



<https://theses.gla.ac.uk/>

Theses Digitisation:

<https://www.gla.ac.uk/myglasgow/research/enlighten/theses/digitisation/>

This is a digitised version of the original print thesis.

Copyright and moral rights for this work are retained by the author

A copy can be downloaded for personal non-commercial research or study,  
without prior permission or charge

This work cannot be reproduced or quoted extensively from without first  
obtaining permission in writing from the author

The content must not be changed in any way or sold commercially in any  
format or medium without the formal permission of the author

When referring to this work, full bibliographic details including the author,  
title, awarding institution and date of the thesis must be given

Enlighten: Theses

<https://theses.gla.ac.uk/>  
[research-enlighten@glasgow.ac.uk](mailto:research-enlighten@glasgow.ac.uk)

**THE MODE AND TIMING OF MICROPLATE  
DOCKING ALONG THE HIGHLAND  
BOUNDARY FAULT ZONE, SCOTLAND**

**BY**

**RICHARD RAIMES JONES**

Thesis submitted for the degree of Doctor of Philosophy  
to the Faculty of Science, Department of Geology and  
Applied Geology, University of Glasgow.

September, 1990

© Richard Jones 1990

ProQuest Number: 11007609

All rights reserved

INFORMATION TO ALL USERS

The quality of this reproduction is dependent upon the quality of the copy submitted.

In the unlikely event that the author did not send a complete manuscript and there are missing pages, these will be noted. Also, if material had to be removed, a note will indicate the deletion.



ProQuest 11007609

Published by ProQuest LLC (2018). Copyright of the Dissertation is held by the Author.

All rights reserved.

This work is protected against unauthorized copying under Title 17, United States Code  
Microform Edition © ProQuest LLC.

ProQuest LLC.  
789 East Eisenhower Parkway  
P.O. Box 1346  
Ann Arbor, MI 48106 – 1346

This thesis is dedicated to Luis, Sherif, Greg, and Joanne,

And to the one who helped me find the way, but who can  
no longer follow it with me.

# ACKNOWLEDGEMENTS

This thesis was initiated and supervised by Dr. P.G.W. Tanner and Prof. B.J. Bluck. Sincere thanks to Geoff, who's scientific integrity, careful criticism, and meticulous analysis has done much to improve this thesis. Many, many thanks too, to Brian, for the endless hours of discussion and lively debate; this has served as a constant and vital source of motivation and interest, as well as helping to expand my geological knowledge and to broaden the scope of this thesis.

The thesis was examined by Professors D.J. Sanderson and D.M. Ramsay. Their constructive criticism has undoubtedly changed this work for the better, and has lead me to widen my thoughts about the HBFZ.

Throughout my time in Glasgow, Peter Haughton has shown keen interest and has offered valuable advice and guidance, to me as to many other postgraduate students, in his own modest and unassuming way.

Similarly, Colin Farrow has not only given invaluable technical advice and practical assistance, but has had such influence as to radically change the direction that my research has taken.

Thanks to Prof. Leake and the faculty of the Department of Geology (more recently the "Department of Geology & Applied Geology"), all of whom have played some part in this work, to a greater or lesser extent. Particular mention must be made of the other "HBC" workers, especially Chris Burton, Joe Crummy, Gordon Curry, Tim Dempster, Mike Dentith, Keith Ingham, Zayd Kamaliddin, Alan Owen, Allan Trench, and Gill Whelan.

Many thanks to Mike Russell for being interested. Far out man.

This thesis benefited greatly from the assistance of the technical staff in the department. Thanks to Roddy-the-Gaffer, Bob (still sane [just] after all these years as a geophysicist), Big Robert, Big George, Big Kenny, Big (?) Allan, and thanks even to Huge Eddie. Kenny and Big George made a fantastic prototype of the clay-box shown in Fig. 4.21. Humble apologies to the cleaners for the spilt tea and the festering socks in 109.

Special thanks to Douglas for the smutty jokes, the marriage guidance, the observations on life, as well as the photography lessons. Too much bromide and not enough daylight, I'd say. I still haven't found your mags after three years searching.

Thanks, of course, to Donny Hutton, Rob Butler, Tim Needham, Dewey, and the Durham Mafia (Chris and Ken, who gave a wild guided tour of the Ox and Clew Bay, Thuggy - of "tadger tectonics" fame, Steve, Richard - the "MAD" cover star, Pete, *etc.*, as well as all the sheep near High Close

youth hostel), without whom I would undoubtedly be an accountant, or worse.

Thanks to Des Smallwood at Sheffield for the slides of Arran S-C fabrics.

Thanks to Harveys Map Services Ltd (Doune), Clydeside Orienteering Club, and Gareth Bryan-Jones for helping find some excellent base maps.

Thanks to Luis Fernandes, who, amongst other things, showed me the pain that thesis preparation can involve. Smile, you pessimistic old sot.

My gratitude to Reg Maddocks, Kerris Owen, and Willy Cotterill, who first kindled my interest in the Earth Sciences.

Hi! to Emil (who re-taught me a valuable lesson), Sherif (who did too), Mark (ditto), Steve (who's sofa bed collapsed at a very unfortunate time), Morgan (thanks again for the floor-space), Paul, Sharif, Lifta, Amar, Youcef-the-mad-Algerian, Omar, Gawen, Fawzi, Neil, Debbie, Tomas, Erica, Ma, Shaladi (despite trying to make me into a seismic geophysicist), Mohamed (the Spy), Ali, Salam, Simon (see you in NSW), Adrian, Ros, Maggy, Derek, Bountiful Spider, Clark, Peter, Calum, Gian, Lindsay, Bubbly-head, Rachel, Julian, Erik, Kenneth, the Boy Gersh, *et al.*, all of whom haven't had a mention yet, but thoroughly deserve one. Soz to those missed out; not deliberate, honest. Hello to the lovely librarian who always smiles.

Special thanks to Martin Hyman, Peter Palmer, Tony Thornley, Graham McIntyre, Øyvinn Thon, and Squaddies past and present, who have given much motivation (and food for thought), each in their own particular way.

Large amounts of pie to Colin, Pakit, Mark, Jock, Freddy, Australia *et al.* for the soup and pecan ice cream on Tuesdays. Why does cheese and bread taste so good in the Hyman Household? Thanks Margaret.

Could it have been done without Ian Curtis, Jim Morrison, Robert Zimmerman, Greenmantle, Viz, the Plantation, or the Campsies?

Thanks to Dave (the Cistern Smasher), for invading my tent, setting up night-time surveillance on my bedroom, filling the bank, completely alienating the neighbours, falling in love, and saving me from total insanity with his unending witty banter. Ahhh, *Caluna Vulgaris*. It's coming Mrs. Brown.

A very special thanks to my long-suffering parents and grandparents, who have given constant support and encouragement. Words cannot express..... Suffer no longer!

Sincere thanks to you all!

# CONTENTS

Page

Dedication	ii
Acknowledgements	iii
Contents	v

<u>Summary</u>	x
----------------	---

## CHAPTER 1: INTRODUCTION

1.1 Research philosophy	1
1.1.1 Aims of the research project	1
1.1.2 Rationale of research and the scope of the thesis	1
1.1.3 Thesis organisation	1
1.2 Regional geology	2
1.3 Abbreviations	3
1.4 Thesis production	4

## CHAPTER 2: POST-CARBONIFEROUS MOVEMENT WITHIN THE HIGHLAND BOUNDARY FAULT ZONE

2.1 Introduction	6
2.2 Recent HBFZ tectonism	6
2.3 Mesozoic & Cenozoic HBFZ tectonism	6
2.4 Summary of Post-Carboniferous tectonism	7

## CHAPTER 3: CARBONIFEROUS MOVEMENT WITHIN THE HIGHLAND BOUNDARY FAULT ZONE

3.1 Introduction	8
3.2 Tectonic setting	8
3.3 Localised Carboniferous extension in the northern and eastern Midland Valley	9
3.4 Carboniferous extension within the HBFZ	9
3.4.1 The southern strand of the HBFZ	10
3.4.2 The northern strand of the HBFZ	11
3.5 Evidence for the timing of movement on the Gaulann Fault Zone	13
3.6 Summary of Carboniferous tectonism	13

## **CHAPTER 4: MID-DEVONIAN DEFORMATION IN CENTRAL SCOTLAND**

4.1	Introduction	15
4.2	Regional geology and previous research	15
4.2.1	Evidence for a mid-Devonian age of deformation	15
4.2.2	Sense of mid-Devonian movement on the HBF	17
4.2.3	Amount of mid-Devonian movement on the HBF	17
4.3	Linked macrofault systems in central Scotland	18
4.3.1	Fault arrays in the Scottish Highlands	18
4.3.2	Fault arrays in the northern Midland Valley	20
4.4	Brittle microtectonics - methodology	22
4.4.1	Choice of sampling sites	22
4.4.2	Analysis of mesofractures	23
4.5	Geometric and kinematic analysis	24
4.5.1	Magnitude of brittle strain	24
4.5.2	Rock rheology	25
4.5.3	Geometric and kinematic data	26
4.6	Dynamic analysis	43
4.6.1	Theory of interpretation	43
4.6.2	Complications in dynamic analysis	48
4.6.3	Mid-Devonian stress orientations	60
4.7	Mid-Devonian folding	80
4.7.1	Fold geometry	80
4.7.2	Mechanism of folding	80
4.7.3	Section balancing and transpression	81
4.7.4	Application of transpression models to the Midland Valley folds	83
4.7.5	Conclusions	87
4.8	Strain partitioning: modification of the simple transpression model	87
4.8.1	The strain partitioning model	87
4.8.2	Partitioned transpressive strain across the HBFZ	90
4.8.3	Partitioned strain across other major fault zones	92

## **CHAPTER 5: TERRANE ACCRETION ALONG THE HBFZ**

5.1	Introduction	95
5.2	Structural description of the Highland Border Complex	95
5.2.1	Structural description of the HBC at Stonehaven	96
5.2.2	Description of the Highland Borders at Drumtochty Castle	102
5.2.3	Structural description of the HBC at Clattering Brig	102

5.2.4	Structural description of the HBC at Edzell	102
5.2.5	Structural description of the HBC at Cortachy	110
5.2.6	Description of the Highland Borders at Lintrathen and West Cult	111
5.2.7	Description of the Highland Borders at Birnam Wood, Tayside	112
5.2.8	Description of the Highland Borders from Meikle Obney to Glen Shee	114
5.2.9	The Highland Borders at Keltie Water, Callander	115
5.2.10	Structural description of the HBC at Lime Craig Quarry, Aberfoyle	116
5.2.11	Structural description of the HBC at Balmaha, Loch Lomond	118
5.2.12	Description of the Highland Borders at Ben Bowie	121
5.2.13	Structural description of the HBC at Innellan	121
5.2.14	Structural description of the HBC at Toward	122
5.2.15	Structural description of the HBC at Scalpsie Bay, Bute	123
5.2.16	Structural description of the HBC around Glen Sannox, Arran	125
5.3	Evidence for Terrane Accretion on the HBF in Ireland	128
5.3.1	Introduction	128
5.3.2	Tyrone	129
5.3.3	The Ox Mountains	129
5.3.4	South Mayo Trough	131
5.4.5	Clew Bay	131
5.4.6	Summary of evidence from the FCL in Ireland	134

## **CHAPTER 6: TERRANE ACCRETION ALONG THE HBFZ - SYNTHESIS, DISCUSSION AND INTERPRETATION**

6.1	Introduction	135
6.2	Synthesis of the structural description of the Highland Border Complex	135
6.2.1.	Amount of exposure along the HBFZ, a summary of the structure of the HBC, and the proportion of highly sheared rocks	135
6.2.2.	Summary of exposures showing high shear strain	137
6.3	Discussion of the theoretical significance of mylonites	137
6.3.1.	Introduction	137
6.3.2.	Characteristics of mylonites	138
6.3.3.	Deformation in four dimensions	143
6.4	Interpretation of the significance of HBC mylonites	145
6.5	Theoretical concepts of terrane tectonics	145
6.5.1.	Plate tectonics and terrane tectonics	145
6.5.2.	Problems associated with structural and stratigraphical correlations	148
6.5.3.	The mode and timing of microplate docking in the Highland Borders of Scotland: philosophical discussion	150
6.5.4.	A strategy for the future analysis of disrupted terranes	156

6.5.5. Concluding remarks concerning objectivity and subjectivity	157
6.6 Interpretation of ductile deformation along the HBFZ	159
6.6.1. An Interpretation of regional HBC stratigraphy	159
6.6.2. The HBFZ as a terrane boundary	163
6.7 A speculative account of the mode and timing of microplate docking (and post-accretion movements) along the HBFZ.	168
<b><u>CHAPTER 7: CONCLUSIONS</u></b>	177
7.1 Conclusions relating to terrane accretion along the HBFZ	177
7.2 Conclusions relating to geological processes	179
<b>Photographic plates 1-4</b>	P1-P4
<b><u>REFERENCES</u></b>	181
<b><u>Appendix 1: MESOFRACTURE ANALYSIS USING A COMPUTER</u></b>	
A1.1 Introduction	A1.1
A1.2 Summary of MASS macros	A1.1
A1.3 Details of the MASS structure	A1.2
A1.3.1 Details of the MASS controlling macros	A1.2
A1.3.2 Details of MASS commands	A1.3
<b><u>Appendix 2: CONSTRUCTING GEOLOGICAL CROSS-SECTIONS USING A COMPUTER</u></b>	
A2.1 Introduction	A2.1
A2.2 Limitations of the program	A2.2
A2.3 Program structure	A2.2
A2.4 Examples of geological cross-sections	A2.3
A2.4.1 Foreland fold and thrust belts	A2.3
A2.4.2 Kink-band folds	A2.6
A2.4.3 Transpressional folds	A2.6
A2.4.4 Chevron folds	A2.6
A2.5 Program listings	A2.8

### **Appendix 3: THE ROTATION OF LINEATIONS DURING FLEXURAL-SLIP FOLDING**

A3.1	Introduction	A3.1
A3.2	The orientation of a palaeomagnetic vector with respect to tilted bedding	A3.1
A3.3	The orientation of palaeomagnetic vectors around parallel folds	A3.4
A3.4	Parallel folds that form during simple shear	A3.4
A3.5	Transpressional parallel folds	A3.8
A3.5.1	Introduction	A3.8
A3.5.2	Fold development in the Harland model of simple transpression	A3.9
A3.5.3	Further discussion of the application of the Harland model of simple transpression to the mid-Devonian folding in the Midland Valley	A3.13
A3.5.4	Computer programs used to model transpression	A3.15
A3.6	Sign Conventions	A3.18
A3.7	Summary	A3.18

# SUMMARY

The Highland Boundary Fault Zone is a major crustal fracture with a long and complex structural history, in which brittle deformation was superimposed upon pre-existing fabrics produced by ductile deformation. This thesis describes and interprets the history of HBFZ tectonism, presented in reverse chronological order (youngest events first).

Although the HBFZ still experiences small-scale earthquakes, there is evidence to show that significant fault displacement has not occurred since the end of the Carboniferous. Extensional deformation during the Upper Devonian and the Carboniferous was small-scale and localised.

Upper crustal deformation in mid-Devonian times, possibly caused by the accretion of the Avalonian terrane with Laurentia, was low in magnitude but widespread in aerial extent.

The results and interpretations of a mesofracture analysis are presented to help constrain mid-Devonian brittle deformation across central Scotland. The results show that regional north-south compression caused transpressional reactivation of the pre-existing HBFZ.

Because our existing understanding of transpression is incapable of explaining the results of the mesofracture analysis, an alternative transpression model is proposed, in which transpressive strain is "partitioned" into two components; a strike-slip component restricted to the fault zone, and a thrust component deforming the rocks that flank the zone. The "strain-partitioning" model, with some elaboration, helps to explain the mid-Devonian deformation seen in central Scotland.

The balance of evidence from the Highland Border, Dalradian, and Midland Valley terranes suggests that ductile deformation along the HBFZ occurred in response to terrane accretion, which probably took place in Ordovician times. A palaeo-tectonic model is presented in which Highland Border and Midland Valley terranes were accreted and laterally displaced, with a sinistrally transpressive sense, onto the Laurentian margin in the Llandeilo and/or Caradoc, and again in the Ashgill and/or Llandovery. The extreme difficulties of postulating the palaeo-tectonic histories of disrupted terranes are discussed in detail.

# CHAPTER 1: INTRODUCTION

## 1.1 Research philosophy

### 1.1.1 Aims of the research project

This thesis presents the results of a NERC-funded PhD research project that I carried out between October 1986 and August 1990.

The original aim of the research project was to document the evidence (particularly the *structural* evidence) for the amount, sense, and timing of microplate docking events that may have occurred along the Highland Boundary Fault Zone ("HBFZ").

### 1.1.2 Rationale of research and the scope of the thesis

Regional geological evidence suggests that microplate docking *may* have occurred along the HBFZ at some time(s) during the Precambrian and/or the Palaeozoic. When analysing evidence of ancient tectonic events it is imperative to be able to separate those structures produced early in the geological history of a terrane, from those relating to subsequent episodes of overprinting and reactivation.

Consequently, this project provided an opportunity to attempt the first comprehensive synthesis of the *structural history* of the Highland Boundary Fault Zone.

Hence, the aims of this thesis are wider than the original proposed aims of the research project. This thesis aims to give a comprehensive structural history of HBFZ tectonism, with particular emphasis on those "early" structures that relate to terrane accretion, but also giving adequate consideration to those structures produced during reactivation of the HBFZ.

### 1.1.3 Thesis organisation

The chapters of this thesis are organised to cover successively older episodes of HBFZ tectonism. In Chapter 2 I summarise evidence that suggests that there has probably been little significant fault displacement since Permo-Carboniferous times. The effect of Carboniferous reactivation is discussed in Chapter 3. Chapter 4 presents evidence that north-south compression caused the HBFZ to experience sinistrally transpressional

reactivation. This event is of wide structural significance, and consequently is discussed in some detail. The evidence for the mode and timing of microplate docking is described in Chapter 5, and finally discussed, and critically analysed in Chapter 6.

## 1.2 Regional geology

The Highland Boundary Fault Zone in Scotland separates the Precambrian rocks of the Dalradian Highlands from the Palaeozoic rocks of the Midland Valley, and lies between Stonehaven on the east coast, and Glen Sannox (Arran) on the west coast (Fig. 1.1).

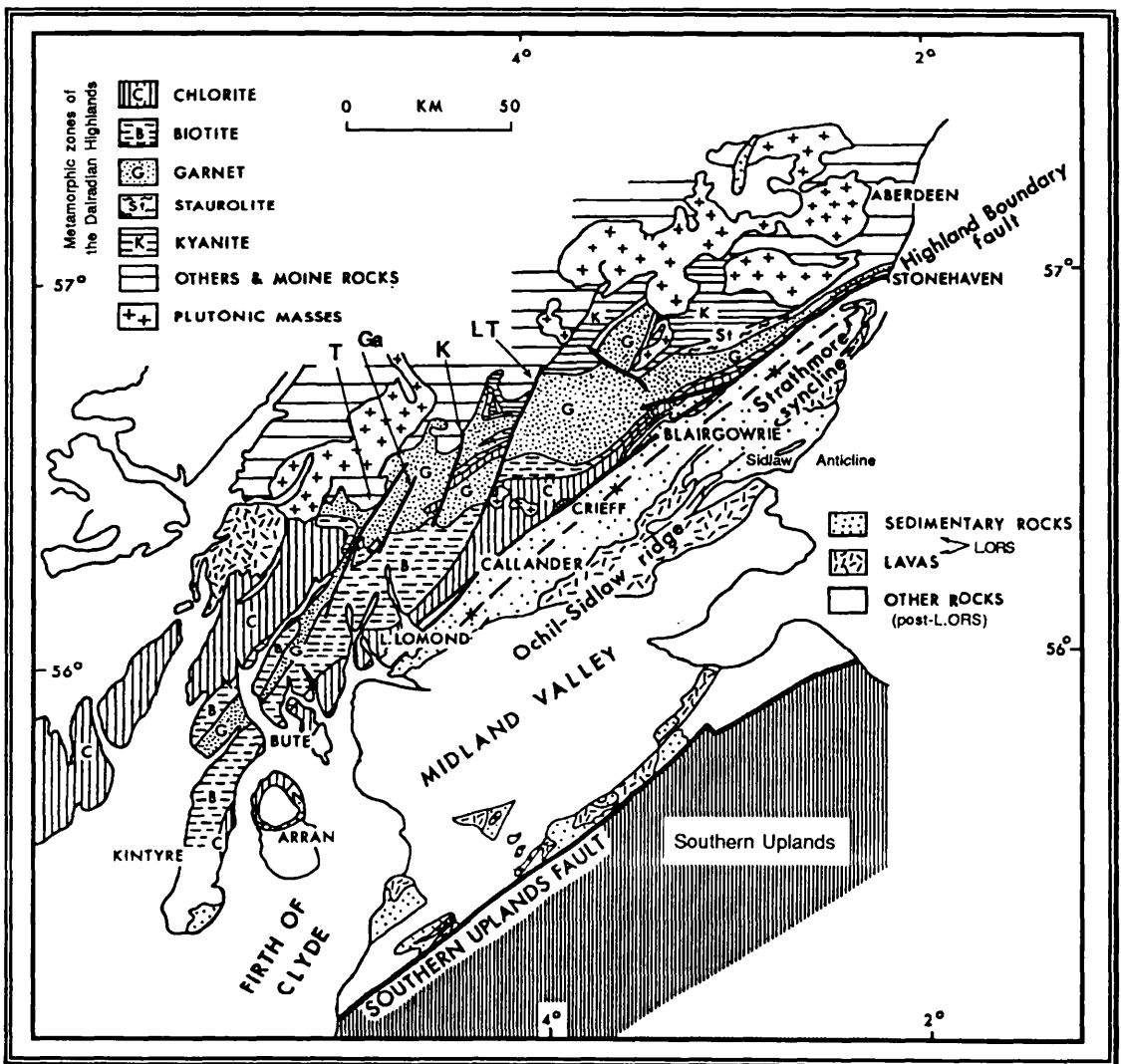


Fig. 1.1. The generalised regional geology of central Scotland. T, Ga, K, & LT are faults of the Tydrum/Garabal/Killin/Loch Tay fault array.

The HBFZ is marked by an irregular zone of highly enigmatic rocks now called the Highland Border Complex ("HBC"). A detailed resumé of the nature and terminology of the HBC is given in Curry *et al.* 1984. The HBC is composed of a melangé of disparate lithologies, many of which have been tectonised, and/or metamorphosed, and/or metasomatised, progressively changing the HBC into a melangé of rocks that are extremely difficult to analyse in the field. In addition, exposure in the zone is generally poor, and most outcrops are small and isolated, and consequently the structural relationships between most outcrops are unknown. Good exposure is restricted to a few type localities (Chapter 5).

The boundary between the HBC and the ORS of the Midland Valley (*i.e.* the southern margin of the HBFZ) was generally considered to be the Highland Boundary Fault (*sensu stricto*), but has since been shown to be unconformable in places. The northern margin of the HBFZ, separating the HBC from the Dalradian Highlands, is also generally depicted as a continuous fault, though because of the lack of continuous exposure this cannot be confirmed. This boundary is probably the result of more than one phase of deformation, and some parts of it at least, may have a more typical duplex geometry rather than being a single planar fault (Boyer & Elliot 1982, Woodcock & Fischer 1986).

Over two hundred years of research in Scotland has provided a wealth of geological map data and a voluminous literature (Curry *et al.* 1984). More recently, geophysical studies have provided constraints on the sub-surface structure of central Scotland. Seismic studies have helped to constrain the overall layered structure of the crust (Bamford *et al.* 1977,1978). Regional and local gravity and magnetic modelling (summary in Davidson *et al.* 1984; Dentith *et al.* in prep.), together with xenolith data (Brian Bluck, pers. comm.), suggest that the HBC dips northward steeply, beneath the Dalradian block, to deep structural levels.

### 1.3 Abbreviations

I have used the following abbreviations extensively throughout this thesis;

a.s.l.	above sea level
CBS	Clew Bay Supercomplex
FCL	Fair Head/Clew Bay Line
GFZ	Gualann Fault Zone
G.R.	Grid Reference

HBC	Highland Border Complex
HBF	Highland Boundary Fault
HBFZ	Highland Boundary Fault Zone
L.ORS	Lower Old Red Sandstone
Ma	Million years before present
ORS	Old Red Sandstone
U.ORS	Upper Old Red Sandstone

## 1.4 Thesis production

This thesis was written using Apple® Macintosh™ micro-computers (Macintosh Classic, SE, II, and IIcx), using the "Microsoft® Word 4.0" document processing program. Word 4.0 allows all the text layout, pagination, size & position of diagrams, and formatting to be completely controlled. Diagrams were produced in a number of different ways, but were all then "pasted" into the Word 4.0 documents.

Many diagrams (*e.g.* Figs. 3.1, 4.28, 5.17) were drawn "free-hand" straight on the computer using the "Superpaint 2.0" graphics software. In contrast, graphs, cross-sections, fault off-set maps, rose diagrams, and stereonet (*e.g.* Figs. 4.29, A2.3, 4.6, 4.4, 4.9 respectively) were produced by linking the Macintosh with a Sun work-station, using "telnet" and "text-term" communication software. The diagrams were created on the Mac screen by the relevant S macros (see Appendices 1 & 2), and these were then pasted into Superpaint for modification.

Other diagrams were produced using a Hewlett Packard "ScanJet Plus", by "scanning" a rough pen & ink outline, or a neat diagram 'stolen' straight from an original paper (*e.g.* Figs. 5.3, 4.5 respectively). The scanned images (at 300 d.p.i.) were pasted into the "Deskpaint" graphics package, to fill-in areas of shade and pattern, and to tidy-up the scanned image where necessary. Text was added (*e.g.* Fig. 3.3) by pasting the newly-modified diagram into Superpaint, before finally pasting it into its correct position in the Word 4.0 document. I also tried a similar method, using a GTCO "Macintizer ADB™" graphics tablet to trace diagrams directly into Superpaint (*e.g.* Figs. 5.5 & 5.6), but this proved too time-consuming, and surprisingly, resolution was not as good as with the scanner.

Fig. 4.1 is a scanned image of a colour print. The resolution is not perfect; this is a function of the printer rather than the scanner (the printer does not support grey-scale printing). In this thesis, only the photographic plates were not incorporated into the Word 4.0 thesis documents. I think

that true 'desktop publishing' of PhD theses will happen in the very near future!

In total, this thesis is stored using 5,166 kilobytes of memory, though this can be greatly reduced (to less than 3 Mb) by using a 'compressing' application such as "DiskDoubler" or "Stuffit™". The thesis was printed using an QMS-PS800 LaserWriter.

# CHAPTER 2: POST-CARBONIFEROUS MOVEMENT WITHIN THE HIGHLAND BOUNDARY FAULT ZONE

## 2.1 Introduction

The rationale of this chapter is to examine two related questions: firstly, whether any fabrics or structures now found along the Highland Boundary Fault are the result of post-Carboniferous deformation, and secondly, whether the present-day distribution of stratigraphic units along the HBF has remained unchanged since Carboniferous times.

## 2.2 Recent HBFZ tectonism

The Highland Boundary Fault is a major crustal fracture with a long geological history. Seismological records gathered during the past two hundred years show that the fault still acts as a significant plane of crustal weakness and a site of stress release (Davison 1924; Dollar 1950). The Comrie area is one of the most seismically active areas in the UK; four hundred and thirty-four quakes were recorded between 1788 and 1949, the largest (Oct.23 1839) was felt over 26,500 square miles, and caused chimneys to topple and some walls to crack (Fig. 2.1).

Quakes have also been recorded at other places along the HBF, from Strathmore in the northeast, through to Dunkeld, Dunoon, and Bute, to Kintyre in the southwest, and on faults of the Loch Tay, Tyndrum, and Killin array (see Fig. 1.1).

## 2.3 Mesozoic & Cenozoic HBFZ tectonism

There is good geological evidence that for the past 290 Ma the HBF has been no more tectonically active than it is today, and hence the HBF was not reactivated as a *major* fault during the formation and disintegration of the Pangaea super-continent.

Late Carboniferous quartz-dolerite and tholeiite dykes cut across the HBC and HBFZ fault strands. The dykes, part of a regional arcuate swarm extending from the Outer Hebrides to the North Sea (Russell & Smythe 1983), are generally orientated W-E or WSW-ENE (*i.e.* at high angle to the HBF). In places the dykes swing into the HBF trend, and run along HBFZ fault strands for short distances (*e.g.* Dounans Quarry [Aberfoyle], and Gourdie [Dunkeld]).

Field relationships from east Fife suggest that the dykes are of Late Carboniferous age (Armstrong *et al.* 1985). This observation is supported by a K-Ar whole rock age of 290-295 Ma for a dyke in Fife (de Souza 1979, p.196-201).

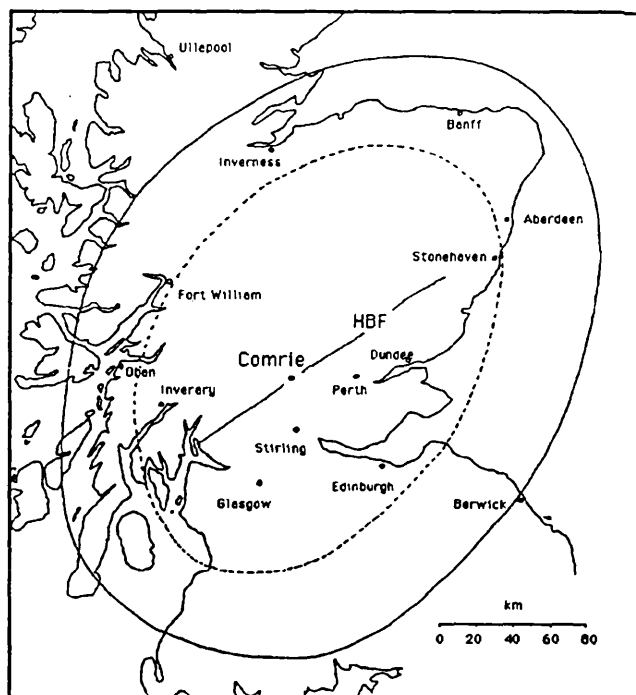


Fig. 2.1. The Comrie earthquake of October 23, 1839, showing the approximate position of two isoseismals. The inner circle represents the limit at which the ground was felt to fall or rise. The outer circle represents the limit at which windows and doors *etc.* were made to rattle (after Davison 1924).

## 2.4 Summary of Post-Carboniferous tectonism

Stratigraphical evidence shows that significant displacement on the HBF had ceased by late Carboniferous times. Since then, the HBF has been the focus of many low-intensity earthquakes that have allowed intra-plate stresses to be released, without causing large fault displacement.

# CHAPTER 3: CARBONIFEROUS MOVEMENT WITHIN THE HIGHLAND BOUNDARY FAULT ZONE

## 3.1 Introduction

This chapter reviews the evidence for a deformation event that post-dates the mid-Devonian tectonism discussed in chapter 4. It is essential to identify the structural style of late tectonic events in order to be able to distinguish them from earlier structures.

As with mid-Devonian deformation, evidence from rocks on either side of the HBF is generally easier to interpret than evidence from within the fault zone itself. Upper ORS and Carboniferous strata give the most reliable evidence, as they are not affected by mid-Devonian or earlier tectonism.

## 3.2 Tectonic setting

The Carboniferous stratigraphy of the British Isles represents a regional marine incursion on to the ORS Laurentian continent (Anderton *et al.* 1979). Tectonically, the basin stratigraphy of Northern Britain marks a period of regional extension and rapid subsidence, represented in Scotland by the emplacement and extrusion of large volumes of alkali basalts.

Carboniferous extension in the southern and western Midland Valley had a profound effect on sediment accumulation, with Coal Measures deposition occurring in fault-bounded pull-apart basins in a dextral transtensional fault system (Alan Gibbs, pers. comm., *e.g.* Hamilton basin, BGS sheets 23 & 31; Douglas Basin, sheets 15 & 23).

In contrast, I have no evidence that the Lower ORS rocks of the northern and eastern Midland Valley have experienced *regionally significant* extension at any time since their deposition. However, the Carboniferous and Upper ORS strata have mostly been removed by erosion, and this makes it more difficult to identify deformation of Carboniferous age. Evidence for extension within the northern Midland Valley is seen only in occasional isolated outcrops; these are described below. Significant Carboniferous extension did occur *within* the HBFZ south-west of Aberfoyle, as discussed below.

Localities where both Upper and Lower ORS sediments are exposed are critical in showing the relative importance of mid-Devonian tectonism compared with the Carboniferous deformation events, and are described and

discussed in chapter 4. Direct comparison of Upper and Lower ORS at Arbroath and Balmaha demonstrates that the magnitude of brittle deformation (folding and fracturing) is significantly greater in the Lower ORS than in the adjacent Upper ORS.

### 3.3 Localised Carboniferous extension in the northern and eastern Midland Valley

Local extension is occasionally recognisable in outcrop by diagnostic mesofracture geometries (the methodology of mesofracture analysis is discussed in detail in section 4.4). At Killearn (G.R. NS 522853) Upper ORS sandstones are cut by an array of listric and planar extensional mesofaults:

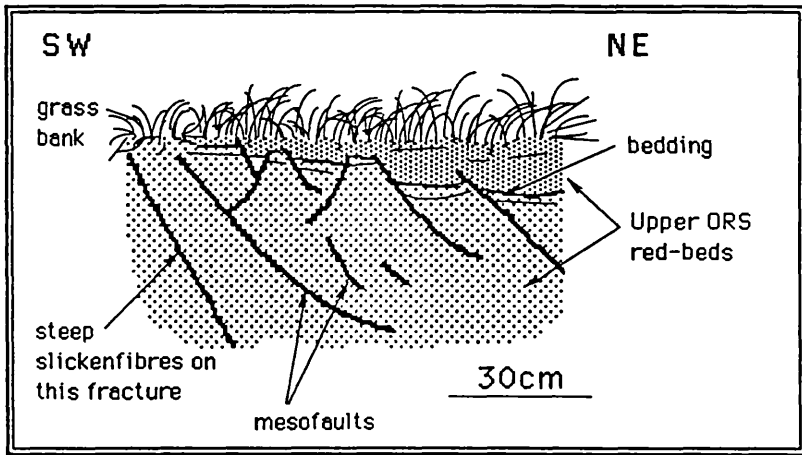


Fig. 3.1. Small-scale extensional mesofaults in Upper ORS sediments at Killearn.

A roadside exposure south of Doune (station 27, G.R. NS 717993) shows a triaxially compressive mesofracture array overprinted by a set of extensional mesofaults (see Chapter 4 for details).

### 3.4 Carboniferous extension within the HBFZ

South-west of Aberfoyle the HBF bifurcates into two well-defined fault strands. In this region within the HBFZ the nomenclature of individual faults is inconsistent and confused, and attaching a name to a particular fault has encouraged workers to assume that the faults can be directly correlated between widely-spaced outcrops. Well-exposed examples of linked fault systems show that such simple correlations may be spurious (thrust duplexes, Butler 1982; strike-slip duplexes, Woodcock & Fisher 1986; extensional duplexes, Gibbs 1984).

### 3.4.1 The southern strand of the HBFZ

The southern branch of the HBFZ contains the fault that has been labelled as the "Highland Boundary Fault" *sensu stricto*. This term refers to the most south-easterly fault of the HBFZ (Anderson 1946), and so is synonymous with the "Highland Fault" of Jehu & Campbell (1917). In general, the HBF separates the HBC from the ORS of the Midland Valley, though in places this boundary is an unconformity.

The southern branch of the HBFZ is referred to here as the "Gualann Fault Zone" or "GFZ"<sup>1</sup>. In the field it is marked by a 100m-wide slice of serpentinites of the Highland Border Complex (see chapter 5). The contact between the Lower ORS and the serpentinites was generally taken as the "Highland Fault" (Jehu & Campbell 1917), but at Balmaha is locally an unconformity (Brian Bluck, pers.comm.).

The Gualann Fault Zone downthrows Upper ORS sediments to the north, though the actual movement vector is unknown (*i.e.* the fault may have a component of strike-slip). The throw on the fault cannot easily be determined from published map data (Fig. 3.2), but by Ben Bowie (G.R. NS 340829) an estimated thickness of over 3 km of Upper ORS is downthrown to the NW (Bluck 1980).

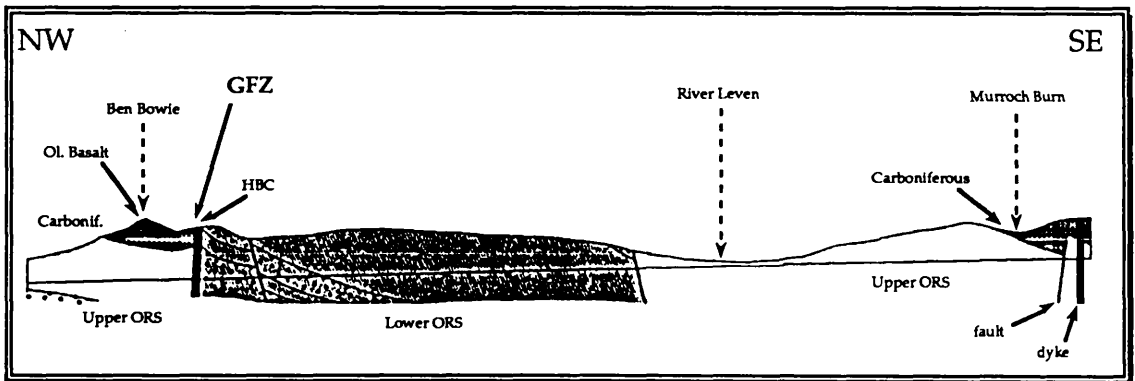


Fig. 3.2. NW/SE cross-section across the Gualann Fault Zone (GFZ), from G.R. NS 325837 to G.R. NS 405797. From BGS sheet 30S. Section is 9km long. Vertical exaggeration: x2.

It is possible to derive an estimate of the throw on the GFZ using a stratum contour solution (Fig. 3.4), derived from detailed field mapping (Fig. 5.12), and this suggests that the displacement on the GFZ at Balmaha might not be so large. It must be stressed that exposure around Balmaha is limited, and there is

<sup>1</sup> Note on terminology: I propose here that the term "Gualann fault zone" be used collectively for those faults that comprise the southern strand of the HBFZ in the region south-west of Aberfoyle. This zone contains the "Highland", "Gualann" and "Jasper" Faults of Jehu & Campbell 1917.

no unique solution based on the data that I have collected. The solution I have chosen predicts the maximum likely thickness of U.ORS near Conic Hill (358m a.s.l.; G.R. NS 430923) to be 200m. Other solutions suggest that the minimum thickness may be as little as 30m, and thus the required *minimum* displacement on the GFZ at Conic Hill is only 65m.

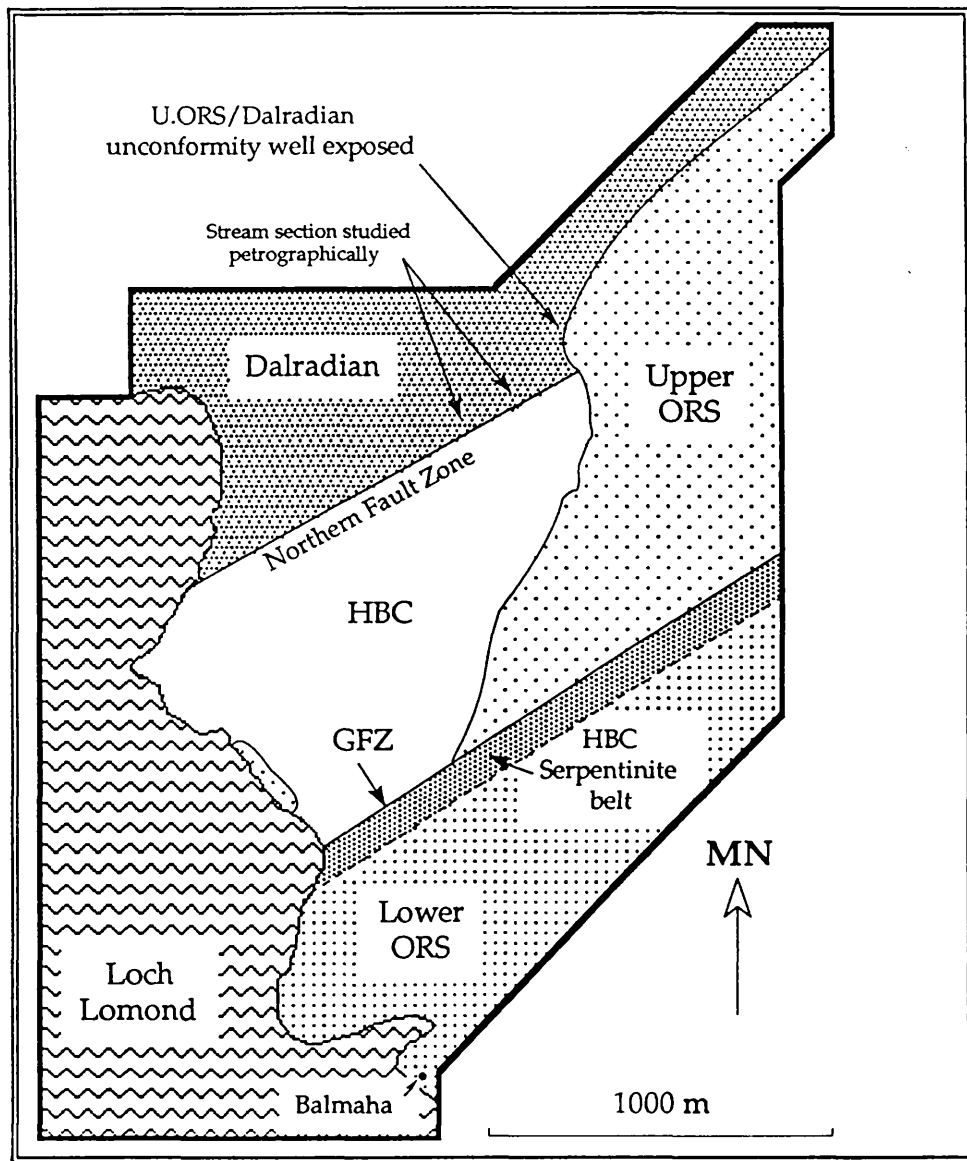


Fig. 3.3. Interpretative map showing the solid geology of the Balmaha area, based on detailed outcrop field mapping (this interpretation is based on the detailed outcrop map shown in Fig. 5.12).

### 3.4.2 The northern strand of the HBFZ

The northern branch of the HBFZ contains the "Leny Fault" of Jehu & Campbell (1917), marking the boundary between the Dalradian metasediments and the Highland Border Complex. The northern fault zone is likely to be a

structurally complex system of anastomosing linked fault strands, rather than one single continuous fault.

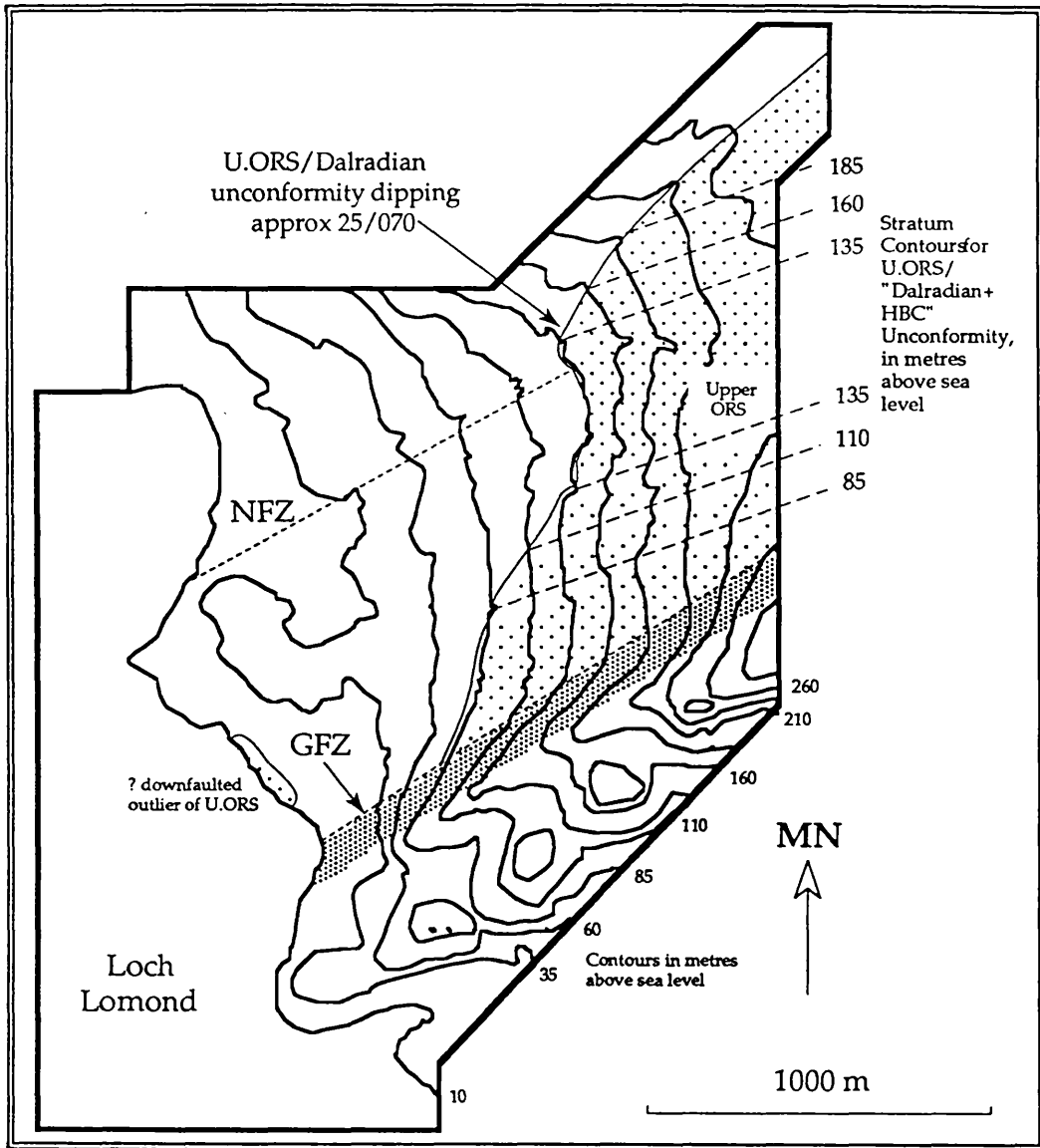


Fig. 3.4. Interpretive stratum contour map for the Upper ORS of the Balmaha area, showing the U. ORS overstepping the NFZ (northern branch of the Highland Boundary Fault Zone), and downfaulted to the north by the GFZ (Gualann Fault Zone). This interpretation is based on the detailed outcrop map shown in Fig. 5.12.

Field evidence suggests that the northern branch of the HBF at Balmaha has been inactive ever since the time of Upper ORS deposition. Upper ORS red-beds appear to overly both the Dalradian and the HBC, on an unconformity surface that shows no obvious displacement by the northern HBF strand (Figs. 3.3 & 3.4). Obviously, this evidence is critical to unravelling the history of HBF movements, and consequently is discussed in detail below.

Like the southern fault, the northern strand of the HBFZ is also marked by a thin wedge of HBC serpentinite (see Fig. 5.12). Between the serpentinite slices lie arenites of the Highland Border Complex; the "Loch Lomond clastics" of Henderson & Robertson (1982), or the "Achray Sandstone Fm." of Curry *et al.* (1982). Northeast of Arrochymore Point the northern serpentinites are either tectonically cut-out, or lie within a 100m exposure gap. The Dalradian and the HBC grits can appear so alike that distinguishing between them in the field is sometimes practically impossible, and they have to be separated petrographically. I used the following criteria in thin section:

<u>HBC</u>	<u>Dalradian</u>
Quartz extinction is only occasionally undulose	Quartz extinction is usually strongly undulose
Chlorite absent	Most detrital grains have chlorite beards
Tectonic fabric is weak	Tectonic fabric is more penetrative
Some chromite grains present	Chromite not seen
Black shale, chert, and igneous fragments present	These grain types not seen

### 3.5 Evidence for the timing of movement on the Gualann Fault Zone

The maximum age of deformation on the GFZ is well constrained because Carboniferous sediments and lavas are affected by the faulting. The minimum age of deformation is generally taken to be Permo-Carboniferous, because of the dyke that appears to stitch the fault at Aberfoyle (Curry *et al.* 1984). However, the field evidence at Dounans Quarry, Aberfoyle, is ambiguous because the dyke lies parallel to, and within, the GFZ. Consequently, though the deformation southwest of Aberfoyle is *likely* to be of similar age to that further to the northeast (*i.e.* Late Carboniferous), I am unable to demonstrate this beyond all reasonable doubt.

### 3.6 Summary of Carboniferous tectonism

South-west of Aberfoyle the HBF bifurcates into two fault strands; the northern and the Gualann Fault Zones. Reliable stratigraphical evidence shows that significant movement on the northern zone had ceased prior to U.ORS

overstep, whereas the GFZ was active during (or possibly after) the Carboniferous.

Northeast of Aberfoyle there is no reliable stratigraphic or structural evidence for post-mid-Devonian movement on the HBF. However, this issue remains unresolved; some Carboniferous deformation may have occurred.

# CHAPTER 4: MID-DEVONIAN DEFORMATION IN CENTRAL SCOTLAND

## 4.1 Introduction

This chapter consists of a review of regional mid-Devonian faulting and folding, together with the results of a mesofracture analysis of central Scotland. The overall aims of the study were twofold:

- 1) to constrain the timing, sense, and amount of movement on the HBF during late, brittle phases of deformation.
- 2) to ascertain the effect that late deformation had upon the geometry of pre-existing structures (particularly those that might represent terrane docking).

The evidence for Carboniferous extension along the HBF, and the cessation of significant movement on the HBF by Permo-Carboniferous times are discussed in chapters 2 & 3. Early (ductile) deformational events (related to terrane accretion) are described in Chapter 5. This chapter relates to an intervening phase of tectonism, in which rocks of Lower Old Red Sandstone age are deformed.

## 4.2 Regional Geology and Previous Research

### 4.2.1 Evidence for a mid-Devonian age of deformation

In the Midland Valley of Scotland rocks of Lower ORS age that form the limbs of the Strathmore syncline/Sidlaw anticline fold pair are unconformably overlain by gently inclined to horizontal Upper ORS strata (Fig. 1.1, Fig. 4.1, and section 4.7). This is taken to indicate that central Scotland experienced a phase of deformation in M.ORS times (*e.g.* Armstrong *et al.* 1985 p.62). Accurate dating of this deformation relies on the palaeontological dating of the ORS sediments (House *et al.* 1977, Richardson *et al.* 1984). The youngest sediments that are involved in the folding episode are of Emsian age, suggesting that the deformation occurred at some time between the Emsian and Givetian ages.

Throughout this thesis, therefore, I use the term "mid-Devonian" for the Emsian to Givetian time period.

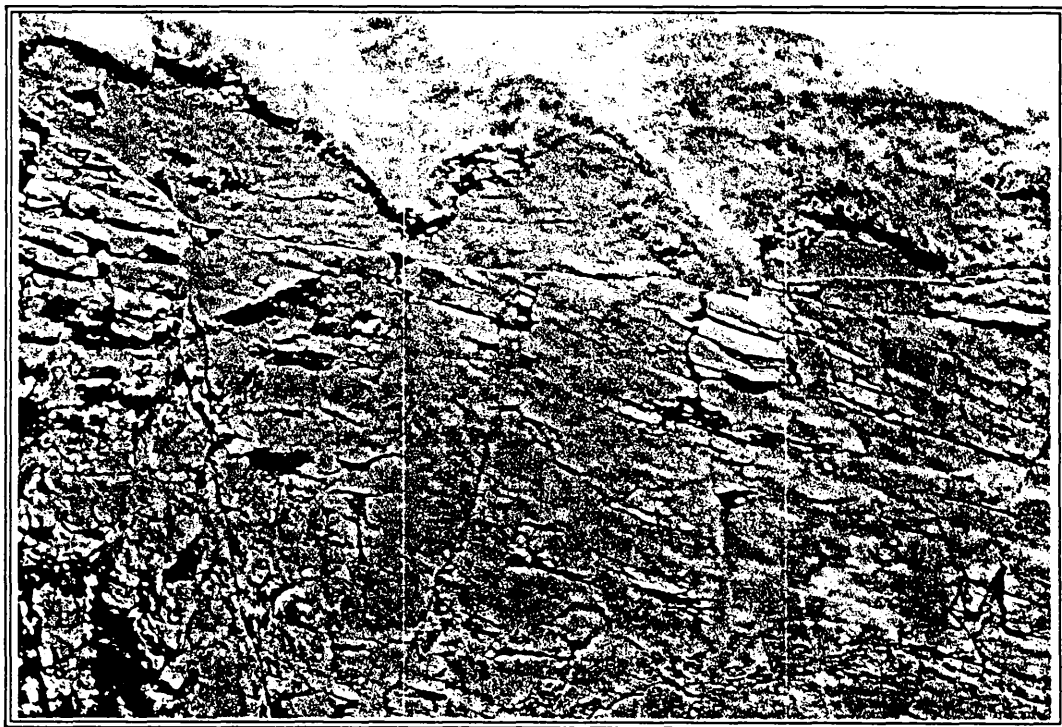
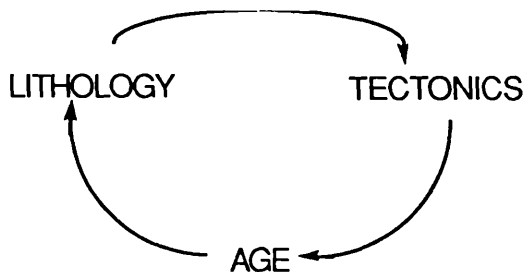


Fig. 4.1. Angular unconformity between faulted Lower and unfaulted Upper ORS arenites, at Dickmont's Den, Arbroath (G.R. NO 667417). Unconformity surface is highlighted by a white line. Vertical height of the section shown is approximately 15m. Looking NE.

Some of the assumptions and limitations inherent in the dating of this deformation must be emphasised. I have assumed that the age ascribed to each Devonian fossil by House *et al.* and Richardson *et al.* is correct, and that the age range of each fossil assemblage is sufficiently well constrained to allow accurate dating of stratigraphic units. The number of exposures that show the unconformity between Lower and Upper ORS is not great, and this, combined with the paucity of zonal fossils in continental red-bed lithologies, gives rise to some difficulties in stratigraphic correlation of the ORS sediments.

In general, mapping of the ORS has been based on lithological correlation. The structural control of L.ORS sedimentation on a regional and a local scale is poorly understood, but it seems probable that lithology is at least partially dependent on the tectonic regime active at the time of deposition (the L.ORS was possibly deposited in one or more pull-apart basins; Haughton 1988, Bluck 1990). Consequently, those arguments dealing with tectonic interpretation that are based on evidence from outcrops where palaeontological control is absent, are likely to involve logic that is somewhat circular:



#### 4.2.2 Sense of mid-Devonian movement on the HBF

There has been little agreement regarding the sense of displacement on the HBF.

Brittle fracturing of clasts in Lower ORS conglomerates adjacent to the HBF (Du Toit 1905) was studied in detail by Ramsay (1962, 1964), who concluded that the HBF acted as a high-angled thrust in mid-Devonian times, carrying the Dalradian metasediments on top of the L.ORS of the Midland Valley. Southerly directed overthrusting of the Dalradian over Ordovician and other rocks can be seen in Tyrone in Ireland (Hutton 1987, 1990). The age of the overthrusting in Ireland is unknown.

The Dalradian rocks of the Grampian Highlands are also pervasively fractured. The Tyndrum/Killin/Loch Tay fault array (Fig. 1.1) is dominated by left-lateral faults (e.g. Shackleton 1957, Smith 1961); this array was first interpreted by Anderson (1951) as representing major sinistral transcurrent movements on the Highland Boundary and Great Glen faults. Evidence for the timing, sense and amount of movement on this fault array is discussed in section 4.3.

#### 4.2.3 Amount of mid-Devonian movement on the HBF

Reliable stratigraphic markers of pre-M.ORS age (that would unequivocally show the amount of mid-Devonian offset on the HBF) have not been found in Scotland or Ireland, and consequently less direct evidence must be used. Until recently most estimates of the magnitude of movement were non-quantitative.

The possibility that the Midland Valley of Scotland was exotic with respect to the Grampian Highlands *until mid-Devonian* times was highlighted by Bluck (1984, 1985), based on the lack of sedimentary detritus of proven Dalradian provenance in the L. ORS strata of the Midland Valley. Inherent in this hypothesis is the inference that the mid-Devonian deformation would represent the first accretion event between Dalradian and Midland Valley terranes (see Chapter 5). A Lower ORS linkage between

the two terranes has since been established on sedimentary provenance grounds (Haughton 1988; Haughton *et al.* 1990), and the post-L.ORS movement constrained palaeomagnetically and geochemically to less than about 2,255 km (Trench & Haughton 1990). Despite this, the nature of tectonic control of L.ORS sedimentation still remains enigmatic.

To summarise; regional geological evidence suggests that Middle Devonian tectonism along the HBFZ may have included components (of unknown magnitude) of both thrusting and sinistral strike-slip.

### 4.3 Linked macrofault systems in central Scotland

This section discusses, in more detail, the movement on macro-scale fault arrays in the Dalradian Highlands and Midland Valley. Macrofaults are widely shown on published BGS maps (1:50,000/1:63,360, sheets 14-77), and have also been imaged using Landsat (Johnson & Frost 1977).

#### 4.3.1 Fault arrays in the Scottish Highlands

In map view the SW/NE faults of the Tyndrum/Killin/Loch Tay array offset Dalradian stratigraphy with a dominant left-lateral sense (Fig. 1.1). The curvature of faults into the HBF, and the change of trend of the HBF at branch lines does suggest a dynamic link between the HBF and the above fault array. This led Anderson (1951) to infer major left-lateral movement on the HBF zone; a hypothesis since incorporated into many tectonic models for the development of the British Caledonides (*e.g.* Watson 1984; Hutton & Soper 1984; Hutton, 1987).

More detailed (three dimensional) movement vectors for four of the main faults have been derived from field mapping and fault plane interpretations by Dr. J.E. Treagus (Manchester Univ., pers. comm.):

Tyndrum	8.1km sinistral + 1.8km dip-slip, downthrow to the SE.
Killin	1.2km sinistral + 1.5km dip-slip, downthrow to the SE.
Loch Tay	7.0km sinistral + 0.7km dip-slip, downthrow to the NW
Glen Strae	4.2km sinistral + 1.7km rotational slip, downthrow to SE (maximum in north).

There is a possible complication in interpreting the kinematic significance of these results, because the net displacements for most of the faults may result from more than one phase of movement. In general

terms, though, the fault array (including the less -well-developed E-W dextral conjugate set), is *extensional* with respect to the Dalradian stratigraphy (in the sense of Norris 1958). This is an important conclusion; the shortening that was directed across the Dalradian strike resulted in oblique fault slip, with stratigraphy extending parallel to strike both horizontally and vertically (*i.e.* triaxial flattening strain). This is regionally consistent with the results of mesofracture analysis presented later in this chapter.

The timing of fault movement remains a matter of some uncertainty. Smith (1961) and Johnstone & Smith (1965) postulated that the main fault movement occurred prior to the emplacement of L.ORS intrusives; however this view must now be questioned. Sarah Curtis (Manchester Univ., pers. comm.) has shown that the Tyndrum fault has two distinct phases of fault movement, one preceding and the other post-dating, the emplacement of felsite intrusives. The age of the intrusives, previously assumed to be Lower Devonian (Smith 1961), awaits corroboration.

Evidence for the earliest possible onset of faulting is provided by radiometric cooling ages for Grampian deformation. A period of rapid uplift, dated at 430-400Ma (Tim Dempster 1984, and pers. comm. 1989), represents the lower age limit for brittle faulting on the Tyndrum/Killin/Loch Tay fault array. The array also cuts the Newer granites of the eastern Grampians (*e.g.* Fig. 4.2), dated at 415-390 Ma (summary in Stephens & Halliday 1984).

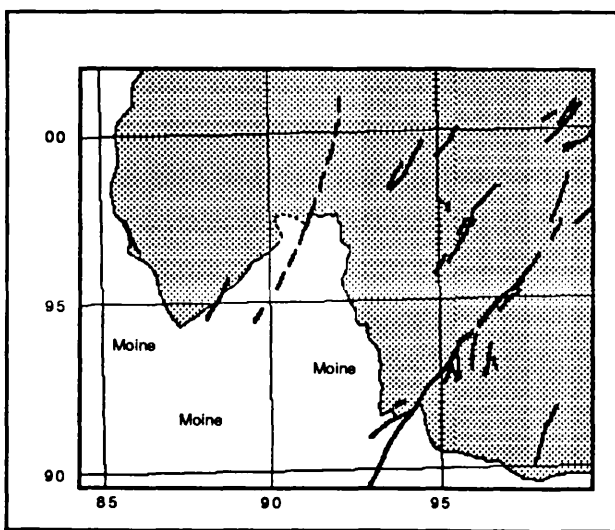


Fig. 4.2. Sketch map showing left-lateral displacements of the Newer Granites of the Cairngorms, simplified from BGS sheet 64 (Kingussie). The granite is shaded. Thick lines are faults. The grid has a 5km spacing.

As with the HBF, the ending of significant fault displacement within the Dalradian tract occurred before the emplacement of Permo-Carboniferous dykes (see Chapter 2).

In summary, the Tyndrum/Killin/Loch Tay fault system was probably initiated during end Silurian/early Devonian uplift, and was subsequently reactivated following the emplacement of the Newer Granites. Overall movement shows a net left-lateral oblique offset, consistent with a regional rotational triaxial flattening strain. Principal compression was orientated within the NW-NE/SE-SW quadrant (Fig. 4.3).

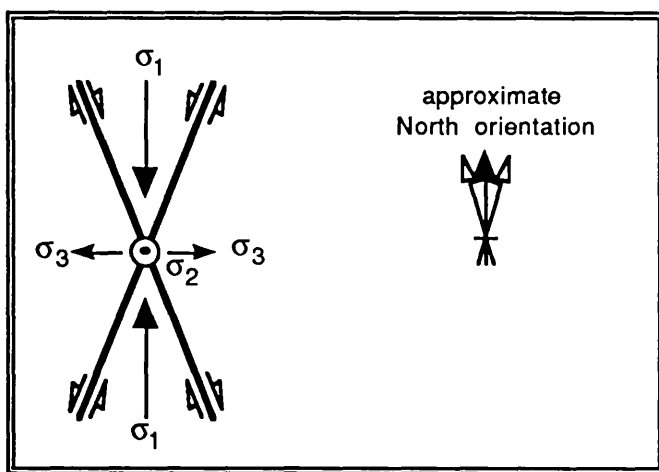


Fig. 4.3. Schematic representation of macrofault geometry in the Dalradian Highlands (map view).  $\sigma_{1-3}$  are principal compressive stresses, such that  $\sigma_1 > \sigma_2 > \sigma_3$ .

#### 4.3.2 Fault arrays in the northern Midland Valley

Macrofaults cutting Lower ORS rocks of the northern Midland Valley are shown on BGS 1:50 000 sheets 39, 48, and 49. In general, Upper ORS rocks are cut by fewer faults than adjacent Lower ORS strata, and many faults traces within the L.ORS stop abruptly at the U.ORS boundary. The strike orientations of sixty-four macrofaults from the above BGS sheets are plotted below. Faults are separated according to their *apparent* sense of strike-slip displacement, *i.e.* the horizontal component of movement (some may have considerable throws).

It is possible to interpret the geometry of faults shown in Fig. 4.4 as a set of conjugate faults orientated symmetrically about a  $\sigma_1$  direction at approximately  $150^\circ/330^\circ$ . Although this interpretation gives a result which

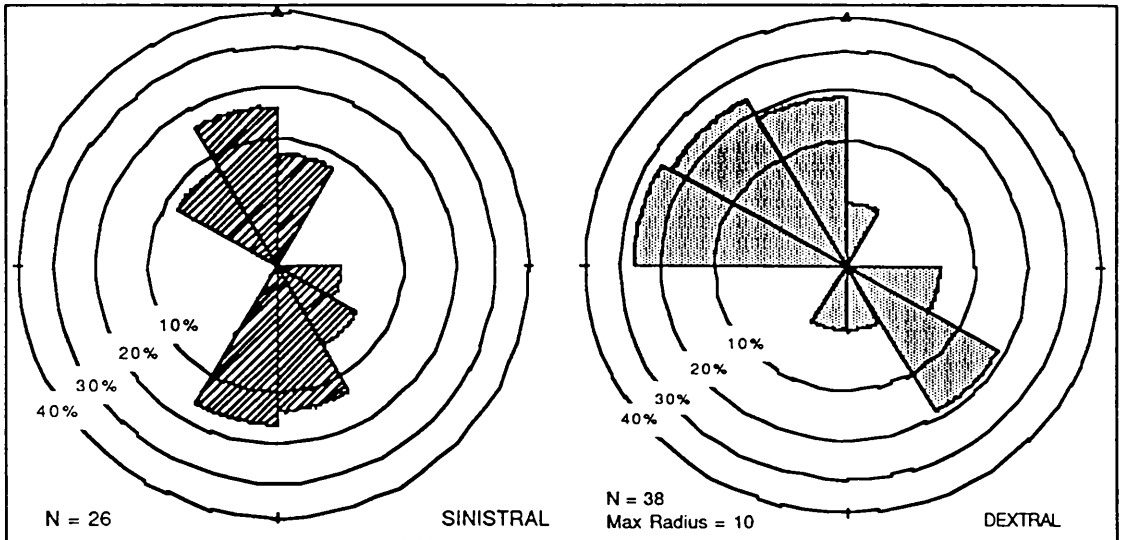


Fig. 4.4. Equal-area rose diagrams showing the orientations of faults (*i.e.* the azimuth of the fault plane, using the left hand rule) within LORS rocks of the Midland Valley. The scale is the same for both plots (see appendix 1 for details of the plotting of rose diagrams).

is consistent with arguments that I shall develop later in the chapter, the method used above is not scientifically rigorous, and great significance must not be placed in this line of evidence.

Problems are three-fold: firstly the upper age of all faults is uncertain - some faults are possibly due to Carboniferous (or later) deformation. Secondly, the *absolute* sense of displacement is unknown; the map view gives only an apparent horizontal offset. Finally, (and most importantly), the database used is not necessarily detailed enough to allow this type of analysis. This criticism, which cannot be applied to *mesofracture* analysis, requires further explanation:

BGS 1:50,000 maps show the survey's geologic *interpretation* (based on fieldwork), but it is not clear from the published maps exactly how much reliable observation lies behind each individual interpretation. Consequently the orientation of each fault, the amount of offset, the dip direction of the fault plane, (and even the existence of the fault at all) may all be inadequately constrained, and the room for radical re-interpretation might be large.

The main conclusion must be that the scientific objectivity of most published maps is not adequate. This would be rectified if workers published outcrop maps that show accurately the exact position and extent of all outcrops found during the survey. The users of such maps can then: (1) assess for themselves the amount of information used in a given interpretation, without having to unnecessarily duplicate field work, and (2) locate those critical outcrops that allow published hypotheses to be tested.

An outcrop map of Balmaha (Loch Lomond) is shown in Fig 5.12, together with an interpretation of macro-scale faulting. The Balmaha area contains a high level of exposure of Lower ORS sediments, allowing a correlation to be made between the results of macro- and meso-fault analyses.

#### 4.4 Brittle microtectonics - methodology

Brittle microtectonics is defined as the application of mesofracture analysis in solving tectonic problems (Hancock 1985). The rationale of the method is to analyse several sampling sites ("stations") across a region, allowing a representative picture of regional brittle deformation to be assimilated.

Mesofractures are fractures of outcrop scale. I use the term 'fracture' to include both faults and joints. 'Joints' are fractures that have no discernible displacement to the naked eye, but can show diagnostic features of displacement with a hand lens. Such joints, including "shear" and "hybrid" joints (Hancock 1985) are extremely useful in the mesofracture analysis of stations in which brittle strain is low.

The *geometry* and *kinematics* of mesofractures at each individual station are studied in detail, in order to describe the total state of brittle strain within that station. These results can then be interpreted collectively, to give a *dynamic* analysis of the regional stress regime that gave rise to the deformation. Many of the details of brittle microtectonics are described in a review article by Hancock (1985). The most important aspects of the methodology are emphasised in the following sections.

##### 4.4.1 Choice of sampling sites

Stations were carefully chosen to provide the best constraints on the *timing* of deformation. One of the greatest difficulties of mesofracture analysis lies in determining the age of individual fractures. Consequently, wherever possible two stations were sited in adjacent areas of Lower and Upper ORS, in order to try to quantify any difference in the amount of brittle strain.

Where possible, stations were chosen in areas of good exposure. This ensured that an adequate number of fractures could be analysed, thus enabling the *magnitude* of brittle strain to be estimated. Good exposure in the area surrounding the station also allows any adjacent macrofaults to be

recognised and avoided more easily, as these often cause second order fracturing, which complicates the dynamic interpretation (see below).

In order to make valid interpretations on a regional scale, stations should be widely separated, in order to cover as large an area as possible. As with ductile strains, brittle strains can be heterogeneous on a very large scale.

#### 4.4.2 Analysis of mesofractures

Dynamic interpretation is most reliable when based on as much kinematic data as possible. Consequently, as well as recording the geometry (strike and dip) of individual fractures, the movement vector along the fracture plane (*i.e.* azimuth, plunge, slip sense and amount of movement) was recorded whenever possible, using an accurate hand-made compass/clinometer and a ruler.

Movement vectors obtained by matching both halves of offset conglomerate clasts. More commonly, slickenline orientations were used to ascertain the azimuth and plunge components of fault movement. Shear sense indicators used include offset lithological markers, asymmetric vein "pull-aparts", and occasionally, second order fault plane fractures (Fig. 4.5) as described by Petit (1987).

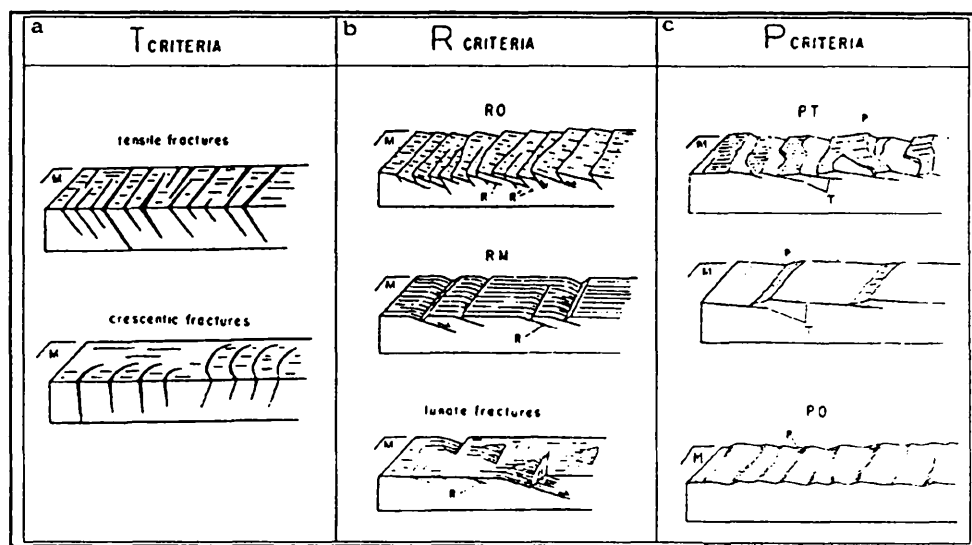


Fig. 4.5. Second order fault plane fractures, used in mesofracture analysis to indicate shear sense (after Petit 1987). M shows the direction of movement of the blocks shown. R, R', P, and T are kinematically equivalent to the fractures shown in Fig. 4.19 (T are extension fractures).

Although joints are defined as fractures with no macroscopic movement they can nevertheless be kinematically diagnostic on a microscopic scale (Hancock 1985). Joints were examined with a hand lens

for evidence of shear, then measured as faults above. Where necessary, fractures were cleaned with a tooth brush before examination.

## 4.5 Geometric and Kinematic Analysis

In total the geometry and kinematics of 2,600 brittle fractures from 40 stations (Fig. 4.8) were recorded. The orientations of the fractures and slip vectors, together with their shear sense, are plotted stereographically for each station, using computer software (appendix 1). The stereonetts are presented below, and are interpreted dynamically in section 4.6.

### 4.5.1 Magnitude of brittle strain

A precise measure of the total amount of brittle strain is only possible when a station displays total three-dimensional exposure, and all fractures can be fully described kinematically. Though these conditions were never fully met in Scotland, it is nevertheless possible to give a subjective estimate of the amount of brittle strain within each station, based on typical fracture spacing, and typical offsets.

In general the magnitude of strain is dominated by the host lithology. This often masks the overall observation that those stations closest to the HBF show slightly higher brittle strains. Brittle deformation in crystalline metasediments (*i.e.* Dalradian and Moine lithologies) and coarse conglomerates (common L. ORS lithology) tends to result in widely spaced macro-faults with large offsets. Consequently the strain magnitude within individual stations is probably not truly representative of regional strain. In contrast, thinly bedded L. ORS arenites and argillites are affected by closely

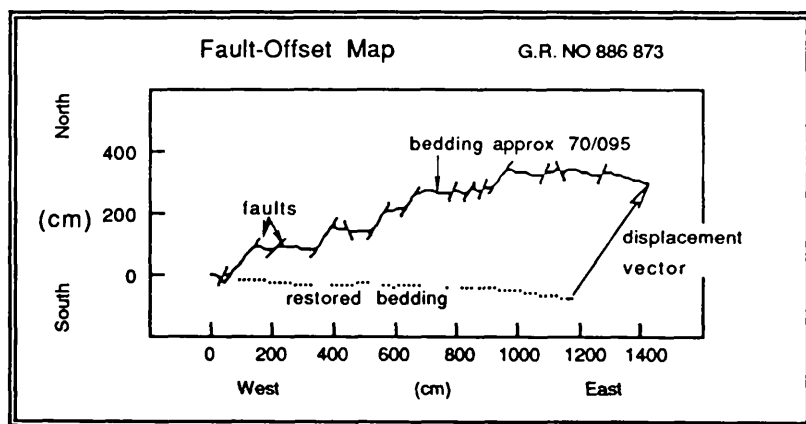


Fig. 4.6. Fault offset map from the L.ORS of Old Kirk Shore, Stonehaven. The bed shown is a coarse, resistant arenite. Bedding is restored by removing the effects of faulting; this shows that bedding experienced 27% extension (assuming biaxial strain and vertical  $\sigma_2$ ), and approximately 20° of rotation.

spaced mesofaults with offsets of centimetres or decimetres.

Excellent coastal exposure at Stonehaven allows brittle strain to be estimated with reasonable precision (Fig. 4.6).

Note that the balancing reconstruction used in Fig. 4.7 calculates strain in terms of changes in bed-length and overall rotation. Back-rotation of individual faults is not measured, even though fault block rotations are likely to have occurred in rocks adjacent to the HBF. This is discussed further in section 4.6 below entitled "Dynamic Analysis".

#### 4.5.2 Rock rheology

The rheological behaviour of rock subjected to stress depends upon several factors including:

- 1) lithology
- 2) prevalent temperature and pressure conditions
- 3) strain rate
- 4) fluid pressure

Low strain rates and elevated temperatures promote ductile rheological response. All lithologies in central Scotland displayed entirely brittle behaviour - the fractures are very sharp, discrete cohesion-less surfaces, and en-echelon vein arrays and "drag" folding are almost always absent (these structures are normally associated with semi-brittle deformation, *e.g.* Ramsay & Huber 1987, p596), suggesting that strain rate was high and that deformation occurred in the upper-most crust.

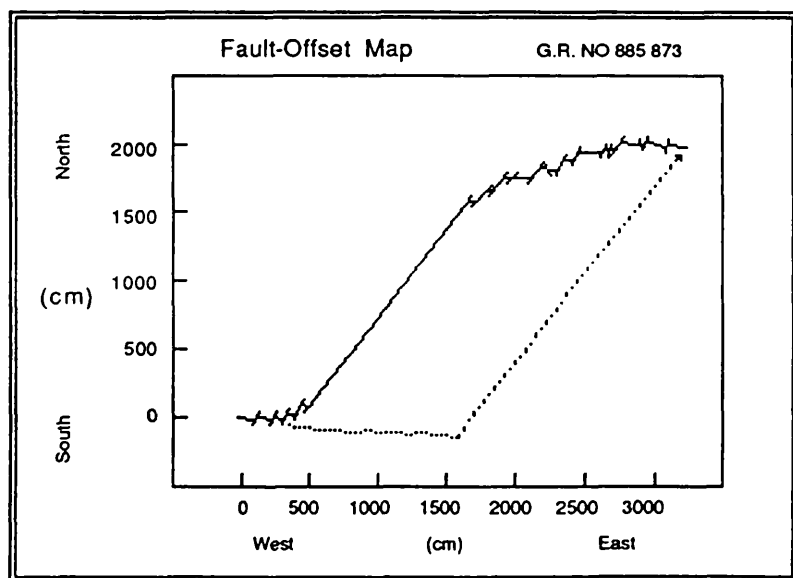


Fig. 4.7. Fault offset map from Old Kirk Shore, Stonehaven, showing overall sigmoidal shape of bedding, produced by multiple brittle faulting. For the section shown, bedding experienced 34% extension (assuming biaxial strain and vertical  $\sigma_2$ ), and approximately 40° of rotation, but note that the deformation at this scale is heterogeneous.

The brittle fractures can represent *heterogenous* deformation on various scales. On an outcrop scale the displacement on fractures can vary systematically, to give beds an overall "sigmoidal" outcrop pattern (Fig. 4.7). Here the fault spacing decreases and the offset increases into a large macrofault with a 19m sinistral displacement.

#### 4.5.3 Geometric and Kinematic Data

The localities of the mesofracture stations used are shown in Fig. 4.8.

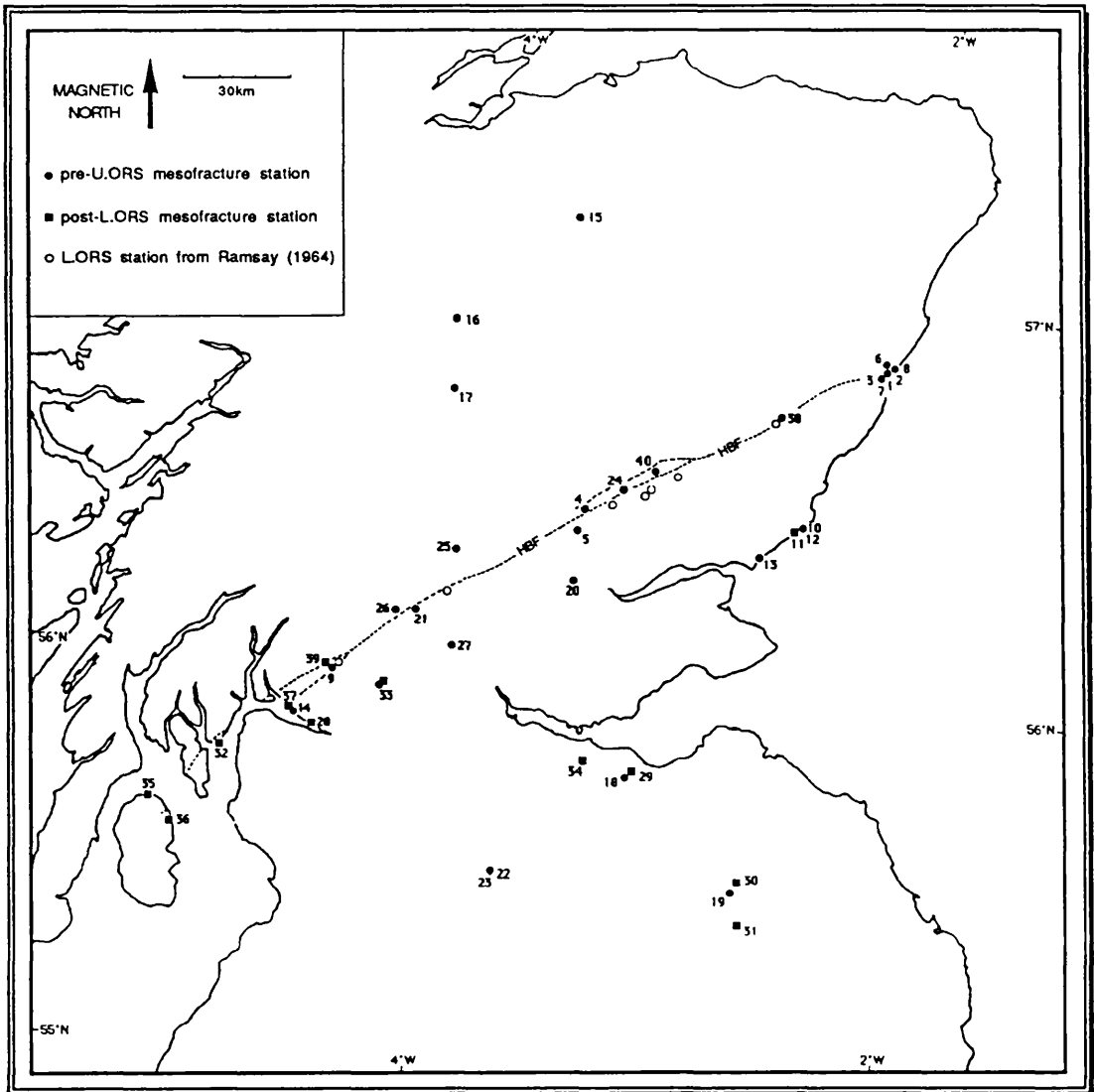
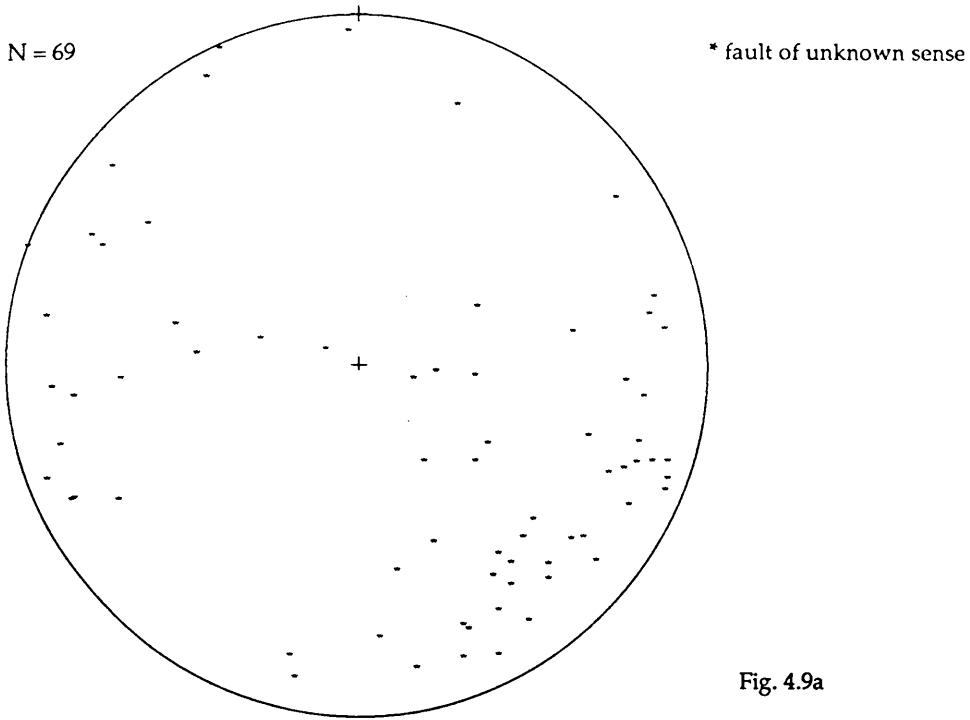


Fig. 4.8. Map of central Scotland, showing the localities of the mesofracture sampling stations.

The geometric and kinematic data for each station are presented on lower hemisphere equal-area stereonet (Figs. 4.9). The nets show poles to

planes for different types of mesofracture (see Appendix 1 for details of the method used). The data are plotted with respect to magnetic north.

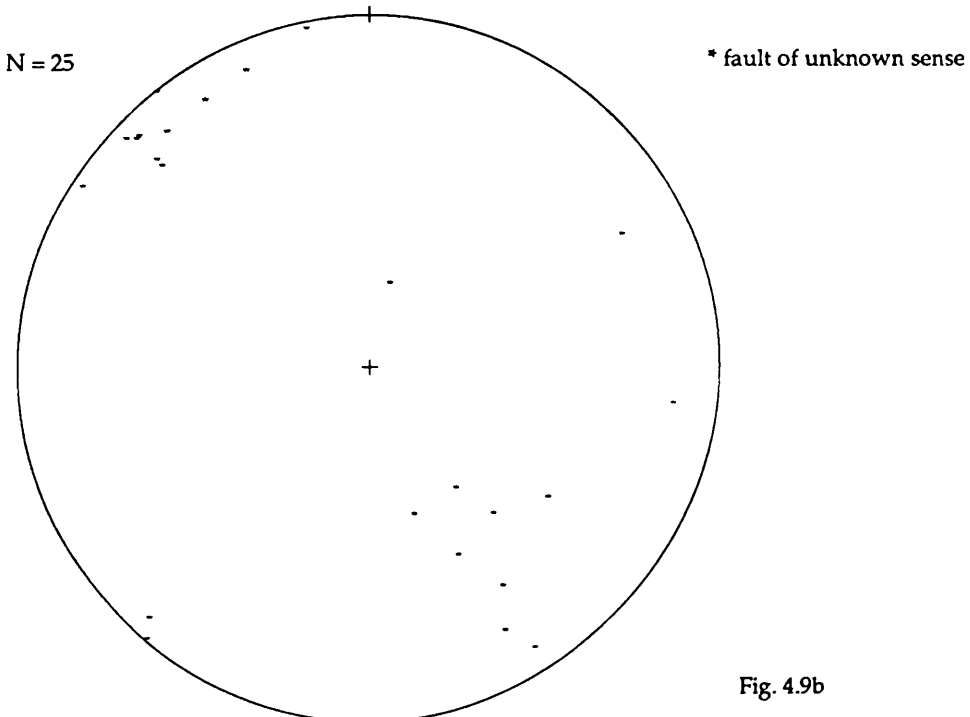


Station no.: S1

Grid Reference: NO 886873

Locality: Old Kirk Shore, Stonehaven

Lithology: weathered ORS spilites



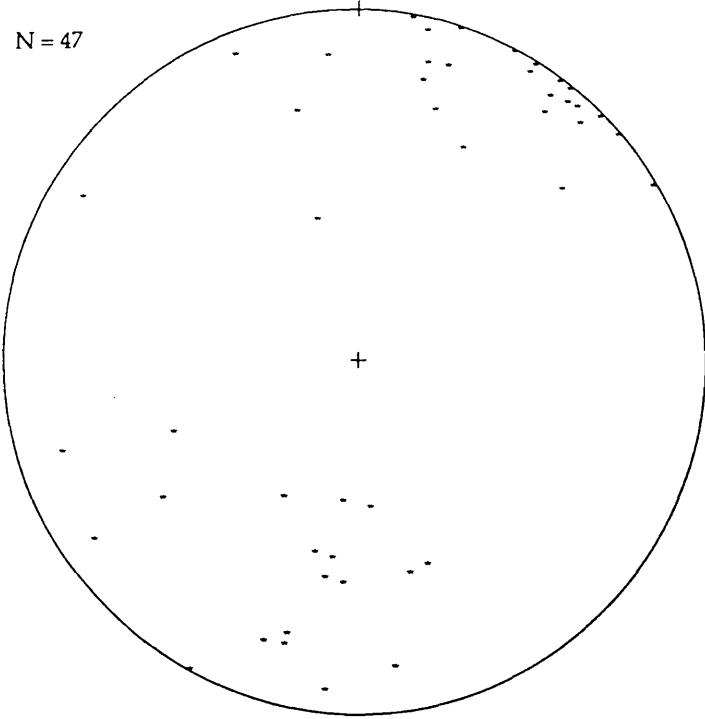
Station no.: S2

Grid Reference: NO 887873

Locality: Slug Head, Stonehaven

Lithology: ORS spilites

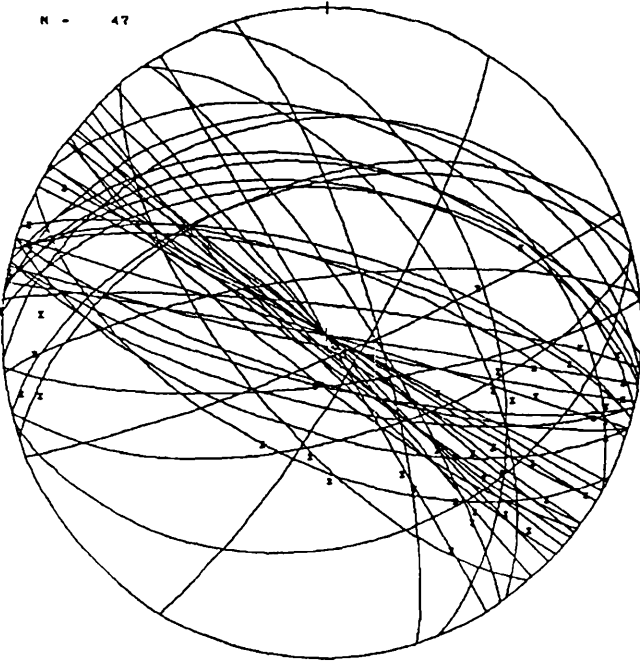
N = 47



\* fault of unknown sense

Fig. 4.9c

N = 47



plot of lineations and great circle  
fault traces

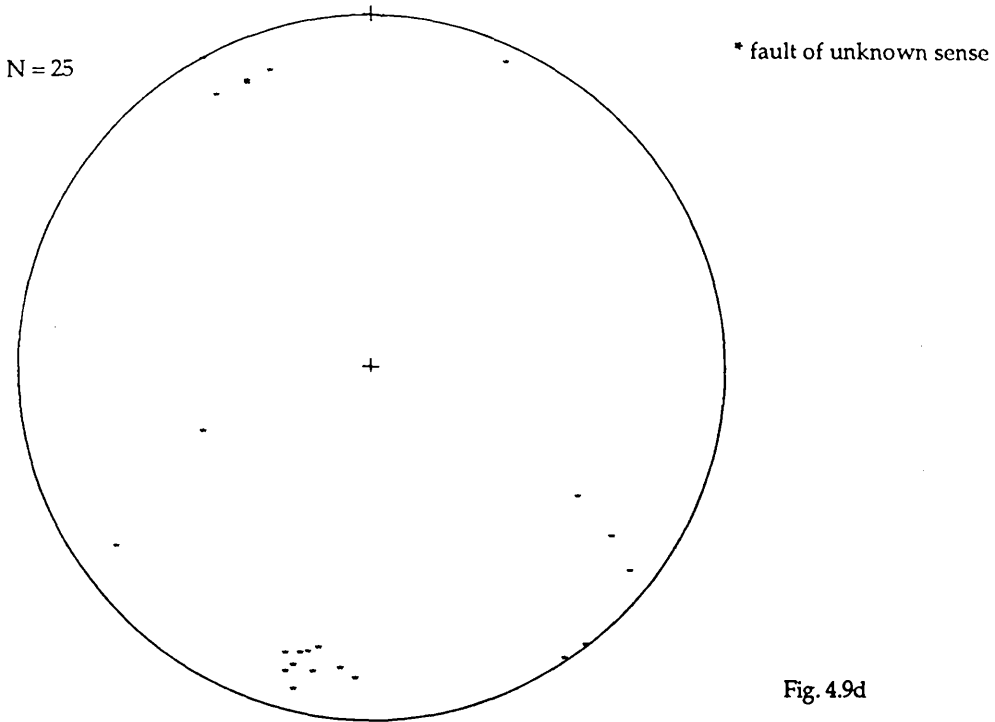
Fig. 4.9c (continued)

Station no.: S4

Grid Reference: NO 067406

Locality: Stenton, Tayside

Lithology: L.ORS lavas

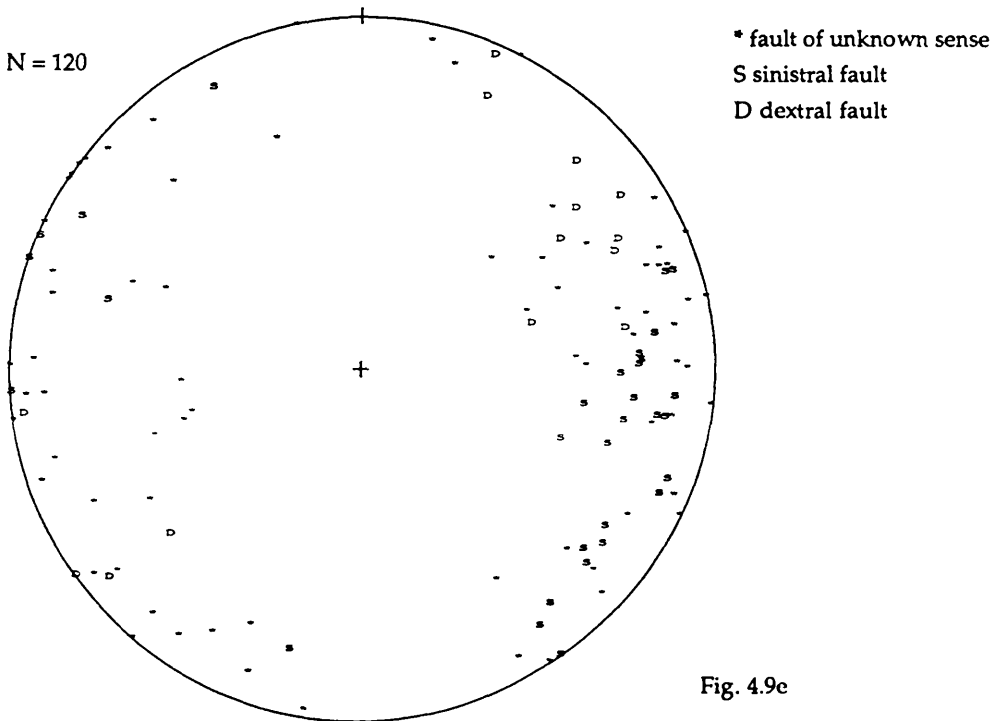


Station no.: S5

Grid Reference: NO 041378

Locality: Meikle Obney, Tayside

Lithology: L.ORS conglomerates



Station no.: S6

Grid Reference: NO 887875

Locality: Craigeven Bay, Stonehaven

Lithology: Dalradian schists

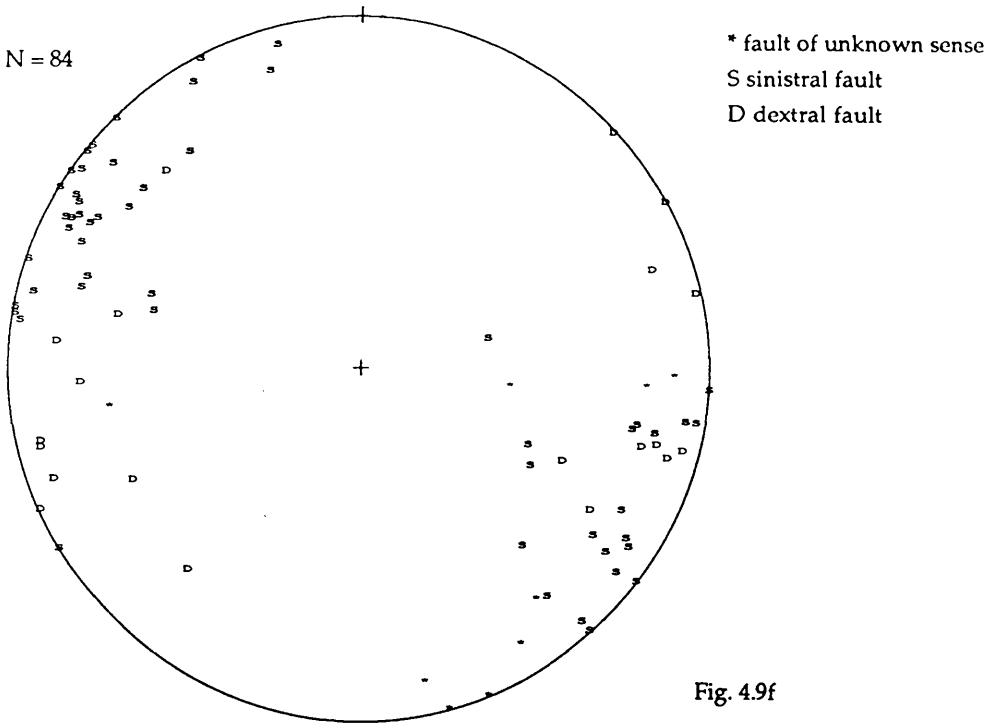


Fig. 4.9f

Station no.: S3/7

Grid Reference: NO 886872

Locality: Old Kirk Shore, Stonehaven

Lithology: L.ORS sandstones

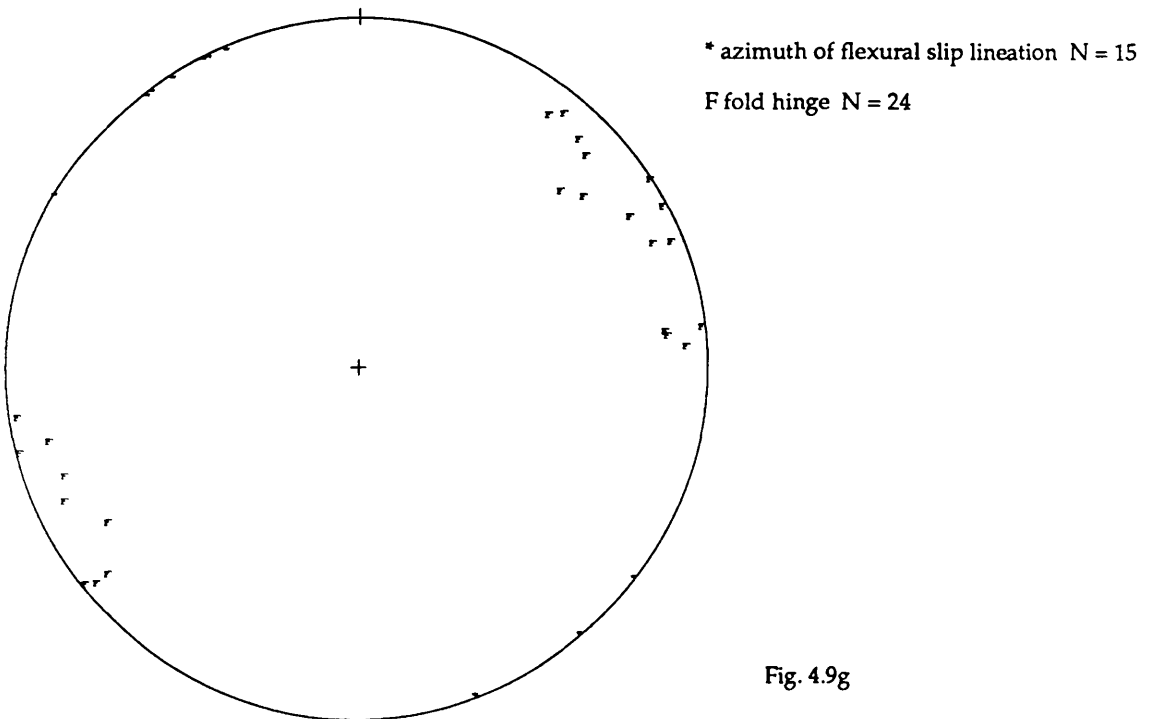


Fig. 4.9g

Station no.: S8

Grid Reference: NO 890875

Locality: Craigeven Bay, Stonehaven

Lithology: HBC mafic lavas

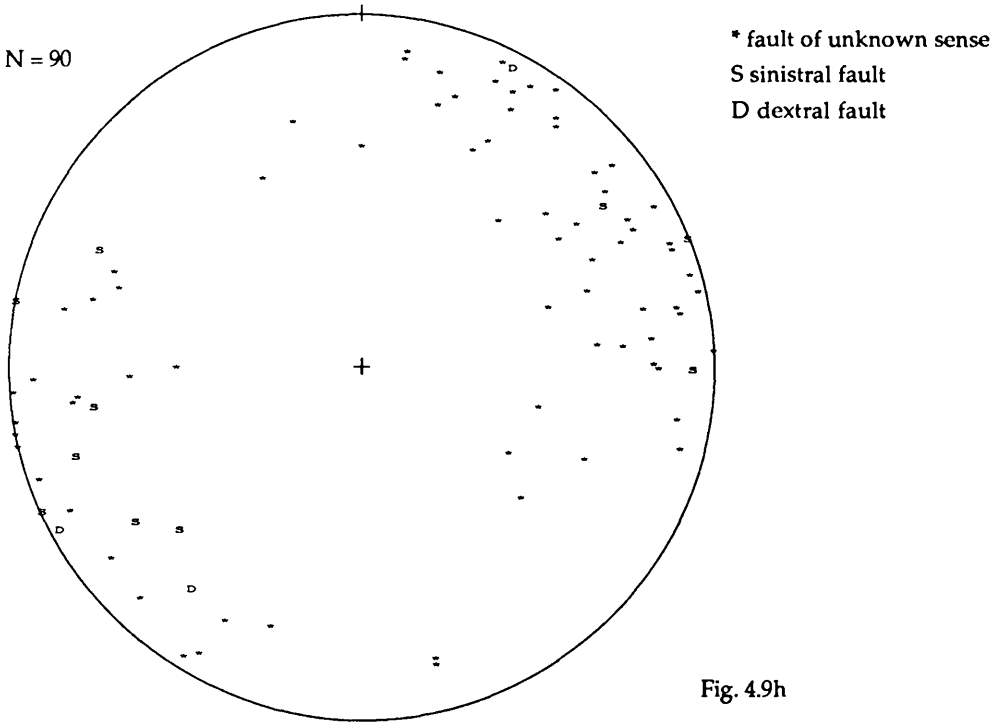
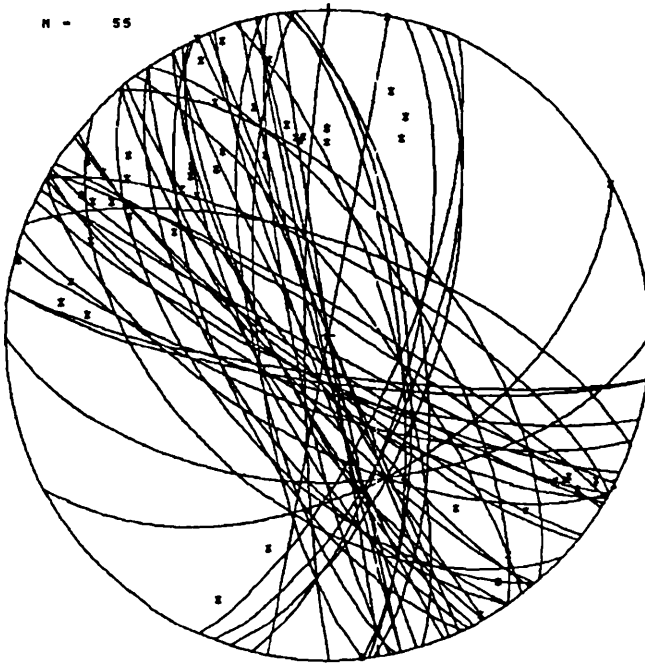


Fig. 4.9h



plot of lineations and great circle  
fault traces

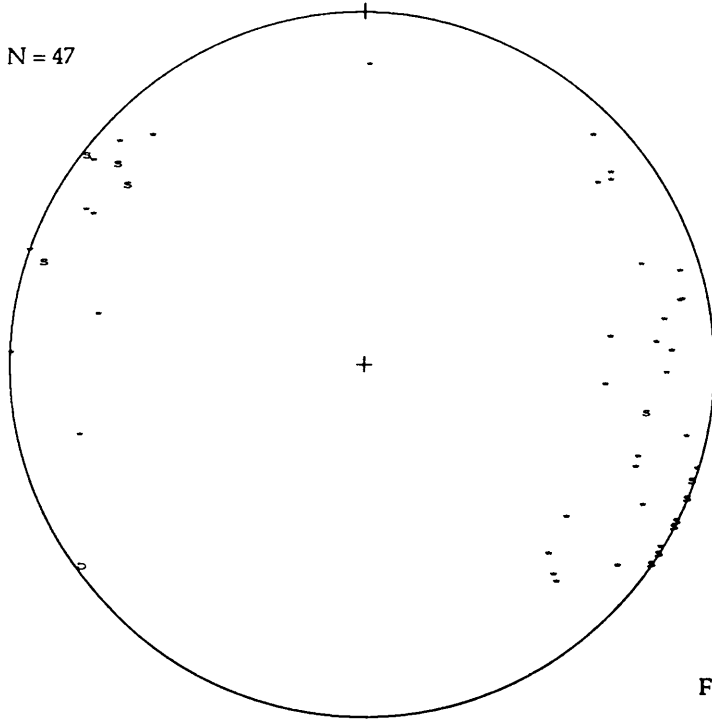
Fig. 4.9h (continued)

Station no.: S9

Locality: Old Pier, Balmaha

Grid Reference: NS 515908

Lithology: L.ORS conglomerates

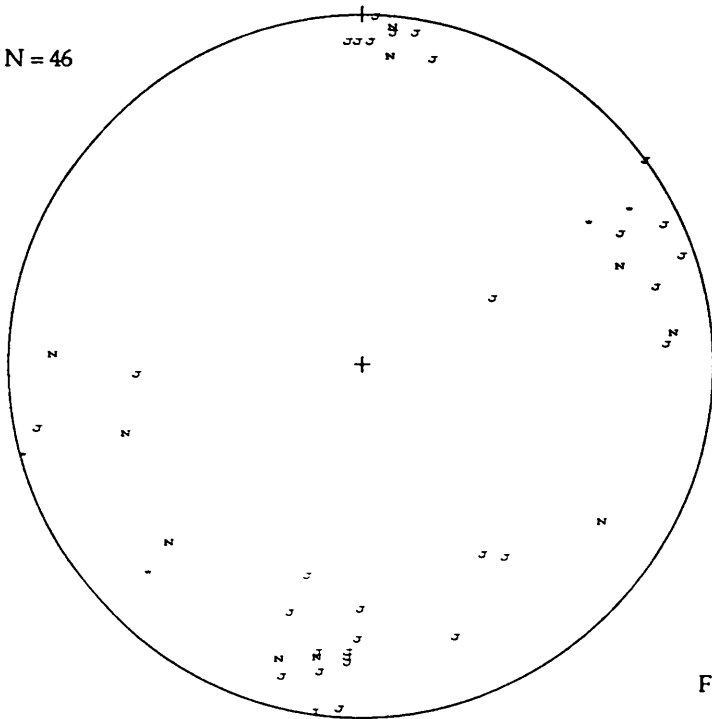


\* fault of unknown sense  
 S sinistral fault  
 D dextral fault

Fig. 4.9i

Station no.: S10/12  
 Locality: Needle E'e, Arbroath

Grid Reference: NO 665414  
 Lithology: L.ORS sandstones/conglomerates



\* fault of unknown sense  
 N normal fault  
 J joint

Fig. 4.9j

Station no.: S11  
 Locality: Whiting Ness, Arbroath

Grid Reference: NO 660411  
 Lithology: U.ORS sandstones/conglomerates

Station no.: S13  
 Locality: Carnoustie shore  
 Comments: strong joint set suggests north-south compression.

Grid Reference: NO 572344  
 Lithology: L.ORS sandstones

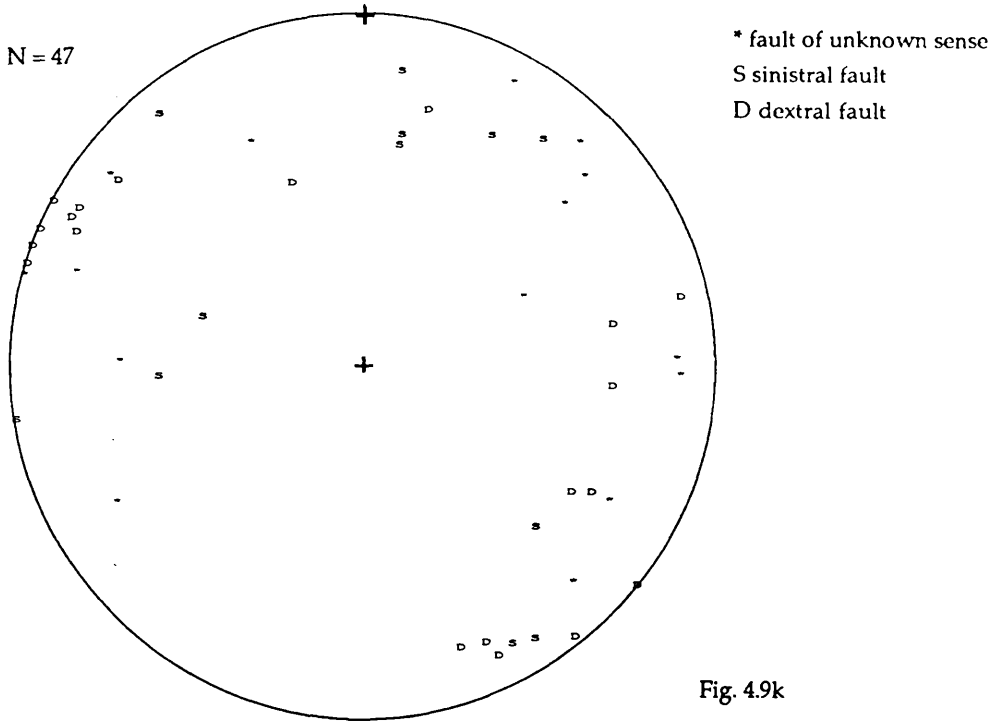


Fig. 4.9k

Station no.: S14

Grid Reference: NS 313785

Locality: Ardmore Point

Lithology: L.ORS sandstones/conglomerates

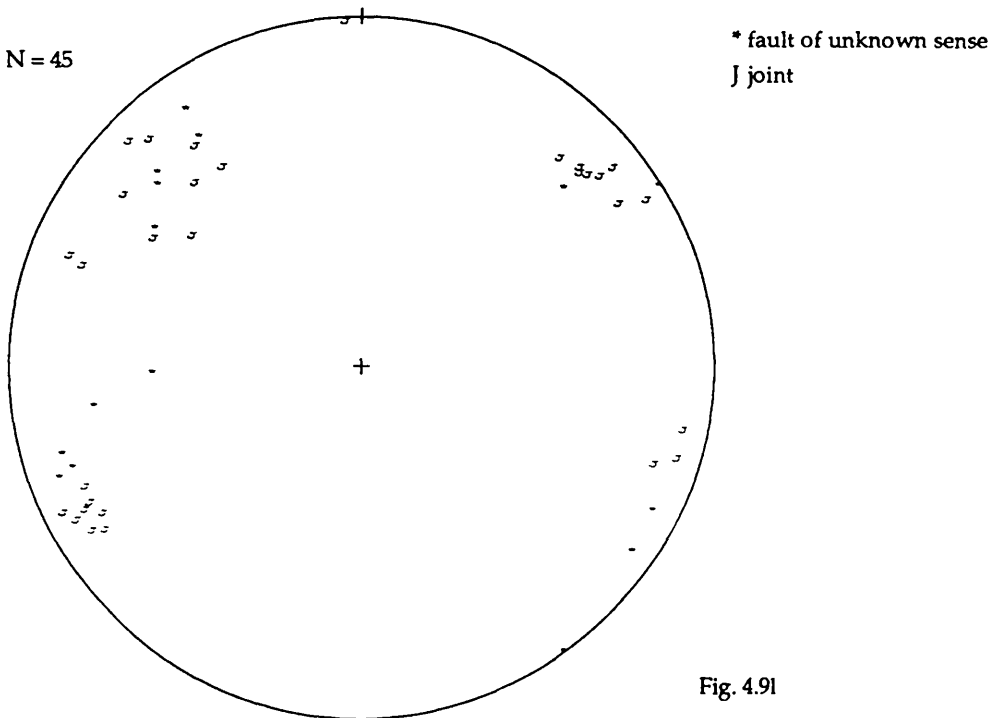


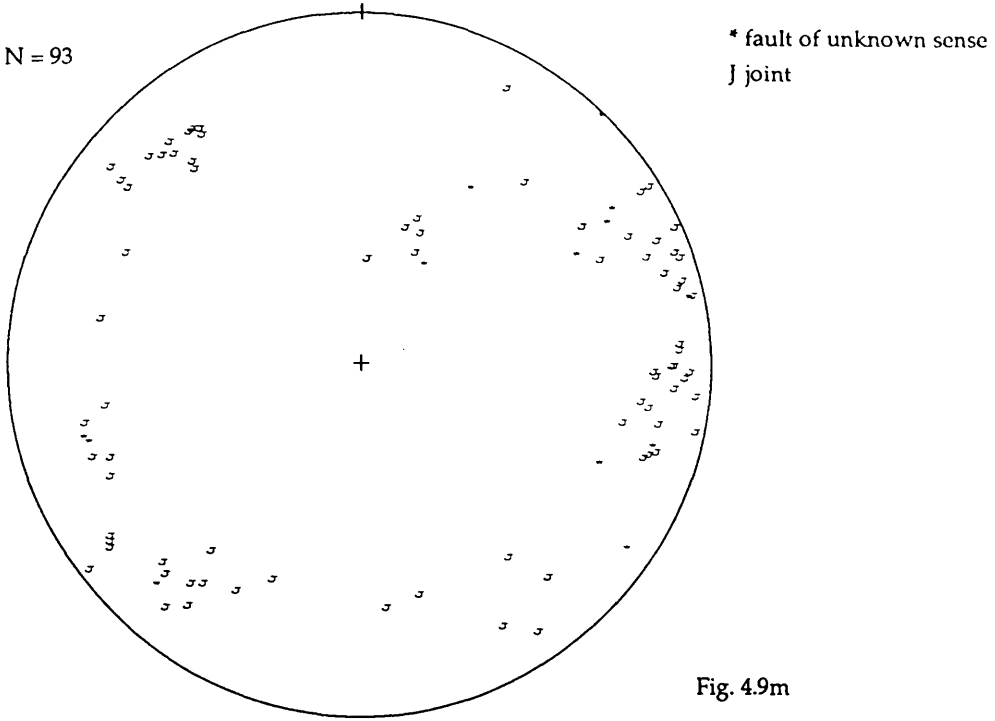
Fig. 4.9l

Station no.: S15

Grid Reference: NH 995229

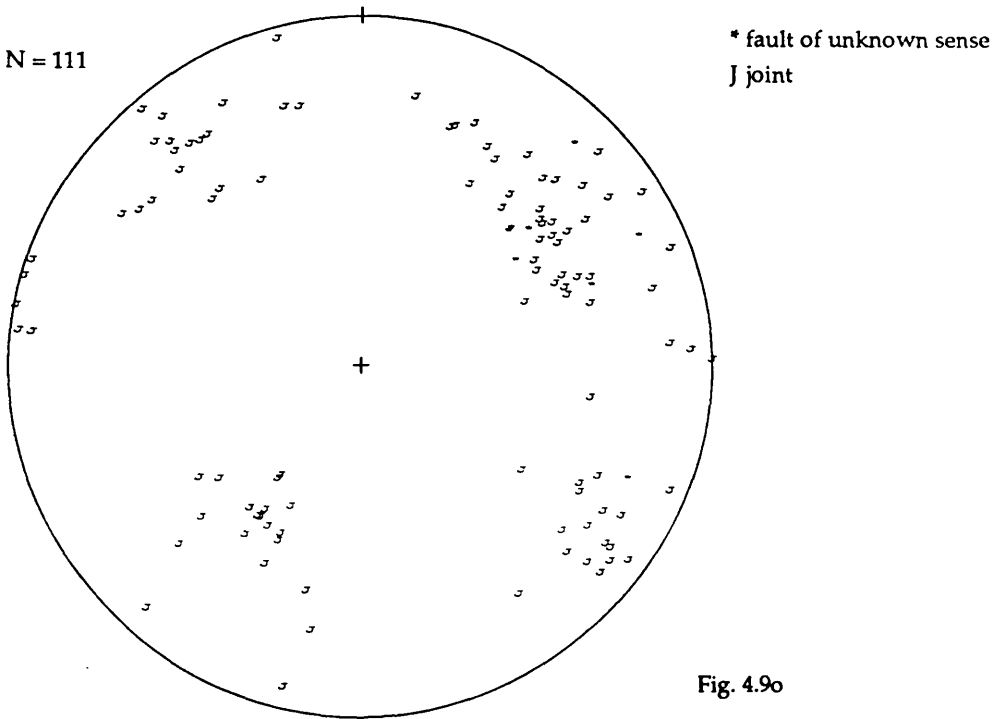
Locality: Grantown-on-Spey

Lithology: Moine schists



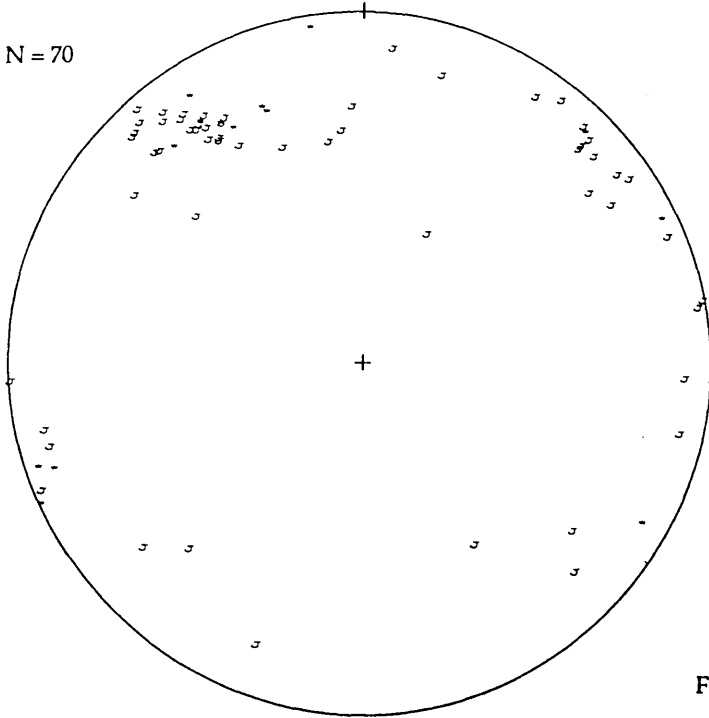
Station no.: S16  
Locality: Glen Truin

Grid Reference: NN 678908  
Lithology: Moine schists



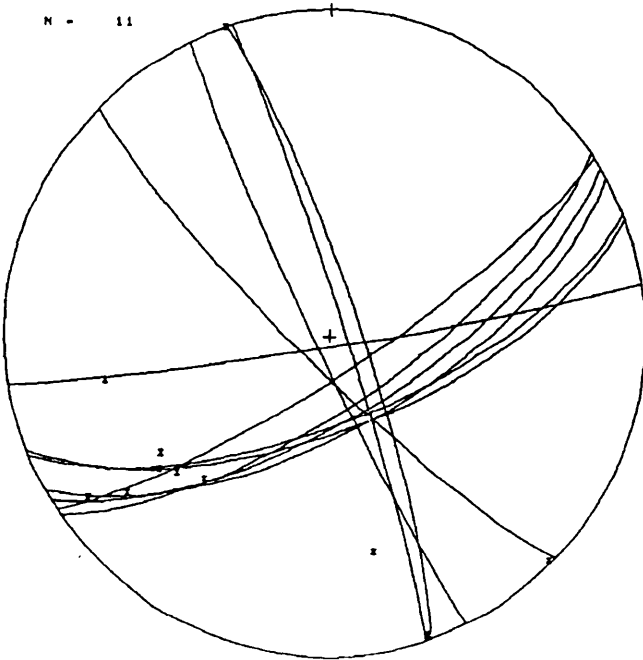
Station no.: S18  
Locality: Blackford quarry, Edinburgh

Grid Reference: NT 260703  
Lithology: L.ORS lavas



\* fault of unknown sense  
J joint

Fig. 4.9n



plot of lineations and great circle  
fault traces

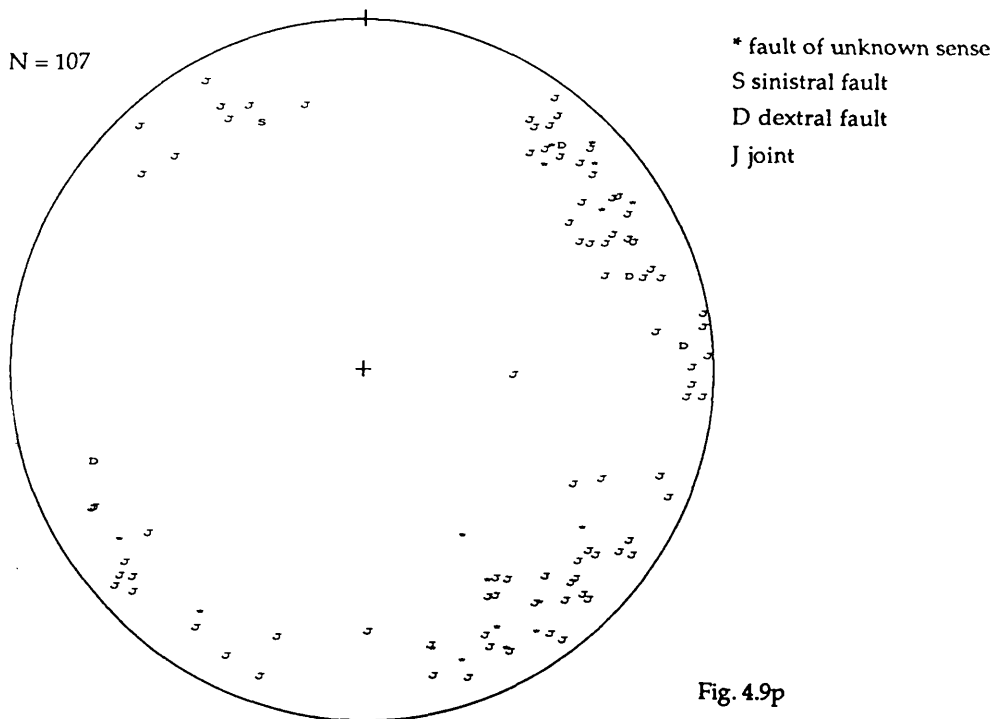
Fig. 4.9n (continued)

Station no.: S17

Grid Reference: NN 672719

Locality: Drumochter Summit

Lithology: Moine schists

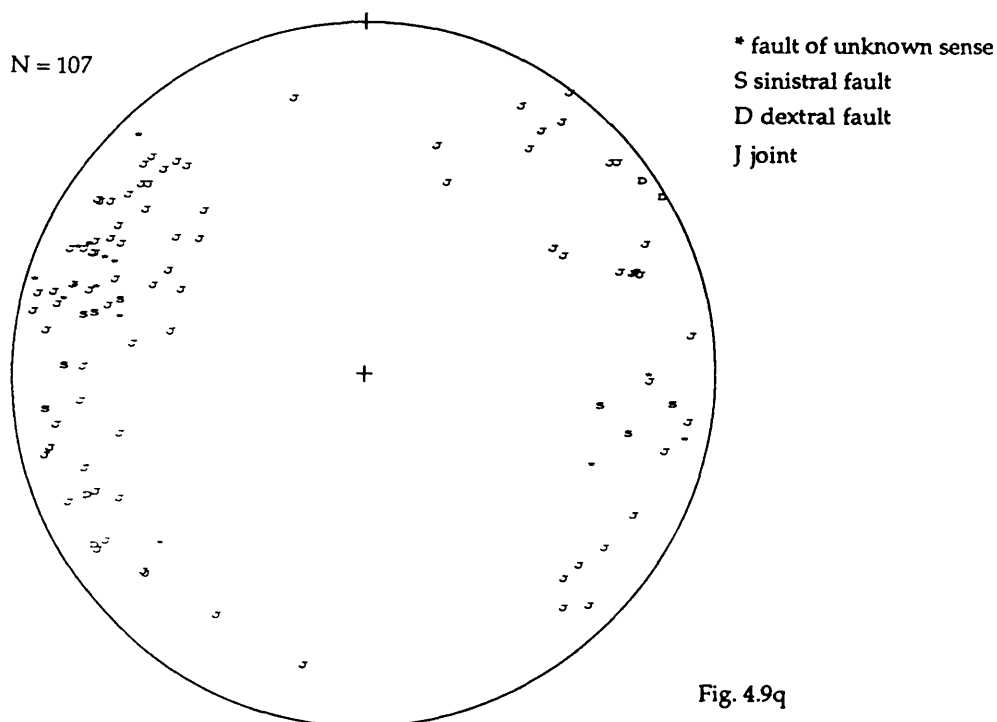


Station no.: S19

Grid Reference: NT 565402

Locality: Earlston

Lithology: L.ORS conglomerates



Station no.: S20

Grid Reference: NO 012182

Locality: Chapelbank, Strathearn

Lithology: L.ORS sandstone

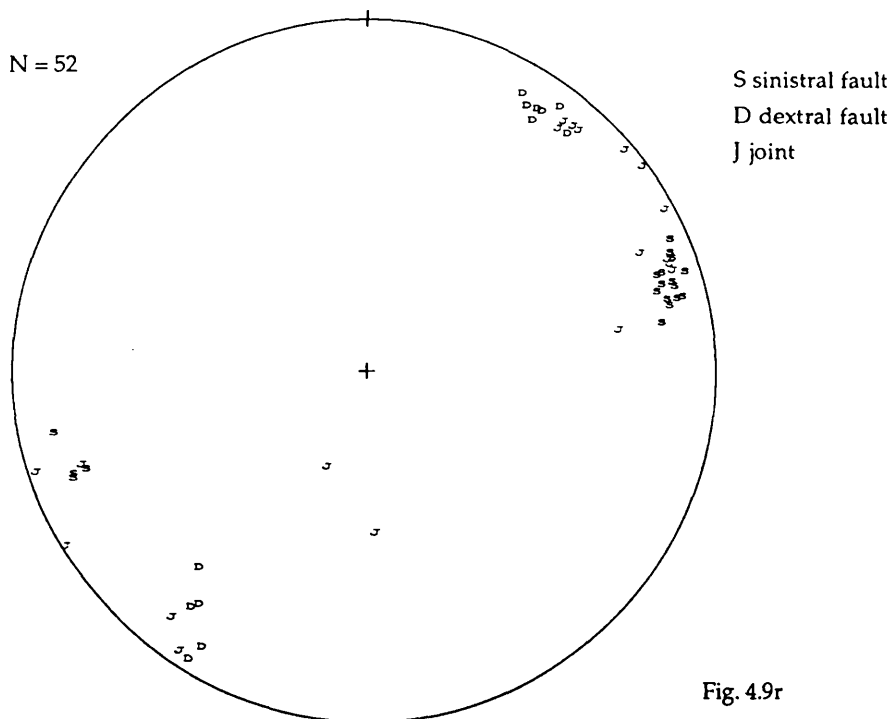


Fig. 4.9r

Station no.: S21

Grid Reference: NN 645084

Locality: Bracklinn Falls, Callander

Lithology: L.ORS pebbly sandstone/siltstone

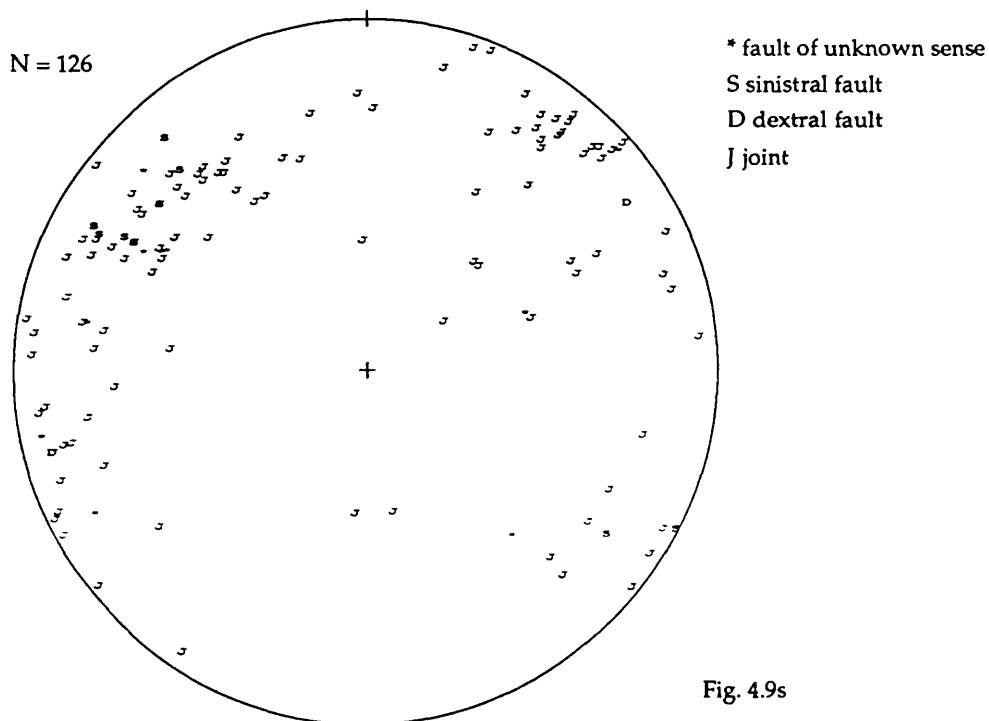


Fig. 4.9s

Station no.: S22/23

Grid Reference: NS 920386

Locality: Westgate, Carmichael

Lithology: L.ORS lavas

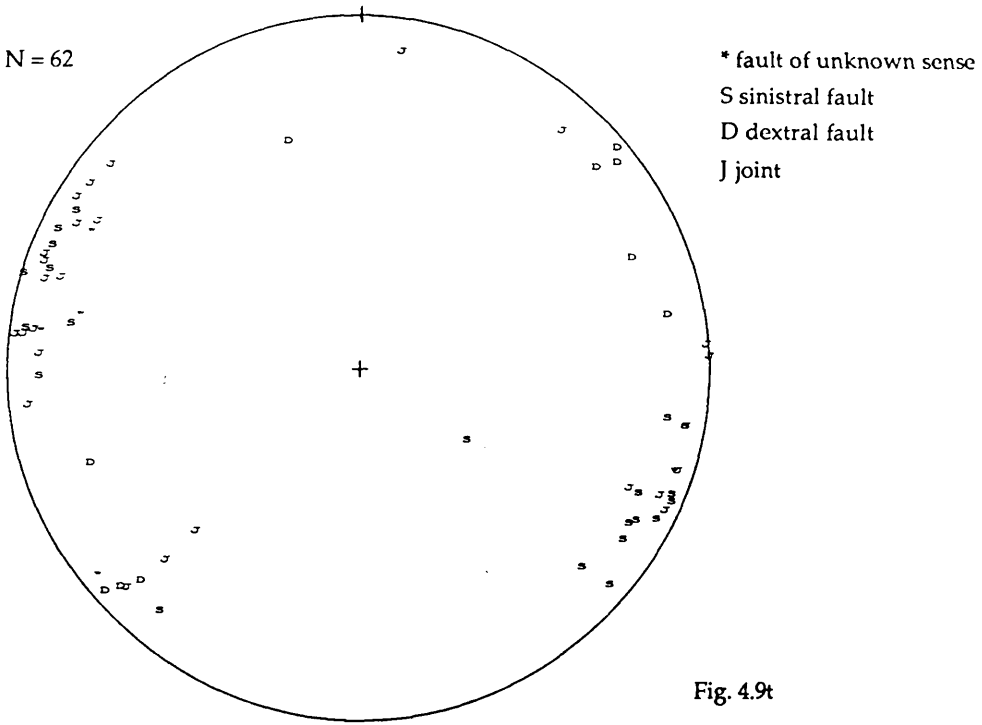


Fig. 4.9t

Station no.: S24

Grid Reference: NO 172480

Locality: River Ericht, Blairgowrie

Lithology: L.ORS conglomerates

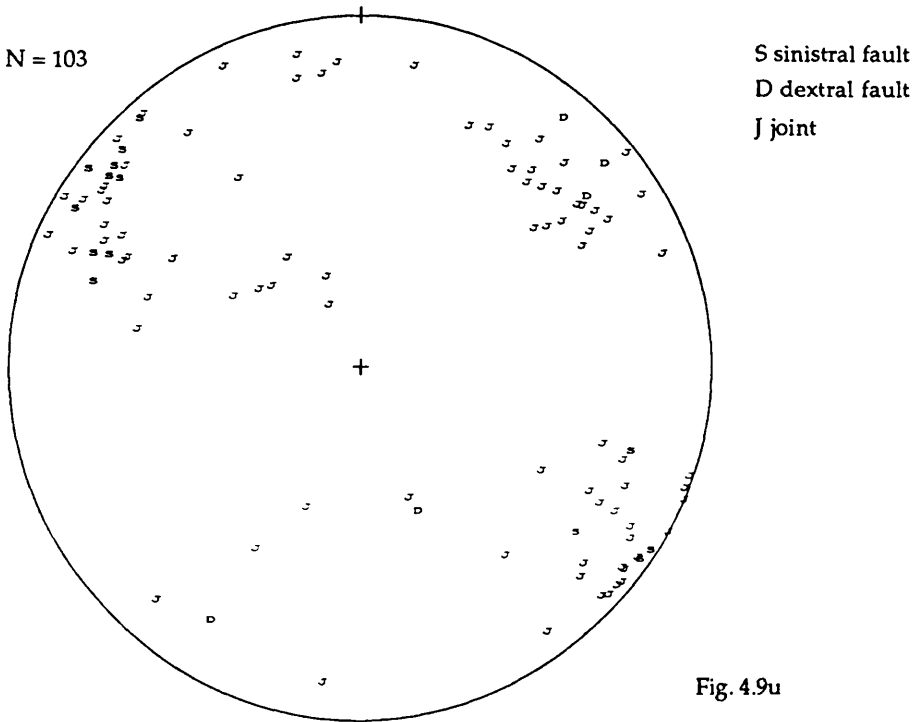


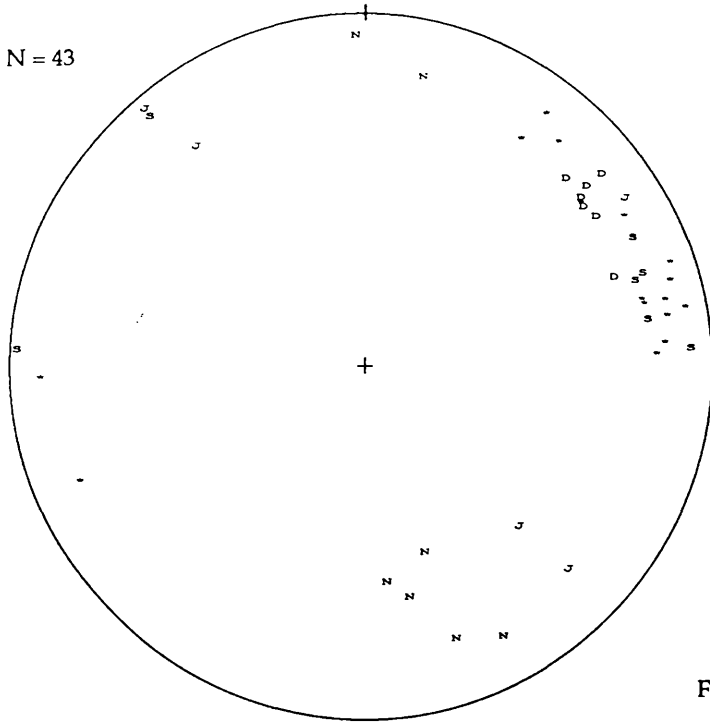
Fig. 4.9u

Station no.: S25

Grid Reference: NN 728290

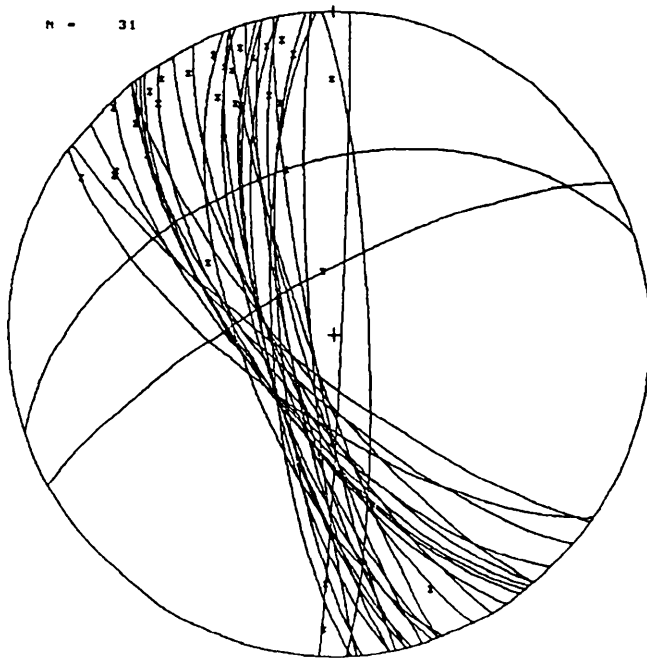
Locality: Loch Lednock, Comrie

Lithology: Comrie diorite



\* fault of unknown sense  
 S sinistral fault  
 D dextral fault  
 N normal fault  
 J joint

Fig. 4.9w



plot of lineations and great circle  
 fault traces

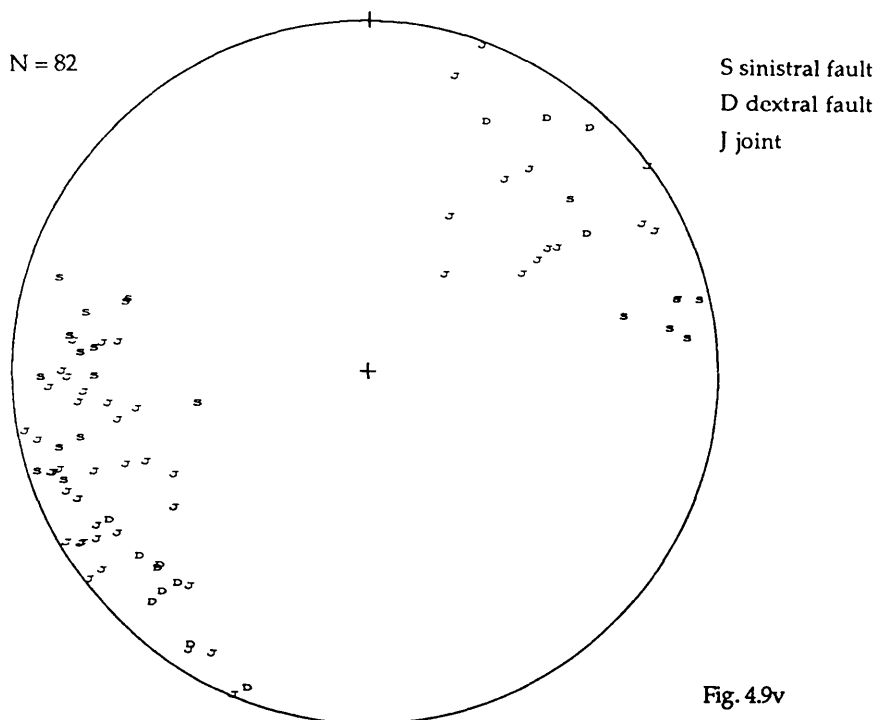
Fig. 4.9w (continued)

Station no.: S27

Locality: Doune

Grid Reference: NS 717993

Lithology: L.ORS sandstone



Station no.: S26

Grid Reference: NN 592088

Locality: Falls of Leny, Callender

Lithology: Dalradian pelites

Station no.: S28

Grid Reference: NS 383755

Locality: Brucehill Cliffs, Dumbarton

Lithology: U.ORS sandstones

Comments: Relatively unfractured compared with nearest L.ORS.

Station no.: S29

Grid Reference: NT 290710

Locality: Craigmillar Quarry, Edinburgh

Lithology: U.ORS sandstones

Comments: Relatively unfractured compared with nearest L.ORS.

Station no.: S30

Grid Reference: NT 582428

Locality: Legerwood, near Earlston

Lithology: U.ORS conglomerates

Comments: Relatively unfractured compared with nearest L.ORS.

Station no.: S31

Grid Reference: NT 588320

Locality: River Tweed, Dryburgh

Lithology: U.ORS conglomerates

Comments: Style of fracturing is markedly different to nearest L.ORS (two orthogonal sets of vertical joints).

Station no.: S32

Grid Reference: NS 266808

Locality: Rosencath

Lithology: U.ORS conglomerates

Comments: Relatively unfractured compared with nearest L.ORS.



The data presented here can be supplemented by data from a study on fractured pebbles by Ramsay (1962,1964). Ramsay measured a total of 4,000 fractures from 1,000 pebbles at nine localities in the L.ORS adjacent to the HBFZ. The study used fracture geometry and kinematics to infer movement on the HBF; in this respect the study was a type of mesofracture analysis, though the results are given only in terms of fracture azimuth (*i.e.* the results are two-dimensional only). Nevertheless, the work gives a full description of the type of fracturing commonly seen in the L.ORS near the HBFZ, and the dynamic results of the study are entirely consistent with the conclusions from the dynamic analysis that I shall present in the next section. Furthermore, the model that I present in section 4.8 to explain the dynamic analysis, helps to account for the 'anomalous' vertical  $\sigma_2$  and horizontal  $\sigma_3$  that originally puzzled Ramsay.

The validity of using Ramsay's pebble data to support the arguments developed in this thesis has been tested by Dr. Geoff Tanner, who has studied the fracturing of L.ORS clasts at the Old Pier, Balmaha, Loch Lomond (G.R. NS 515908). The data, presented below (Fig. 4.9x), shows close agreement with both Ramsay's study (Ramsay 1964, p.236-239), and the mesofracture results shown here in Figs. 4.9h and 4.23d.

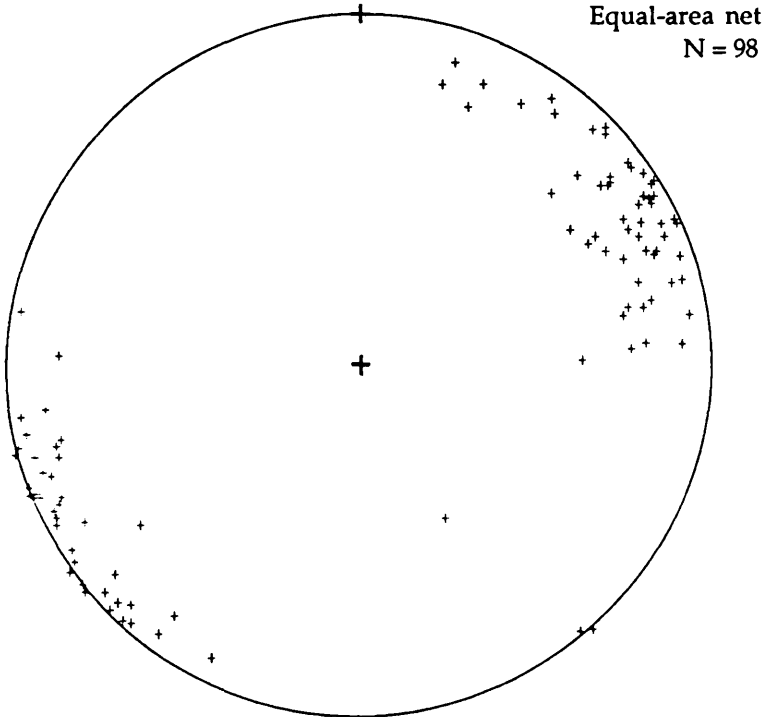


Fig. 4.9x. Poles to fracture planes from faulted conglomerate clasts in the L.ORS at Balmaha (G.R. NS 515908).

## 4.6 Dynamic Analysis

The stress conditions at the time of fracture initiation can be inferred from a dynamic interpretation of the geometric and kinematic results of mesofracture analysis. Interpretation relies on an understanding of the relationship between stress and brittle failure.

### 4.6.1 Theory of interpretation

Conjugate fractures have long been recognised in rocks, and have been directly compared with fractures resulting from experimental compression of isotropic materials (*e.g.* Daubree 1879). Such field and experimental conjugate shears are also predicted theoretically (*e.g.* Anderson 1942). The relationship between principal stresses and conjugate fractures is well understood;  $\sigma_2$  lies along the intersection of the conjugate fractures, and the acute angle between the pair of fractures represents the  $\sigma_1/\sigma_2$  plane. Conjugate fractures result from both pure shear and simple shear (*e.g.* Anderson 1942, and Cloos 1928, respectively).

Conjugate fractures represent plane strain (the effect of  $\sigma_2$  is neutral). Plane strain should be considered as a special case within a general spectrum of deformation from extreme flattening through to extreme constriction. A slip model, in which brittle deformation is non-plane strain, has been developed by Reches (1978,1983) to explain multiple faults (three or four coeval sets of faults in orthorhombic symmetry) that have been observed experimentally (Oertel 1965, Reches & Dietrich 1983) and in the field (Aydin & Reches 1982, Krantz 1988).

Brittle fractures developed under plane and non-plane strain conditions are shown schematically in Fig. 4.10.

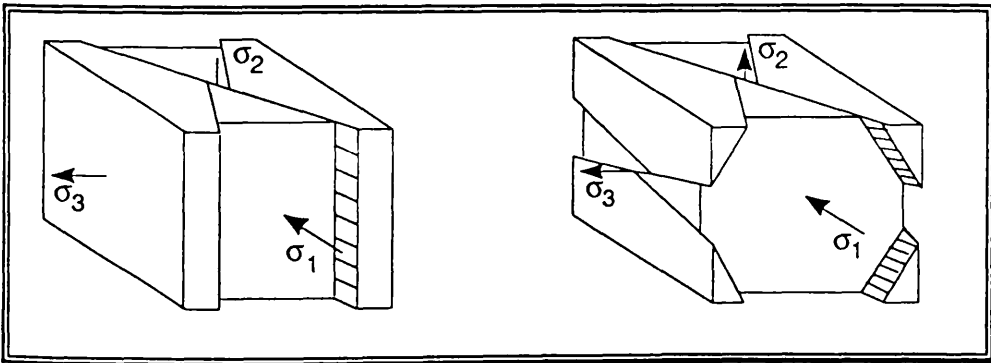


Fig. 4.10. Biaxial and triaxial (oblate) brittle strains.

The slip model of Reches uses tensor analysis to derive the orientations of preferred slip surfaces and slip vectors for given stress ratios. There are

important assumptions inherent in the model, and these are outlined below:

- 1) the model derives the yielding stresses required to initiate slip along sets of pre-existing surfaces of discontinuity, in rock that contains a random array of such surfaces. This approach is therefore different to the *yield criteria* model of Anderson (1942). Though this suggests that the slip model cannot be directly applied with absolute rigour to unfaulted rock, experimental results have validated the practical application of the model (Reches & Dietrich 1983).
- 2) resistance to slip on each surface obeys Coulomb's friction law (Jaeger & Cook 1969), *i.e.* slip is cohesive and frictional.
- 3) strain is constant volume and irrotational.
- 4) it is assumed that the density of faults is such that on the required observational scale, deformation is approximately homogeneous.

The slip model of Reches predicts four sets of faults with an overall orthorhombic symmetry (Fig. 4.9). The orientation of the faults and their slip vectors depends upon  $k$ , the ratio of principal strains, and  $\phi$ , the angle of internal friction (an inherent property of the deformed material). This relationship is expressed in equations 26 and 27 of Reches (1983). These are shown here for oblate strains, when  $-0.5 \leq k \leq 0$  (where  $k$  is the strain ratio  $E_2/E_1$ ;  $E_2$  is the intermediate compressive strain, and  $E_1$  the maximum compressive strain).

The direction cosines of poles to slip planes are given by:

$$N_1 = \pm (\sqrt{2}/2) (1 - \sin \phi)^{1/2}$$

$$N_2 = \pm (\sqrt{2}/2) |k|^{1/2} (1 + \sin \phi)^{1/2}$$

$$N_3 = (\sqrt{2}/2) (1 - |k|)^{1/2} (1 + \sin \phi)^{1/2}$$

The direction cosines of the slip vectors are given by:

$$S_1 = \pm (\sqrt{2}/2) (1 + \sin \phi)^{1/2}$$

$$S_2 = \pm (\sqrt{2}/2) |k|^{1/2} (1 - \sin \phi)^{1/2}$$

$$S_3 = (\sqrt{2}/2) (1 - |k|)^{1/2} (1 - \sin \phi)^{1/2}$$

By changing the signs of two of the three direction cosines four sets of slip planes and slip vectors are derived (the sign of the third direction cosine remains unchanged as only vectors pointing downwards [*i.e.* in the lower hemisphere of the stereonet] are needed). The equations are solved for a range of  $k$  and  $\phi$  values, and plotted on equal area stereonets in Fig.4.11:

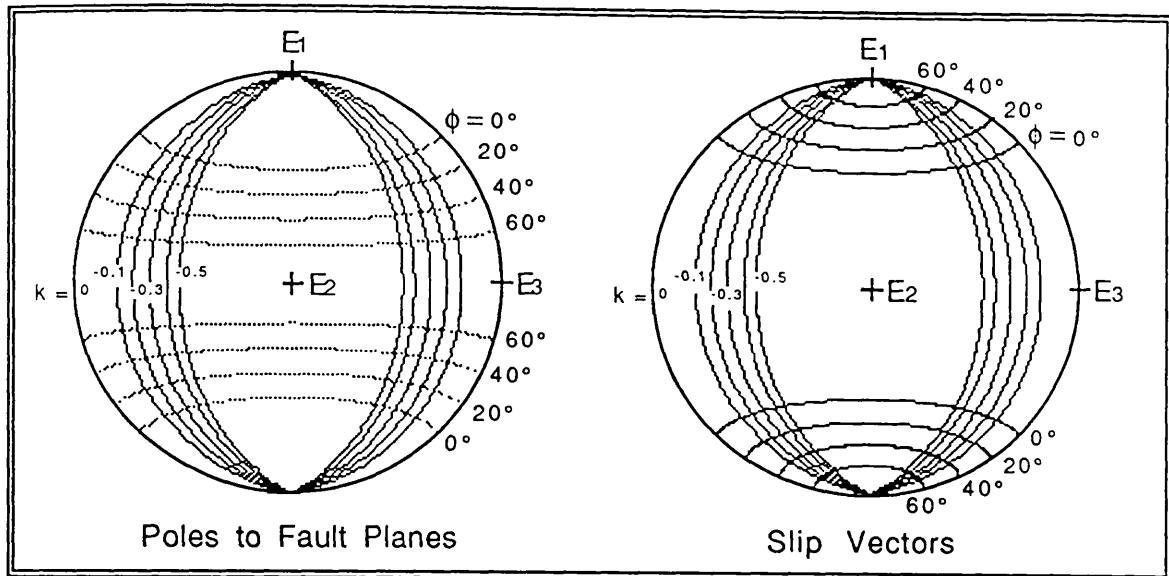


Fig. 4.11. Equal area stereonets showing the predicted loci of slip vectors and poles to fault planes (for a range of  $k$  and  $\phi$  values) in relation to a horizontal  $E_1$  and vertical  $E_2$ . The stereonets are derived from the equations for the direction cosines given in equations 27 of Reches 1983.

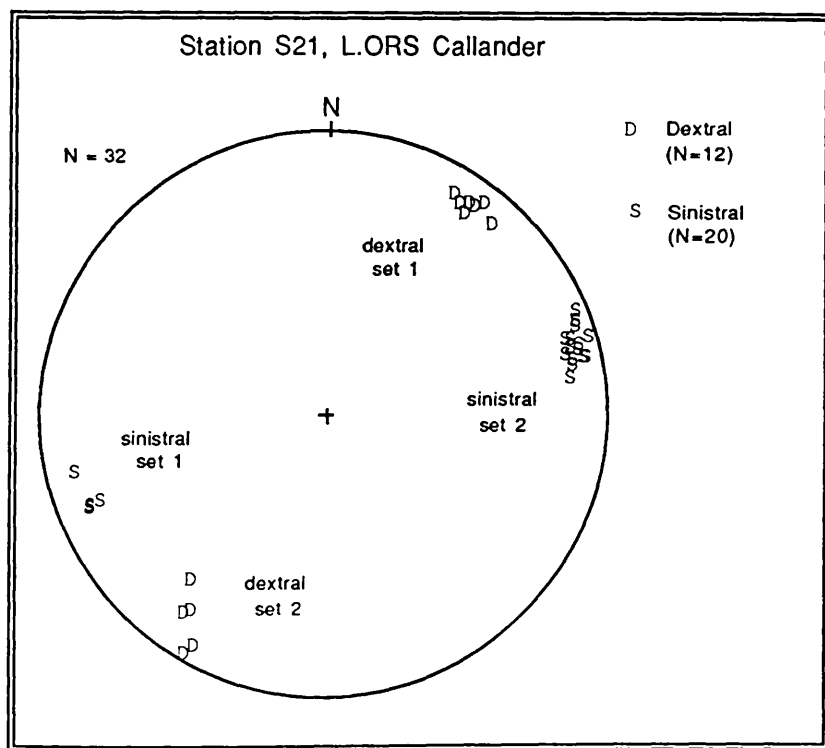


Fig. 4.12. Lower hemisphere equal-area stereonet showing the geometric and kinematic results of mesofracture analysis of L.ORS pebbly sandstones from Station S21 at Bracklinn Falls, near Callander. Results are given as poles to fracture planes, for different senses of fracture offset. Brittle strain is very low within this station; fractures shown are shear joints, with offset sense based on microscopic shear sense criteria (see section 4.4). "N" is magnetic north.

The stereonet in Fig. 4.11 provide a template with which to compare the geometric and kinematic results already presented (Figs. 4.9). This is done below, by way of example, for a particularly well-constrained station from the L.ORS near Callander.

Firstly, it is clear from the plotted data (Fig. 4.12) that faults and shear joints of different offset sense form quite discreet clusters, and so the different senses of fracture are contoured separately (Fig. 4.13).

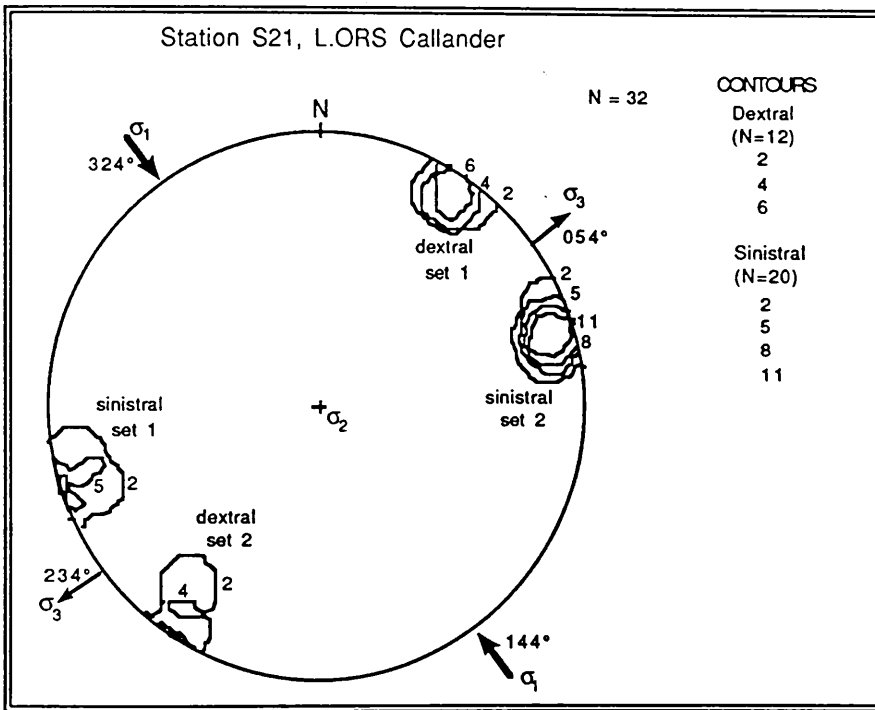


Fig. 4.13. Lower hemisphere equal area stereonet showing contoured poles to fracture planes from Station S21. Sinistral and dextral mesofractures are contoured separately. The maximum principal compression,  $\sigma_1$  lies parallel to the obtuse bisector of adjacent clusters of faults, hence  $\sigma_3$  is parallel to the acute bisector.  $\sigma_2$  is vertical and tensile.

The plot is then rotated (Fig. 4.14) to enable comparison with the theoretical stereonet in Fig. 4.11.

The dynamic interpretations from station S21 are:

- 1)  $\sigma_1$  is horizontal and trends  $144^\circ$ - $324^\circ$ .  $\sigma_1$  is the obtuse bisector of the poles to fracture planes (*i.e.* the acute bisector of the planes).

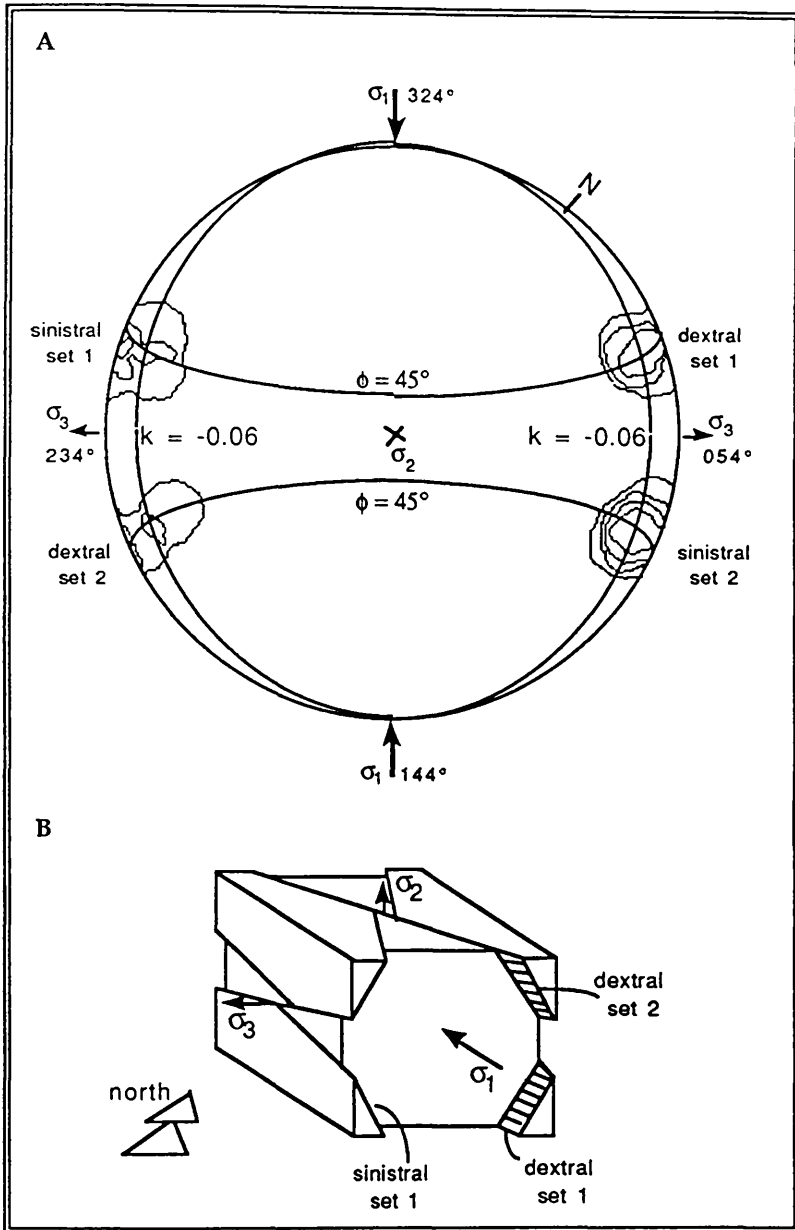


Fig. 4.14. (A) The stereonet of Fig. 4.13 has been rotated until  $\sigma_1$  is aligned "N-S" to allow comparison with Fig. 4.11. Also shown are the great circles representing loci of poles for  $k = -0.06$ , and the small circles with loci representing  $\phi = 45^\circ$ . (B) Deformation of a cube, schematically representing the geometry and kinematics of mesofractures at station S21 at Callander.

2) stress was triaxial; the effect of  $\sigma_2$  was small but not neutral. The strain ratio,  $k$ , = -0.06. Fractures are steep but not vertical. The poles to fracture planes do not quite cluster on the perimeter of the net and hence form four sets of fractures rather than one conjugate pair.  $k$  is derived from the  $k/\phi$  loci in Fig. 4.11. For plane strain  $k=0$ ; the  $k$  value of -0.06 represents a slight departure from plane strain.

- 3) Both  $\sigma_2$  and  $\sigma_3$  were extensional, giving rise to flattening (oblate) strains. This is reflected in the negative  $k$  value.
- 4) The angle of internal friction,  $\phi$ , was approximately equal to  $45^\circ$  at the time of fracture initiation. This is derived from the  $k$  and  $\phi$  loci in Fig. 4.11.
- 5) There is a slightly greater abundance of fractures in dextral set 2 and sinistral set 1 than in the other two sets, but it is not clear in a station of low strain whether this difference is significant. Such a feature may be due to sampling bias, to a heterogeneity of strain on an outcrop scale, or to a genuine dominance of one or more fracture sets which can represent a component of simple shear strain. This is generally recognisable only in areas of higher brittle strain.

The geometry and kinematics from station S21 are shown diagrammatically as the deformation of a unit cube (Fig. 4.14B).

#### 4.6.2 Complications in dynamic analysis

Not all stations can be interpreted with such objectivity as station S21. Complications in interpretation arise for two main reasons; firstly, because of inherent limitations in the methodology of mesofracture analysis, and secondly because some stations yielded results that cannot be interpreted in terms of the model of brittle deformation as outlined in section 4.6.1.

#### **Methodological complications:**

1) It is extremely difficult to date the age of individual fractures, and consequently some of the fractures used may be initiated or re-activated in post-mid-Devonian times ( $\sigma_1$  in the present day stress field is orientated NW-SE, paralleling  $\sigma_1$  for many of the stations I analysed [Paul Hancock, pers. comm. 1988]). In particular, Carboniferous rocks in central Scotland are often pervasively fractured, indicating significant syn- or post-Carboniferous brittle deformation. However, wherever U.ORS rocks could be observed in close proximity to the L.ORS mesofracture stations, there was a marked difference in both the magnitude and style of brittle deformation.

2) The contouring routines used by the SODS computer programs (see Appendix 1) follow an identical methodology to manual contouring, in which a circle with an area 1% of the area of the stereonet is used as a counting template. This method of contouring yields results that are not accurate, because the shape of the template used for counting should be changed for different regions of the stereonet (a circle should only be used

for the centre of the net - away from the centre the template becomes irregularly elliptical). This would clearly be impractical for manual contouring but would be possible using a computer. This complication is most significant towards the perimeter of the stereonet, and so will most affect the results of mesofracture stations that contain predominantly steeply dipping planes, such as those typifying central Scotland. A demonstration of this problem is shown in Fig. 4.15.

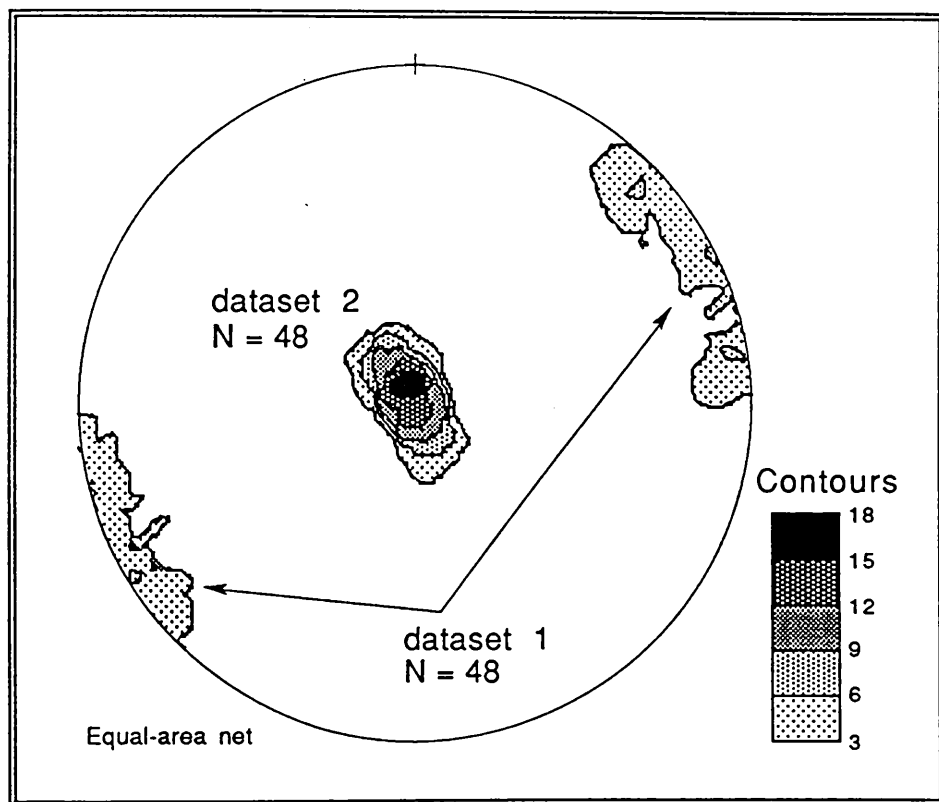


Fig. 4.15. Equal-area net showing the effect of using the traditional method of contouring data. Dataset 1 is real data showing the orientation of fold hinges from mesofracture station S8, at Stonehaven. Dataset 2 is composed of the same data rotated through  $90^\circ$  in a vertical plane. Note the marked difference in *apparent* statistical significance of the two (identical) sets.

### Complications in interpretation

These complications arise because for some stations the assumptions of mesofracture analysis and/or the Reches model are not all valid (see section 4.6.1):

- 1) Fractures may be of more than one generation. Earlier fractures result in the rock having a pre-existing anisotropy when subsequently deformed, whilst later fractures can "overprint" (*i.e.* complicate) existing kinematic information. Fortunately, this is usually clear in stations that are

kinematically well controlled, such as Station S27 in which a typical triaxial pattern of four fault sets is overprinted by NE-SW normal faulting.

2) Deformation is assumed to be homogeneous on the required scale of observation. An important assertion of mesofracture analysis is that the interpretation of *outcrop-scale* fractures can lead in turn to the interpretation of *regional* dynamics. In reality, however, fracture sets tend to occur in domains and sub-domains (etc.), on a variety of scales, because large fractures can have several orders of associated secondary fractures<sup>1</sup> (Fig.4.16). On our scale of observation, *i.e.* the "outcrop" scale, it may be impossible to know which order of fracture is represented within the outcrop. For instance, the aim of my analysis is to interpret *regional* HBFZ movements, but are the fractures at each station first order, second order, third order etc. *with respect to the HBFZ*? Serious difficulties in interpretation can arise when the mesofractures measured within a station are lower order fractures to larger, unrecognised macrofaults.

Fortunately though, most stations close to the HBF appear to be dominated by second order fracturing, and so of are of great use in determining the sense of offset on the HBF itself. Station S16 may be an exception to this (see Fig. 4.9m and Fig. 4.23g), and is probably dominated by second order fractures to the nearby Loch Ericht fault.

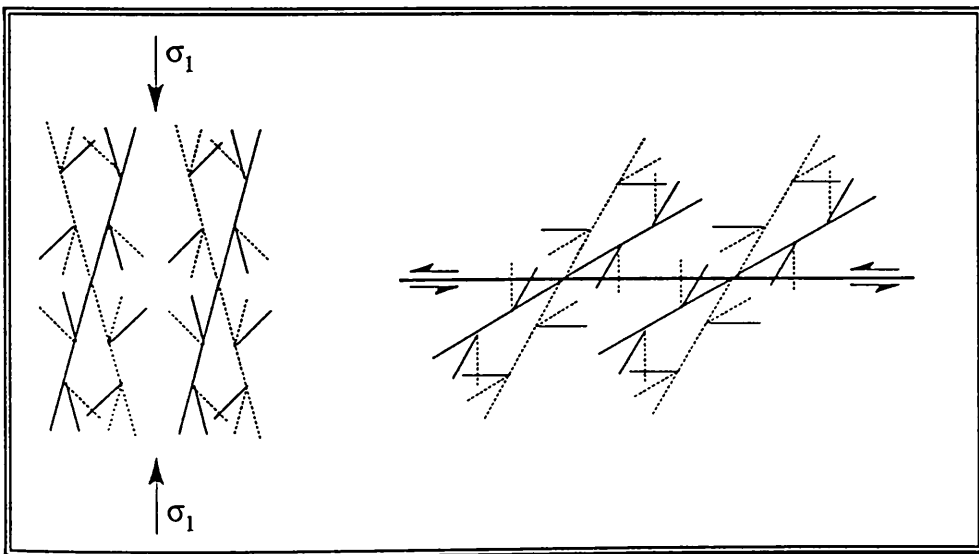


Fig. 4.16. Complicated fracture patterns resulting from multiple orders of fractures in pure shear and left-lateral simple shear. Sinistral faults are solid, dextral faults are dashed.

<sup>1</sup> Do mesofractures display fractal geometry?

3) Deformation is assumed to be irrotational. Rotation (due to a simple shear component) may be recognised in stations showing moderate to high brittle strain, by a predominance of faults of one sense of offset. Station S3/7 at Stonehaven is such a station (see below).

However, such interpretation is not without difficulty, because such fault sets can result from a range of different boundary conditions (Fig. 4.17). This is unfortunate, because one aim of mesofracture analysis is to *deduce* large-scale boundary conditions from a study of local-scale fracture sets.

Therefore, in order to interpret the dynamics of a mesofracture station in which rotation may have occurred, the boundary conditions must be measured or assumed.

A very relevant example of such reasoning was presented by Robertson (1987), who inferred a period of syn-sedimentary sinistral transpression from the L.ORS Strathlethan Formation, near Stonehaven, by *assuming* that the HBF acted as a boundary to basin deposition. Although this is possible, it remains difficult to prove, because the steep limb of the Strathmore syncline has been denudated<sup>1</sup>.

Fig. 4.17 shows three types of rotational deformation resulting from slip along one preferred fault set, namely "boundary rotation", "simple shear", and "fault block rotation". The latter has been widely recognised in fault zones. It is not possible to distinguish between these in the field, because the geometry and kinematics are identical. However, they are dynamically very different, and consequently have contrasting implications for interpretation of regional stress and strain.

Boundary rotation can result if faults and fault blocks do not rotate during deformation; the rotational component is manifested by a change in orientation of the margins to the deforming zone (Fig. 4.17A). In contrast, all the rotation can be accommodated without boundary rotation, by simple shear or fault block rotation. The zone width is maintained during simple shear, though the zone boundaries must move laterally with respect to each other (Fig. 4.17B). Transpressional deformation results in both lateral movement of zone boundaries, as well as shortening across the zone (Fig. 4.17C), as the faults (and therefore the fault blocks between them) rotate during deformation. Note that during fault block rotation the faults move *anti-thetically* with respect to the component of simple shear acting on zone boundaries.

---

<sup>1</sup> Furthermore, the NNW-SSE principal compression direction reported by Robertson (1987) is *orthogonal* to the HBFZ, and therefore (for reasons developed in sections 4.7, 4.8 and Appendix 3) can not be explained by the transpression models that existed in 1987!

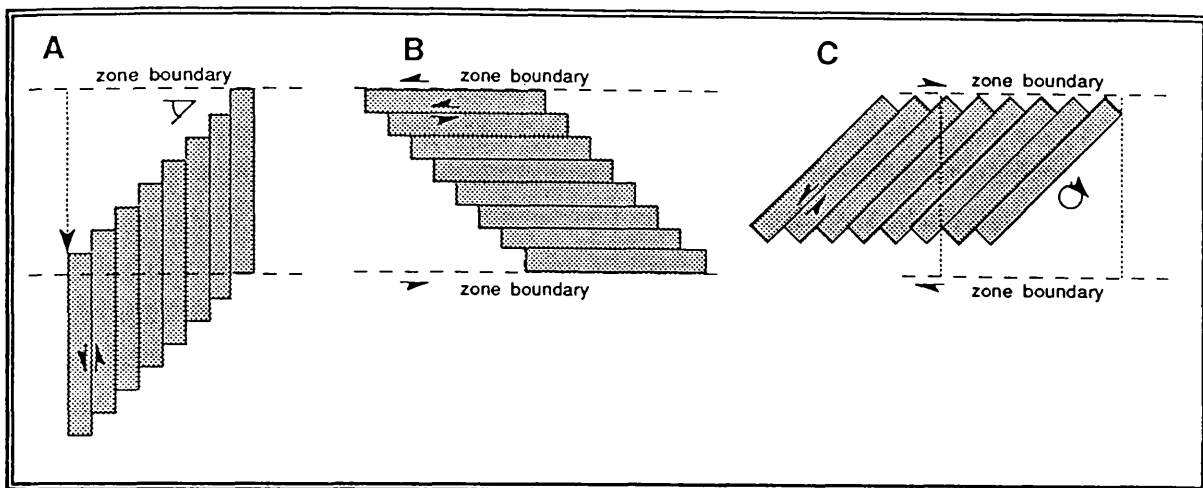


Fig. 4.17. Three types of rotational deformation produced by brittle faulting. A dominant left-lateral faulting with no fault block rotation must be associated with rotation (and elongation) of the deformation zone boundaries. B simple shear deformation with respect to the zone boundaries (dashed lines). C dominant left-lateral faulting is associated with rotation of faults and fault blocks. Deformation with respect to the zone boundaries (dashed lines) includes pure shear and simple shear (*i.e.* transpression).

In many tectonic settings, including oblique fault slip and oblique basin closure (*i.e.* "simple transpression" of Harland 1971 - see section 4.7.3), deformation within the deforming zone is due to the external movement of non-rotating zone boundaries. In other words, the deformational boundary conditions prevent the deformation zone boundaries from rotating, and consequently fault block rotation is more widely applicable than zone boundary rotation.

Fault block rotation has been widely described and well quantified using palaeomagnetic studies (*e.g.* Ron 1987, Ron *et al.* 1984, 1986). The models shown in Fig. 4.17 show rotational deformation; in contrast, pure shear deformation has also been approximated by Ron *et al.* (1984, figure 1), in a model in which adjacent domains of fault blocks have opposing displacement senses, though strictly speaking this has shown to be imprecise (Garfunkel & Ron 1985, figure 4a,b).

Some of the models that describe block rotation quantitatively have provided an invaluable framework in interpreting field data (Ron *et al.* 1984, 1986; Garfunkel & Ron 1985, Ron 1987). Each of these models is based on a rigorous fault block geometry and specified boundary conditions, and the model is then used to determine the strain at any stage during deformation. For a given fault geometry the block rotation model allows only one deformation path, irrespective of the applied stress. This approach

is oversimplified and unrealistic, because strain occurs *in response to* applied stress, (to some extent at least).

The limitation of the rigid block rotation model is that it assumes rigidity of the fault blocks (which generally requires that the width of the deformation zone decreases; Fig. 4.17C). Given perfect rigidity of fault blocks, *and* zero resistance to slip on the fault surfaces, the model aims to predict the resulting kinematics, after yield has occurred (*i.e.* a sophisticated version of the model might incorporate a yield criterion to predict the initial orientation of the faults, but after failure has occurred the applied stress cannot change the deformation path).

Both the above assumptions are groundless because:

1) fault blocks are not totally rigid (Fig. 4.18); blocks can flex, and stress can be stored elastically (otherwise every fracture would have to circle the entire globe, and furthermore, fractures would be unable to propagate; they would have to instantaneously "exist"!).

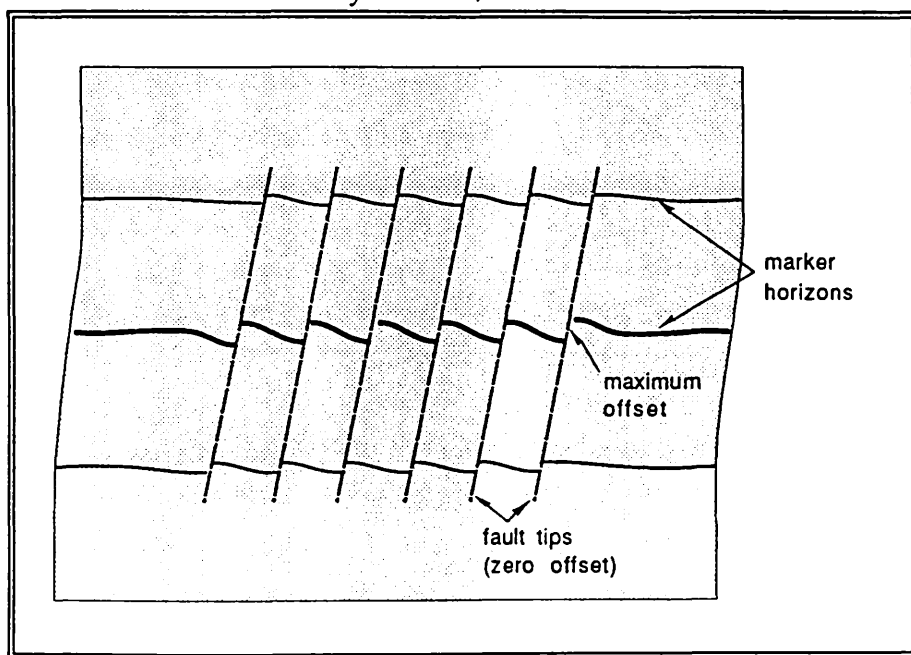


Fig. 4.18. Faulting in non-rigid rock; displacement decreases towards the crack tip. Stress is stored elastically around the fault tips.

2) resistance to slip can become so great during progressive deformation that it becomes kinematically favourable to initiate new fractures, rather than continue to slip along pre-existing ones. This is expected even under conditions of coaxial constant incremental stress (*i.e.* a relatively simple situation).

This criticism of the rigid block rotation model in no way underestimates the value of palaeomagnetic studies of fault zones.

Palaeomagnetism provides an invaluable tool in testing other fault zone models.

There are other models that help to explain observed fault block rotation. These models, based on clay- and sand-box deformation, explain the resulting faults and fault rotations in terms of progressive change of the strain ellipse produced under well-defined stress conditions. The models show that during simple shear a conjugate fracture set is initiated such that the acute bisector ( $\sigma_1$ ) is at  $45^\circ$  to the zone boundaries (Tchalenko 1970, Wilcox *et al.* 1973). These fractures are termed "Riedels" (or "synthetic" faults) and "anti-Riedels" (or "antithetic" faults). The Riedel/anti-Riedel conjugate pair is analogous to the conjugate fractures produced during pure shear (section 4.6.1; Daubree 1879; Anderson 1942). The Riedel faults, together with related fractures and other en-echelon structures are shown in Fig. 4.19.

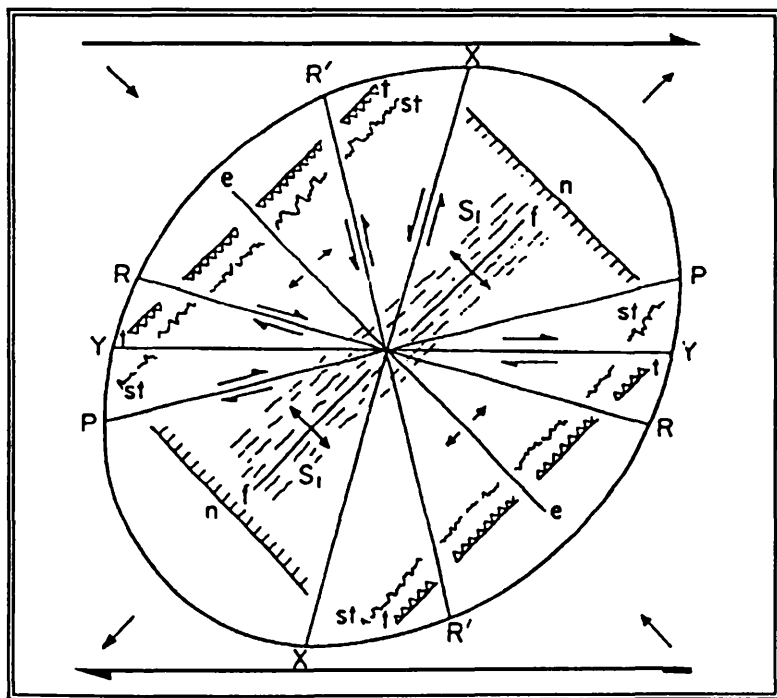


Fig. 4.19. En-echelon structures showing the relationship between fracture geometry, kinematics, and the finite strain ellipse during right-lateral simple shear (from Hancock 1985). R: Riedels; R': anti-Riedels; P, X and Y: P, X, and Y shears; e: extension joints, fissures and veins; n: normal faults; t: thrusts; st: stylolites; f: folds;  $S_1$ : cleavage or other foliation.

To emphasise; the dynamic significance of both the Riedel conjugate fractures (simple shear) and the Andersonian conjugate fractures (pure shear) is that they serve to change the shape of the three-dimensional incremental strain ellipsoid. The difference between the two lies in the

respective strain boundary conditions; the terms 'pure shear' and 'simple shear' are themselves statements of boundary strain.

Consequently, unless the boundary conditions are known, it is difficult to distinguish between conjugate fracture sets resulting from pure shear, from equivalent sets produced in response to simple shear.

This has important consequences for mesofractures analysis, because, as outlined in section 4.4, the rationale of mesofracture analysis is to use small-scale fractures to infer large-scale boundary conditions. However, if the *kinematics* of a mesofracture station are well constrained, evidence of overall rotation can be taken to be indicative of simple shear.

Conjugate fractures have been very widely recognised in many upper-crustal fault zones around the world, and the Riedel model has often been invoked to explain the geometry and kinematics of fractures in these zones (*e.g.* Tchalenko & Ambreyes 1970, Tchalenko 1970, Wilcox *et al.* 1973; many other examples are given in Sylvester 1988). However, as pointed out by Sanderson & Marchini (1984), many such fault zones, though conforming qualitatively to the Riedel model, have conjugate fractures and en-echelon structures that depart from the *quantitative* geometry predicted theoretically and recorded experimentally. Many fault zones have fracture set geometries that imply that  $\sigma_1$  is orientated at an angle greater than  $45^\circ$  to the shear zone, and Sanderson & Marchini (1984) interpret this as representing a departure from both pure shear *and* simple shear strain; the deformation is transpressional.

Clay-box experiments (*e.g.* Wilcox *et al.* 1973) have shown that rotation of non-rigid fault blocks can occur during simple shear. In clay this occurs by plastic deformation (and is therefore of limited relevance to the HBFZ in mid-Devonian times), but might also occur by a combination of elastic deformation (including folding), together with brittle fracturing on many scales.

The kinematic effect of all the fractures shown in Fig. 4.19 is to *collectively* change the shape of the finite strain ellipse.

Contemporaneous brittle deformation on several orders of fracture can allow deformation to be homogeneous on a regional scale, even during progressive rotational strain, though deformation might be heterogeneous at some scales of observation<sup>1</sup>.

---

<sup>1</sup> This is an important feature of fractal geometry.

In the experimental models, and in the many field examples that have been interpreted using the model, there is usually a dominance of Riedel faults over anti-Riedels (in this way the strain ellipsoid rotates as well as elongates). Consequently, the geometry of many fault systems are similar in both the rigid block rotation model (Fig 4.17C) or the Riedel model, and either can be invoked to explain the geometry and kinematics of faults and fault blocks observed in many fault zones.

It is important to note the dynamic difference between the Riedel and rigid block rotation models. In the Riedel model, second order faults at low angles to the main fault are synthetic to the overall sense of shear. This is the converse of the rigid block rotation model (Fig. 4.17C).

The Riedel model is valid, because it attempts to use the observed finite strain to interpret the operative stress regime. In contrast, the rigid block rotation model uses a combination of measurement (palaeomagnetic rotation) and assumption (boundary conditions) to predict the finite strain.

This assertion suggests that the whole philosophy of the rigid block rotation model is scientifically invalid. The yield criteria and slip criteria models (Anderson 1942; Reches 1983) are not open to such criticism because neither aims to *totally* describe brittle deformation; each refers to only one parameter of the brittle deformation process.

In fact, I think that during *progressive* brittle deformation, infinitesimal strain will depend on both infinitesimal stress *and* finite strain (*i.e.* there is probably a complex relationship between stress and progressive brittle strain).

An analogous relationship exists during ductile deformation, in the "strain softening" process, in which finite strain affects infinitesimal strain. However, the problem is exacerbated because at our scale of observation brittle deformation is more difficult to model than ductile deformation, due to the large heterogeneity that *inevitably* exists as soon as brittle failure (*i.e.* yield) occurs.

Consequently, a realistic description of progressive brittle deformation must aim to incorporate yield criteria, slip criteria, and stored (elastic) stress, under both coaxial and non-coaxial conditions.

I use the Riedel model to interpret Station S3/7 Fig. 4.20 (also see Figs. 4.6, 4.7). The contoured data shows a swathe of poles to steep or vertical

sinistral faults clustering near the perimeter of the net. Fractures appear to comprise a conjugate fracture set, and therefore deformation is due to simple shear (*i.e.* plane strain), at least at the available resolution.

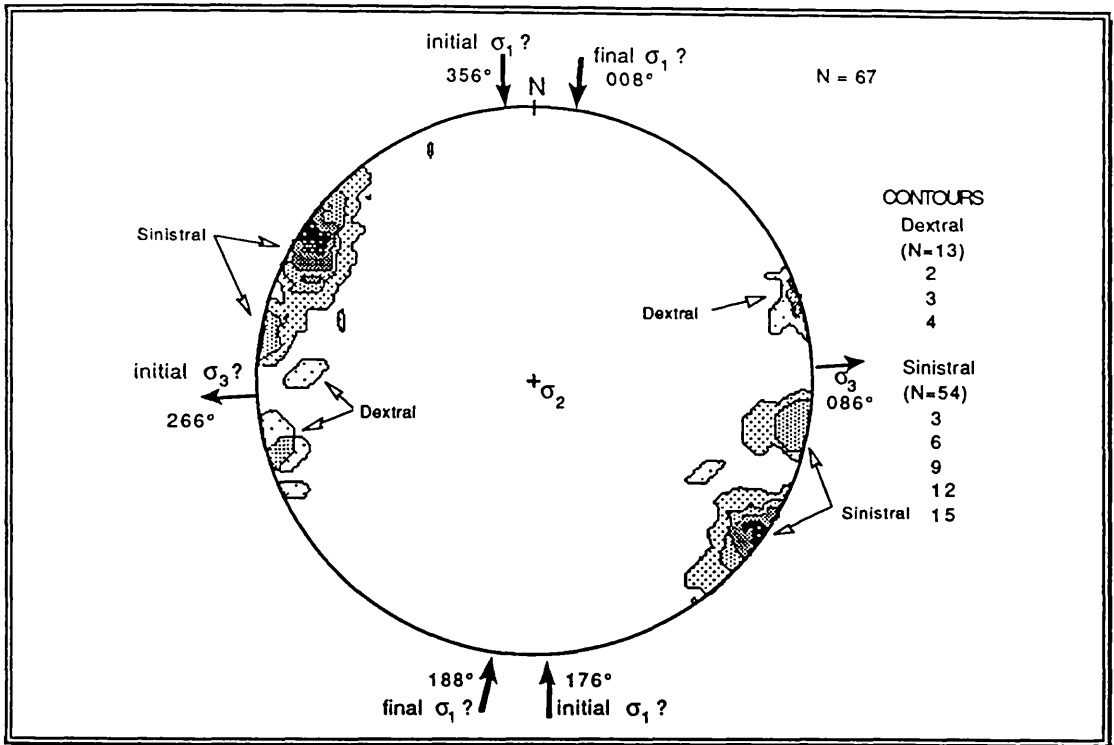


Fig. 4.20. Equal area stereonet showing contoured poles to fault planes, for station S3/7 from the L.ORS, Old Kirk shore, Stonehaven. Sinistral and dextral faults are contoured separately. Note the swathe of sinistral faults.

The spread of sinistral poles is as predicted; sinistral faults are progressively rotated clockwise during block rotation. If rotation progresses far enough, the orientation of the faults is unsuitable for further slip, and new faults tend to propagate. The antithetic dextral faults have a tendency to rotate clockwise in response to the simple shear and anticlockwise due to the changing strain ellipse, and so do not undergo significant rotation. This is reflected by the tight clustering of dextral faults.

The swathe of sinistral faults can be used to estimate the progressive change in orientation of  $\sigma_1$  during simple shear. The result is not accurate enough to calculate the exact amount of simple shear, but should provide a constraint on regional dynamics. In station S3/7 the  $\sigma_1$  rotated within the approximate range 176/356° through to 008/188°. These values probably underestimate both limits of the range, but further constraint is beyond the limitations of the method of interpretation.

Note that it is sometimes difficult to separate the effects of second order fracturing from fault-block back-rotation, because both result in similar fracture geometry (*i.e.* both give rise to an increased spread of azimuthal values, particularly for faults that are synthetic to regional shear). To emphasise; dynamic *interpretation* will depend upon the quality of kinematic data available.

Conjugate and multiple fractures are not limited to pure shear and simple shear. The three-dimensional irrotational slip model of Reches (1978, 1983) can be combined with the Riedel model of simple shear to predict fracture geometries expected in response to infinitesimal 3D *rotational* stress (*i.e.* "transpression", including components of both simple shear and pure shear; Sanderson & Marchini, 1984).

Strictly speaking, the combined model can only be used to quantitatively describe the *initiation* of slip, and would be limited by the combined assumptions of *both* models. However, clay-box modelling of simple shear has shown qualitatively how faults rotate during simple shear, and the inferences from this can be utilised to qualitatively predict progressive transpressional deformation.

Transpressional flattening (*i.e.* transpression not transtension) under brittle conditions will lead to the initiation of four sets of faults, all of which collectively act to rotate and flatten the 3D finite strain ellipsoid. Two of the fault sets are synthetic to the direction of overall simple shear (kinematically equivalent to Riedels), and two sets are antithetic (equivalent to anti-Riedels). Such predictions can be tested using a 3D clay-box that allows shortening or extension across the deforming zone (Fig. 4.21).

Some mesofracture stations along the Highland Borders, together with macrofault arrays close to the HBF, show a dominance of *oblique sinistral* fault offsets, and these fit the general predictions outlined above. As an example Station S9 is interpreted in Fig. 4.22. The contoured data show two elongated sets of poles to steep sinistral faults and two sets of poles to dextral faults, all clustering near the perimeter of the net. I interpret this as representing flattening of the stress ellipsoid (*i.e.* an oblate strain).

The spread of sinistral poles is as predicted; the strikes of sinistral faults are progressively rotated clockwise during block rotation (fault blocks themselves undergo complex rotations about non-vertical axes that progressively change orientation during deformation; this has great significance to palaeomagnetic studies). If rotation progresses far enough, the orientations of the faults are unsuitable for further slip, and new faults

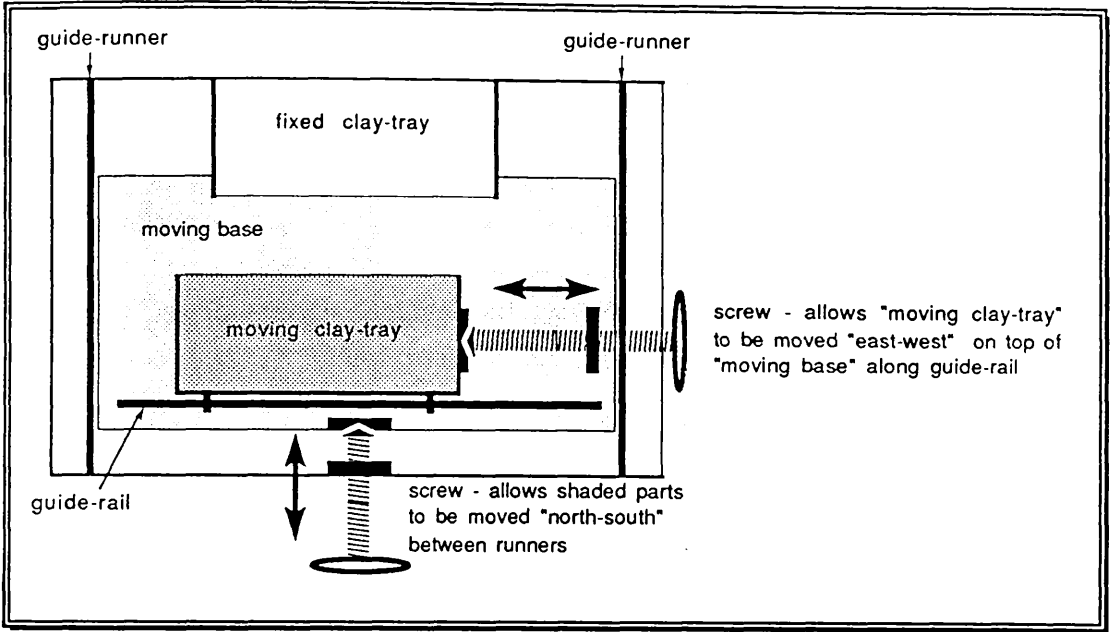


Fig. 4.21. A clay-box used to model transpression and transtension.

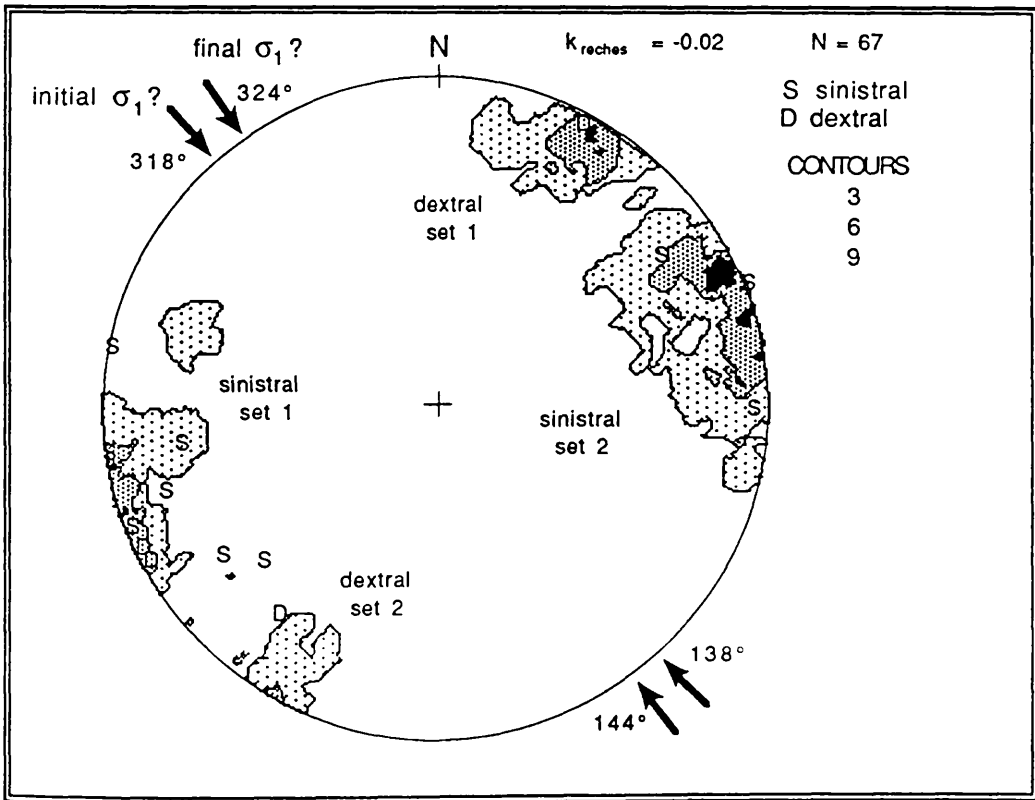


Fig. 4.22. Equal area stereonet showing contoured poles to fault planes, for station S9 from the LORS, Balmaha, Loch Lomond. Sinistral, dextral and unknown faults are contoured collectively, because there is not enough shear sense data to plot separately.  $K = -0.02$ , *i.e.* slightly non-plane strain. This is supported by slickenside data (section 4.5.3).

tend to propagate. The antithetic dextral faults have tendencies to rotate clockwise in response to the simple shear and anticlockwise due to the flattening of the strain ellipsoid, and so do not necessarily undergo significant rotation at all.

Because of the present lack of reliable high-resolution palaeomagnetic data, it is not possible to distinguish between block rotation and boundary rotation (Fig. 4.17). Consequently the interpretation of such stations is still somewhat subjective, though a new study by Alan Trench (Oxford Univ.) may soon provide further constraint.

**In summary:** mesofracture sets should be explained by a general model that describes deformation in three-dimensions, and that allows for rotational components of strain. Plane strain, simple shear, and pure shear are just three special types of strain in a complete deformational spectrum.

#### 4.6.3 Mid Devonian stress orientations

Twenty-three mesofracture stations sited in pre-U.ORS rocks have mesofracture geometries and kinematics that can be interpreted dynamically in the way described in this section (4.6). Only one station (S14, Ardmore) in which a reasonable amount of data was collected could not be interpreted in this way. Twelve stations sited in post-L.ORS rocks either had insufficient mesofractures to allow an interpretation, or contained fracture sets that could not be attributed to compressional deformation of the type described here. The dynamic interpretations from each mesofracture station are presented below (Figs. 4.23).

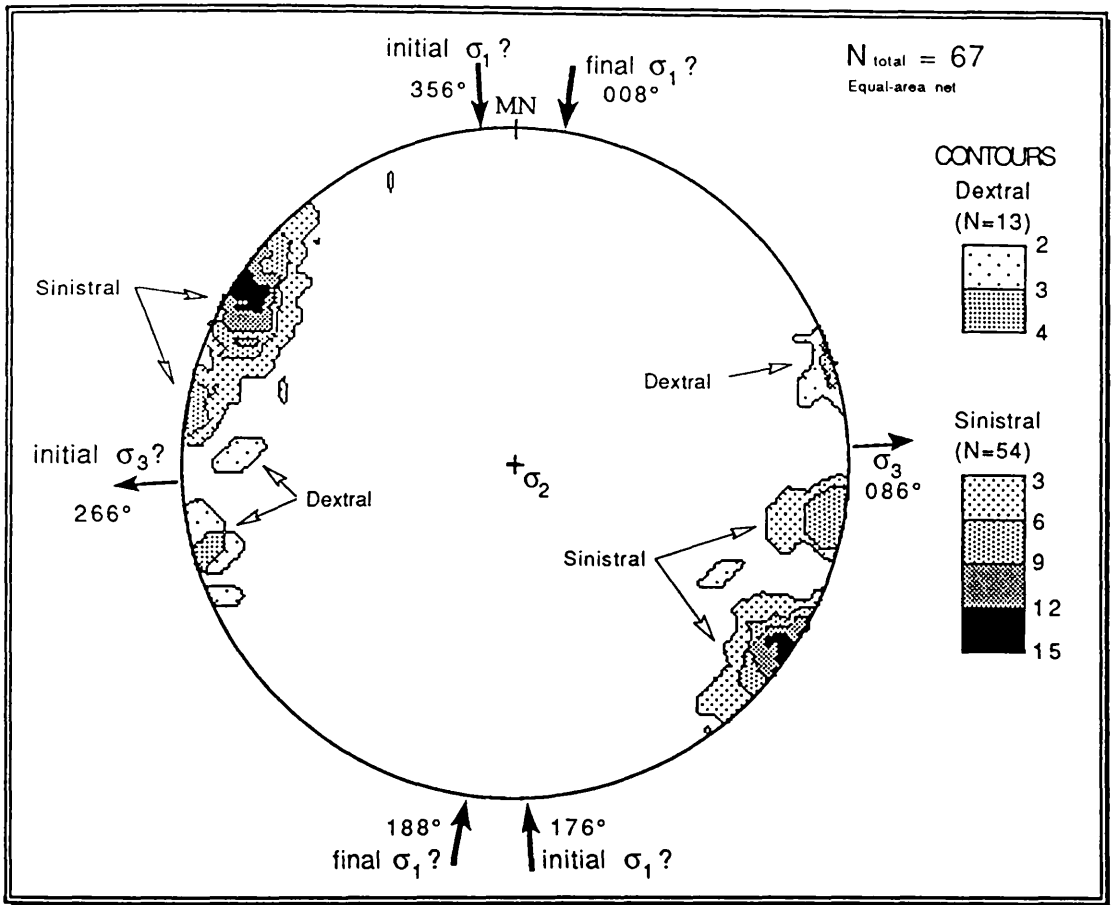


Fig. 4.23a. Dynamic interpretation of mesofracture station S3/7, from the L.ORS, Old Kirk Shore, Stonehaven. Sinistral and dextral faults are contoured separately (using the "faces" macro described in Appendix 1). Strain is biaxial and rotational, with  $\sigma_1$  rotating within the approximate range 176/356° through to 008/188°.  $\sigma_2$  is vertical.

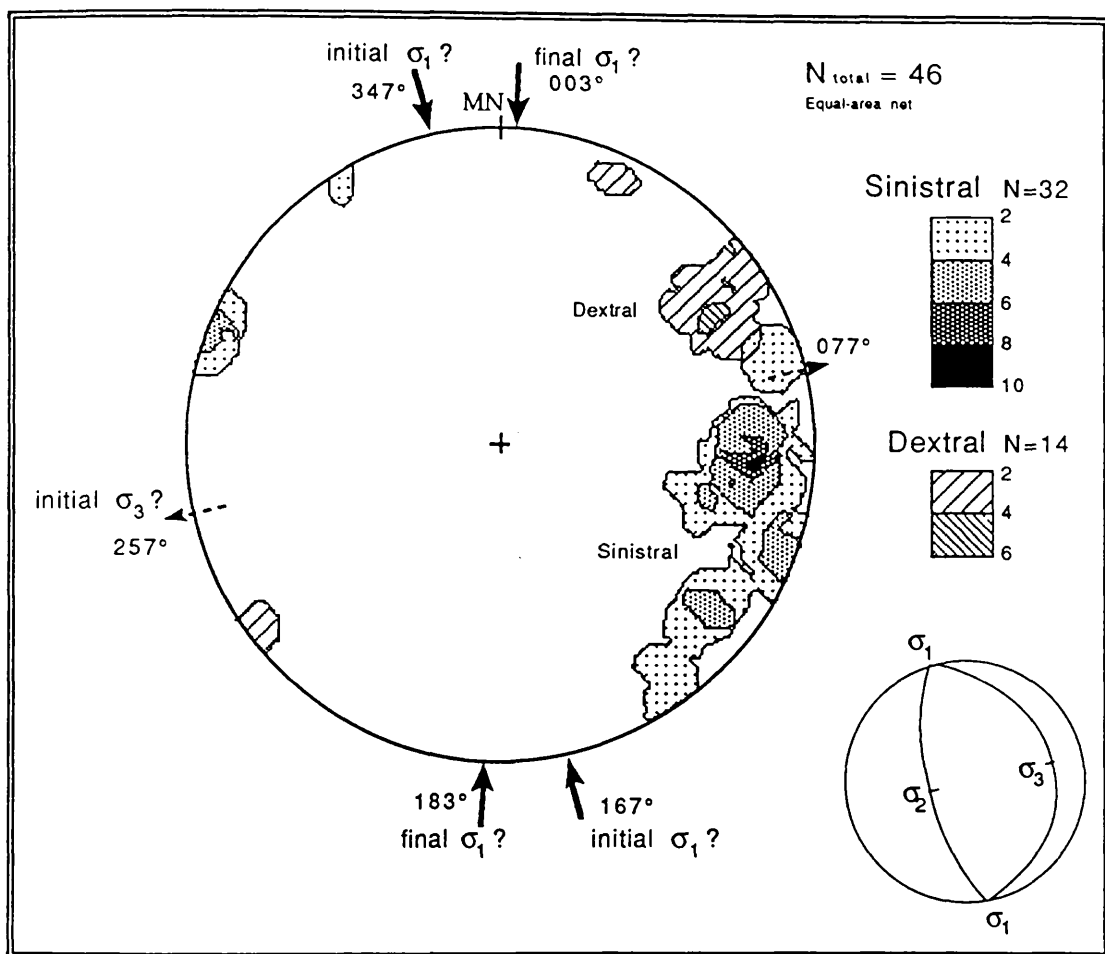


Fig. 4.23b. Dynamic interpretation of mesofracture station S6, from the Dalradian, Craigeven Bay, Stonehaven. Sinistral and dextral faults are contoured separately (using the "faces" macro described in Appendix 1). Strain is biaxial and rotational, with  $\sigma_1$  rotating within the approximate range 167/347° through to 003/183°. The small diagrammatic stereonet shows the initial orientations of principal strain axes at the time of brittle yield, and shows that  $\sigma_2$  is steep, but not vertical.

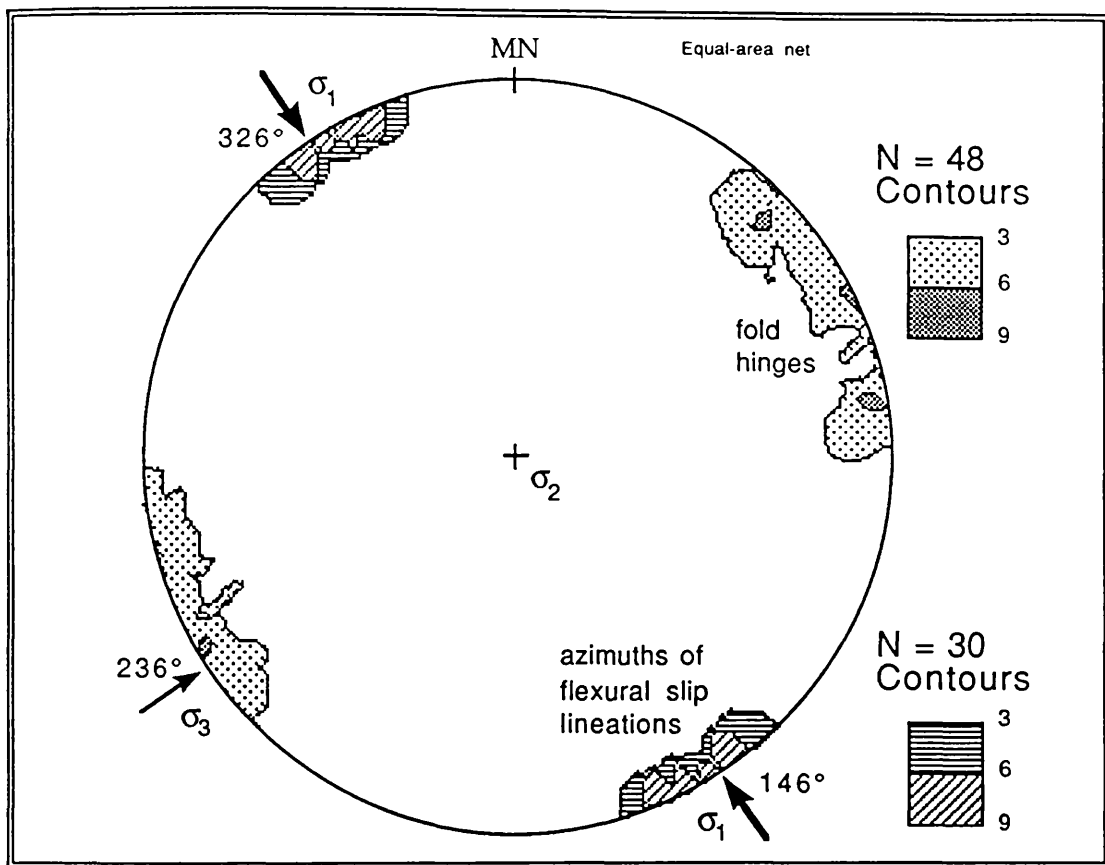


Fig. 4.23c. Dynamic interpretation of mesofracture station S8, from the HBC metaspilites, Craigeven Bay, Stonehaven. Fold axes are contoured, as are the azimuthal values of flexural-slip lineations associated with the folding (only the azimuth is shown, because the lineations curve in the vertical plane). Strain is biaxial. The orthogonal relationship between the fold axes and the flexural slip lineations suggests that  $\sigma_1$  lies perpendicular to the fold axes (this is not necessarily the case with all folds).

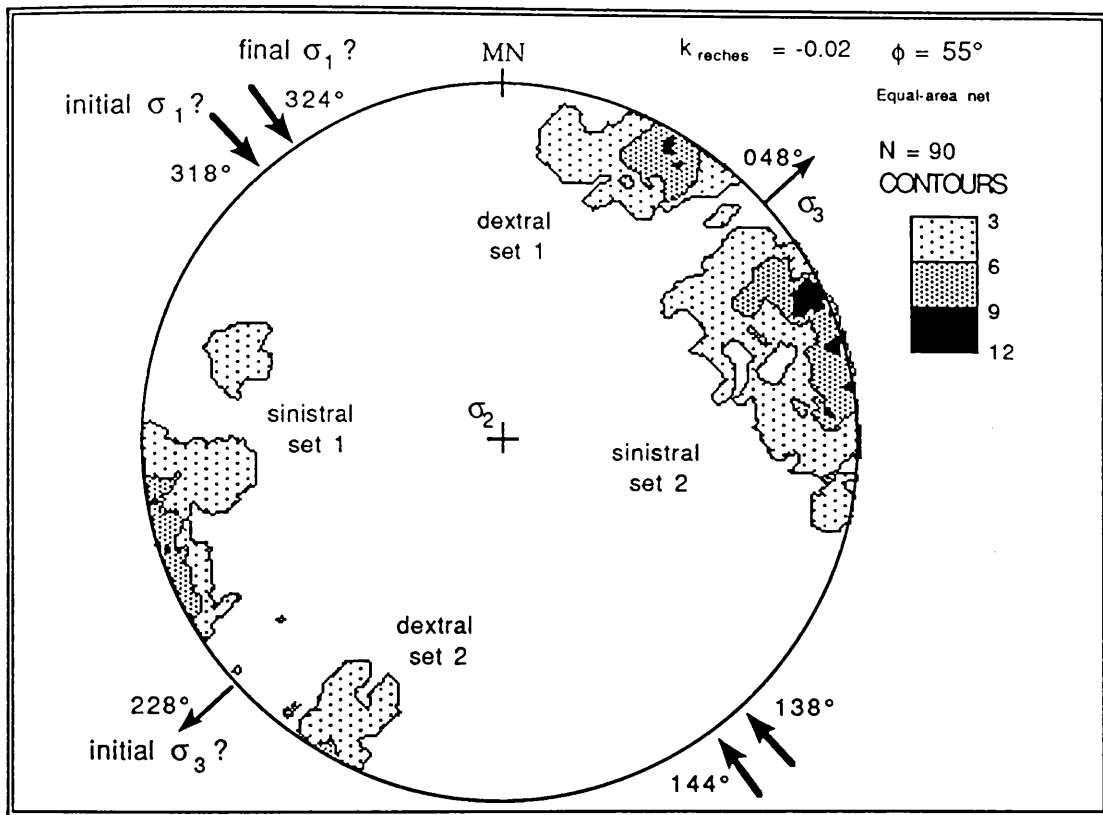


Fig. 4.23d. Dynamic interpretation of mesofracture station S9, from the L.ORS, Balmaha, Loch Lomond. Sinistral, dextral and undifferentiated faults are contoured together (using the "pufs" macro described in Appendix 1). Strain is triaxial and slightly rotational (hence the estimate of  $\phi$  is only approximate), with  $\sigma_1$  rotating within the approximate range 138/318° through to 144/324°.  $\sigma_2$  is vertical, and extensional;  $k = -0.02$  (*i.e.* slightly non-plane strain).

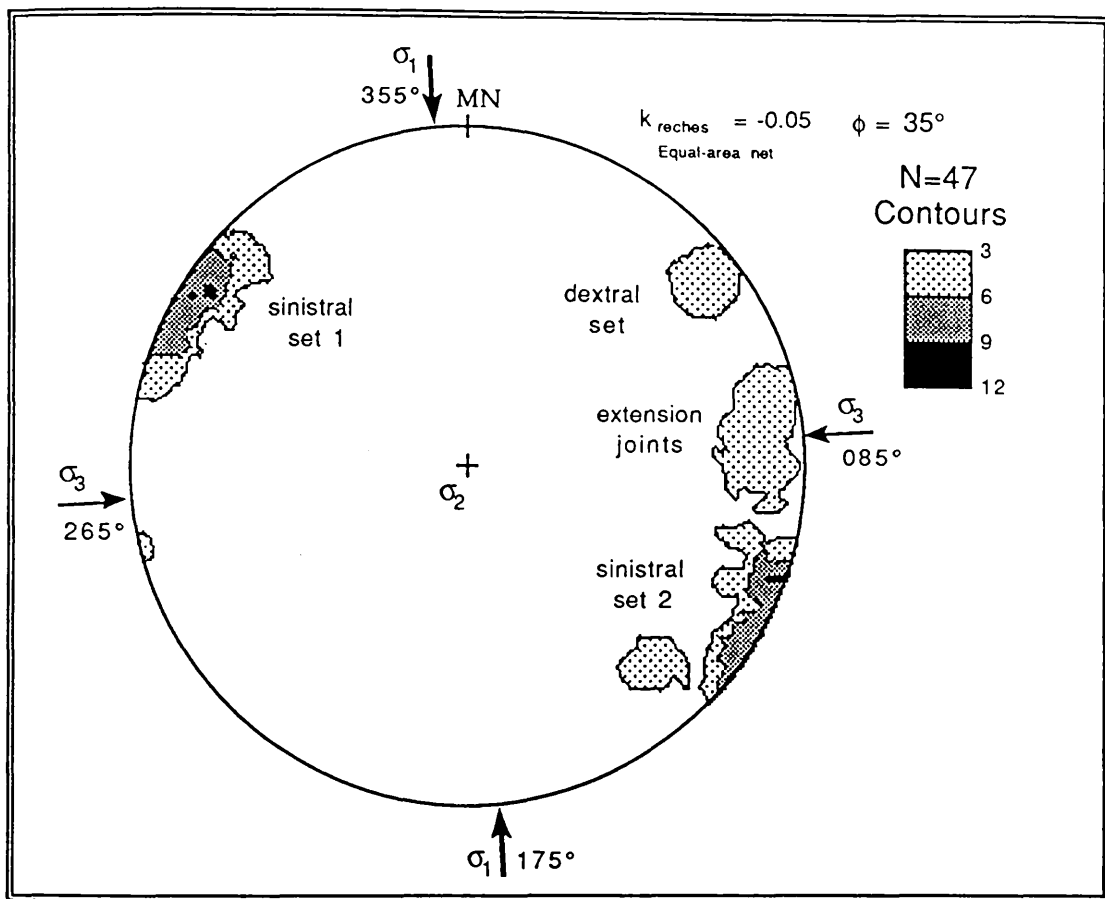


Fig. 4.23e. Dynamic interpretation of mesofracture station S10, from the L.ORS, Arbroath. Sinistral, dextral and undifferentiated faults are contoured together (using the "pufs" macro described in Appendix 1). Strain is triaxial and probably irrotational; the apparent dominance of sinistral faults is more likely to be due to sampling bias than a simple shear component.  $\sigma_2$  is vertical, and extensional;  $k = -0.05$  (i.e. slightly non-plane strain).

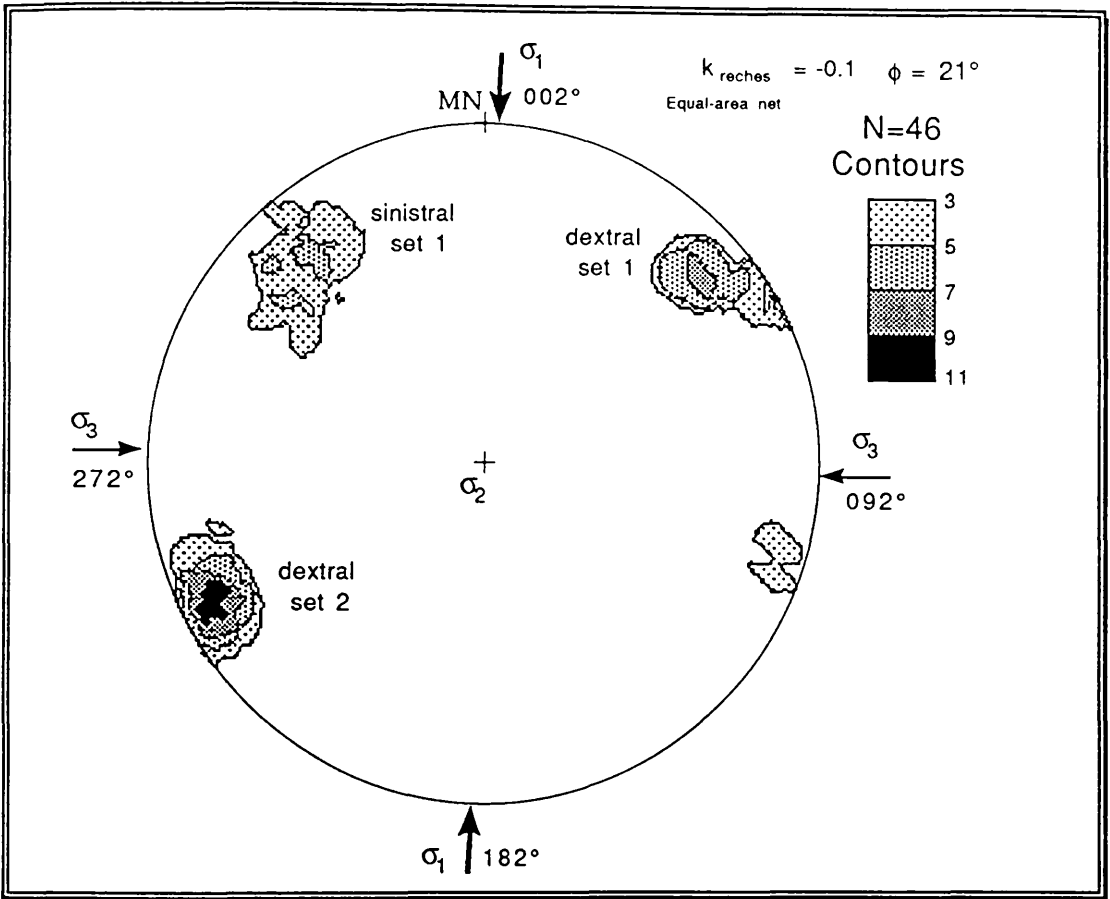


Fig. 4.23f. Dynamic interpretation of mesofracture station S15, from Moine schists, near Grantown-on-Spey. Joints and undifferentiated faults are contoured together (using the "pufs" macro described in Appendix 1). Strain is triaxial and irrotational.  $\sigma_2$  is vertical, and extensional;  $k = -0.1$  (i.e. non-plane strain).

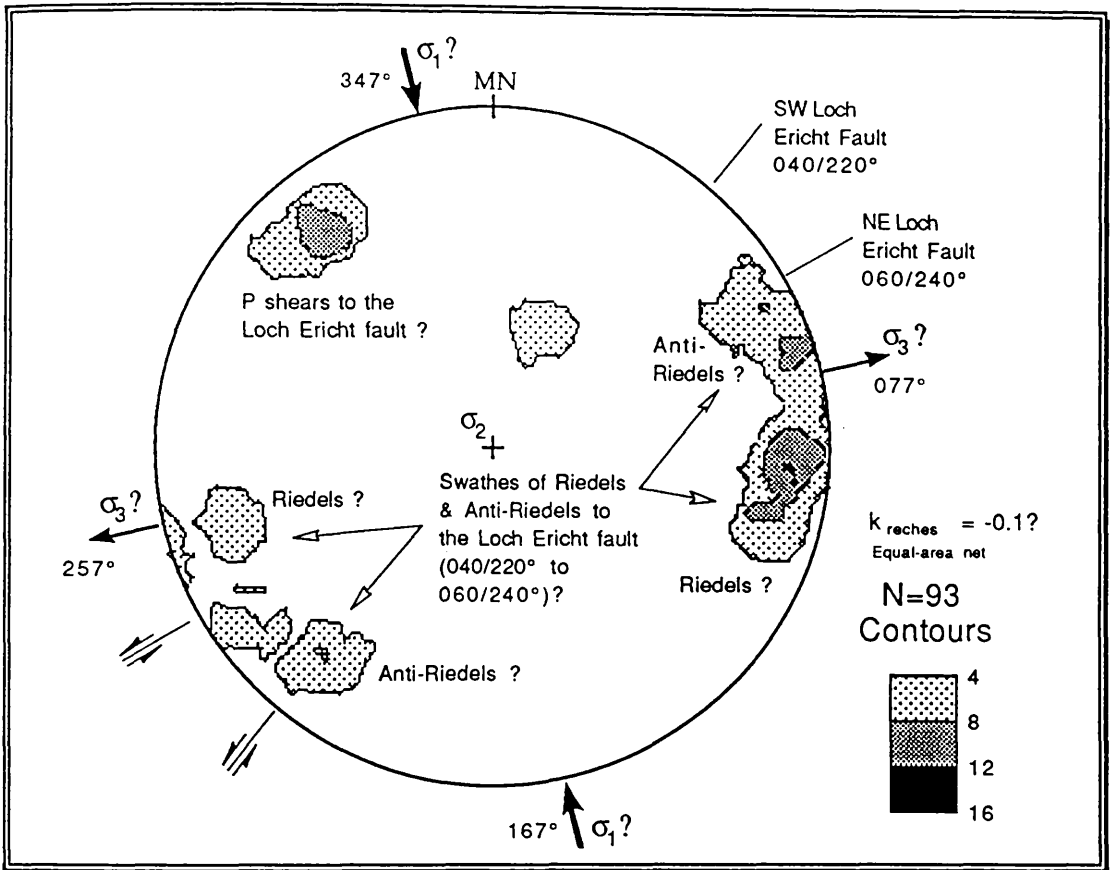


Fig. 4.23g. Tentative dynamic interpretation of mesofracture station S16, from Moine schists, Glen Truin, showing how the complex mesofracture pattern might relate to the change in orientation of the nearby Loch Ericht fault. Joints and undifferentiated faults are contoured together (using the "pufs" macro described in Appendix 1). Strain is triaxial,  $\sigma_2$  is vertical and extensional;  $k = \text{approx. } -0.1$  (i.e. non-plane strain).

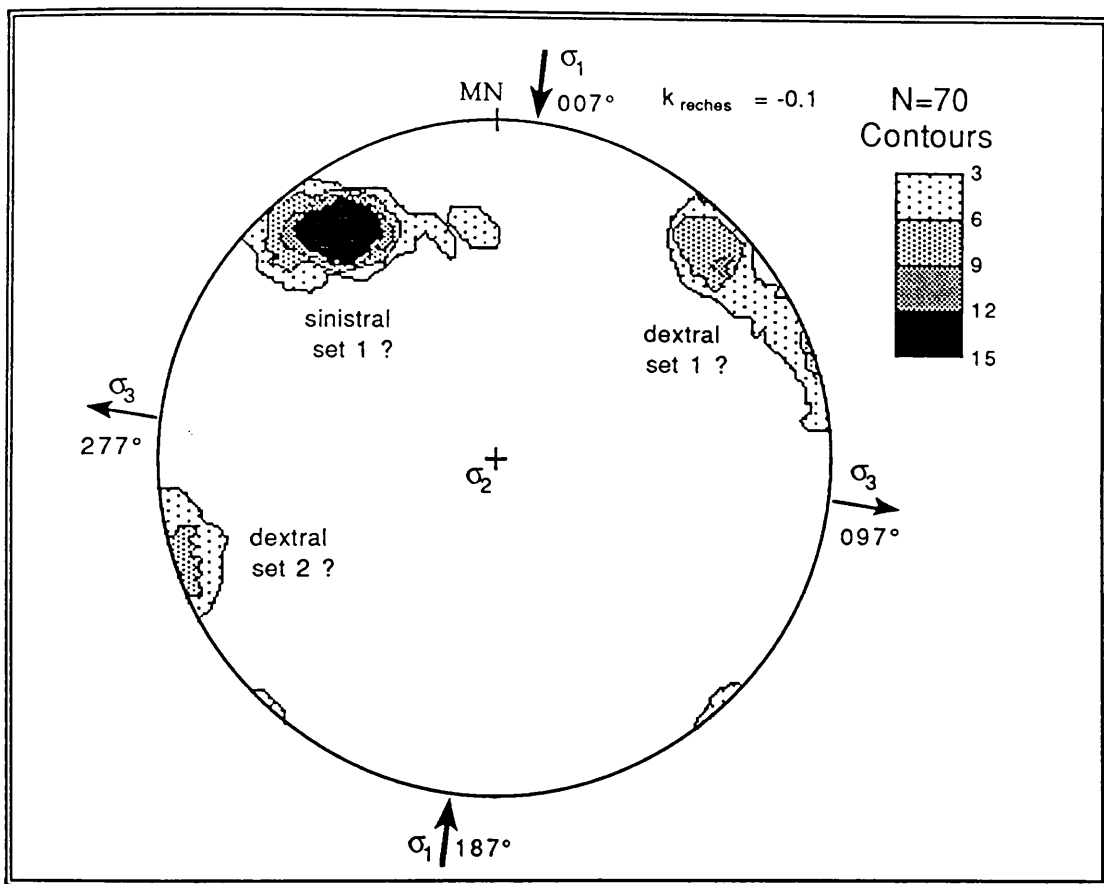


Fig. 4.23h. Dynamic interpretation of mesofracture station S17, from Moine schists, Drumochter Summit. Joints and undifferentiated faults are contoured together (using the "pufs" macro described in Appendix 1). Strain is triaxial and irrotational.  $\sigma_2$  is vertical, and extensional;  $k = -0.1$  (*i.e.* non-plane strain).

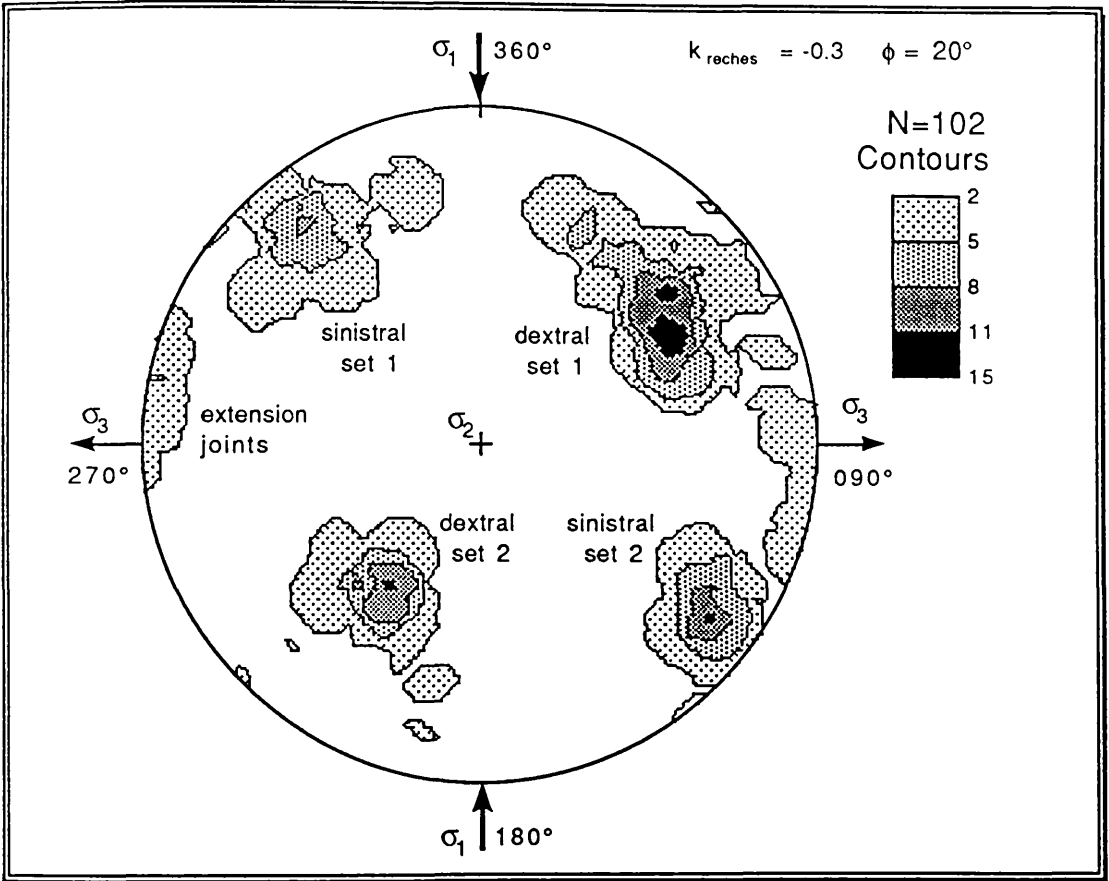


Fig. 4.23i. Dynamic interpretation of mesofracture station S18, from L.ORS lavas, Edinburgh. Joints are contoured using the "faces" macro described in Appendix 1. Strain is triaxial and irrotational.  $\sigma_2$  is vertical, and extensional;  $k = -0.3$  (*i.e.* non-plane strain).

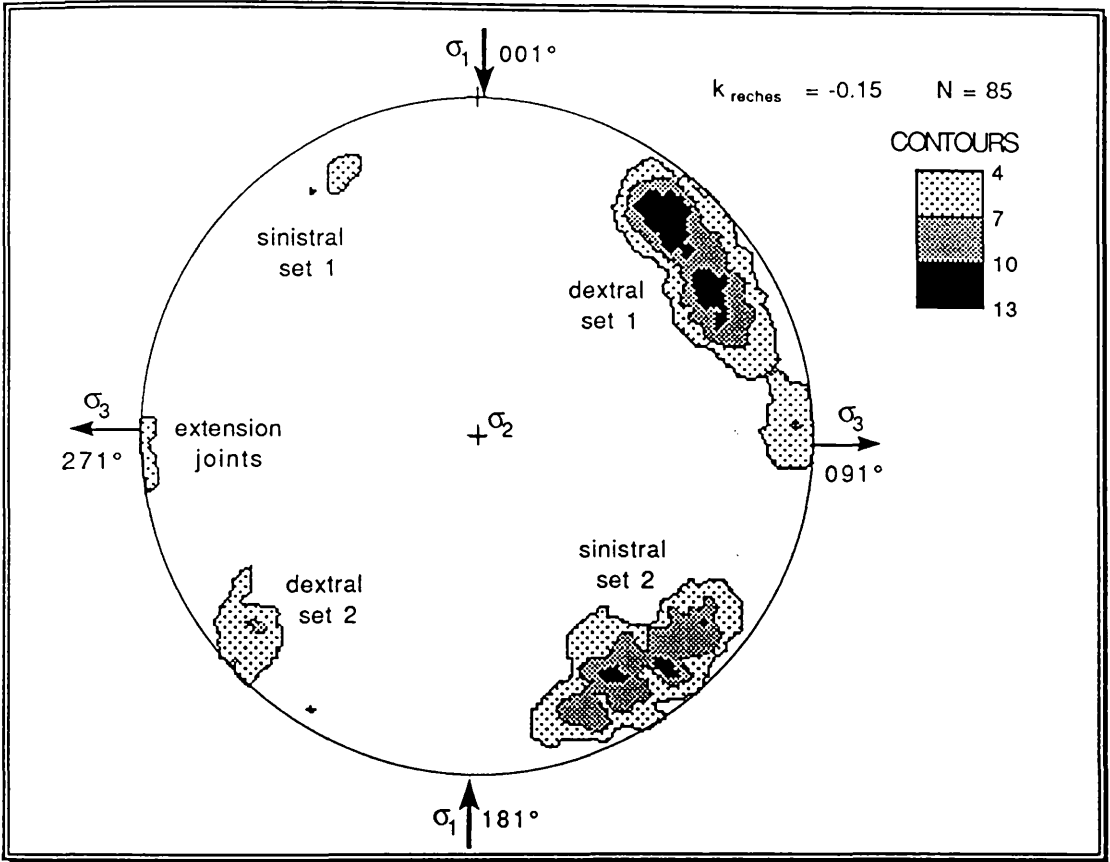


Fig. 4.23j. Dynamic interpretation of mesofracture station S19, from the L.ORS, Earlston. Joints are contoured using the "faces" macro described in Appendix 1. Strain is triaxial and irrotational.  $\sigma_2$  is vertical, and extensional;  $k = -0.15$  (*i.e.* non-plane strain).

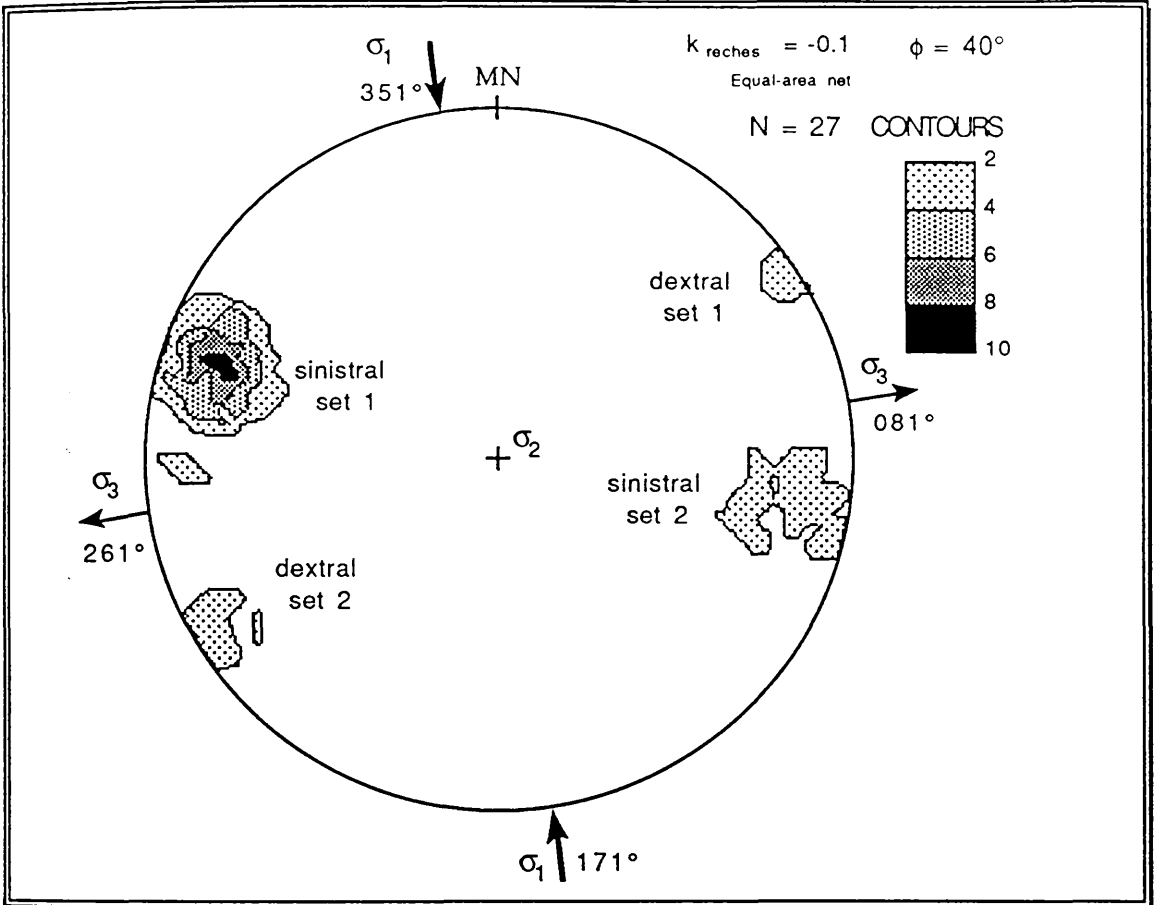


Fig. 4.23k. Dynamic interpretation of mesofracture station S20, from the L.ORS, Chapelbank, Strathearn. Sinistral, dextral and undifferentiated faults are contoured together (using the "pufs" macro described in Appendix 1). Strain is triaxial and irrotational.  $\sigma_2$  is vertical, and extensional;  $k = -0.1$  (*i.e.* non-plane strain).

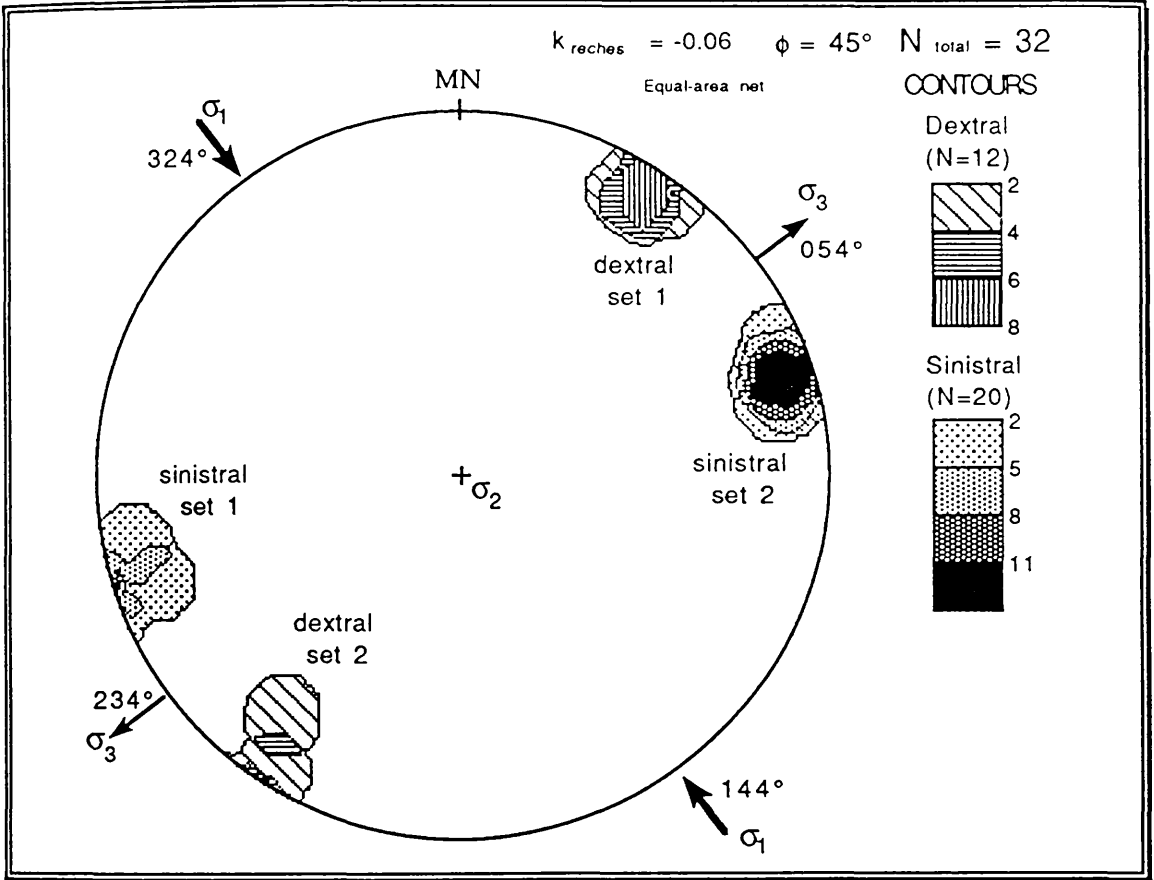


Fig. 4.231. Dynamic interpretation of mesofracture station S21, from the L.ORS, Bracklinn Falls, near Callander. Sinistral and dextral faults are contoured separately (using the "faces" macro described in Appendix 1). Strain is triaxial and irrotational.  $\sigma_2$  is vertical, and extensional;  $k = -0.06$  (i.e. slightly non-plane strain).

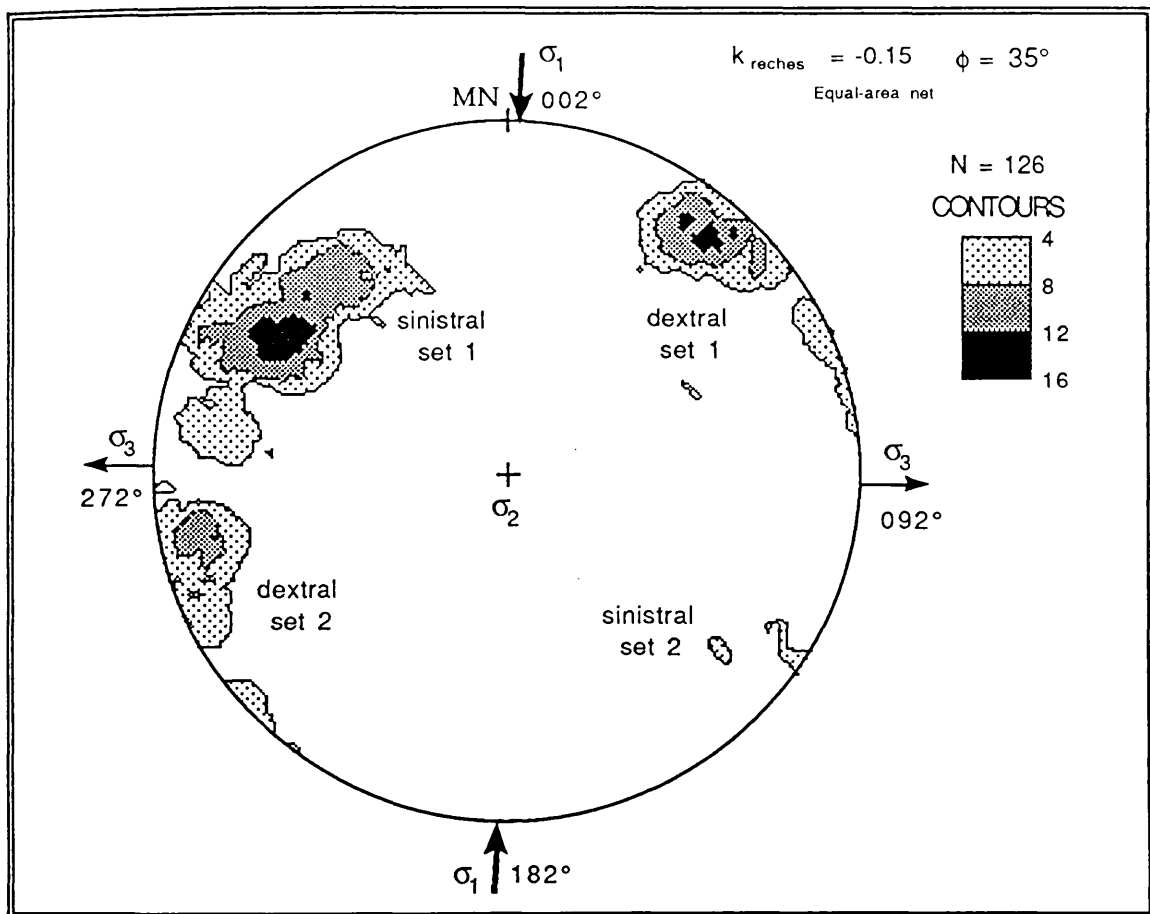


Fig. 4.23m. Dynamic interpretation of mesofracture station S22/23, from the L.ORS, Carmichael. Joints, and sinistral, dextral and undifferentiated faults are contoured together (using the "pufs" macro described in Appendix 1). Strain is triaxial and irrotational.  $\sigma_2$  is vertical, and extensional;  $k = -0.15$  (*i.e.* non-plane strain).

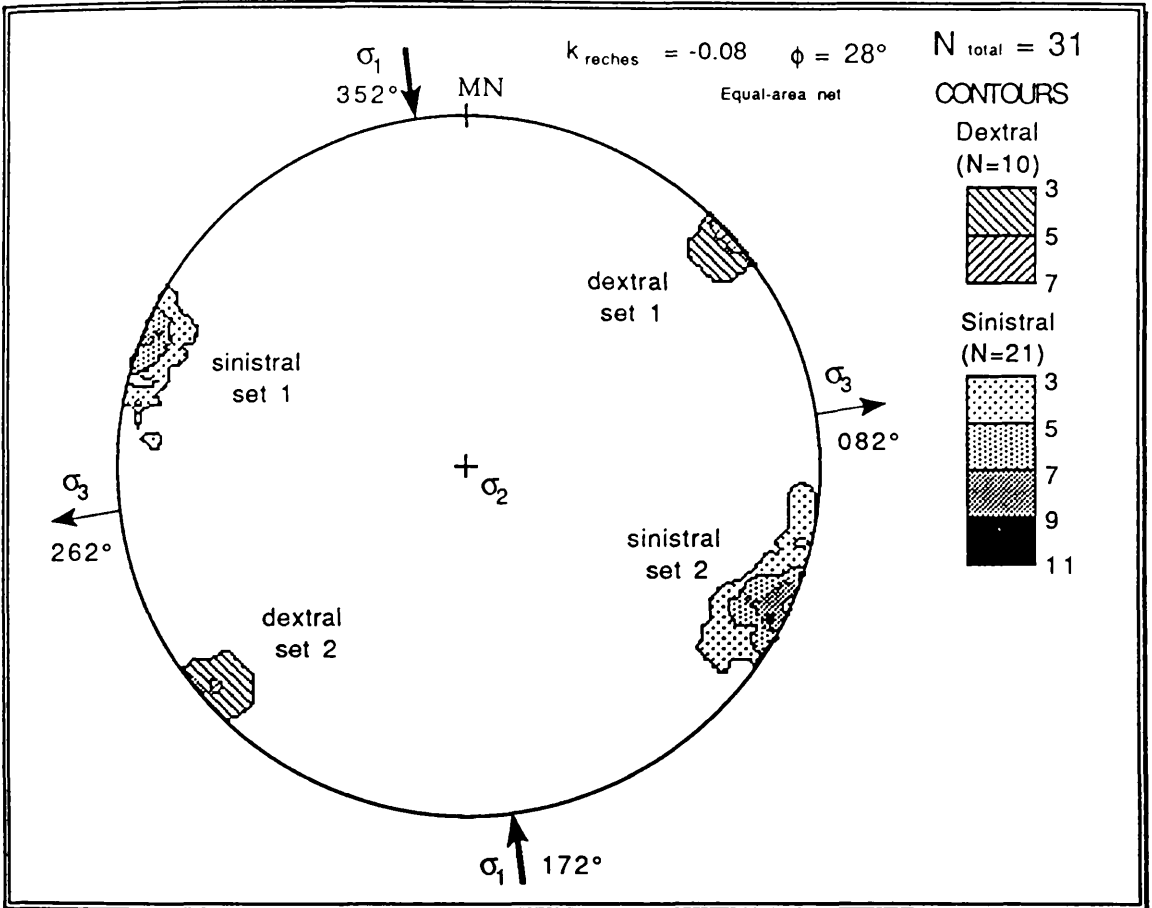


Fig. 4.23n. Dynamic interpretation of mesofracture station S24, from the L.ORS, River Ericht, near Blairgowrie. Sinistral and dextral faults are contoured separately (using the "faces" macro described in Appendix 1). Strain is triaxial and irrotational.  $\sigma_2$  is vertical, and extensional;  $k = -0.08$  (*i.e.* slightly non-plane strain).

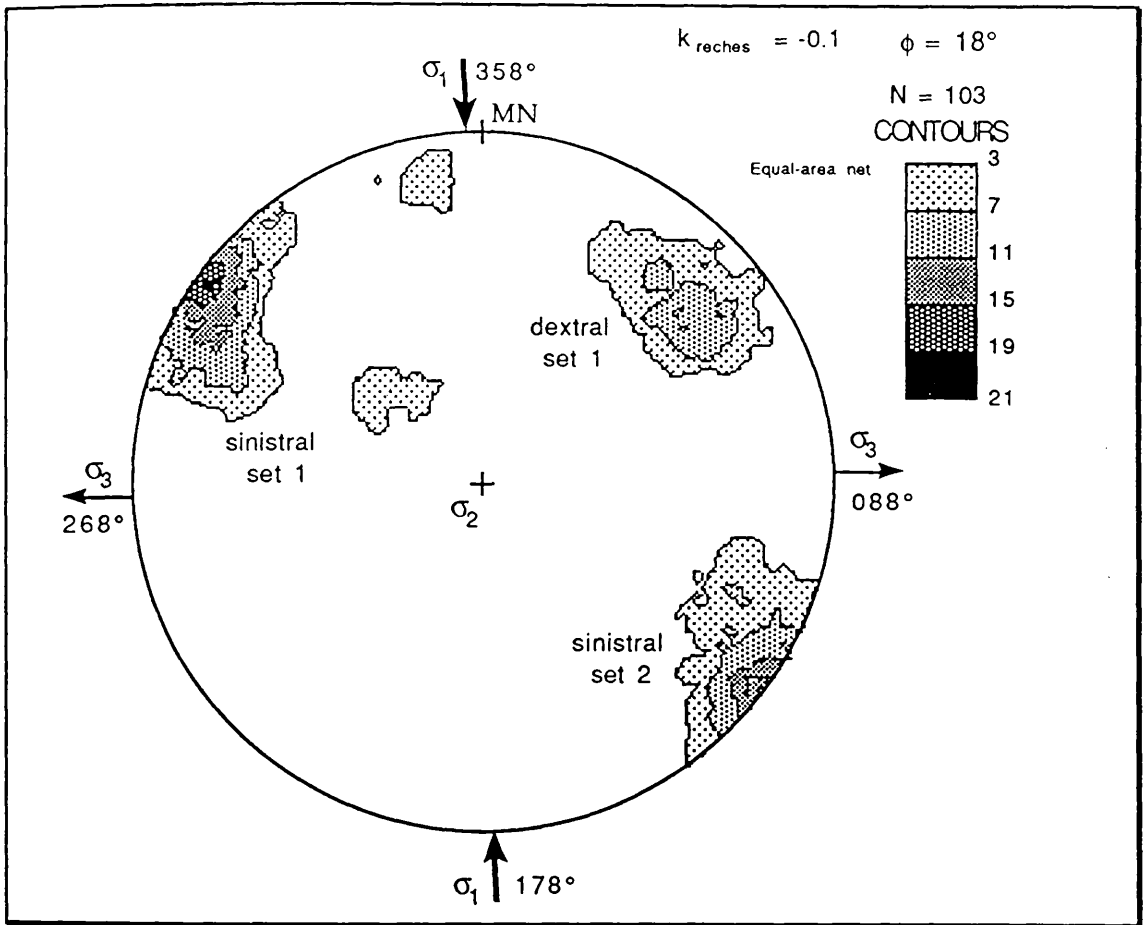


Fig. 4.23o. Dynamic interpretation of mesofracture station S25, from the Comrie Diorite, Loch Lednock. Joints, and sinistral, dextral and undifferentiated faults are contoured together (using the "pufs" macro described in Appendix 1). Strain is triaxial and irrotational.  $\sigma_2$  is vertical, and extensional;  $k = -0.1$  (*i.e.* non-plane strain).

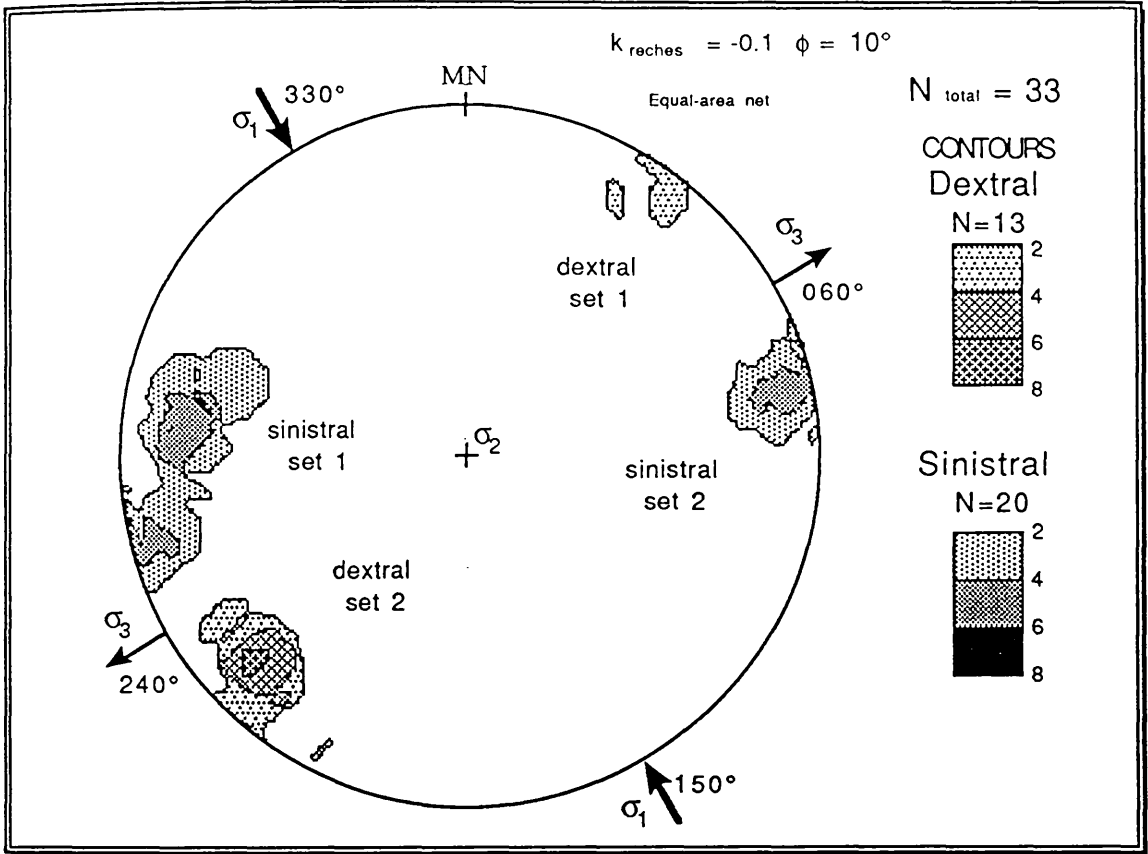


Fig. 4.23p. Dynamic interpretation of mesofracture station S26, from the Dalradian, Falls of Leny. Sinistral and dextral faults are contoured separately (using the "faces" macro described in Appendix 1). Strain is triaxial and essentially irrotational (a small component of rotation might be present).  $\sigma_2$  is vertical, and extensional;  $k = -0.1$  (i.e. non-plane strain).

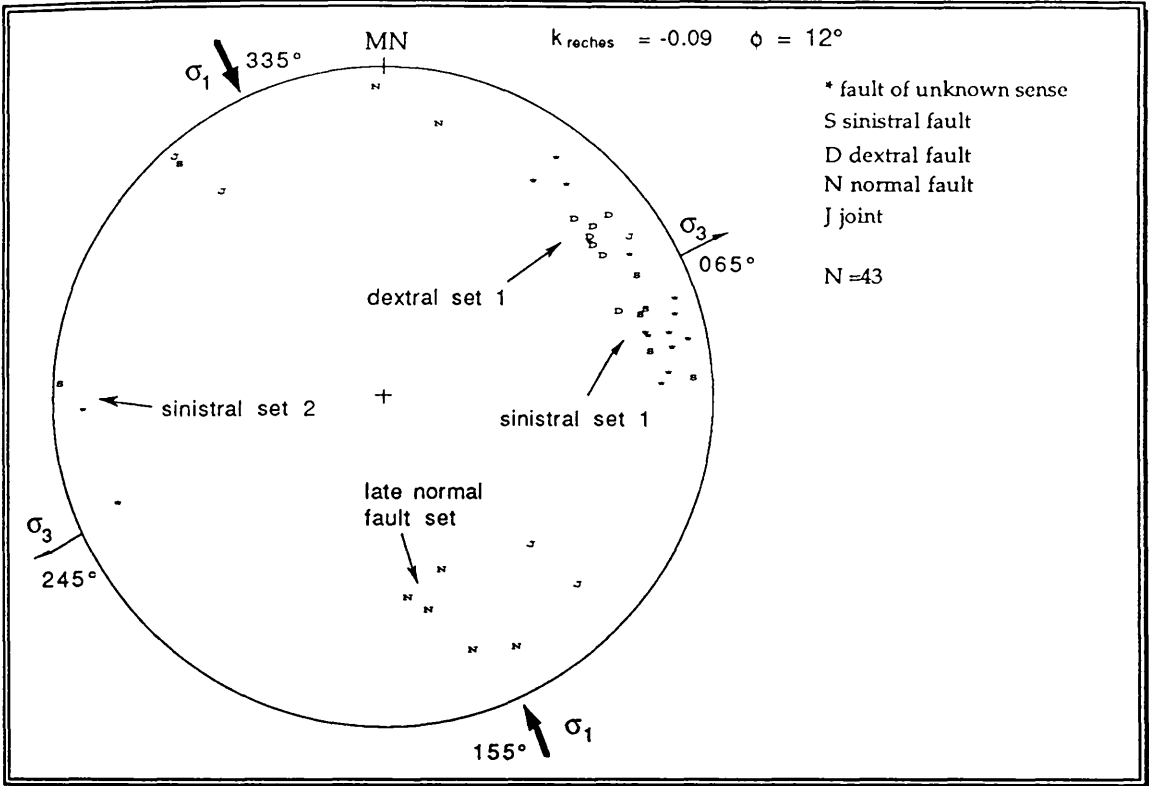


Fig. 4.23q. Dynamic interpretation of mesofracture station S27, from the L.ORS, Doune. The very friable nature of the arenites gives the outcrop a heavy bias of south-westerly dipping fracture planes, and consequently the plot is not contoured. However, strain is triaxial and appears irrotational.  $\sigma_2$  is vertical, and extensional;  $k = -0.09$  (*i.e.* non-plane strain).

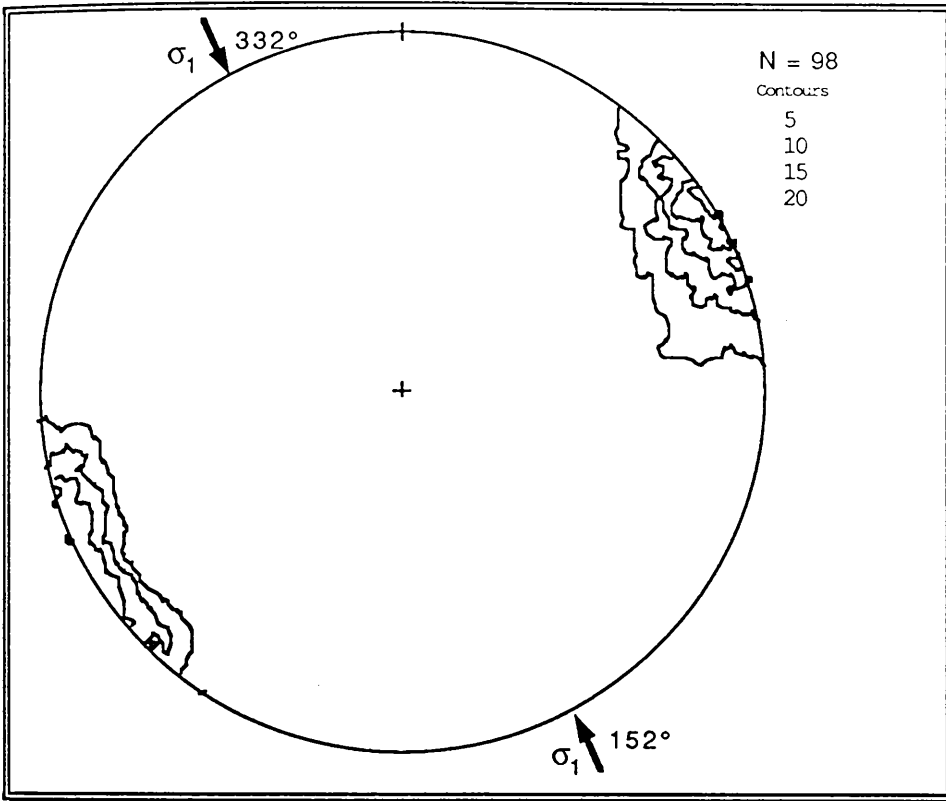


Fig. 4.23r. Dynamic interpretation of a study of faulted conglomerate clasts from Balmaha, Loch Lomond, made by Dr. P.W.G. Tanner (see Fig. 4.9x).

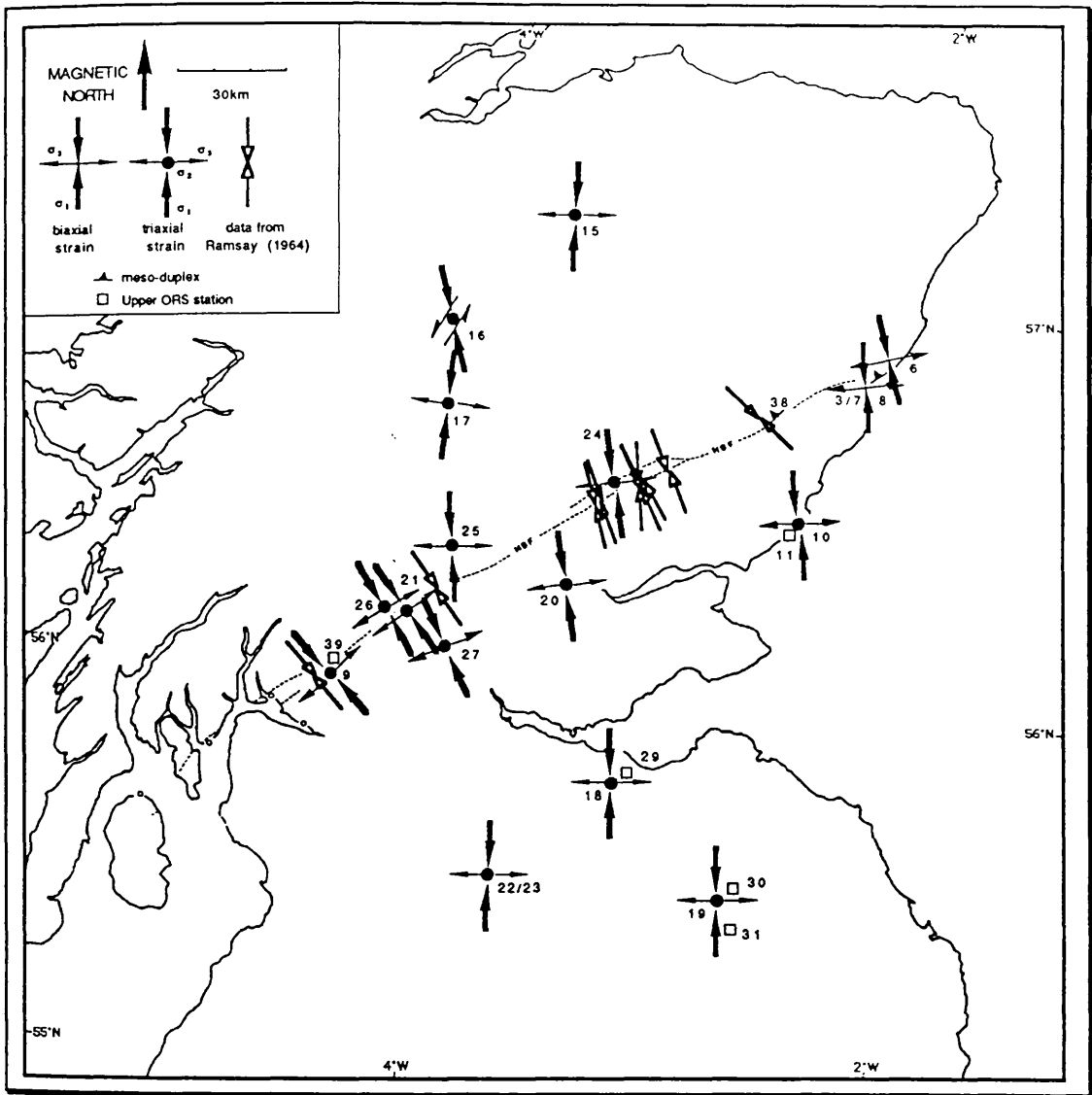


Fig. 4.24. Regional interpretation of mid-Devonian deformation in central Scotland, based on the dynamic analysis of mesofractures. Numerals refer to the mesofracture station numbers, as given in section 4.5.3. The symbol depicting station 16 represents the possible relation between the mesofractures and the nearby sinistral Loch Erich fault.

In summary: mesofracture analysis has shown that the Reches model can be directly applied, at least qualitatively, to the brittle deformation in central Scotland; many stations show non-plane strain, having four sets of non-vertical fractures of the predicted fault sense, with non-horizontal (*i.e.* oblique) slip vectors.

## 4.7 Mid Devonian Folding

The aim of this section is to determine in three dimensions the extent of mid-Devonian deformation that is represented by folding (as opposed to fracturing) of the L.ORS sediments. As with the fracture analysis in the preceding sections, this must consider deformation in three dimensions, including possible rotational strain.

### 4.7.1 Fold geometry

The Strathmore syncline and Sidlaw anticline (Fig. 1.1) form one of the largest fold pairs in Great Britain, with a wavelength of over 30km and a 200km axial trace spanning the entire length of the Midland Valley. The overall fold structure seems clear from BGS 1:50 000 maps, however it should be noted that a reversal of dip direction does not exclusively prove the presence of a fold axis; such changes in dip can represent angular unconformities that typify, for instance, the structural inversion of strike-slip basins (*e.g.* Galdeano 1987).

A further complication exists in the interpretation of Midland Valley fold geometry, as it is unclear how much of the present day "fold" geometry represents the original structure of the L.ORS sedimentary basin(s) (*i.e.* what was the pre-folding basin geometry of the L.ORS?). Some primary influence is suggested by the facies changes across the Strathmore syncline (Armstrong & Paterson, 1970), but the clearest indication that tectonic deformation is largely responsible for the present geometry is found on the steep, northern limb of the Strathmore syncline. Several NW-SE sections across the Midland Valley show that dips decrease rapidly but progressively from steep, vertical or even overturned, through to horizontal towards the SE (*e.g.* River N.Esk, Glen Artney, Menteith Hills, Drymen).

### 4.7.2 Mechanism of folding

The geometry of folds is strongly dependant upon the operative fold mechanism. An understanding of the likely style of folding is essential in constructing geological cross-sections and in restoring these sections to calculate the amount of tectonic shortening represented by the folds.

The geometry of large-scale folds is often difficult to determine. Syn-genetic small-scale parasitic folds are useful in revealing the geometry of higher order folds, but minor folds have not been recognised in the Midland Valley, and more indirect evidence must be used.

The following evidence suggests that the Strathmore and Sidlaw folds were produced by flexural-slip mechanisms, to give a parallel fold geometry (in the classification of Ramsay 1967; Tanner 1989):

- a) the folding is intimately associated with brittle deformation that characterises the uppermost part of the crust.
- b) no macro- or microscopic cleavage is visible in the ORS rocks.
- c) ORS sediments appear unstrained in thin section.
- d) some bedding parallel meso-scale fractures do exist, though they are difficult to recognise and characterise because there are very few bed-transecting markers to demonstrate the amount and sense of displacement that has occurred.

Field evidence at Stonehaven may indicate why unequivocal bedding-parallel flexural slip surfaces are not easily recognised within the ORS strata. On Old Kirk Shore (G.R. NO 88608723) a L.ORS dyke (Hutchison 1925) has been imbricated along a bedding-parallel slip surface. The surface is situated within a well-laminated fine-grained argillaceous bed that shows *no* other evidence of slip (such as the development of fibre veins *etc.*).

Based on the assumption that the folds have parallel geometry it is possible to construct a geological cross-section to show the present day fold structure. A computer program, based on a rigid set of geometric rules to give parallel fold geometries, was used to construct and plot a section across the northern Midland Valley, using dip data from surface outcrop (Fig. 4.25). Appendix 2 contains details of the construction method and the program used.

The section constructed is probably a reasonable approximation to the present geometry of the Midland Valley folds. However, the cross-section cannot be used to calculate the amount of tectonic shortening represented by the folds, unless it can be shown that the section is orientated parallel to the regional shortening direction, and that deformation was plane strain and irrotational (*i.e.* not transpressional). This is discussed in detail in the following sections.

#### 4.7.3 Section balancing and transpression

Since the pioneering work of Dahlstrom (1969) the technique of section-balancing has been used extensively to calculate both shortening across orogenic belts (*e.g.* Hossack 1983) and extension across sedimentary basins (Gibbs 1983). The most important assumption inherent in section

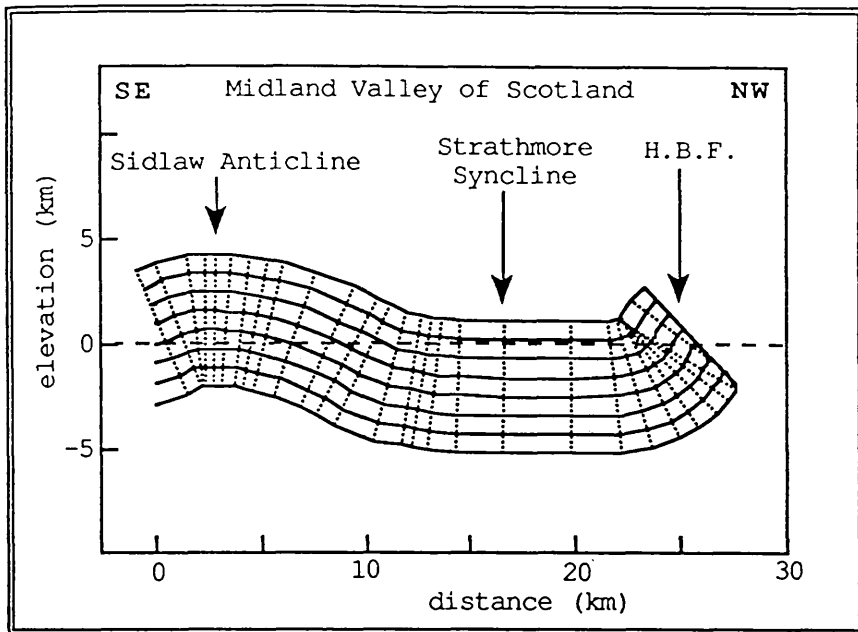


Fig. 4.25. SE/NW composite section across the northern Midland Valley of Scotland showing present day fold geometry, based on 30 representative dip values from the BGS Stirling sheet.

balancing methodology is that the deformation is plane strain and the cross section contains both the maximum and the minimum principal strain axes (the intermediate axis of the strain ellipse is neutral in plane strain). This assumption does not hold when the deformation contains either of the following components of strain:

1) non-plane strain (Fig. 4.26a). Flattening strains ( $0 < k_{\text{flinn}} < 1$ ) move material out of the plane of the section, and section balancing gives rise to underestimates of shortening. Conversely, constrictional strains ( $\infty > k_{\text{flinn}} > 1$ ) introduce additional material into the plane of section, and section balancing gives rise to underestimates of extension.

2) a simple shear (*i.e.* rotational) strain, about any axis non-perpendicular to the plane of cross-section (Fig. 4.26b). This does not alter the area of a cross-section, but does lead to a restored section that is incorrect.

Transpressional and transtensional deformation (Harland 1971) contains both of the above strain components (Sanderson & Marchini 1984).

The results of the mesofracture analysis presented in section 4.6 show that mid-Devonian deformation was triaxial and was *regionally* transpressive with respect to the Highland Boundary Fault. Consequently, normal section balancing procedures cannot immediately be applied to the Midland Valley folds, and the effect of transpressional deformation must first be investigated.

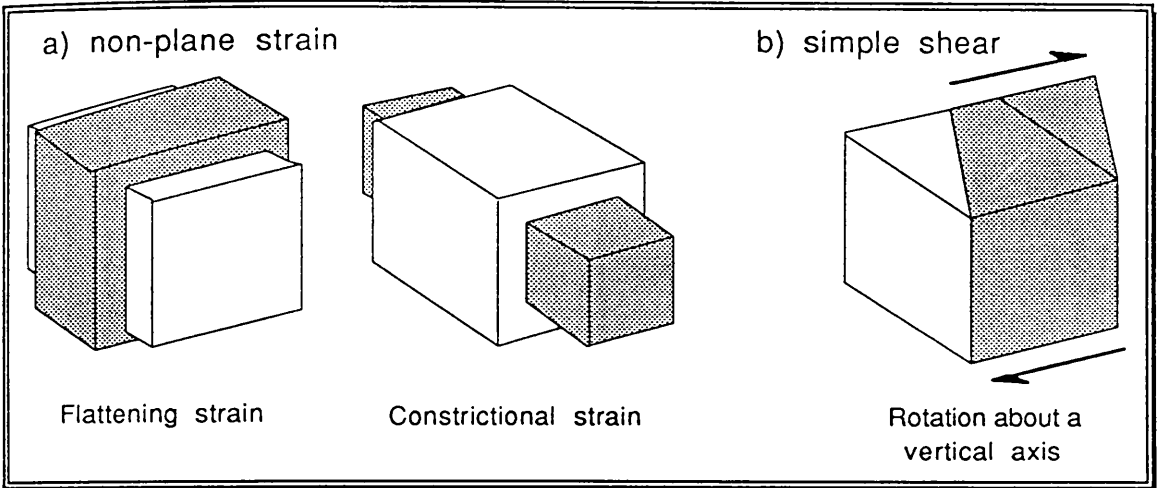


Fig. 4.26. Strain components that invalidate the principles of two dimensional section-balancing.

#### 4.7.4 Application of transpression models to the Midland Valley folds

The purpose of this section is to determine whether existing models of transpressional deformation can explain the present orientation of the Strathmore/Sidlaw folds; and hence whether these models can be applied without modification to the Lower ORS in the Midland Valley of Scotland, in order to derive the magnitude of folding deformation.

The least complicated description of transpression is given by Sanderson & Marchini (1984), who fully describe the deformation mathematically by assuming homogeneous strain. Harland (1971) identified a form of deformation which he labelled "simple transpression", and which he described in terms of a set of boundary conditions in which basin closure results from the oblique approach of two rigid basin margins. Harland envisaged that basin closure would occur by folding, and hence the deformation is heterogeneous and more difficult to describe. Shortening of the transpressional zone causes folds to rotate progressively, towards parallelism with the transpression zone boundaries, due to the component of simple shear (Fig. 4.27).

The equations given by Sanderson & Marchini (1984, p.453) show the relationship between the pure and simple shear components and the amount of shortening across the transpression zone (see Fig.4.28).

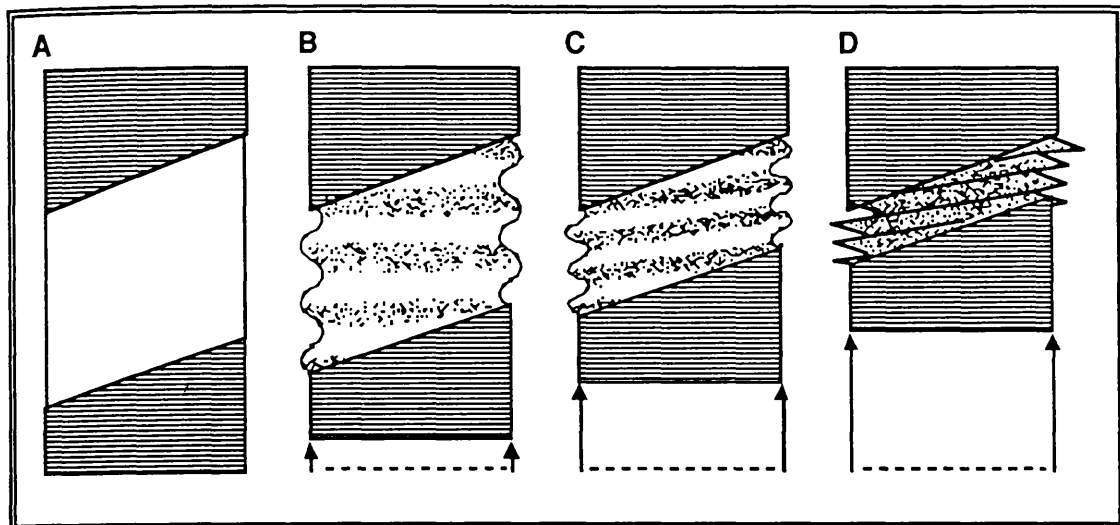


Fig. 4.27. Schematic representation of "simple transpression" from figure 3 of Harland (1971). The four stages show oblique closure of a basin, with progressive rotation of fold hinges towards parallelism with the zone boundaries.

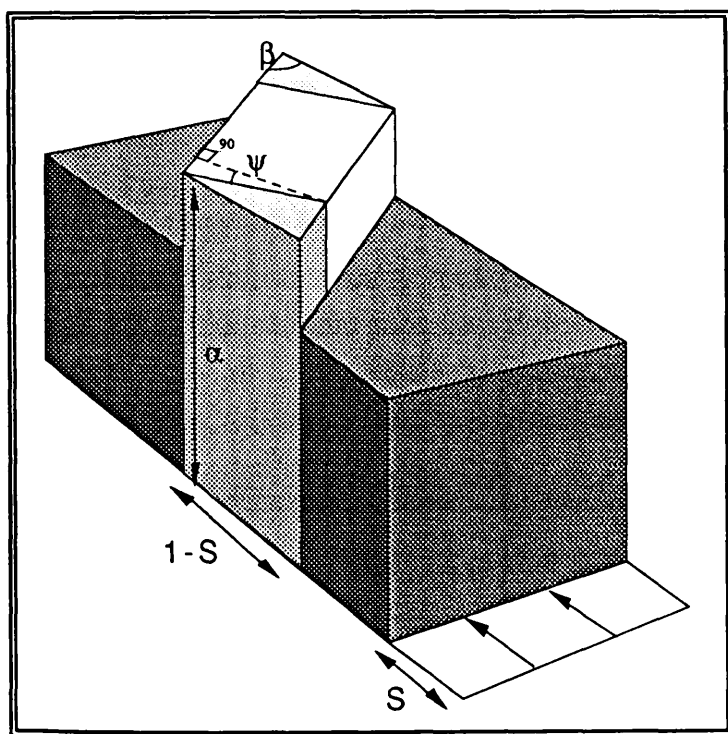


Fig.4.28. Homogeneous simple transpression, illustrating the parameters given in equations 1 and 2.

$$\text{pure shear contraction; } \alpha^{-1} = (1-S) \quad (\text{EQ.4.1})$$

$$\text{simple shear strain; } \gamma = \tan \psi = S (1-S)^{-1} \cot \beta \quad (\text{EQ.4.2})$$

where:  $S$  is the amount of shortening in the external  $\sigma_1$  direction

$\beta$  is the angle of external  $\sigma_1$  to the transpression zone boundaries

( $\psi$  is angular shear strain )

The variation of  $\gamma$  during progressive shortening is shown graphically for different  $\beta$  values in Fig. 4.29. At 100% shortening  $\gamma$  is infinite.

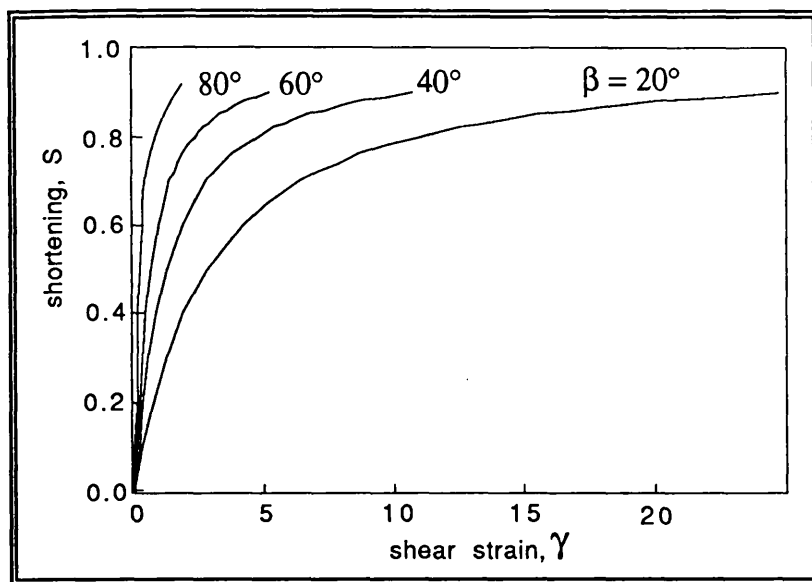


Fig. 4.29. Graph showing how shear strain  $\gamma$  increases with shortening during simple transpression, as described by EQ.4.2. Four curves are shown, representing different  $\beta$  values. The X-axis coincides with  $\beta = 0$  (simple shear), and the Y-axis with  $\beta = 90$  (pure shear).

Deformation manifested by folding is not homogeneous; consequently the model of simple transpression as originally envisaged by Harland is complex, and difficult to describe mathematically (appendix 3). However, the *qualitative* predictions of the "heterogeneous" Harland model are supported by the *quantitative* description of the "homogeneous" Sanderson & Marchini model.

One prediction of the Harland model that has relevance to the Midland Valley folds is that folds will progressively rotate during transpressional shortening. Importantly, if shortening is great, the folds *tend towards* parallelism with the zone boundaries, but some obliquity remains (Fig. 4.27D). This prediction agrees with the rotation of the finite stress ellipsoid, as described during homogeneous simple transpression.

The finite strain ellipsoid rotates due to the component of simple shear. The orientation of the long axis of the strain ellipse in the horizontal plane,  $\theta'$ , can be derived from the strain matrix of Sanderson & Marchini (1984):

$$\tan 2\theta' = 2\gamma / (\alpha^2 + \gamma^2 - 1) \quad \text{EQ.4.3}$$

By substituting EQ .4.1 and EQ.4.2 into EQ.4.3 the rotation of the strain ellipsoid is expressed in terms of shortening,  $S$ . This is shown graphically in Fig. 4.30;

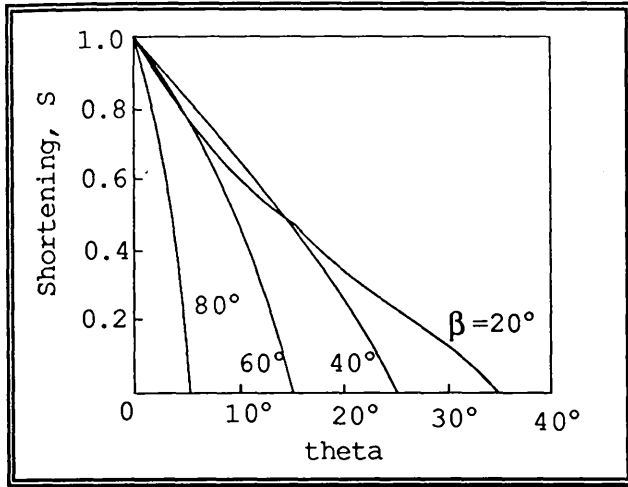


Fig. 4.30 Rotation of the long axis of the finite strain ellipse in the horizontal plane, during simple transpression. Four curves are shown, representing different  $\beta$  values. The strain ellipse only achieves parallelism with the zone boundary at 100% shortening.

Before applying the above discussion to the Midland Valley folds, the following salient points from preceding sections must be emphasised:

- a) the axes of the Strathmore/Sidlaw folds lie parallel to the HBF.
- b) the principal stress orientations at the time of brittle failure have been derived from mesofracture analysis; *regional* shortening was approximately north-south, though many stations close to the HBF show NNW-SSE shortening (*i.e.* approximately orthogonal to the HBF).
- c) mesofracture analysis shows that deformation was regionally triaxial, giving oblate strain.

Both the "quantitative" homogeneous transpression model (Fig. 4.28 - 4.30), and the "qualitative" heterogeneous transpression model (Fig. 4.27), show that folds can only achieve parallelism with infinite transpressional shortening. This inference is incompatible with:

- 1) the present orientation of the Strathmore and Sidlaw fold axes,
- 2) the low amount of shortening ("low", but not yet quantifiable, at this stage of the discussion) represented by the open folds, and,
- 3) the orthogonality of  $\sigma_1$  (with respect to the HBFZ) represented by many of the mesofracture stations situated close to the HBF.

Such incompatibility suggests that the current models for transpression cannot be applied to the mid-Devonian folds of the Midland Valley.

Palaeomagnetic studies have been used by structural geologists to help constrain the amount of rotation by block faulting (*e.g.* Ron *et al.* 1984, 1986), the rotations of microplates (*e.g.* Kissel *et al.* 1986), and to measure the amount of folding in rocks that have a poorly defined palaeo-horizontal (*e.g.* Kent 1988). The potential use of palaeomagnetic studies in measuring the rotation of folds that develop during transpression, is discussed in detail in Appendix 3, together with further analysis of the Midland Valley folds.

#### 4.7.5 Conclusions

There is no evidence of rotation of the Strathmore and Sidlaw fold axes. Thus, the folds appear to have developed parallel to the HBF due to a local, orthogonal  $\sigma_1$ , during regional N-S shortening. This is incompatible with our existing understanding of transpression, and an alternative model is therefore developed in the following section.

### 4.8 Strain partitioning: modification of the simple transpression model

The conclusions from the previous section suggest that the Midland Valley folds represent predominantly pure shear deformation, and therefore the Harland model of simple transpression cannot apply. However, a pure shear origin for the folding gives rise to a serious strain-incompatibility problem on a regional scale, because there is then no expression of the component of simple shear that must result from oblique regional shortening.

#### 4.8.1 The strain partitioning model

In the alternative model for transpression that I propose here, the simple and pure shear components are completely partitioned into separate domains of deformation. Thus, the deformation is regionally heterogeneous, but there is no regional strain incompatibility.

The "strain-partitioning" transpressional model developed here has particular relevance to transpressional shortening across faults, to the

closure of fault-bounded basins, and to oblique orogenic shortening across elongate mountain belts.

Many major faults are long-lived crustal fractures that can undergo repeated re-activation. Although such faults are often complicated anastomosing shear zones (e.g. the HBFZ), they are here assumed to be planar vertical fractures of no finite width. A further condition, which can also never be fully realised, is that the faults are surfaces of zero friction (*i.e.* there is no resistance to slip).

Transpression across such a pre-existing frictionless fracture allows the entire simple shear component to act along the fracture. No pure shear

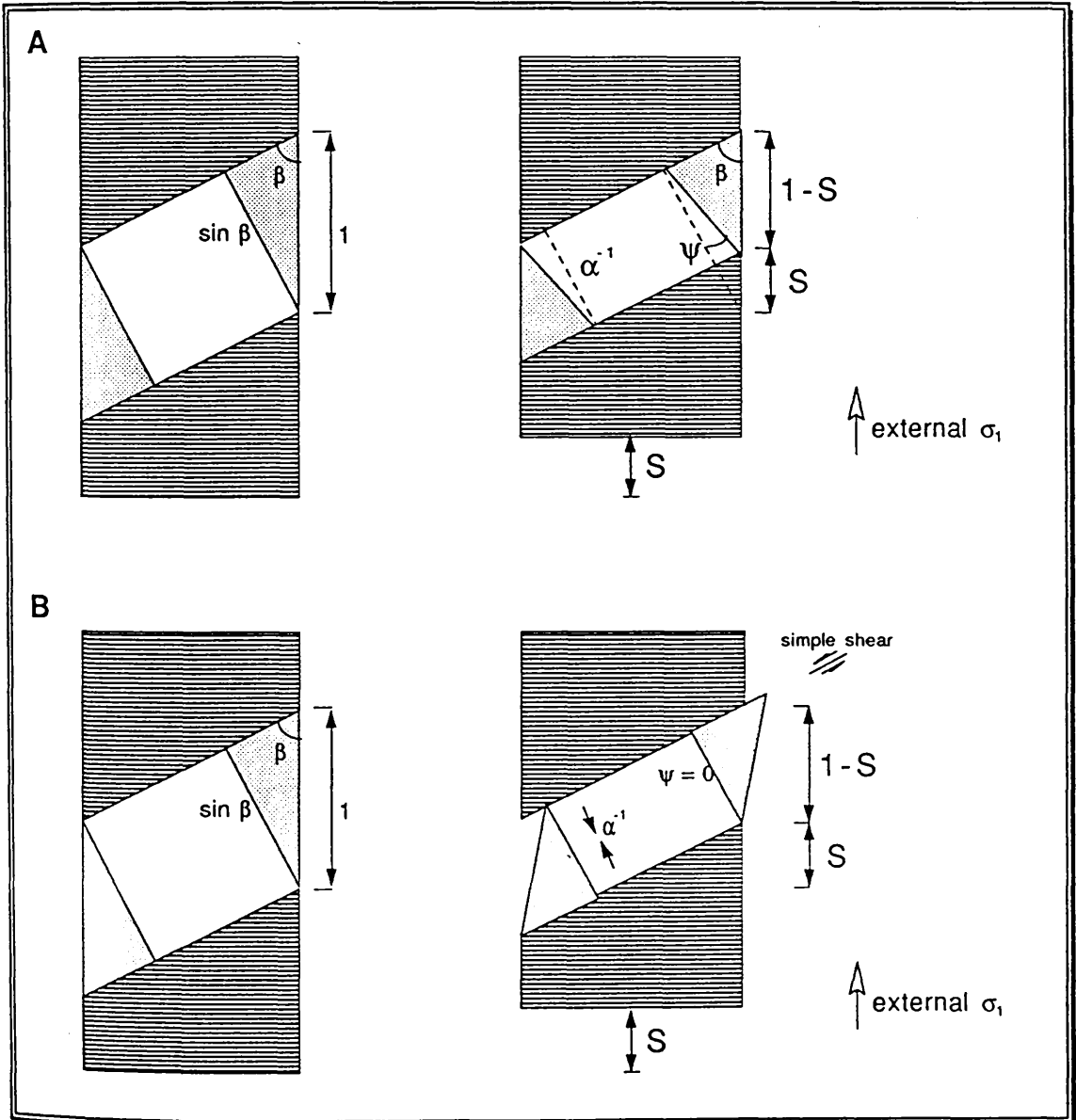


Fig. 4.31. A comparison of two models of simple transpression (plan view). (A) homogeneous transpression, with no loss of cohesion at the zone boundaries (from figure 6 of Sanderson & Marchini, 1984). (B) strain-partitioning model in which one of the zone boundaries is a pre-existing vertical frictionless fault.

across the vertical fracture is possible because the fracture has no width. The pure shear component therefore affects the rocks on one or both sides of the fracture. No simple shear affects these rocks, because it is taken up preferentially on the frictionless fracture. The strain-partitioning model of simple transpression is compared with the model of homogeneous simple transpression from Sanderson & Marchini (1984) in Fig. 4.31.

The assumptions of the strain-partitioning model, though unreasonable, allow one extreme deformational regime to be described. The two models shown in Fig. 4.31 can be considered to be "end-members" of transpressional deformation. Where structural heterogeneities form one or both of the boundaries of transpression zones, some strain partitioning is likely.

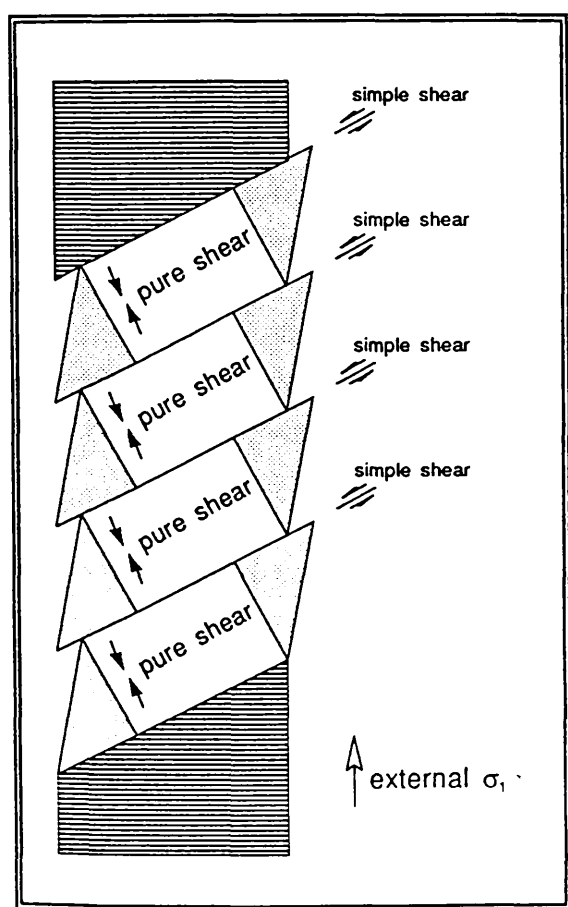


Fig. 4.32. Oblique shortening of a faulted basin (or a faulted orogenic belt), showing that stretching directions are only parallel to regional  $\sigma_1$  outside the deformation zone (plan view).

The strain-partitioning model has important implications for the deformation of anisotropic crustal material. For example, Fig. 4.32 shows the oblique closure of a faulted basin, in which all pure shear is evenly

distributed within fault blocks, whilst simple shear is taken up along the faults. An equivalent situation might exist during the oblique shortening of a faulted orogenic belt.

The importance of the strain-partitioning model is that the stretching lineations observed across the entire deformation zone do not lie parallel to the direction of regional shortening (*c.f.* Shackleton & Ries, 1984).

This implies that the foreland to deformation zones must be studied (if preserved) in order to predict the regional  $\sigma_1$  direction.

Construction of two-dimensional balanced cross-sections is only valid when it can be demonstrated that a component of simple shear strain has not been partitioned along faults that have high angles to the plane of section.

#### 4.8.2 Partitioned transpressive strain across the HBFZ

The strain-partitioning model helps to explain the kinematics of mid-Devonian transpression across the HBFZ. As a first order approximation, strain is partitioned into a component of pure shear in the Midland Valley, and a component of simple shear within the HBFZ. However, strain is not partitioned perfectly. The mesofracture analysis given in sections 4.5 & 4.6, together with the study of mid-Devonian folding (section 4.7), allow the various components of mid-Devonian strain to be characterised in more detail. Strain is partitioned into the following deformational domains (Fig. 4.34):

- 1) the northern Midland Valley is deformed by pure shear, manifested by upright open folds, and a pervasive non-plane strain (oblate) mesofracture array. Because the folding is irrotational the section across the Midland Valley shown in Fig. 4.25 can be restored, and indicates a typical shortening of approximately 7%. This is an underestimate, because deformation is non-plane strain, but the  $\sigma_3$  extension out of the plane of section cannot be quantified (unless it is assumed that the  $\sigma_1 : \sigma_2 : \sigma_3$  ratio for folding is the same as the average  $\sigma_1 : \sigma_2 : \sigma_3$  ratio derived from mesofracture analysis).
- 2) the pre-existing HBFZ is deformed principally by simple shear, further disrupting the HBC melange already produced during terrane accretion (see chapter 5). The amount of simple shear within the HBFZ is unknown.
- 3) some small domains in the L.ORS close to the HBFZ have experienced both pure shear and sinistral simple shear - this is because not all the simple

shear component is contained entirely within the HBFZ. This deformational component is represented in the stations that show evidence of overall rotation (*i.e.* a dominance of sinistral Riedel faults over dextral anti-Riedels). The effect of this component is shown schematically in Fig. 4.33.

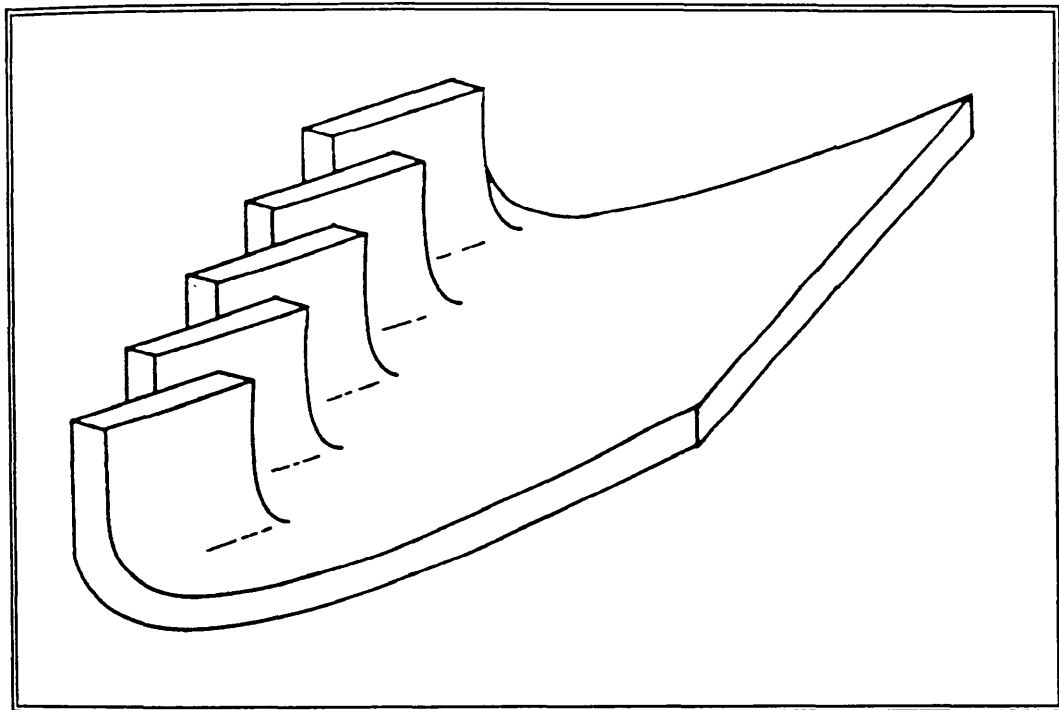


Fig. 4.33. Schematic diagram to show how some simple shear is seen in sub-domains close to the HBFZ, in stations that are dominated by faults that have offsets predominantly synthetic to HBFZ movement (*i.e.* Riedel-type fractures).

- 4) the Dalradian block north of the HBFZ is deformed by both pure and simple shear, represented by a non-plane strain mesofracture array and the oblique Tyndrum/Killin/Loch Tay macro-fault array.
- 5) the fault that is generally seen marking the northern margin of the HBFZ experienced a component of pure shear of unknown magnitude, carrying the Dalradian block on top of the HBC and the Midland Valley.
- 6) the southern Midland Valley and the northern Dalradian rocks are deformed by irrotational triaxial (oblate) strain, and so appear to lie beyond the margins of the transpression zone (*i.e.* they are the outside the area in which mid-Devonian deformation was influenced by the large heterogeneity of the reactivating HBFZ).

It is not possible to reliably quantify the collective magnitude of mid-Devonian deformation in central Scotland represented by all the above domains. As a rough estimate though, I think that the total amount of shortening is unlikely to exceed 20%. This corresponds to approximately 40km of shortening between mesofracture station 15 in the north, and station 19 in the south, with the extent of deformation generally diminishing away from the structurally weak (*i.e.* easily reactivated) HBFZ.

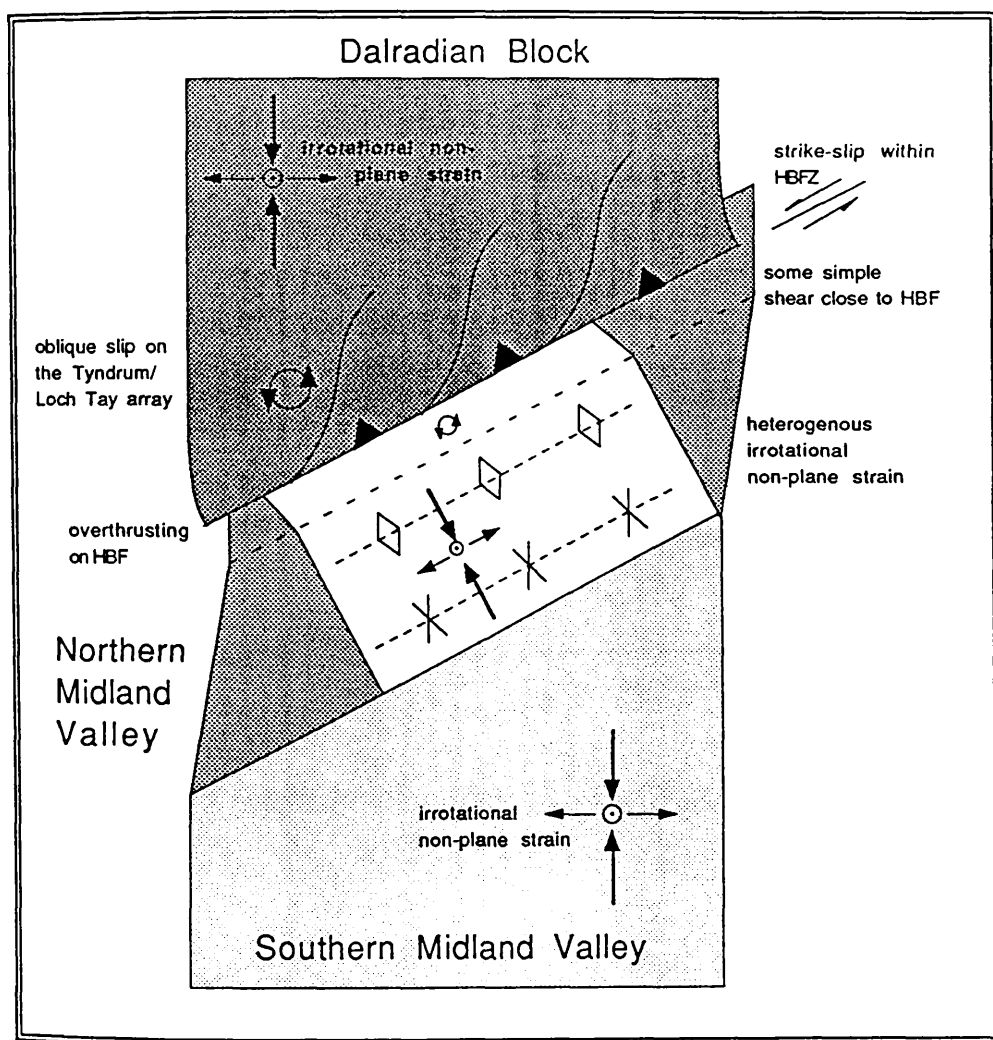


Fig. 4.34. Simplified plan view of the partitioned components of mid-Devonian transpression across the HBFZ.

#### 4.8.3 Partitioned strain across other major fault zones

Although many of the World's major fault zones have been the focus of much geological research, there are few well-documented examples of fault zones in which strain partitioning (or "stress decoupling") has been recognised. This may in part be due to an un-questioning acceptance of the applicability of the Riedel model in explaining strike-slip zones. In addition,

our understanding has been hindered by the historical segregation of faults into strike-slip, normal and reverse, and by the undue attention afforded to the pure shear and simple shear "end members" of deformation.

Strain partitioning *has* been recognised along the San Andreas fault in California (Andrews 1986, Mount & Suppe 1987). Andrews (1986) observed that deformation in the Mecca Hills transpressional restraining bend was partitioned onto separate thrust and strike-slip faults.

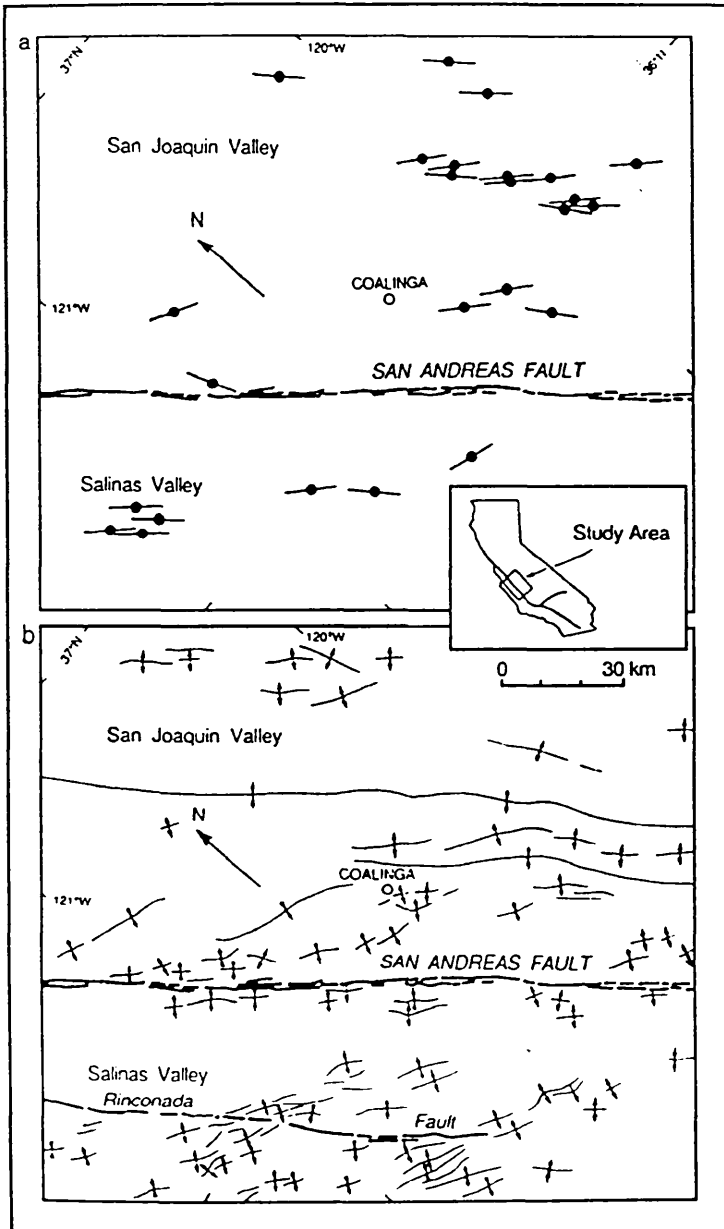


Fig. 4.35. Dynamic interpretation of data from San Andreas fault zone, central California, after Mount & Suppe 1987. (a) borehole elongation data; bars with circles indicate the direction of borehole elongation (minimum horizontal stress). (b) young fold axes and faults

More significantly, Mount & Suppe (1987) have documented neotectonic stresses (based on borehole elongations and breakouts) in rocks

flanking a 150km "straight" (Woodcock and Fischer 1986) section of the San Andreas fault. The borehole data, together with fold axial trace data, show that in some domains flanking the fault, the principal stress is perpendicular to the fault (Fig. 4.35).

Mount & Suppe used this data to hypothesise that the classic wrench tectonics model of Wilcox *et al.* 1973 may be inapplicable to real strike-slip zones, but as commented by Harding (1988) and Wickham (1988) this is unreasonable. Mount & Suppe imply that the San Andreas fault (and probably other faults also) actually *initiated* as a fracture surface with very low frictional coupling and drag. With the strain partitioning model that I have presented in section 4.8.1, this need not be so.

Mount & Suppe realised the dynamic effect of low frictional coupling across a fault, but their interpretation of its significance is questionable. In contrast, the strain partitioning model helps to explain the existence of some domains of en echelon folds, together with younger, fault-parallel fold domains. Unlike the HBFZ, the San Andreas fault appears to have initiated (or perhaps to have reactivated after burial by a sedimentary sequence) as a fault with *high* frictional coupling. Subsequently, during progressive deformation, the amount of strain partitioning increased as frictional coupling decreased.

**In summary:** the strain partitioning model, when combined with the classic wrench tectonic model, can give a more complete understanding of *progressive* fault zone movement, and fault zone *reactivation*.

# CHAPTER 5: TERRANE ACCRETION ALONG THE HBFZ

## 5.1 Introduction

The aim of this chapter is to describe and interpret the evidence of movement on the HBF *prior* to the Devonian brittle deformation already discussed in chapter 4. Earlier ductile tectonism had deformed rocks of the Highland Border Complex (HBC), a disparate suite of igneous, sedimentary, and metamorphic tectonic slivers. The HBC lies along the HBFZ and so marks the topographical and geological boundary between the Dalradian Highlands and the Midland Valley.

## 5.2 Structural description of the Highland Border Complex

The rationale of this research was to examine the HBC for evidence of high strain associated with major displacement along the HBFZ. Where possible, the aim of the study was to constrain the timing, sense, and amount of deformation, in order to build a rigorous model of the history of terrane accretion along the Highland Borders.

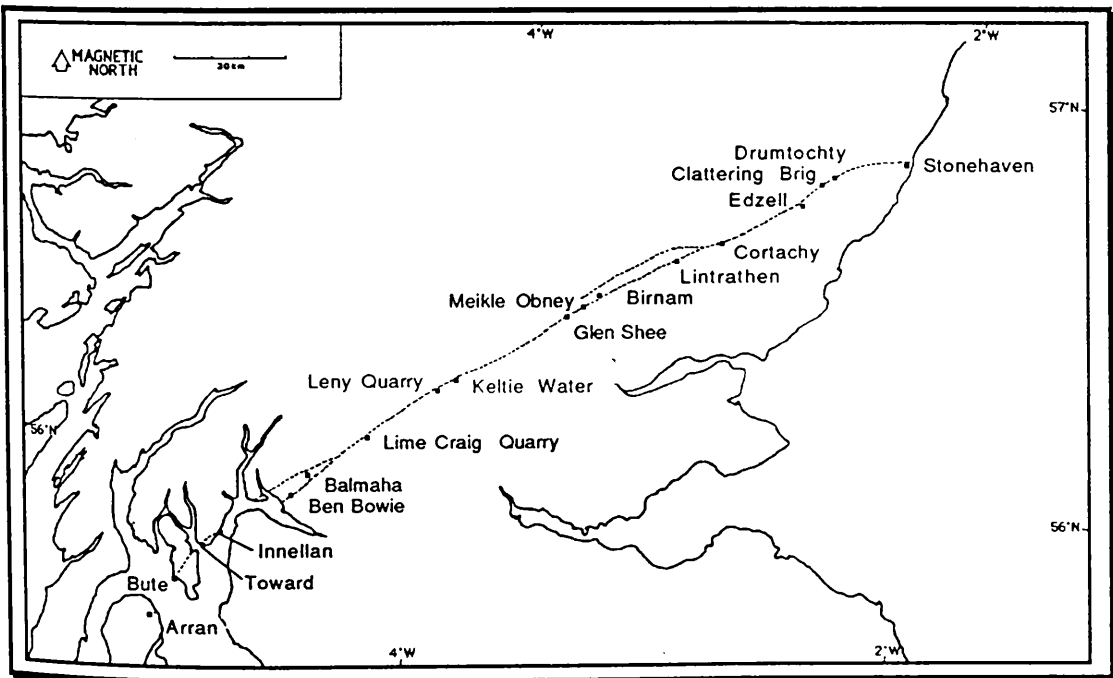


Fig. 5.1. Location map of HBC localities.

The *correlation* of geological structures, particularly those associated with high shear strain, is often more problematical than the correlation of stratigraphy. Because of this, I have described each locality individually, in order to present the data as objectively as possible. A regional synthesis and an *interpretation* of the data is given in chapter 6, together with a discussion of the uncertainties associated with such interpretation.

### 5.2.1 Structural description of the HBC at Stonehaven

The coastal exposures north of Stonehaven represent the largest and most continuous outcrop of HBC in Scotland. The sea cliffs afford clean exposure and vertical relief of up to 30 metres.

#### Previous research:

Published papers relating to the geology of Stonehaven include the following; Imrie 1812, Campbell 1911, Traquair 1912, Campbell 1913, Hutchison 1925, Anderson 1946 (p. 488), Ikin 1979, Booth 1985, Henderson & Robertson 1982 (p. 437), Ikin & Harmon 1983, Curry et al. 1984 (p. 124-125), Robertson & Henderson 1984, Whelan 1988 (p. 35-37), Marshall 1989.

#### Stratigraphy:

The Stonehaven section consists of Mid Silurian (ORS) arenites lying unconformably upon HBC metaspilites, with Dalradian grits thrust southwards over the HBC (Figs. 5.2, 5.3).

There have been a number of palaeontological discoveries from the HBC at Stonehaven, particularly from black shale horizons that are interbedded with the metaspilites (Campbell 1913). The reliability of Campbell's original biostratigraphical assignment has been questioned by Curry *et al.* 1984, and they assign a *probable* mid Ordovician age (*i.e.* Llanvirn-Llandeilo) to the black shales, based on a discovery of inarticulate brachiopods. A graptolite and a fragment of trinucleid trilobite have been rediscovered from the collection of the late Professor Gordon, and give confirmation of a Llanvirn-Llandeilo age (Alan Owen, pers. comm. 1990).

#### Field description, petrography & structural analysis:

The L.ORS ("Downtonian") Stonehaven Group is comprised of sandstones and siltstones, with occasional pebbly bands, and is of probable Late Wenlockian age (Marshall 1989). The tectonostratigraphic affinity of the sequence is not understood, and the obvious contrast with the rest of the L.ORS of the Midland Valley is difficult to explain. Unlike the coarse

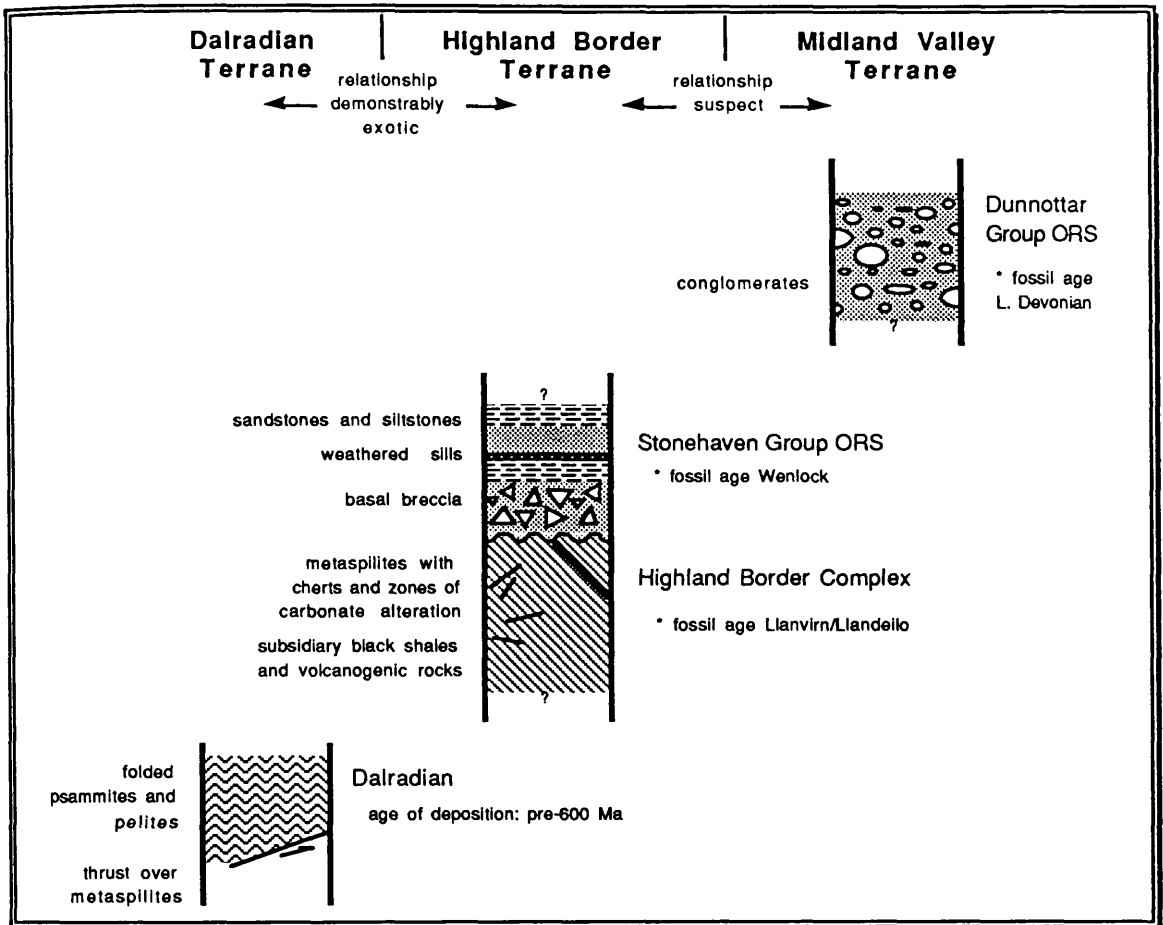


Fig. 5.2 Summary of stratigraphy at Stonehaven.

rudites that typify much of the Strathmore ORS, the Stonehaven Group probably represents distal deposition. The soft-sediment deformation that is widespread in the Stonehaven Group is not widely recognised in the younger ORS strata, and may indicate active tectonism during Mid Silurian times.

The relationship between the Stonehaven and Dunnottar Groups is uncertain. At normal tide levels there is a large gap in coastal exposure between Cowie and the cliffs south of Stonehaven Harbour. Further inland exposure is generally very poor, but a fault has been inferred on the B.G.S. (sheet 67). Campbell (1913) stated that the two Groups were conformable, though the recent palaeontological dating has shown the presence of a significant time-gap in deposition. Thus, this boundary must be viewed as tectonostratigraphically suspect (in the sense of Coney *et al.* 1980).

The unconformity between L.ORS and the HBC was first recognised by Campbell (1913) on Old Kirk Shore (G.R. NO 8865 8727). In the field it is difficult to identify, because of heavy fracturing and penetrative iron

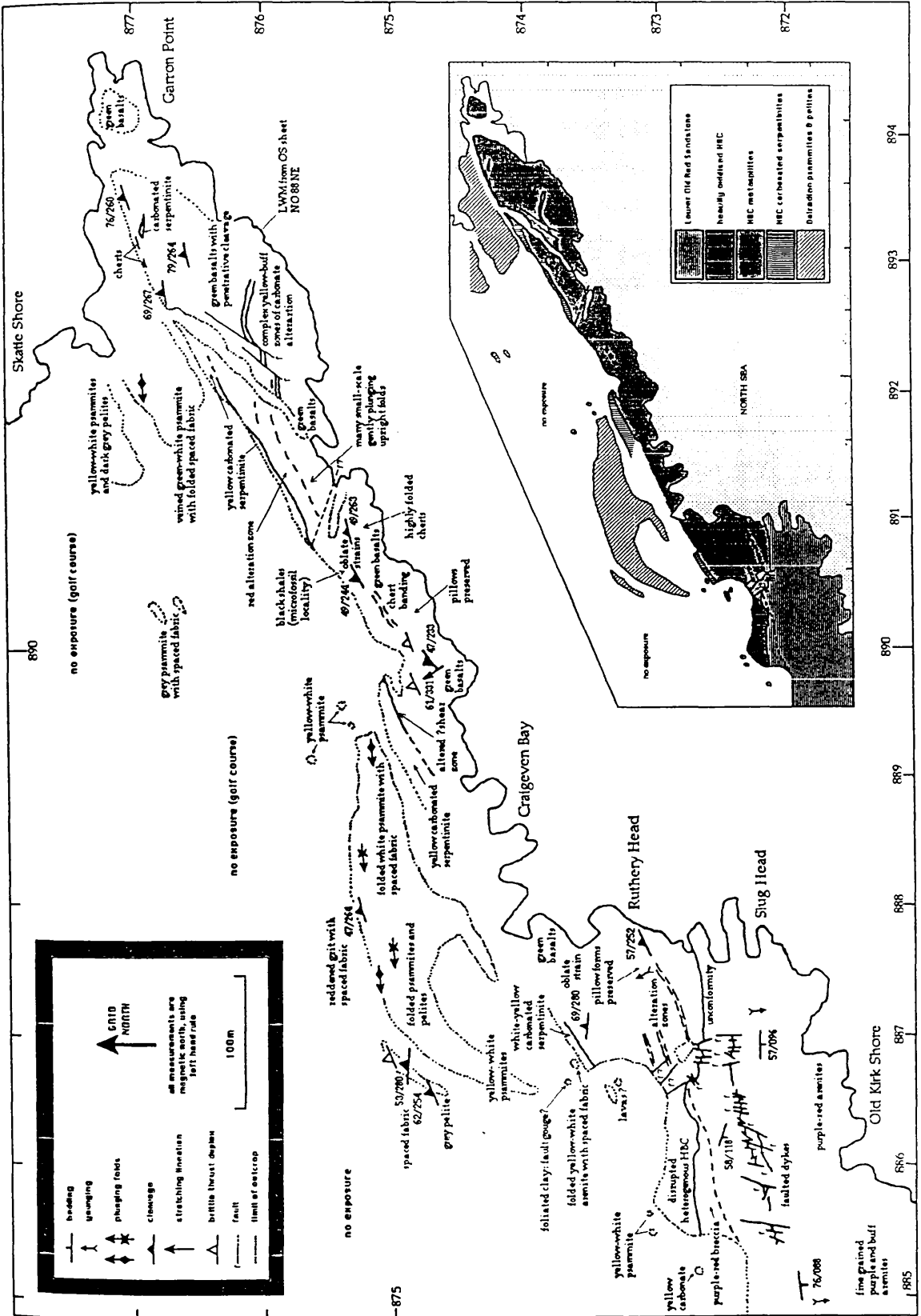


Fig. 5.3. Outcrop map of the shore section NE of Stonehaven. Inset is a tectonostratigraphic interpretation.

staining, but nevertheless is certainly present. The unconformity surface is cut by steeply dipping brittle faults (these probably originated during the mid-Devonian deformation event discussed in Chapter 4). The faults also offset two thin, highly weathered, basic sheets within the ORS on Old Kirk Shore (sample numbers S006, S007, S008). Hutchison (1925) considered the basic rocks to be an extrusive flow. This has important implications because they have been drilled by palaeomagnetists, to whom the exact age of the rocks is of great importance. I think that the field evidence is not conclusive, and that the 'lavas' may be intrusive sills.

HBC rocks below the unconformity are heavily oxidised, giving them a similar macroscopic appearance to the overlying ORS, and obliterating much of the microscopic evidence of their origin and original character (sample numbers S005, S011, S025). It is not even clear whether these rocks are of igneous, sedimentary, metamorphic or tectonic origin. It is possible, though not certain, that the reddened HBC is a heavily weathered HBC spilite. Some less oxidised blocks within the red HBC rocks of Old Kirk Shore (sample numbers S009, S010) resemble the metaspilites of Slug Head, both petrographically and in hand specimen. The heterogeneous nature of the reddened HBC is typical of the arid weathering of basic lavas (the volcanic Canary islands are a modern day analogue, in which the complexity and heterogeneity of the HBC rocks of Old Kirk Shore is certainly matched in the present day soil profile of weathered, oxidised basalts).

The contact at Slug Head (G.R. 8867 8728) between the red oxidised HBC and the green HBC spilites is not fully exposed and is difficult to interpret. The HBC has experienced a brittle deformation not seen in the overlying ORS, but this is difficult to characterise using mesofracture analysis, and may simply reflect the structural and lithological heterogeneity of the HBC.

The green HBC lavas of Ruthery Head, Craigeven Bay, and Garron Point have been interpreted as metamorphosed spilitised MORB basalts, based on 'stable' element geochemistry (Henderson & Robertson 1982, p.435). Pillow structures are preserved at G.R. NO 8875 8732 and G.R. NO 8902 8749. Caution is needed in interpreting the results of geochemical analyses because of the complex geological history and consequent level of alteration that typifies the metaspilites. Henderson & Robertson (1984) record that some samples show 'within-plate' or 'arc tholeiite' compositions.

The metaspilites (sample numbers S001, S002, S003, S016) have a penetrative cleavage with an overall orientation sub-parallel to, or slightly clockwise of the HBF (approximately  $50^{\circ}/250^{\circ}$ ). Strains are dominantly oblate, as defined by micas and flattened vesicles (sample number S016), . In thin section there is usually no significant alignment of micas and feldspar laths in the plane of cleavage, though steep stretching lineations can be seen in a few places (Fig. 5.3). Great care must be taken when using phyllosilicates to indicate stretching direction because of the flaky habit of these minerals. Erosion surfaces in the field, and thin sections for petrographic study, must both be cut exactly parallel to the plane of cleavage to see oblate strains; slight obliquity of even  $2-3^{\circ}$  will make round flakes appear extremely elongate (Fig. 5.4).

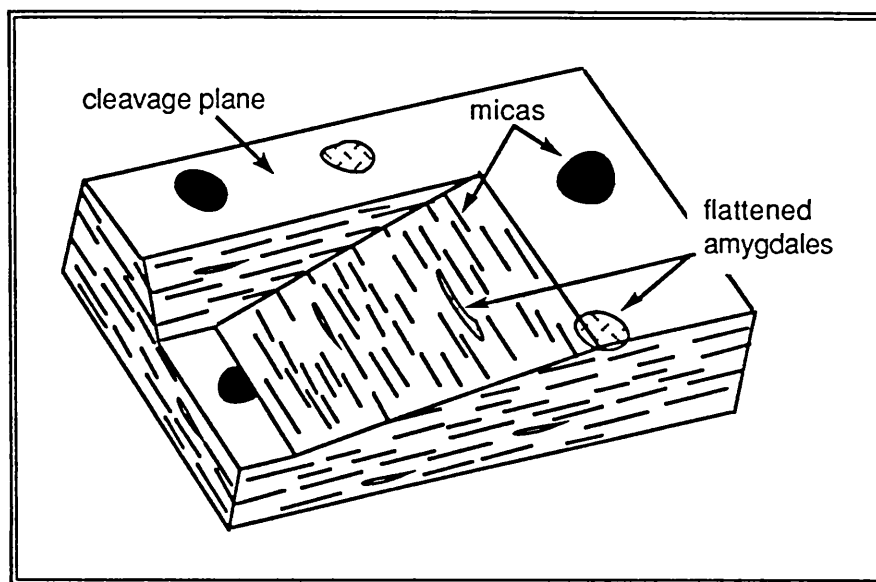


Fig. 5.4. Oblate strain in HBC spilites.

In places the orientation of the cleavage has been affected by later brittle deformation. Block faulting back-rotation has rotated the cleavage to give slight clockwise obliquity with respect to the HBFZ, and thrust-related folding of the pre-existing cleavage can be seen at G.R. NO 8897 8748 and G.R. NO 8901 8749. These features are described and interpreted in Chapter 4.

The metaspilites are cut by numerous thin yellow banded veins. These were interpreted as shear zones by Campbell (1913), but I have not yet seen reliable evidence for ductile simple shear within the veins. Slight cataclasis may have accompanied the precipitation of fluids along some of the veins (sample numbers S003, S004). This is indicated by occasional fragmentation of grains and invasion of carbonate along the fractures.

The HBF at Stonehaven is marked for much of its length by a 5 - 12 metre wide zone of yellowy-white massive heterogeneous carbonate rock (sample numbers S012, S013, S022), (Plate IIA in Anderson 1946). Campbell (1913) postulated that this rock represents a shear zone, an assumption adopted by most subsequent workers. Dolomitisation, alteration, veining, and fracturing are collectively so pervasive that the original character of the rock is difficult to ascertain with certainty in the thin sections that I have studied. Some sections (sample numbers S017, S018, S019) show relic structures and mineralogy, and indicate that the carbonate has replaced existing serpentine minerals. Campbell (1913 p. 928) documented angular metaspilite fragments within the dolomite, though I have been unable to corroborate this observation (these may be small zones of relic serpentinite, rather than discreet fragments).

In thin section the best-preserved (*i.e.* the least dolomitised) relic serpentinites show a crude fabric, defined by fine-grained anastomosing serpentine forming 'tails' around coarser elongate serpentine xenoblasts. I have *not* seen any asymmetric porphyroblasts or secondary cleavages in the serpentinite fabric that might indicate that the rock was mylonitic - *i.e.* produced by simple shear. A further, more extensive petrographic study could possibly uncover less altered relic zones with earlier mineralogy and tectonic fabrics better preserved. Petrographic study shows the following tentative geologic history for the carbonate rock:

7. brittle fracturing *youngest*
6. oxidation along veins & fractures
5. carbonate veining - 2nd generation
4. carbonate veining - 1st generation, possibly associated with cataclasis
3. carbonate alteration (replacement by cryptocrystalline & euhedral carbonate [?dolomite]), with subsidiary quartz mineralisation.
2. serpentine minerals strained to give LS tectonite fabric
1. serpentinitisation of existing ?ultramafic body *oldest*

Because of the high level of alteration further study is needed to confirm the composition and structural history of the HBC rocks.

The boundary between the metaspilites and the dolomitised serpentinites is well exposed on the east side of Craigeven Bay (G.R. NO 8895 8750). At this locality the contact is marked by a 2-3 metre wide alteration zone with well developed irregularly anastomosing fabric. These rocks have a similar appearance to a typical ductile shear zone, but the kinematic relevance of the exposure is difficult to ascertain (sample number S014).

### 5.2.2 Description of the Highland Borders at Drumtochty Castle

A xenolithic feldspar porphyry (sample number D01), with poorly defined bedding, is exposed in a 50m-long stream section in Luther Water near Drumtochty Castle (G.R. NO 694 804). Carbonate and brick-red opaques (iron oxide?) occur both as finely disseminated material and also concentrations in fine veins. Together they comprise 10-20 % of the groundmass.

The exposure is isolated, so the relationships with adjacent lithologies are unknown. Pelites (presumed Dalradian) lie 120m to the north, and ORS conglomerates lie just south of the porphyry.

### 5.2.3 Structural description of the HBC at Clattering Brig

The HBC rocks at Clattering Brig were studied in detail by Barrow (1901). Unfortunately the limestone quarry exposures described by Barrow (1901, p.337) were already obscured by the time of Anderson's review of the Highland Borders (Anderson 1946).

Exposure is very poor immediately west of the B 974 at Clattering Brig. East of the road, on the wooded east banks of Dueat Water, there is an incomplete section through the HBC (Fig. 5.5). HBC breccias are separated from presumed Dalradian by a 15m gap in exposure (marked by a shallow gully).

The purple-red HBC rocks are coarse, heterogeneous breccias, with angular and sub-angular clasts up to 3 cm in size (typically 4-10mm). The grain composition varies, but is dominated by quartz grains and quartz arenite rock fragments. The rocks consist of up to about 15% opaques, and as much as 40% carbonate mineralisation. The groundmass is probably composed of cryptocrystalline alteration products (this is beyond the resolution of the Zeiss Axioplan microscope, even with x40 objective).

### 5.2.4 Structural description of the HBC at Edzell

Rocks exposed in the River North Esk near Edzell represent one of the best sections through the HBC in Scotland. Unlike Stonehaven (where the HBC is not wide and there is good exposure *parallel* to the HBFZ), the river N. Esk provides a narrow cut through two kilometres of HBC, *perpendicular* to the Highland Borders. The river section, generally no more than 50m wide, is not complete, but nevertheless gives a good HBC profile, with

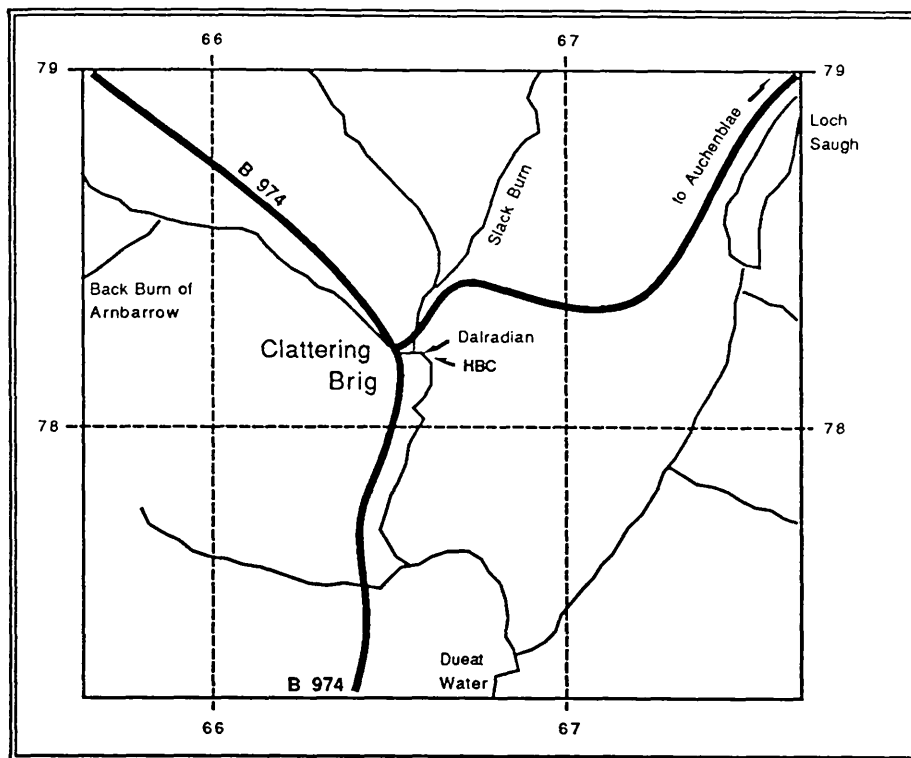


Fig. 5.5. Location map of the HBC exposed in the burn at Clattering Brig (G.R. NO 666 783). Dotted grid lines have a 1 km spacing, and are taken from OS 1:50,000 sheet 45.

vertical relief of up to 30m in places. Some of the contacts between separate lithological units are well preserved, unlike many HBC exposures elsewhere along the fault zone.

#### Previous research:

Published papers relating to HBC geology of the N. Esk section include the following; Barrow 1901, Pringle 1941, Anderson 1946 (p. 489-490), Johnson & Harris 1967, Downie *et al.* 1971, Booth 1985, Henderson & Robertson 1982 (p. 435, 437), Burton *et al.* 1984, Curry *et al.* 1984, Robertson & Henderson 1984, Whelan 1988 (p. 32-34).

The contact between Dalradian metasediments and the Margie series of the HBC is marked by the "North Esk Fault" of Johnson & Harris 1967, ("major thrust" of Barrow 1901, fig. 1). This locality (GR NO 586734) is one of very few along the length of the Highland Borders in which the contact zone between Dalradian and HBC is adequately exposed (the exposure is enhanced by washing the sand and silt from the outcrop).

Field description, petrography & structural analysis:

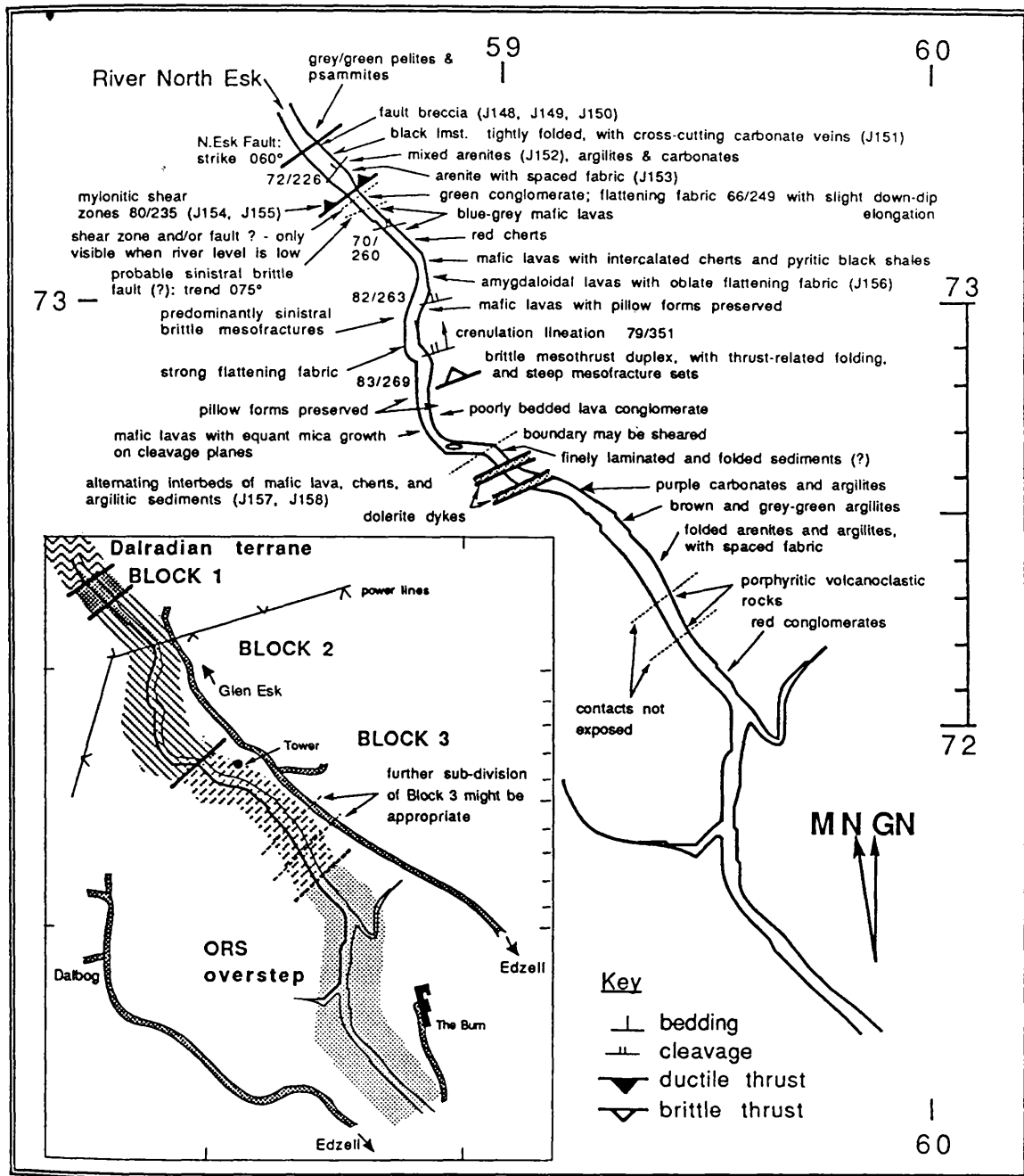


Fig. 5.6. Field map of the N.Esk section. Sample numbers are referred individually to in the text. Inset is a tectonostratigraphic interpretation (see Fig. 5.7).

The fault zone trends 060°-240°, and is marked by a poorly foliated breccia with highly polished, black, striated slickensides (*sensu stricto*; Wise *et al.* 1984). In thin section (sample numbers J148, J150; plate 1) it is clear that deformation is not restricted to slickenside surfaces, but is pervasive through the rock, affecting the (quartz) breccia clasts. Quartz grains are typically 1-5 mm in diameter; marked grain-size reduction has occurred by brittle fracturing. The precipitation of carbonate fluids and the formation of

slickensides are intimately associated with this brittle disintegration of the rock. The slickenside surfaces (thin section number J148(i) & J148(ii) ) are composed of angular quartz fragments (0.001 - 0.5 mm) in a fine grained fibrous phyllosilicate matrix, and are truly cataclastic in nature. No glassy material or fibrous quartz is present.

Internally, the quartz clasts show undulose extinction and weakly developed kink banding<sup>1</sup>, whilst the matrix is characterised by serrated grain contacts and the formation of subgrains. These features are characteristic of *deformation* and *recovery* under ductile conditions, and so the rock fits the very loose definition of a mylonite introduced by Bell & Etheridge (1973). Since their pioneering work, usage of the term "mylonite" has tightened<sup>2</sup>, and the dominance of crystal-plastic deformation over syntectonic recovery; the only slightly diminished grain-size; and the absence of a marked foliation, all preclude the N.Esk fault rocks from being truly mylonitic.

The protolith to the fault breccia was presumably a coarse quartzitic rudite or a metaquartzite. The association of ductile and brittle deformation of the breccia is enigmatic, but need not necessarily represent two entirely separate tectonic events. The overall character of the fault rock suggests that the rate of strain was high and the rate of recovery low, but the rock is not a typical cataclasite, and is difficult to fit into the classification of Wise *et al.* 1984 without invoking a complex progressive strain history (perhaps passing through the protomylonitic field into the cataclasite field).

The sense of fault displacement and the timing of the deformation(s) are unknown. The stratigraphic/structural position and micro-structural style of the breccia is consistent with the model for mid-Devonian deformation outlined in Chapter 4, but does *not* provide conclusive proof for the model. Without a reliable age for the deformation any interpretation of the relevance of the fault must be speculative.

Associated with the fault breccia is a very fine grained, light grey, poorly foliated rock (sample number J149), composed of microcrystalline quartz, phyllosilicates and opaques. The rock is probably a siltstone [the "grey shales" of Pringle 1941], though the resolving power of even the Zeiss

<sup>1</sup> here I use the term "kink band" in the sense of Bell & Etheridge (1973) to describe micro-deformational structures within strained crystals, and this should not be confused with the same term given to (generally macroscopic) angular chevron fold pairs (eg Anderson 1964, Dewey 1965).

<sup>2</sup> Wise *et al.* 1984 propose that the term "mylonite" be used for "coherent rocks with at least microscopic foliation, with or without porphyroclasts, characterized by intense syntectonic crystal-plastic grain-size reduction of the country rock to an average diameter less than 50 microns (0.05 mm) and invariably showing at least minor syntectonic recovery/recrystallisation."

Axioplan (x40 lens with high resolution condenser) is not sufficient to adequately resolve the optical properties of the constituent minerals.

Further south, after a 10m gap in exposure, fine grey ?siltstone (similar in appearance to sample J149) passes into a dark grey limestone (sample number J151). This is the "Margie Limestone" of Barrow 1901, and has been assigned a Caradoc age based on chitinozoan microfossils (Burton *et al.* 1984). The limestone is composed of coarse recrystallised carbonate, with thin interbedded layers of organic material that help to define a crude banding (bedding?). This is folded into tight to isoclinal folds that have subsequently been cross-cut by carbonate veins.

Sample number J152 is a poorly sorted grit [the "Margie Grits"], with quartz grains and subsidiary feldspar up to 1mm in diameter in a fine chlorite, carbonate, and quartz matrix. The rock has a weak foliation orientated at 72°/226°. Locally the beds young to the south, though folding may have disguised the regional younging direction.

Other lithologies (*e.g.* sample number J153) are compositionally similar to the Margie grits (dated micro-palaeontologically) but more closely resemble the Dalradian grits in appearance (both petrographically and in the field). They have a marked fabric defined by flattened quartz grains and aligned phyllosilicates, with a superimposed parallel spaced fabric. The classification of such rocks as belonging to the HBC or the Dalradian remains one of the fundamental problems in Highland Border geology, both in the N. Esk section and elsewhere within the HBFZ, and this is discussed in detail in the next section (section 5.3).

The contact between the Margie Grits and the Green Conglomerate is structurally important, but unfortunately was not exposed during several visits I made in 1987-89. According to Pringle (1941, p.138) the water level must be exceptionally low before the contact is exposed, and this led Barrow (1901) to originally misinterpret the contact as a conformable one.

The rocks that lie within 15 or 20 m of the contact are a heterogeneous mix of different lithologies, and include zones of higher shear strain; one such prominent zone (2 m wide) lies 5 metres north of the contact (sample numbers J154 and J155). Some rocks appear dolomitised, and are similar in field appearance to the yellow-white carbonate rock at Stonehaven (see section 5.2.1).

Sample J154 is composed of a heterogeneous quartz-mica schist, with a crude anastomosing foliation that varies in orientation (average 80°/235°), defined by segregated bands of felsic and mafic minerals. The schistosity is

overprinted by a sub-parallel carbonate replacement, and then later by a second, cross-cutting carbonate phase. In hand specimen the felsic segregations form tailed lenses that have no obvious asymmetry or rotation, and the overall strain appears oblate. In thin section the quartz grains are dominated by deformation banding and polygonisation, extreme grain-size reduction, and the formation of new grains and subgrains with serrated boundaries: these are deformation, recovery, and recrystallisation features that typify mylonites. I have seen no visible microscopic evidence of asymmetric fabric growth or of porphyroclast rotation in sample J154, although the carbonate overprint is extensive, and this makes it difficult to see through to the earlier fabric.

Sample J155, from the same shear zone as J154, more clearly represents strong mylonitisation, though once again this rock is not typical of mylonites commonly described in the literature (see section 6.3). The psammitic field appearance of the rock is misleading, and specimens must be sliced to show the true heterogeneity of structural fabric. The rock is comprised of discrete, elongate pods of varying composition, each with its own well-defined internal fabric. Some pods are very quartz-rich, others are phyllosilicate dominated, but this compositional segregation does not resemble a schistosity. Pods are typically 1-7 mm thick, and up to 50 mm long and wide. They are bounded by sharp curvi-planar pod margins that cut across the internal fabric of the pods. Some pod boundaries have acted as sites of subsequent brittle fracturing (these may represent the incipient development of a crude spaced fabric).

Mylonitisation in sample J155 is only recognisable in thin section. Thin-sections J155(i) and J155(iii) are orientated perpendicular to the rock fabric and parallel to a faint down-dip stretching lineation that has an approximate orientation of  $75^\circ/310^\circ$  (*i.e.* the sections are cut in the XZ plane). Section J155(ii) is cut perpendicular to both the fabric and the X stretching direction (*i.e.* it is cut in the YZ plane).

Quartz pods have been pervasively deformed by intense kink-banding and polygonisation. Some individual quartz polygons within kink-bands are themselves deformed by smaller scale polygonised kink-bands (at high angle to the larger scale bands).

Other pods are comprised principally of fine-grained micas with small porphyroclasts of quartz and subsidiary feldspar. Some pods have shear bands (C surfaces) deforming the S fabric defined by aligned micas. These S-C fabrics, together with occasional tailed porphyroclasts, show a consistent thrust sense of shear in sections J155(i) and J155(iii) (*i.e.* top to the south-east; *apparent* dextral sense in both sections). Section J155(ii) shows no

unambiguous and consistent shear sense indicators, but like the other sections may suggest a strong flattening strain.

The overall geometry of the beds in and around the shear zone(s) has been affected by later brittle fractures and mesothrusts (see chapter 4).

Flattening strain within the Green Conglomerate appears to decrease slightly southwards (*i.e.* away from the shear zone just described). However, this is due, in part at least, to a gradual increase in the clast-to-matrix ratio; the fabric is better defined when there are fewer clasts. Strain within the conglomerate is dominantly a flattening strain, with a smaller component of down dip elongation; clast shapes define an LS fabric, with  $k < 1$  (*i.e.* in the flattening field of the Flinn diagram). An approximate estimate of axial ratios is 4:3:1: note that this is based on brief observation and *not* detailed measurement, and the original clast shape fabric may have had an important effect on present shape fabric. The Green Conglomerate is approximately 20m in stratigraphic thickness, and is composed of lava and jasper clasts that have been assumed to be of local origin (Barrow 1901, Pringle 1941). Younging is to the north (Johnson & Harris 1967).

The contact between the Green Conglomerate and the mafic lavas ("Jasper & Greenrock Series" of Barrow 1901) is not well exposed. Fracturing intensifies near the contact, and a strong sinistral mesofracture set, with shallow plunging slickenlines, suggests that the contact is a steep sinistral fault zone striking 255°. The mesofracture set strike at 210°, and I interpret these as synthetic (*i.e.* Riedels) to the main fault.

The mafic lavas have a similar stable element geochemistry to the lavas at Stonehaven, and are thought to represent MORB type basalts (Henderson & Robertson 1982). In the N.Esk section there are abundant interbeds of chert and black shale. The identification of an Arenig - ?Llanvirn microfauna (Downie *et al.* 1971), has now been retracted (Rogers *et al.* 1989). The beds sampled by Whelan (1988) proved barren. Pillow shapes in the lavas show that the beds young to the north.

Structurally, the lavas have a strong flattening fabric with an average orientation of about 70/260°. This has been crenulated by later deformation. The fabric has been folded by later deformation associated with brittle faulting (see Chapter 4).

The southern contact of the mafic lavas, at the southern end of the river gorge, is marked by thin bands of lava and cherts interbedded or

intersheared with ?tectonised sediments (sample numbers J157 and J158). The sediments are strongly overprinted by carbonate, and this has almost totally destroyed earlier fabrics. The 'original' mineralogy appears to be composed of quartz and mica, and the rock was probably a fine siltstone. Following carbonatisation, the rock was folded irregularly to give a chaotic set of polyclinal folds. This contact between lavas and sediments is complex, and will require much detailed study before a reasonable structural description can be given. I have not seen reliable microscopic evidence that the contact is tectonic.

The beds to the south of the lava/sediment contact are an 800m sedimentary sequence of various lithologies, including a purple shale of Llanvirn - Ashgill age (Whelan 1988). Previously, the sequence has always been equated with the Margie units north of the mafic lavas (Barrow 1901, Whelan 1988), though this was based solely on field appearance. In this southern sedimentary sequence there is also a series of grey/yellow greywackes with a spaced cleavage, that are similar in appearance to the Dalradian metasediments. These have not yet yielded specifically diagnostic microfossils, and their origin remains uncertain.

The sediments are bounded to the south by a porphyry of Lintrathen type. Exposure is poor; the contact was believed to be a fault by Barrow (1901), but may be unconformable (Brian Bluck, pers. comm.). To the south the porphyry is faulted against Lower ORS sandstones.

#### Interpretation of Stratigraphy:

The high level of exposure and the abundance of sedimentary rocks in the N.Esk has enabled palaeontologists to erect a relatively detailed bio-stratigraphy for the HBC at this locality. The Mid and Upper Ordovician Margie Series, previously equated with the Lower Cambrian Leny Limestone (see section 5.2.10), occupies an important tectonostratigraphic position. The palaeontological dating of the Margie Series has highlighted the difficulty of correlating rocks in a fault zone, using either lithological similarity or structural style. The apparent continuation of Grampian-style deformation from the Dalradian into the HBC led Johnson & Harris (1967) to infer that Grampian deformation postdated the deposition of the HBC. This clearly cannot be so, if the age given by Burton *et al.* 1984 for the Margie Series is correct. The difficulties inherent in structural and lithological correlations are discussed in detail in section 5.3.4.

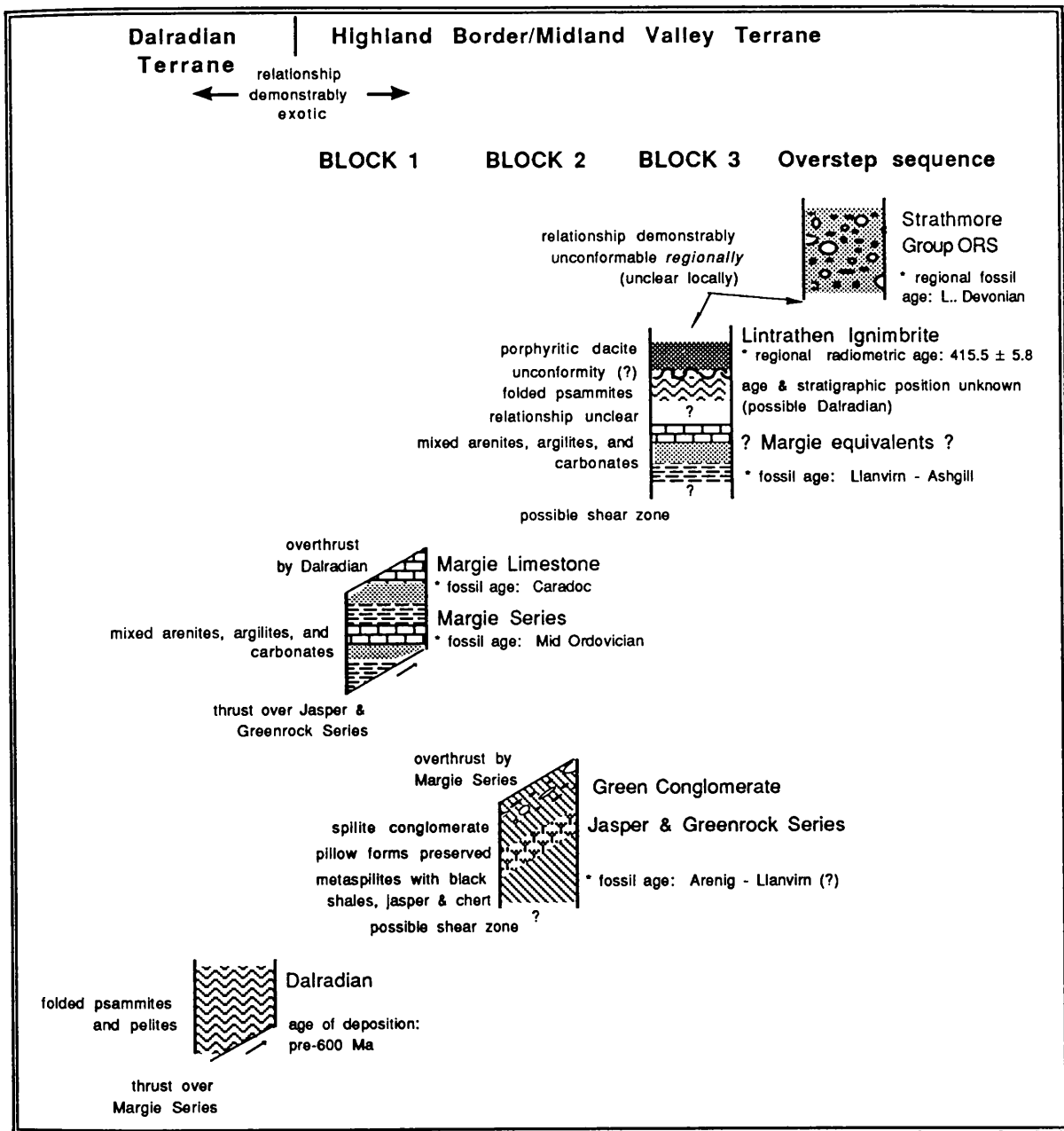


Fig. 5.7. Tentative tectono-stratigraphic interpretation for the Highland Borders in the River North Esk (see text for explanation).

### 5.2.5 Structural description of the HBC at Cortachy

Previous research:

This includes the following; Allan 1928, Anderson 1946 (p. 490), Ikin & Harmon 1981, Ikin & Harmon 1983.

Field description:

Dark green serpentinite conglomerates are exposed in the river S. Esk at the Bridge of Cortachy (G.R. NO 395598). The serpentinites are

1983). The conglomeratic nature of the rocks is probably entirely tectonic in origin, with sub-rounded serpentinite "clasts" floating in an anastomosing penetratively foliated and lineated serpentinitic matrix (sample numbers J0099, J0100).

Future work in the HBC should include a microstructural study of the serpentinites, particularly now that a suitable methodology for the structural analysis of serpentinites exists (Norrell *et al.* 1989).

The contacts of the serpentinite with surrounding lithologies are not exposed.

### 5.2.6 Description of the Highland Borders at Lintrathen and West Cult

Previous research:

This includes the following; Allan 1928, Anderson 1946 (p. 491), Paterson & Harris 1969, Harris & Fettes 1972, Ikin & Harmon 1981, Thirlwall 1983, Armstrong *et al.* 1985, Thirlwall 1988.

Stratigraphy:

Exposures to the south of the Loch of Lintrathen are the type locality for a porphyritic ignimbrite, called the Lintrathen porphyry, that has assumed an important position in the stratigraphy of the Scottish Caledonides.

Though originally mapped as a series of dacitic intrusions (Geike 1897), the porphyry was re-interpreted as a lava flow (Allan 1928), then later as an ignimbrite by Paterson & Harris 1969. These interpretations of a sub-aerial deposition for the porphyry are important, because they provide constraint on the ages of Dalradian peneplanation and ORS sedimentation. Thirlwall (1983,1988) has documented an adjusted age of  $415.5 \pm 5.8$  Ma (Rb/Sr on biotite and whole-rock) for the porphyry (the exact locality is not stated). It is clear from the petrographic description of the ignimbrite given by Paterson & Harris (1969) that great caution should be exercised in the radiometric dating of the Lintrathen porphyry, because of whole-rock alteration (including replacement of plagioclase and biotite), and the high content of xenolithic material enclosed within the ignimbrite.

Field description:

According to Paterson & Harris (1969) the relationships of the Lintrathen porphyry with the Dalradian and ORS are clearly displayed at West Cult (G.R. NO 06 41); their Figure 2 is reproduced here (Fig. 5.8A). However, because of the small amount of rock presently exposed (Fig. 5.8B) other interpretations are feasible, and the overall conclusions of Paterson &

Harris (1969), though probable, are not certain beyond all reasonable doubt. No boundaries between the various lithologies were exposed at the time of my field survey (May 1987).

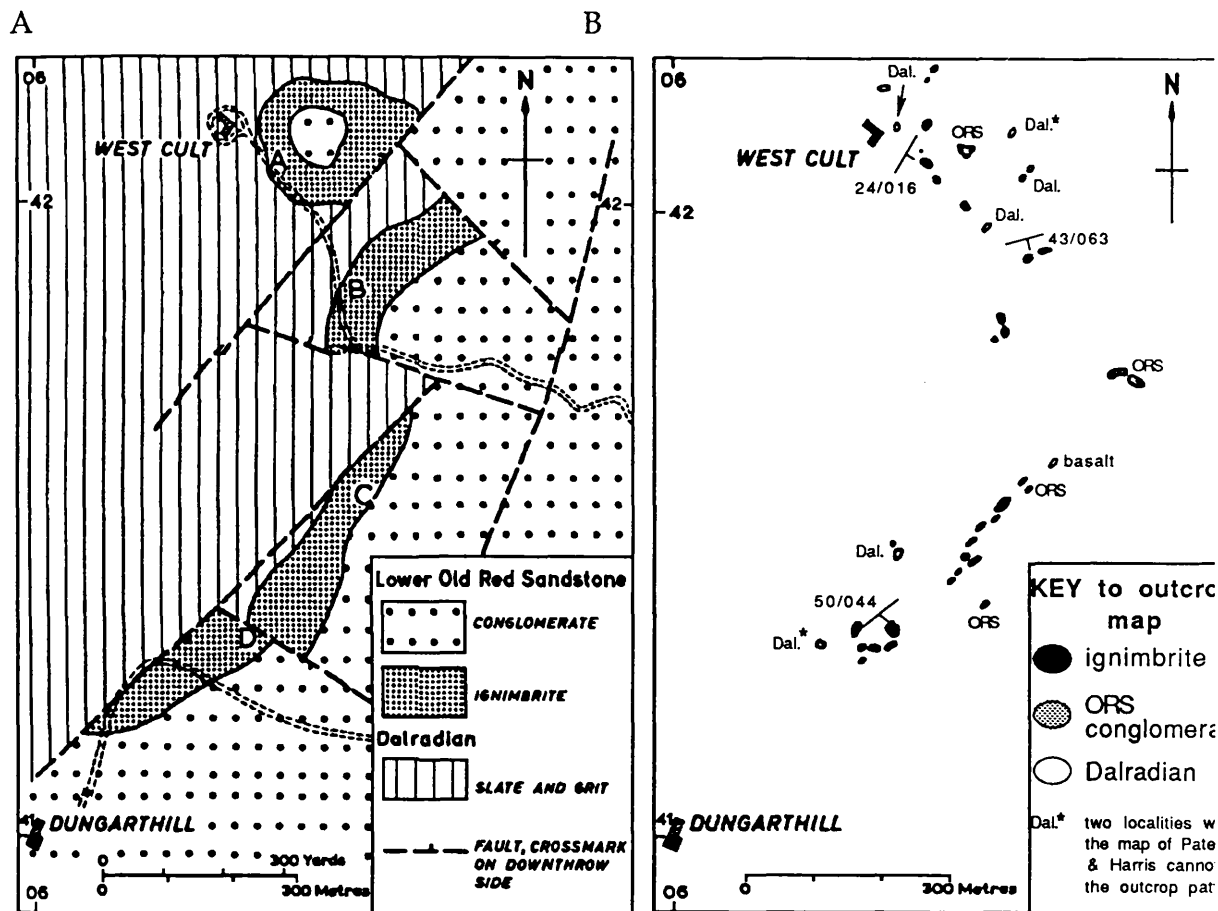


Fig. 5.8. (A) interpretive geological map of the area around W. Cult (Tayside), reproduced from Paterson & Harris 1969. (B) outcrop map of the area around W. Cult, surveyed in May 1987.

### 5.2.7 Description of the Highland Borders at Birnam Wood, Tayside

The tract of land immediately west of the Tay Valley (Fig. 5.1) exemplifies many of the difficulties that face geologists working along the Highland Border. My principle aim was to extend the HBC description east of the Tay Valley (Allan 1928), southwestwards, to an area not previously mapped in detail. The area described by Allan (1928) is of interest because of the presence of L.ORS rocks lying unconformably on the Dalradian, on the northern side of the HBFZ.

Correlation of lithologies and of fault zones across the Tay Valley is hampered by a belt of alluvium up to 1 km wide on the valley floor. It is



Previous research:

Anderson 1946 (p. 492), Harris & Fettes 1972, Armstrong *et al.* 1985.

Field description, petrography & structural analysis:

The area shown in Fig. 5.9 is heavily afforested, and exposures are rare, small, and isolated. I found no structural or lithological contacts, and no exposures of HBC rocks. The sedimentological variation in the ORS conglomerates is interesting, but I was unable to define the boundary between the Dalradian and HBC/Midland Valley terranes. It is important that the position of the HBF is *not* defined by differences in clast composition of the L.ORS conglomerates, because theories about the HBF that depend on such differences will then be based on circular logic (see section 4.2.1). Consequently, I have no basis upon which to locate the HBF, and therefore I have not shown a speculative position for the HBF in Fig. 5.9.

#### 5.2.8 Description of the Highland Borders from Meikle Obney to Glen Shee

At Meikle Obney typical Dalradian-type pelites (G.R. NO 034380) are separated from coarse red ORS-type conglomerates dipping at  $57^{\circ}/033^{\circ}$  (G.R. NO 041378) by a 700m exposure gap. The conglomerate clasts are mostly quartzites, basic volcanics, and acidic plutonics. The position of these conglomerates relative to the various mapped strands of the HBFZ is unclear.

Small exposures of porphyry, similar in hand specimen to the Linthathen ignimbrite, outcrop at Glack (specimen number J0120, G.R. NO 021358; specimen numbers J0121 & J0122, G.R. NO 018359). The contacts with adjacent ORS-type conglomerates (G.R. NO 019358) are not exposed.

In Glen Shee, Dalradian-type psammites and pelites (G.R. NN 991340) are separated from coarse red conglomerates of ORS type (G.R. NN 994339) by a 100m gap in exposure. No exposures of typical HBC lithologies were found.

The psammites and pelites have a composite S1/S2 cleavage that has an approximate overall orientation of  $70^{\circ}/270^{\circ}$ . The conglomerates are orientated at  $25^{\circ}/055^{\circ}$ , and the clasts show clear imbrication. Compositionally, they have a high proportion of acidic and basic volcanic clasts, with clast size typically 1-10cm, ranging up to 60cm. I observed very little brittle deformation in the conglomerates.

### 5.2.9 The Highland Borders at Keltie Water, Callander

This river section has played a crucial part in the history of research in Highland Border geology; some of the interpretations made in the past, despite careful and detailed field observation, have repeatedly led to misunderstandings of Caledonide stratigraphy and tectonism. This situation demonstrates how the geology in fault zones can be so complicated and misleading, and how any lithological or structural correlations along fault zones can be fraught with difficulties.

With the benefit of hindsight, it is now clear that some or all of the following considerations may now apply in the Keltie section, and might have a wider relevance to other Highland Border sections, and to fault zones in general.

Firstly, it now appears that the structural histories of Dalradian rocks and the HBC, though similar in geometry (Harris 1962), cannot have been caused by the same tectonic event, because the pre-D3 Ben Vuirich granite has been precisely dated at  $590 \pm 2$  Ma (U/Pb on single grain abraded zircons; Rogers *et al.* 1989). Note that the utilisation of this new data in interpretation of other areas of the Dalradian rocks does assume that D2 and D3 are each broadly synchronous across the whole Dalradian tract, *i.e.* that S2 at Ben Vuirich is the same as S2 in the Keltie section. The inference to be made from the earlier erroneous interpretations of Harris, is that fault zones are often associated with fault-parallel fabrics, and adjacent blocks may be expected to have similar fabric geometries produced at widely differing times.

Secondly, the limestone in the Keltie Water need not necessarily be equivalent to the Cambrian Leny Limestone found at the type locality at Leny Quarry (section 5.2.10), and may indeed be part of the Dalradian Supergroup. It is now obvious that correlation based solely on field appearance is not always rigorous enough, and the limestone in the Keltie Water has yet not been dated palaeontologically.

Finally, there *are* structural discontinuities within the Keltie section. For example, there is a brittle fault zone, of unknown displacement, 100m north of the thick quartz-dolerite dyke (see map in Harris 1962). Furthermore, there are gaps in exposure that could contain faults of large magnitude, and one of the many (ORS?) felsite dykes may have been intruded along a pre-existing shear zone, *cryptically* stitching a major tectonic boundary.

Previous research:

This includes the following: Anderson 1946 (p. 495), Harris 1962, Harris 1969, Harris & Fettes 1972.

#### 5.2.10 Structural description of the HBC at Lime Craig Quarry, Aberfoyle

Previous research:

This includes the following: Du Toit 1902, Jehu 1912, Jehu 1914, Jehu & Campbell 1917, Anderson 1946 (p. 495-496), Harris & Fettes 1972, Harris 1973, Curry *et al.* 1982, Henderson & Robertson 1982, Henderson & Fortey 1982, Curry *et al.* 1984, Robertson & Henderson 1984, Ingham *et al.* 1985, Whelan 1988, Dempster & Bluck, 1989.

Stratigraphy:

This locality has provided important palaeontological constraints on the stratigraphy of the HBC (Curry *et al.* 1982, 1984). The section comprises components of two (possibly three) separate faunas: a silicified Lower Arenig assemblage has been recovered from the Dounans Limestone, and a Caradoc-Llandovery fauna from the Achray Sandstone Formation. The Achray sandstone may also contain a derived fauna of Llanvirn/Llandeilo age.

The ORS is believed to belong to the Arbuthnot Group.

Field description, petrography & structural analysis:

The outcrop at Lime Craig Quarry (Fig. 5.10) is of regional tectono-stratigraphical importance because it provides convincing exposures of the unconformity between the HBC and the ORS. In places the contact is marked by thin mud drapes and/or a basal sandstone. Overlying conglomerates of ORS type consist predominantly of very well rounded quartzite clasts, with no obvious HBC detritus. In contrast, the Lime Craig conglomerate of the HBC contains a significant proportion of serpentinitic detritus that may have been derived from the *unconformably* underlying Dounans limestone/serpentinite rock.

Apart from late brittle deformation, few tectonic contacts are exposed in the quarry. The faults postulated by Curry *et al.* (1984), particularly those believed to lie parallel to the HBFZ trend, cannot be proven (based on current exposure).

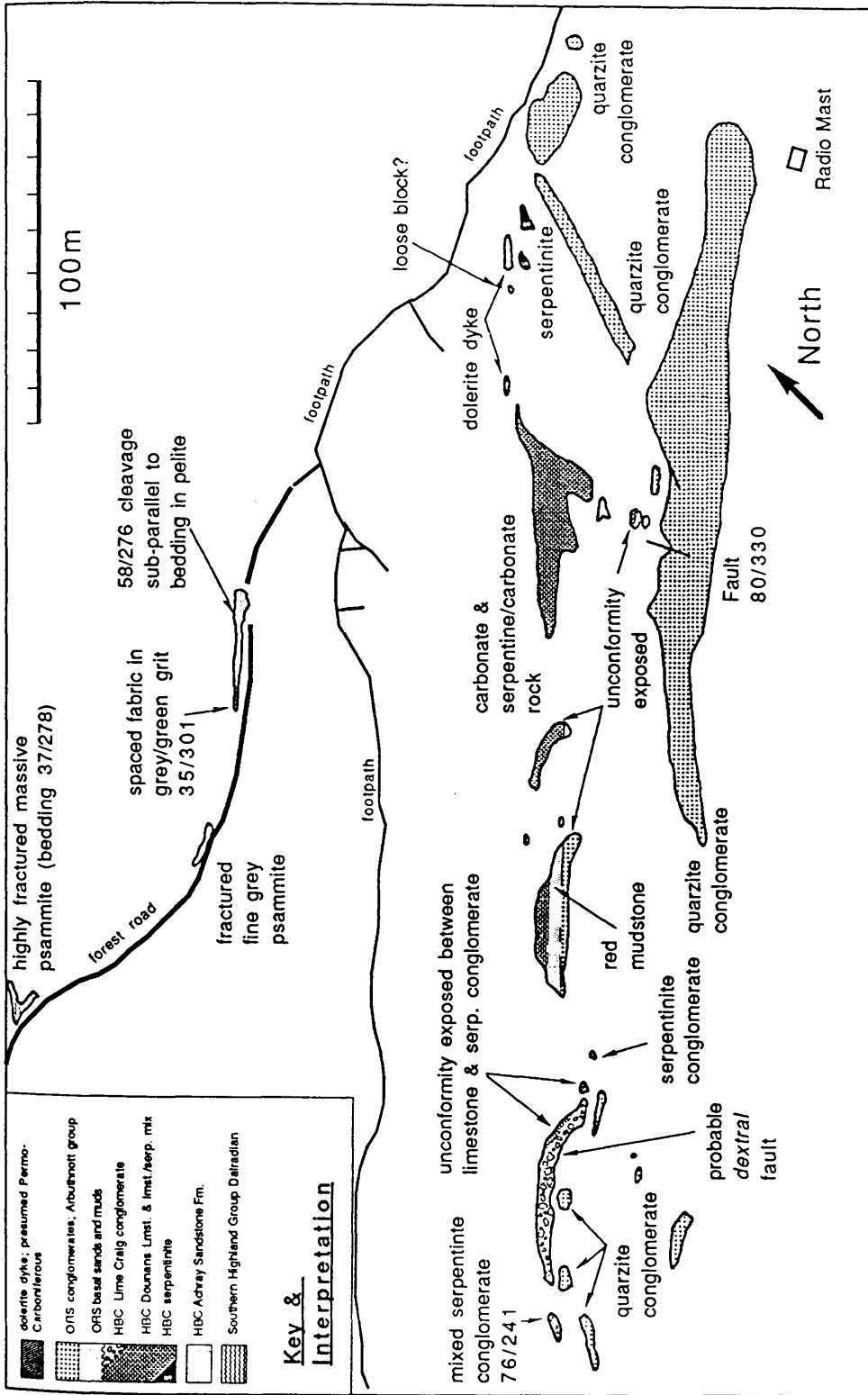


Fig. 5.10. Outcrop map of Lime Craig Quarry, Aberfoyle. Base map from Curry *et al.* 1984 (p.126).

### 5.2.11 Structural description of the HBC at Balmaha, Loch Lomond

The Balmaha area comprises a wide (1.2 km) section across the HBFZ. Although most exposures are small and isolated, overall the area contains important tectono-stratigraphical and structural evidence of several deformation events. Thus, much of the entire HBFZ history that has been pieced together from other Highland Border sections is represented at this one locality. The significance of the Balmaha area to Upper Palaeozoic tectonism is described and discussed in Chapters 3 and 4. This section is concerned with the geological history prior to ORS times.

#### Previous research:

This includes: Du Toit 1902, Jehu & Campbell 1917, Anderson 1946 (p. 496), Tremlett 1973, Henderson 1981, Ikin & Harmon 1981, Henderson & Fortey 1982, Ikin & Harmon 1983, Robertson & Henderson 1984, Dempster & Bluck, 1989.

#### Stratigraphy:

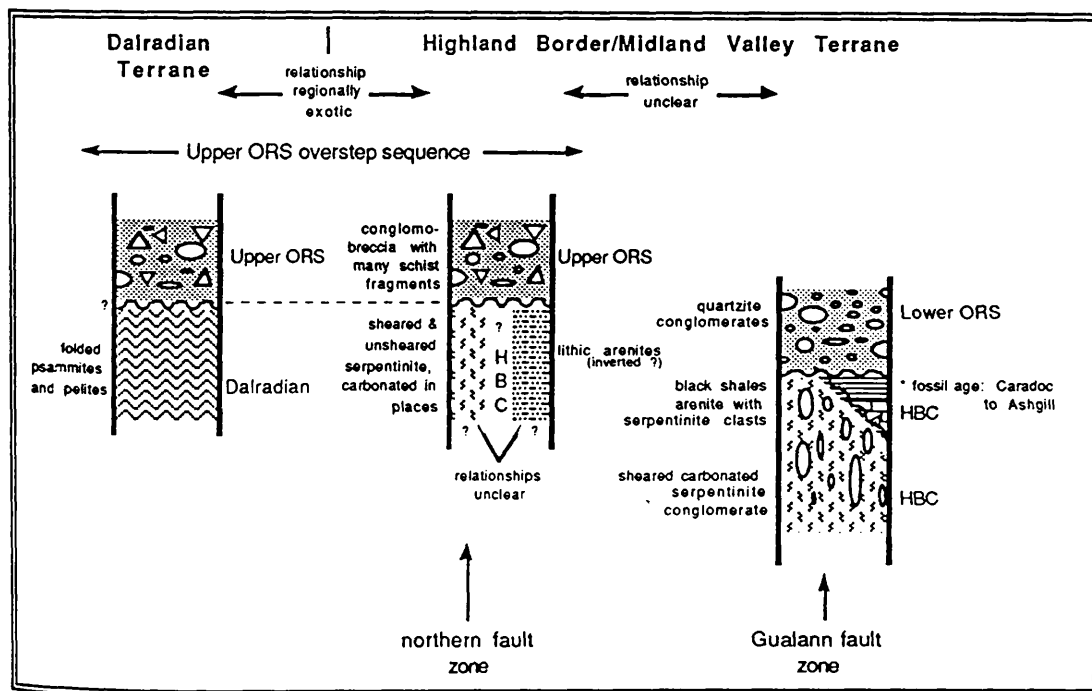


Fig. 5.11. Tentative tectono-stratigraphy at Balmaha, Loch Lomond.

The most important stratigraphical constraints come from exposures that lie below the normal water level of Loch Lomond (Whelan 1988, Brian Bluck, pers. comm.). These show: (1) an intra-HBC

unconformity between the southern belt serpentinites/overlying limestone, and the Caradoc-Ashgill black shales, and,  
 (2) that the HBC lithic arenites at Arrochymore Point are unconformably overlain by a conglomerate of Upper ORS type (Figs. 5.11, 5.12).

The Lower ORS sits unconformably on HBC serpentinites on the west side of Inchcailloch (Brian Bluck, pers. comm.).

Field description, petrography & structural analysis:

Fig. 5.12 is a detailed outcrop map of the Balmaha region. A tectonostratigraphic interpretation is given in Fig. 3.3.

The exposures that are structurally most significant to the analysis of HBC ductile deformation are found in two separate HBC wedges that lie along the Gualann and Northern Fault Zones (see Fig. 3.3). The two HBC belts are both composed predominantly, but not exclusively, of altered serpentinites.

The southern belt consists of heavily veined, ochrous fragmental "serpentinites", now pervasively altered to carbonate. Some outcrops show sedimentary structures (Henderson & Fortey 1982), suggesting that the original serpentinites were detrital. The petrography of the serpentinites is described in detail by Henderson & Fortey (1982). The southern serpentinite belt contains slices of a fine grained, immature grit, though the contacts of the grit with the carbonated serpentinites are not exposed.

The carbonated serpentinites are heterogeneous and structurally complex. Many of the outcrops show a chaotic fabric that is highly variable, but overall is often crudely aligned parallel to the trend of the Gualann Fault Zone ("GFZ"). The rocks are also cut by an irregular array of extensional carbonate veins. The abundance of the veins varies, but in places exceeds 50% of the volume of the bulk rock, suggesting that large extension has occurred.

Whilst some serpentinites of the northern belt have also been heavily carbonated and veined, others are pervasively silicified. In places, extensional fibrous carbonate veins comprise up to 60% of the bulk rock, implying very large extension (at least on a local scale). In a few outcrops the veins have been cut by small sinistral shear bands. A small outcrop on the shore of Loch Lomond (see Fig. 5.12) preserves an un-carbonated sheared serpentinite. A penetrative foliation anastomoses around tectonically rounded serpentinite pods. I could find no reliable shear sense indicators in the serpentinites.



### 5.2.12 Description of the Highland Borders at Ben Bowie

#### Previous research:

Published work includes; Anderson 1946 (p. 497), Whelan 1988.

#### Stratigraphy:

Black shales from Glen Fruin have yielded chitinozoans of probable Caradoc age (Whelan 1988, p.19, 283).

#### Reconnaissance field description:

The Carboniferous lavas of Ben Bowie lie to the NW of the Gualann Fault Zone ("GFZ"; *i.e.* the southern branch of the HBFZ - see chapter 3). Several exposures on the sides of hillocks immediately east and south of Ben Bowie consist of typical HBC-type lithologies. The most abundant rock is carbonated serpentinite, similar in field appearance to the serpentinites marking the GFZ at Balmaha. Due east of Ben Bowie is a small exposure of pale arenite, that may be an equivalent of the Achray sandstone.

### 5.2.13 Structural description of the HBC at Innellan

This is a small coastal section of unknown structural significance. I only carried out a reconnaissance survey, and further structural analysis (with a detailed petrographical study) is needed.

#### Previous research:

This includes the following; Gunn *et al.* 1897, Anderson 1946 (p. 499-500), Ikin & Harmon 1981, Henderson & Robertson 1982, Ikin & Harmon 1983.

#### Stratigraphy:

There are no recorded palaeontological discoveries known from the Innellan section, and hence stratigraphy is currently based on lithological and geochemical correlation.

#### Reconnaissance field description, petrography & structural analysis:

The contact between the HBC and the Upper ORS is not exposed, and I have not (yet) seen the red fault breccia observed by Anderson 1946 (p.500). Adjacent to the ORS are coarse dark grits (grain size up to 2mm),

that change northwards, over a distance of about 30m, into crystalline platey mylonites (sample no. J169).

Further east, after a 10m gap in exposure, the outcrop is comprised of serpentinites and serpentinite "conglomerates" (sample no. J170). The conglomeratic nature of these rocks is probably of tectonic origin; a well defined serpentinite fabric anastomoses around more massive serpentinite pods. In thin section the penetrative fabric is defined by serpentine laths. The fabric is folded, with an axial planar cleavage marked by cross-cutting acicular serpentine laths. The folds are themselves overprinted by a carbonatisation event, though this is not at all pervasive. A third phase of serpentine growth overprints the carbonate.

The serpentinites pass eastwards into cleaved shales and heavily veined Dalradian-type pelites.

#### 5.2.14 Structural description of the HBC at Toward

Brief reconnaissance mapping at Toward has already shown it to be one of the key exposures of Highland Border rocks in Scotland. Coastal exposures are small, but nevertheless have well preserved structural contacts.

Previous research:

Gunn *et al.* 1897, Anderson 1946 (p. 500), Henderson & Robertson 1982.

Stratigraphy:

There are no palaeontological discoveries recorded from Toward, and stratigraphy is currently based only on lithological correlation.

Field description, petrography & structural analysis:

Carbonated serpentinites occur as fault-bounded slices caught in green-grey cleaved grits of unknown tectonostratigraphical affinity. The steeply plunging stretching lineations reported by Henderson & Robertson (1982) are not evident in rocks close to the contact between the serpentinites and the grits. In places, this contact zone is marked by a thin width of mylonites, with horizontal or shallowly plunging stretching lineations.

Sample J165 is a quartz mica mylonite, in which recovery and recrystallisation microstructures (grain-size diminution, new grain/sub grain growth, grain elongation) are pervasive. Secondary fabrics and

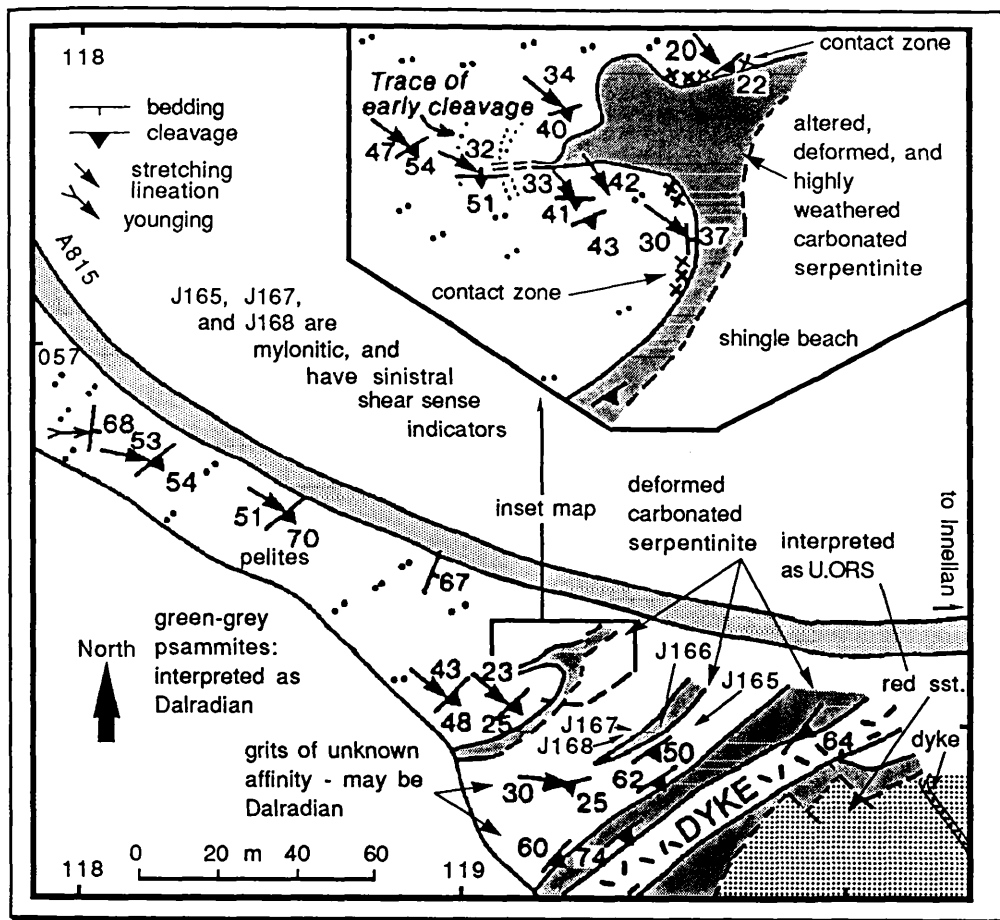


Fig. 5.13. Reconnaissance map of the HBC at Toward, based on Henderson and Robertson 1982.

$\sigma$ -type porphyroclasts show that shear sense is sinistral (plate 2 ).

Sample J166 is a carbonated serpentinite in which relicts of serpentine are still preserved, despite widespread overprinting by multiple generations of carbonate veining.

Samples J167 and J168 are quartz mica mylonites that show reliable sinistral shear sense (S-C fabrics, extensional crenulation cleavage, occasional rotated porphyroblasts). Mica has retrogressed to chlorite.

#### 5.2.15 Structural description of the HBC at Scalpsie Bay, Bute

Exposure of the HBC is not widespread at Scalpsie Bay. However, the section is of importance because it contains lithological units that may not be present in the other well-documented HBC localities. Furthermore, the contacts between some lithologies are relatively well exposed.

The tectonostratigraphic significance of the amphibolite sheet at Scalpsie bay is not fully known, but it may represent part of an ophiolite unit (see section 6.6).

### Previous research:

Smellie 1916, Lamont 1930, McCallien 1938, Anderson 1943, Anderson 1946 (p. 501-503), Ikin & Harmon 1981, Henderson & Robertson 1982, Ikin 1983, Ikin & Harmon 1983.

### Stratigraphy:

There are no palaeontological discoveries recorded from Bute. The amphibolite has been radiometrically dated at 540Ma (K/Ar on hornblendes, Tim Dempster pers. comm. 1990); work is still in progress to refine this age determination.

### Field description, petrography & structural analysis:

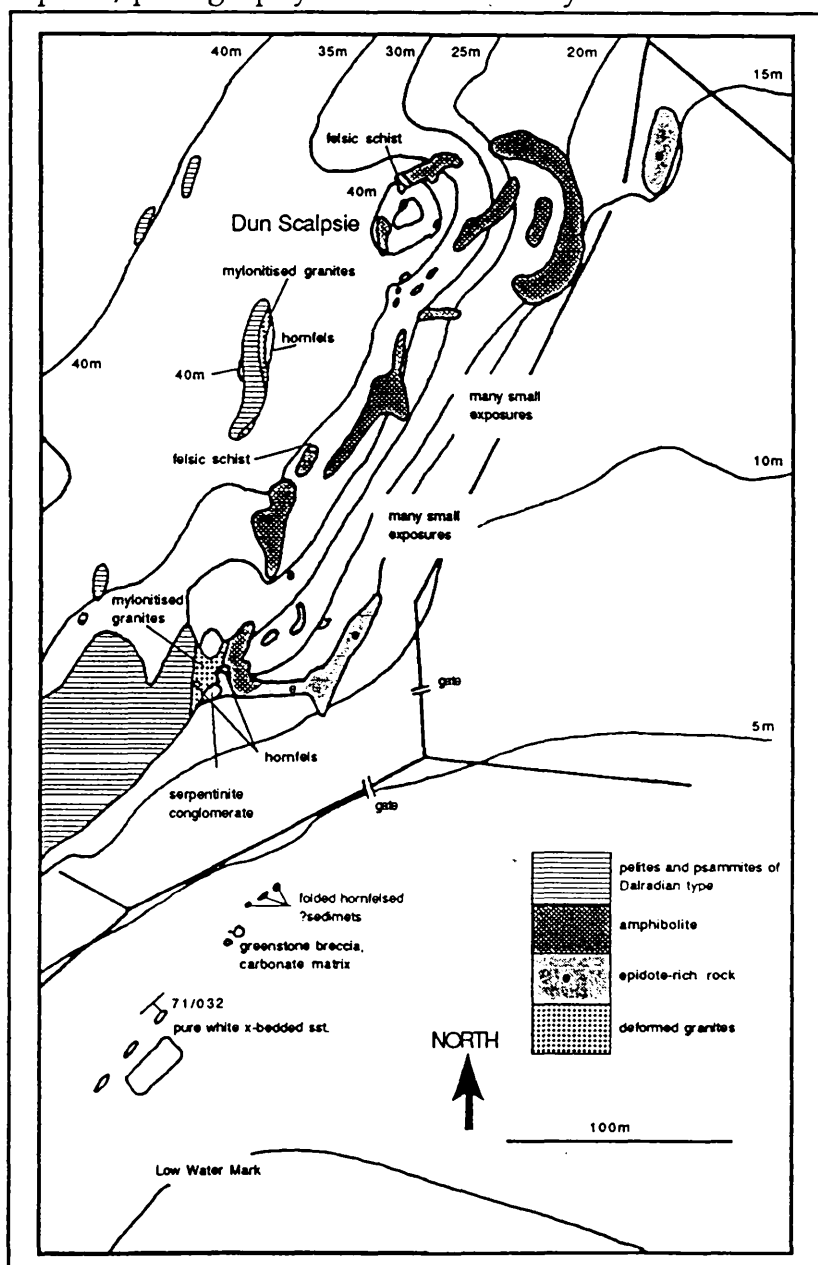


Fig. 5.14. Detailed outcrop map of the HBC at Scalpsie Bay, Bute.

The boundary between Dalradian-type slates and grits and the HBC is marked by a 2-5m wide zone of a felsic crystalline rock that resembles a granite. In hand specimen many of the granites show small discrete ductile shear zones, defined by phyllosilicates. Petrographically, the micas in the rock have completely retrogressed to chlorite, destroying any existing mica fabric, but there is abundant evidence of mylonitisation in quartz and feldspar grains (grain recrystallisation, seriate grain boundaries, new grain growth *etc.*), [samples J0001, J0002, J0004, J0005, J0049, J0050, J0058, J0060]. Interestingly, mylonitic deformational structures are less dominant than recovery and recrystallisation, yet some quartz grains have deformed in a semi-brittle way, by grain fragmentation.

Other lithologies are preserved along the shear zone. Very fine grained hornfelsed ?siltstones crop out adjacent to the mylonitic granite, composed of up to 20% pyroxene, and cross-cut by veins of carbonate, quartz and opaques. Also present are a carbonate cemented breccia that might be of tectonic origin, and a serpentinite conglomerate that appears heavily deformed, but is poorly exposed.

#### 5.2.16 Structural description of the HBC around Glen Sannox, Arran

The exposures in and above Glen Sannox differ from other Highland Border localities, because although there are few well-exposed contacts between adjacent lithologies, there is good evidence of ductile deformation *within* some lithological units. At other localities, ductile deformation is generally restricted to narrow shear zones that *separate* relatively undeformed units.

Previous research:

This includes the following; Gunn *et al.* 1903, Stark 1904, Gunn 1905, Anderson 1944, Anderson & Pringle 1944, Anderson 1946 (p. 503-504), Friend *et al.* 1963, Johnson & Harris 1967, Henderson & Robertson 1982, Ikin 1983, Ikin & Harmon 1983, Curry *et al.* 1984, Robertson & Henderson 1984, Dorning 1985, Whelan 1988.

Stratigraphy:

The HBC series on Arran was considered to be of Arenig age by Anderson & Pringle (1944), based on a discovery of hingeless brachiopods in black shales. However, their taxonomic assignment cannot be corroborated because the original specimens cannot now be

located. No further stratigraphically useful discoveries were documented until Whelan (1988) recorded a Lower Ordovician age for black shales from Allt Cairn Bhain.

Field description, petrography & structural analysis:

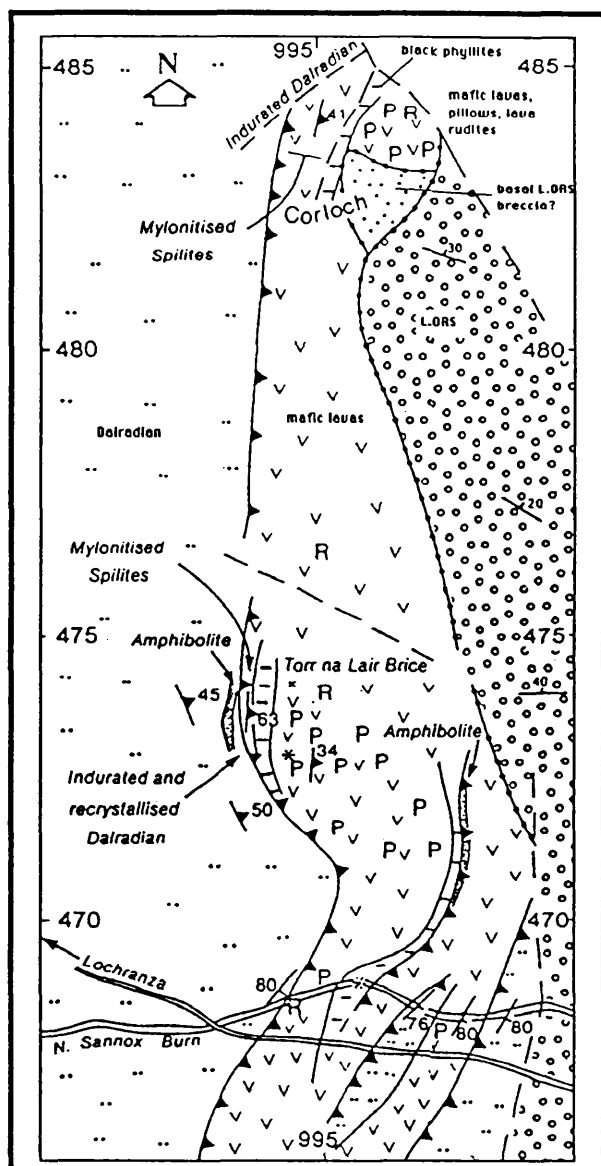


Fig. 5.15. Sketch map of the HBC geology on Arran (from Henderson & Robertson 1982).

Exposures in the North Sannox Burn and at Corloch (Fig. 5.15) contain important evidence of the scale of tectonism along the HBFZ. In the North Sannox Burn evidence of sinistral shear is common, and is based on diagnostic S-C relationships, as well as "Ramsay & Graham" type small-scale sigmoidal shear zones.

At Corloch there are outcrops of ultramylonites that collectively span a zone width of about fifty metres or more. The mylonites are grey-green to bright green in colour, fine grained, very platy, and moderately fissile. They have been crenulated and tightly folded subsequent to mylonitisation (Fig. 5.16), and the entire fault zone is composed of tight to isoclinal *rootless* folds. Unfortunately, this precludes the use of shear sense indicators to interpret terrane movements.

The mylonites contain no clear stretching direction in the XY plane, either macro- or microscopically, yet in thin section there is clear evidence of high shear strain (plate 3). Porphyroclasts are rare; grain size is uniform, and most grains have become extremely elongate. With care it is possible to identify an oblique fabric that defines an S-C relationship (e.g. samples D0011, B0012, B0013, J0013). Extensional crenulation cleavage can also be seen (this is quite separate to the easily distinguishable fold crenulations seen in plate 3).

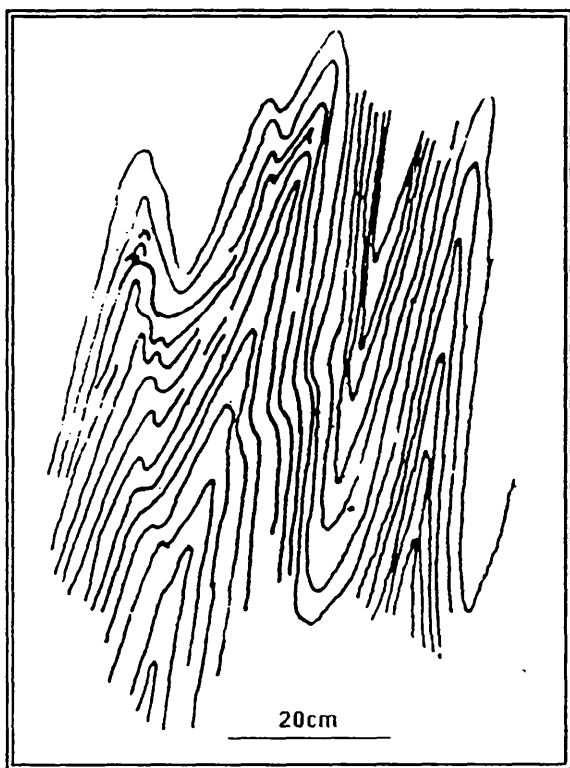


Fig. 5.16. Field sketch of folded rootless mylonites at Corloch, Arran. Looking SSW.

## 5.3 Evidence for Terrane Accretion on the HBF in Ireland

### 5.3.1 Introduction

Many geologists believe that a continuation of the HBF in Scotland can be traced for 300 km across Ireland on a NE/SW trend along the Fair Head / Clew Bay line ("FCL"), (Bailey & Høltedahl 1938; Max & Riddihough 1975). As in Scotland the fault zone broadly separates the "orthotectonic" from the "paratectonic" Caledonides (Ryan et al. 1983), (Fig. 5.17).

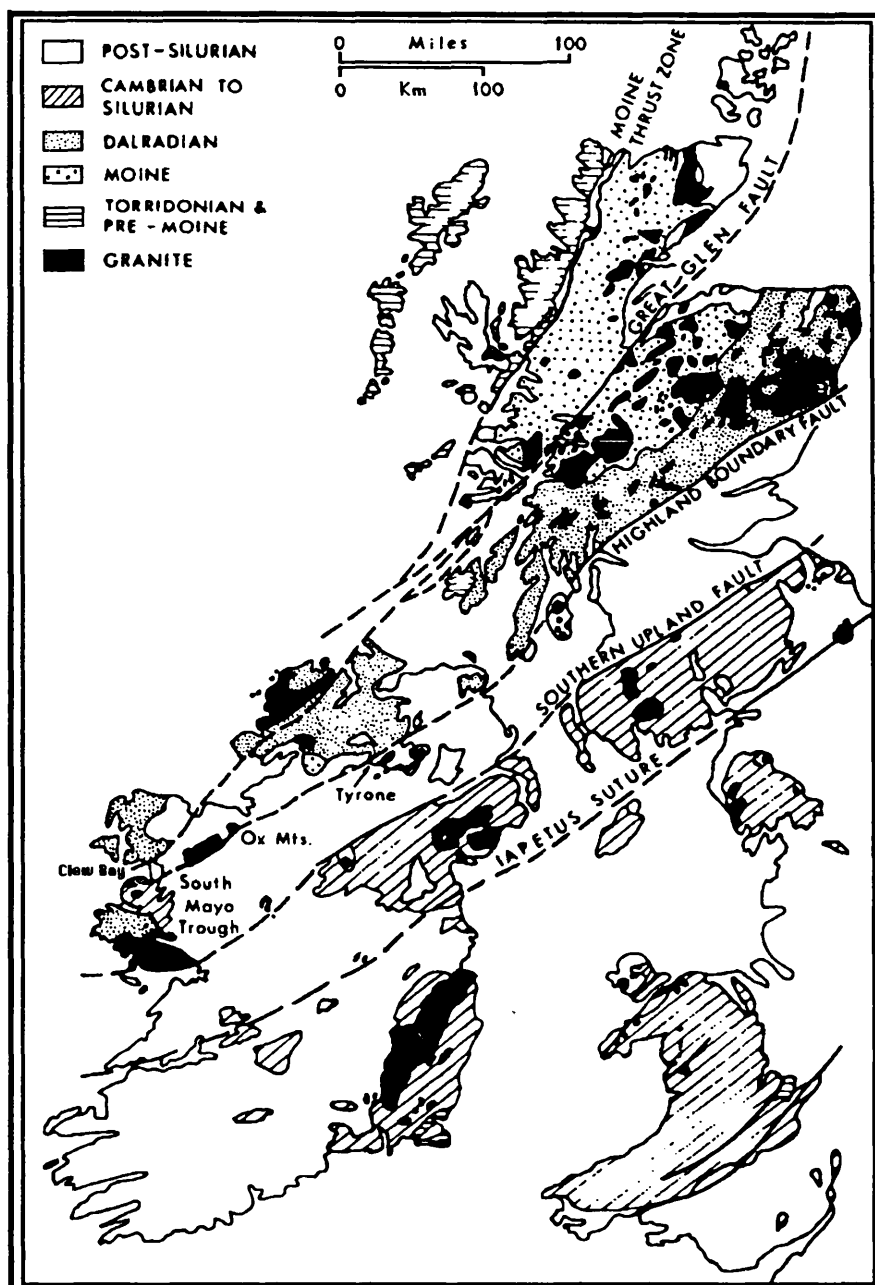


Fig. 5.17. Outline geological map of the British Isles, showing the continuation of the HBFZ across Ireland (after Leake et al. 1983).

Much of the HBFZ in Ireland has been affected by syn- or post-Carboniferous deformation. Despite this, there is good exposure of Lower Palaeozoic rocks along the length of the HBF, and these contain some crucial evidence for Highland Border terrane accretion.

There are four main areas of Lower Palaeozoic rocks flanking the HBFZ (see Fig. 5.17):

- 1) Tyrone
- 2) The Ox Mountains ("Slieve Gamph")
- 3) The South Mayo trough
- 4) Clew Bay.

These are discussed briefly in the following sections.

### 5.3.2. Tyrone

Hutton *et al.* (1985, 1990) have documented the presence of an ophiolitic sequence within the Tyrone igneous complex. U/Pb isotopic dating show the ophiolite to have been formed around  $471^{+2/-4}$  Ma (*i.e.* Arenig), and obducted soon after.

The Tyrone complex, together with the Arenig ophiolite at Ballantrae (Bluck *et al.* 1980), are significant because they give evidence of the nature and the formation of the Midland Valley basement, much of which has since been covered by Old Red Sandstone and subsequent sedimentation.

### 5.3.3. The Ox Mountains

The Ox mountains inlier contains Caledonian metasediments and intrusives in tectonic contact with a high grade gneissic pre-Caledonide basement.

The basement rocks in the NE Ox Mountains (Fig. 5.18) are mainly psammitic gneisses, with some pelites, semi-pelites, marbles, and meta-basic intrusives. The rocks have undergone granulite facies metamorphism, and have yielded a Rb/Sr age of  $895 \pm 60$  Ma.

The younger metasediments of the SW Ox Mountains have been correlated with the Dalradian of S. Donegal by Chris Jones and Ian Alsop (pers. comm.; Jones & McCaffery 1989), and are possibly equivalent to the Southern Highland Group in Scotland. Early Caledonian deformation has been strongly overprinted by transcurrent tectonism.

The Dalradian of the SW Ox Mountains has been intruded by three plutons that show syn-cooling deformation. Their age, and hence the age of the deformation, is of fundamental importance to our understanding of Caledonide geology.

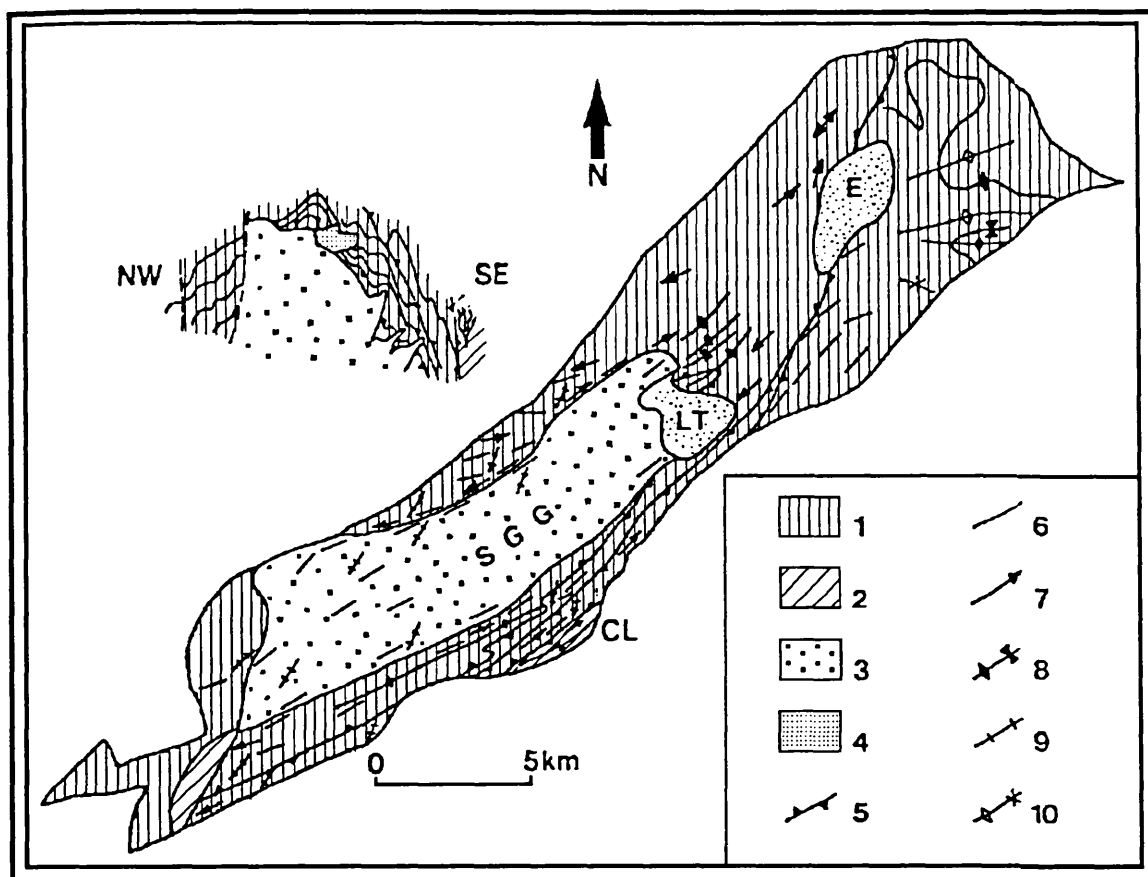


Fig. 5.18. Geological map of the Ox Mountains inlier (after Hutton & Dewey 1986).

Key: 1 = Medium to high grade metasediments; 2 = low-grade metasediments; 3 = SGG Slieve Gamph granodiorite; 4 = Lough Talt (LT) and Easky (E) adamellites; 5 = slides and minor shear zones; 6 =  $S_3$  and average bedding traces (both surfaces generally moderately to steeply inclined); 7 =  $D_3$  stretching lineations (usually low plunges); 8 =  $F_3$  axial traces; 9 = sinistral extensional crenulation cleavage trace; 10 =  $F_4$  axial traces; CL = Callow Loughs

Shear strain is high in many of the exposures in the Ox Mountains, and there is abundant evidence of simple shear. Because this contrasts so noticeably with much of the HBFZ exposed in Scotland, I have described some of the Ox Mountains structures in more detail below.

1) sub-horizontal stretching lineation (e.g. Cloonygowan)

This is associated with a very penetrative pervasive mylonitic fabric (in greenschist grade Dalradian rocks) that is spatially related to tight or isoclinal upright  $F_2$  folds.  $D_2$  deformation was intense, and has almost obliterated the  $D_1$  fabric. There is also a steep well-formed  $D_3$  spaced fabric.

2) sinistral shear bands (e.g. Callow Post Office, and Callow Loughs)

These occur in both low grade and high grade rocks. At Callow, amphibolite grade metasediments are cut by many sinistral shear bands (Plate 4) with S-C and extension crenulation fabrics. Dextral

shear bands also occur locally; these are not as well developed or as abundant as the sinistral bands.

3) sinistral S-C fabrics in Ox granodiorite (*e.g.* Pontoon)

The granodiorite is strongly foliated, and has a spectacular S-C fabric. In places the fabric intensifies into anastomosing mylonitic zones. The pervasive sinistral fabric is assumed to have been superimposed during and after the cooling of the pluton, which has been dated at  $478 \pm 12$  Ma (Rb/Sr, whole rock; Pankhurst *et al.* 1976). The granite is awaiting re-dating at S.U.R.R.C.

4) weak sinistral S-C fabric in the Loch Easky adamellite

Here the fabric is similar to the granodiorite at Pontoon, though the foliation is much more weakly developed. The granite is thought to have been intruded at around 400 Ma (Hutton & Dewey 1986).

#### 5.3.4. South Mayo Trough

The South Mayo Trough is a synclinorium comprised of Ordovician and Silurian sediments and volcanics (Dewey 1963). Conglomerates of the Llandoveryan Owenduff Group overstep the Doon Rock and Lough Nafuoey faults that separate the South Mayo Trough from the Dalradian of Connemara to the south.

Broadly speaking, the South Mayo Trough shares a similar geological history to parts of the HBC of Scotland. Stratigraphically, both contain a Lower Ordovician sedimentary sequence that was deformed prior to the deposition of Upper Ordovician/Lower Silurian clastic sediments.

#### 5.3.5. Clew Bay

Rocks exposed in the area around Clew Bay are considered to represent a continuation of the HBC in Scotland (*e.g.* Phillips 1973, Ryan *et al.* 1973, Hutton 1987, Max 1989). Most importantly, correlation is now based on biostratigraphical as well as lithological evidence (Harper *et al.* 1989, Fig. 5.19).

The stratigraphy of the rocks of Clew Bay has recently been described by Max 1989 and Harper *et al.* 1989<sup>1</sup>. The Clew Bay Supercomplex (CBS) of Harper *et al.* 1989 is defined to include both the Deer Park Complex (Phillips

---

<sup>1</sup> Note that the stratigraphic nomenclature of the rocks around Clew Bay is complicated. Various names have been assigned to the same rocks by different workers; opinions have differed on lithological correlation between outcrops, in the absence of a detailed biostratigraphy.

1973) and the various L. Palaeozoic cover sequences (including those described by Max 1989).

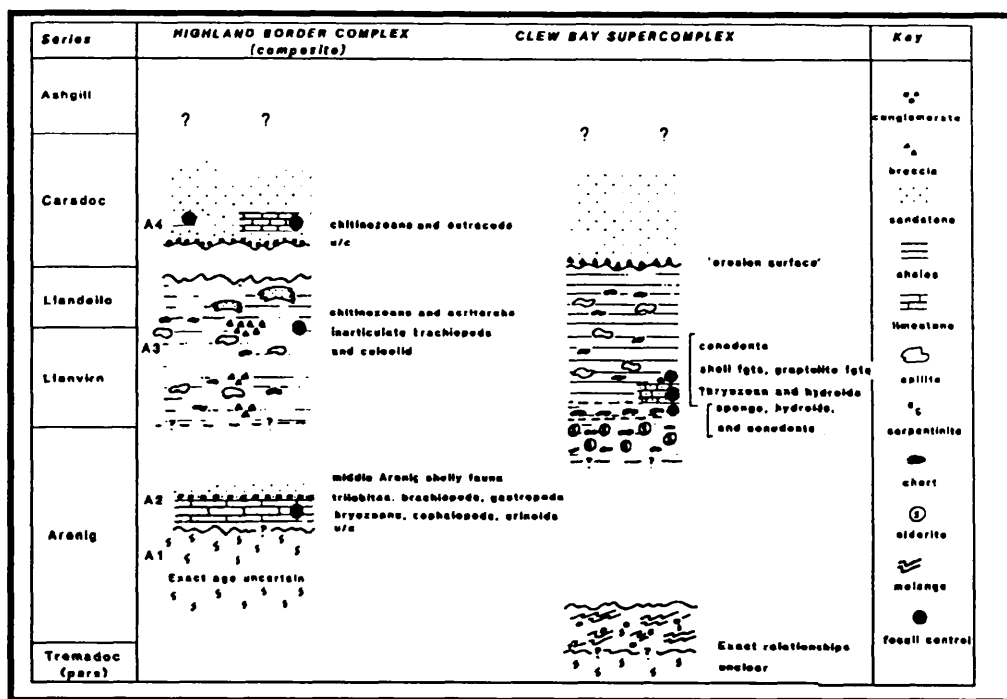


Fig. 5.19. A tentative biostratigraphical and lithostratigraphical correlation between the Clew Bay Supercomplex of Western Ireland and the HBC of Scotland (from Harper *et al.* 1989).

The Clew Bay Supercomplex (CBS) comprises the following formations:

- 1) the Deer Park Complex (Phillips 1973); this is a heterogeneous mix of serpentinites, serpentinite breccias, igneous rocks, dolomite, and schists, cropping out on the south side of Clew Bay (Fig. 5.20), and on Clare Island (the Kill Inlier). The age of the Deer Park Complex remains uncertain.
- 2) the Killadangan Fm. (Graham *et al.* 1985, Max 1989); this is dominated by melange and olistostrome units, comprising conglomerates, quartzites, greywackes, mudstones, impure limestones, cherts, and volcanics, cropping out on the south side of Clew Bay (Fig. 5.20).
- 3) the Portruckagh Fm. (Graham *et al.* 1985); cropping out only on Clare Island, these can possibly be correlated lithologically with the Killadangan rather than the Ballytoohy Formation (Harper *et al.* 1989).
- 4) the Ballytoohy Fm. (Phillips 1973); this crops out on Clare Island, and is composed of mudrocks and greywackes that show pervasive syn-sedimentary deformation. The Ballytoohy Fm. was believed to

be Dalradian, and of likely Cambrian age (Rushton & Phillips 1973), but has recently been shown to contain a Llanvirn macro- and micro-fauna (Harper *et al.* 1989).

5) the South Achill Beg Fm. (Max 1989); this comprises conglomerates, grits and mudstones. On Achill Beg they are separated from Dalradian schists by the Achill Beg fault.

6) the Bill's Rocks Fm. (Max 1989); exposures on and around Bill's Rocks are mainly greywackes and conglomerates.

The Westport Grit Formation (Fig. 5.20) and the Carrowgarve Formation are both of unclear affinity. Either may belong to the CBS, though a Dalradian origin is equally plausible based on present evidence.

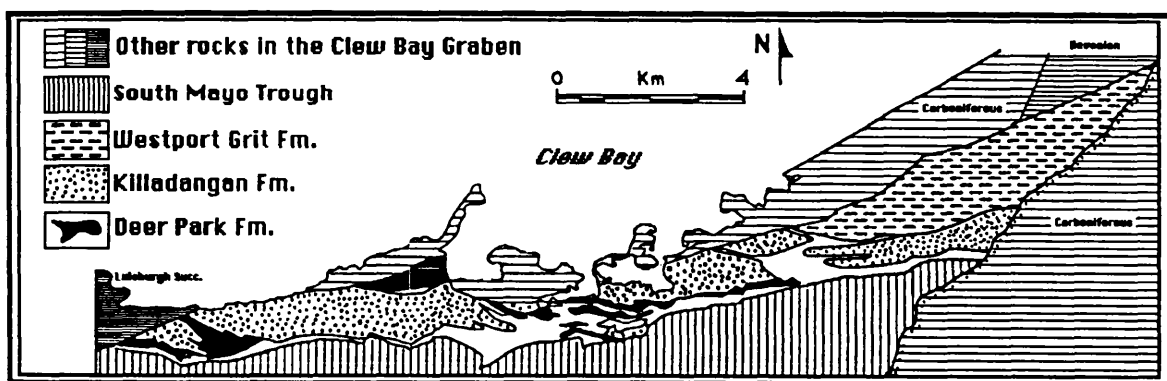


Fig. 5.20. Main tectonostratigraphic elements along the south side of Clew Bay (after Max 1989). The Killadangan and Deer Park Formations are probable equivalents to the Highland Border Complex of Scotland.

Interpretation & relevance of the Clew Bay Supercomplex:

The CBS is of fundamental importance to our understanding of the history of Highland Boundary Fault movements in Scotland if it can be shown that *either*;

- a) parts of the HBC can be correlated with parts of the CBS, *or*
- b) the HBF is structurally linked with the Clew Bay fault zone.

The evidence reviewed above suggests that *both* criteria are met, and the implications of such a correlation are as follows.

Firstly, sheeted dykes, olistostromes, and melanges of the CBS provide further evidence for the ophiolitic nature of the HBC, and probably represent in part a back arc-basin succession.

Secondly, the evidence for sinistral shear is very much more common and unambiguous in the Clew Bay fault zone than along the HBFZ in Scotland. Silurian sediments of the South Mayo Trough sit unconformably on serpentinites, amphibolites, and mylonites of the Deer Park Complex (Max 1989, figure 1), confirming the suspicion from Stonehaven that the

ductile deformation within the HBC had occurred prior to Silurian sedimentation.

#### 5.3.6. Summary of evidence from the FCL in Ireland

The amount of exposure and the clarity of structural evidence are far greater along the FCL in Ireland than the equivalent HBF in Scotland, and provide the following constraints on the HBF movement history.

- 1) Newly formed oceanic crust was obducted in Arenig times in Tyrone. A Lower Ordovician age is also likely (though *not* proven) for the Clew Bay ophiolite.
- 2) In the Ox Mountains, Dalradian metasediments and pre-Caledonian basement experienced significant sinistral deformation around the time of emplacement of the Ox granodiorite ( $478 \pm 12$  Ma; awaiting re-dating); *i.e.* Middle or Upper Ordovician. The ophiolitic rocks and associated sediments of Clew Bay were also deformed in one or more ductile events prior to the overstep of Croagh Patrick sediments.
- 3) Further sinistral deformation occurred during the emplacement of the later Ox granites, *assumed* to be at around 400 Ma (*i.e.* Lower Devonian).

# CHAPTER 6: TERRANE ACCRETION ALONG THE HBFZ - SYNTHESIS, DISCUSSION AND INTERPRETATION

## 6.1 Introduction

This chapter attempts to summarise the data presented in Chapter 5, and then, after a detailed and involved discussion, to interpret this data. Interpretation is directed towards an understanding of the mode and timing of microplate docking, and so forms conclusions that are central to this thesis.

In this chapter I shall state my opinion about the complexities and uncertainties associated with the interpretation of the ductile deformation along the HBFZ. It is because of such uncertainties that I have deliberately separated the data and its interpretation into two distinct chapters.

## 6.2 Synthesis of the structural description of the Highland Border Complex

This section presents a synthesis of the observational data given in Chapter 5.

### 6.2.1. Amount of exposure along the HBFZ, a summary of the structure of the HBC, and the proportion of highly sheared rocks

The HBFZ stretches for 250 km across Scotland. The present-day width of the fault zone, marked by rocks of the HBC, varies from a small gap in exposure, up to two kilometres wide.

In general, the level of exposure of the fault zone is poor or very poor. Large tracts of land are covered by drift, and consequently almost all data from the HBFZ come from a few type localities; these have been studied extensively by previous geologists, and described in this thesis in section 5.2. Some of these type localities have excellent levels of exposure.

As a very crude estimate, I would suggest that there is approximately 1% exposure within the HBFZ overall.

The HBC is a highly disparate melange of disrupted rocks of various affinities. The average size of structurally homogeneous blocks of rock is typically a few centimetres, sometimes a few metres in diameter. However, when exposure is good, much of this fragmentation can be seen to be *brittle* in character, and is therefore likely to be due to "late" fault movements in

the Upper Palaeozoic, as discussed in Chapters 3 and 4 (Late Lower Palaeozoic deformation is also possible, although I have seen no evidence for it in central Scotland).

Furthermore, much of the heterogeneity and complexity that typifies the HBC in the field, though often previously taken as indicative of intense alteration, can often actually be ascribed to fluid flow, and the effects of metasomatism and metamorphism associated with it.

Metasomatic alteration has given rise to extreme difficulties in analysing HBC rocks: not only does it tend to homogenise the field appearance of rocks that would otherwise be easily distinguishable, but it might also heavily overprint earlier fabrics (including fabrics produced by high shear strain).

Most of the rocks of the HBC that have experienced ductile deformation are typified by one or two flattening cleavages (*i.e.* S fabrics) that are orientated sub-parallel to the HBFZ. Stretching lineations associated with the fabric(s) tend to be weakly developed and quite localised. The orientation of such stretching lineations varies, but there appears to be a general tendency for lineations to be dip-parallel in the more north-eastern exposures, and strike-parallel in the more south-easterly exposures.

Most of the rocks of the HBC that have experienced ductile deformation do not show evidence of high shear strain. As a very crude estimate, I would suggest that less than 1% of the presently exposed HBC rocks show high shear strains.

Such a small proportion of mylonitic rocks is an important feature of the HBFZ. There are several possible reasons for this low amount of high shear strain:

- (a) zones of high shear strain may be numerous but are not exposed (due to preferential erosion?)
- (b) perhaps many zones of high shear strain have been overprinted by fluid flow and associated metasomatism
- (c) late deformation may have hidden many zones of high shear strain. In particular, thrusting of the Dalradian over the HBC and Midland Valley during the mid Devonian has probably concealed much of the evidence for high strain within the HBC (see Chapter 4)
- (d) perhaps the HBC never experienced regionally significant high shear strain.

It is possible, if not likely, that more than one of the above factors has had a significant effect on the present-day structure of the HBFZ.

The importance of these complications is that they introduce a *fundamental* uncertainty into any interpretation that a geologist might make, *i.e.* there are additional degrees of freedom in interpretation: the subjectivity of interpretation must increase. This is discussed in detail later in this chapter.

### 6.2.2. Summary of exposures showing high shear strain

There are seven HBC localities described in section 5.2 that show high shear strain.

I interpret that the collective significance of these seven exposures is small in comparison with the extensive mylonites and sinistral shear zones of Slieve Gamp and Clew Bay in Ireland (see section 5.3).

In Scotland, the following exposures contain rocks that show high ductile shear strains (a location map is given in Fig. 5.1, page 95):

1. At Stonehaven there is a 2-3 metre wide zone of alteration that is similar in appearance to a ductile shear zone. The kinematic significance of this exposure is *unknown* (see section 5.2.1., page 101).
2. In the River N. Esk, near Edzell, there is a mylonitised schist, with a *thrust* sense of displacement (section 5.2.4., page 106-108).
3. At Balmaha, some of the northern serpentinites have escaped intense carbonatisation, and show evidence of high shear strain. Sense of shear is *unknown* (see section 5.2.11., page 119).
4. Innellan contains platy crystalline rocks that are probably mylonitic (section 5.2.13., page 121-122).
5. At Toward there are several narrow shear zones that contain high strain mylonites with reliable *sinistral* shear sense indicators (section 5.2.14., page 122-123).
6. On Bute there is a thin mylonitic granite (section 5.2.15., page 124-125).
7. At Corloch, Arran, there is a 50 metre wide ultramylonite. The rock contains reliable shear sense indicators, but the original significance of the shear sense has been lost by subsequent folding (section 5.2.16., page 127).

## 6.3 Discussion of the theoretical significance of mylonites

### 6.3.1. Introduction

An important hypothesis that determined my strategy of research for this thesis is that terrane accretion produces mylonites, at depth, along

terrane boundaries. Hence a study of mylonites is essential in understanding the complexities of terrane accretion.

This section covers two aspects of mylonites. Firstly, the diagnostic characteristics of mylonites are discussed, with particular reference to those features of relevance to the interpretation of individual mylonitic rocks outcropping within the HBFZ. The discussion is then widened, to emphasise the difficulties in interpreting mylonitic rocks on a regional scale.

### 6.3.2. Characteristics of mylonites

Great progress in our understanding of mylonites was made when it was realised that mylonitic microstructures were produced by *ductile* rather than *brittle* processes (Bell & Etheridge 1973). This benchmark paper finally led to the rejection of the intimate involvement of brittle deformation in the production of mylonites, as originally suggested by Lapworth (1885). Bell & Etheridge noted that mylonitic microstructures could be divided into three categories:

- 1) deformation structures, including undulose extinction and deformation bands (also called "kink bands")
- 2) recovery structures, including grain polygonisation, and formation of subgrains
- 3) recrystallisation structures, including serrated grain boundaries, serrated deformation band boundaries, and the formation of new grains.

The very loose definition of mylonites given by Bell & Etheridge (1973) suggested that mylonites were the result of deformation, recovery, and recrystallisation of rocks during ductile deformation.

A tighter definition, also based on Bell & Etheridge's three categories of mylonitic microstructures, was proposed by Wise *et al.* 1984, who suggested that:

"mylonites are coherent rocks with at least microscopic foliation, with or without porphyroclasts, characterized by intense syntectonic crystal-plastic grain-size reduction of the country rock to an average diameter less than 50 microns (0.05 mm) and invariably showing at least minor syntectonic recovery/recrystallisation."

The detailed analysis of mylonitic microfabrics has led to a highly specialised branch of research into deformation mechanisms and flow laws (e.g. White *et al.* 1980, Knipe 1989). Of more direct importance to terrane analysis is the use of shear sense indicators to elucidate the sense of movement in mylonite zones (comprehensive reviews are found in Simpson & Schmid 1983, Sugden 1987, and Barker 1990).

Non-coaxial deformation produces two main groups of asymmetric microstructures that form reliable shear sense indicators;

- 1) rotated porphyroclasts (Passchier and Simpson 1986), and boudins (Hanmer 1986);
- 2) composite fabrics (Berthé *et al.* 1979, Platt 1984, Lister & Snoke 1984).

There are two main forms of asymmetric porphyroclast systems,  $\sigma$ -type and  $\delta$ -type (Fig. 6.1).

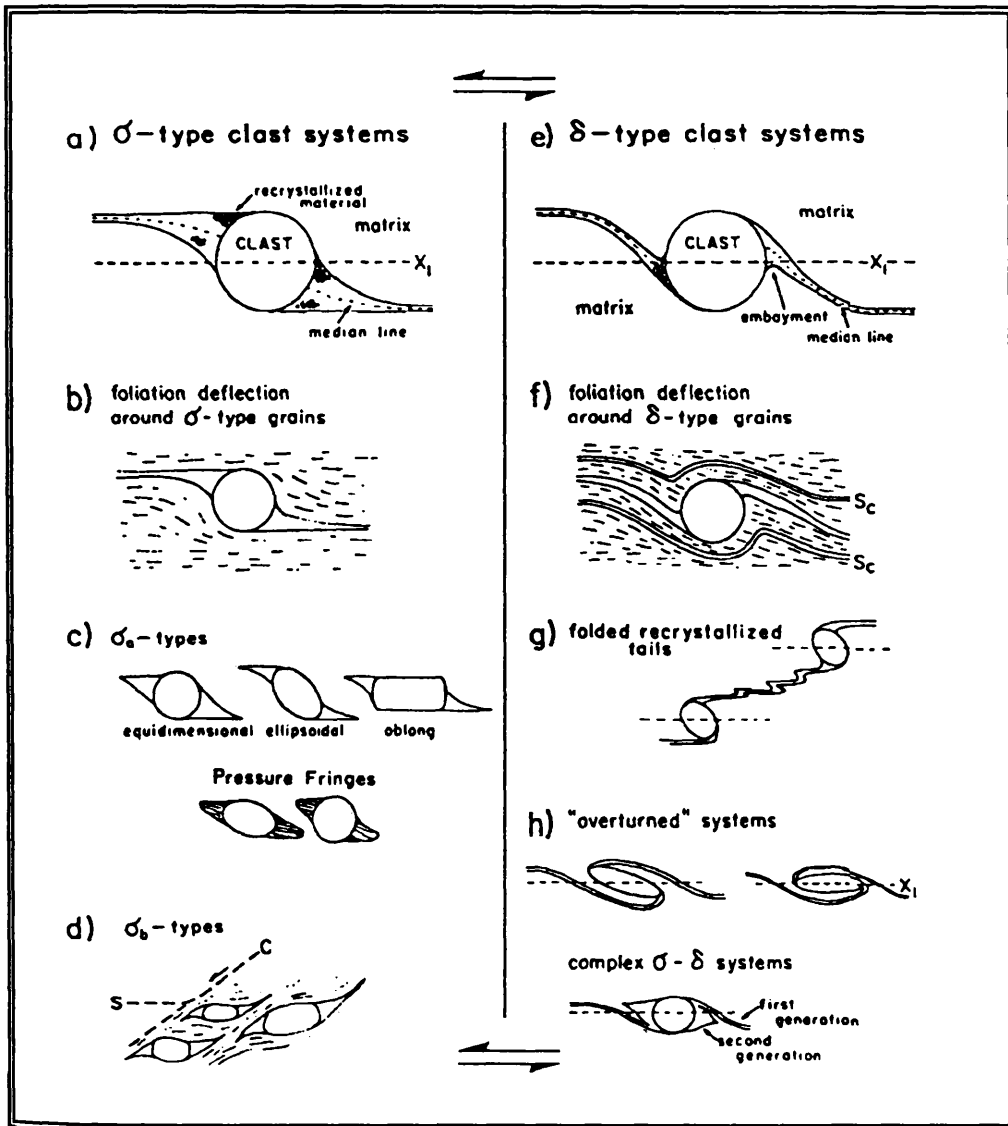


Fig. 6.1. Classification of porphyroclast systems, from Passchier and Simpson (1986). The diagram shows systems having a sinistral sense of vorticity. (a)  $\sigma$ -type system. (b) Foliation deflection around  $\sigma$ -type systems. (c)  $\sigma_a$ -type (equidimensional, ellipsoidal, oblong); pressure fringes. (d)  $\sigma_b$ -type in S-C mylonites. (e)  $\delta$ -type systems. (f) Foliation deflection around  $\delta$ -type systems.  $S_c$ , compositional layering. (g) Folded recrystallised tails. (h) Complex and overturned  $\delta$ -type systems.

Composite fabrics in shear zones can give a valuable indication of shear sense, providing care is taken to understand the kinematic significance and relationships between fabrics. Most shear zones are defined by a sigmoidal ["S"] foliation that represents the accumulation of finite strain (Ramsay & Graham 1970). In some shear zones strain is concentrated into narrow planes that parallel the major shear zone boundaries. These planes are themselves small shear zones, and define a "C" fabric (Berthé *et al.* 1979), and the relationship between S and C foliations is an indicator of shear sense (Berthé *et al.* 1979, Lister & Snoke 1984). With ongoing deformation the S-C fabric can be further extended along secondary cleavage planes (Platt 1984), to give "extension crenulation cleavage" (Fig. 6.2).

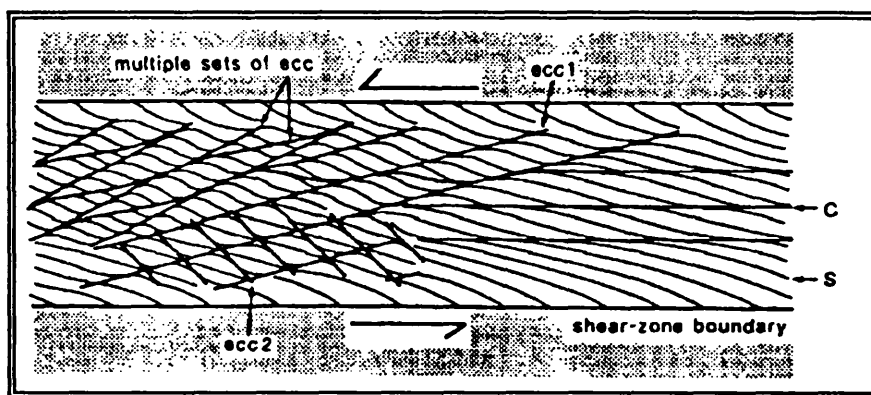


Fig. 6.2. Diagram to illustrate the orientations and mutual relationships of foliations in shear-zones, from Platt (1984). S, shape fabric; C, shear bands, *ecc1* & *ecc2*, conjugate sets of extensional crenulation cleavages.

Most studies of mylonites have investigated the deformation of a limited number of minerals, in particular quartz, feldspar, mica, olivine, and calcite. These minerals comprise the majority of mylonitic rocks, but are not likely to be ubiquitous in many mylonites found in the "disrupted" type of tectonostratigraphic terranes described by Jones *et al.* (1983) from the Western Cordillera. Such disrupted terranes are often characterized by blocks of heterogenous lithology and age set in a matrix of sheared serpentinite (or graywacke). Recent work has focused on the generation of mylonites and the use of kinematic shear sense indicators in sheared serpentinites (Norrell *et al.* 1989). This study could be of great significance in interpreting HBC rocks, and is of wider economic importance, because serpentinitised (and carbonated) shear zones can host gold, cobalt, and nickel mineralisation (Buisson & Leblanc 1985, Leblanc 1986).

Shear sense indicators, such as those described above, are of use in interpreting some of the mylonitic rocks found within the HBC. By

incorporating the kinematic interpretation of individual mylonites into the field descriptions in section 5.2, I am assuming that the use of shear sense indicators, in the way outlined here, is generally accepted by the majority of structural geologists. In contrast, the utilisation of *individual* kinematic interpretations to constrain *regional* plate motions and palaeogeographical constructions is much more ambiguous, and consequently is discussed in more detail in the remainder of this section.

There is some controversy regarding the type of flow involved in the generation of mylonites, that is, regarding the relative importance of pure shear and simple shear (Lister & Snoke 1984, p.617-618). Many mylonites are thought to have formed during simple shear, because of prolific asymmetric porphyroclasts and microfabrics that suggest a consistent sense of rotational deformation. However, the effect of pure shear is generally overlooked. I find it difficult to see why bulk deformation during pure shear will not involve grain-scale displacements similar to those seen in "simple shear mylonites". Hence ductile *pure* shear can be expected to give rise to deformation microstructures, recovery microstructures, and recrystallisation microstructures similar to those produced during simple shear (at equivalent rates of strain and recovery).

Furthermore, though the presence of asymmetric microstructures with consistent sense of vorticity may indeed imply a strong component of simple shear, this does not preclude the possibility that a component of pure shear acted across the shear zone; *i.e.* the deformation is transpressional in the sense of Sanderson & Marchini (1984). In this situation, the finite strain ellipsoid has rotated, and  $k \neq 1$ .

Sanderson & Marchini (1984) make some theoretical predictions that have important implications for "pure shear + simple shear" mylonites (from here termed "transpressional mylonites"). For given values of the pure shear ( $\alpha^{-1}$ ) and simple shear ( $\gamma$ ) components, it is possible to derive the axial ratios of the finite strain ellipsoid (Fig. 2 of Sanderson & Marchini, 1984). Theory predicts that the orientation of the X axis of the ellipsoid (corresponding to the stretching direction), is dependant upon the relative magnitudes of  $\alpha^{-1}$  and  $\gamma$ , and indeed, given a large component of compressional pure shear, the X axis may be orientated *perpendicular*, rather than *parallel*, to the direction of simple shear.

This implies that the stretching lineation in mylonites *might not always* represent the direction of regional simple shear, or the direction of regional shortening (*c.f.* Shackleton & Ries 1984, Ellis & Watkinson 1987,1988, Girard *et al.* 1988, Bamford & Ford 1988).

In fact, in this situation, the orientations of the X and Y axes can actually "switch" during progressive strain along some deformation paths, including some constant incremental strain paths (Fig. 4 of Sanderson & Marchini, 1984).

A further point of significance is that there is a range of relative values of  $\alpha^{-1}$  and  $\gamma$  (defined by the abscissa of the Flinn diagram) for which  $X = Y$  (*i.e.* "flattening",  $k=0$ )<sup>1</sup>. Transpressional mylonites recording such a finite strain might not show a well developed stretching lineation at all, and may show no *consistent* direction of shear sense.

To emphasise: an overall prediction from transpression theory is that it might be very difficult to infer regional stress (*i.e.* plate motions) from local strain patterns, even in the relatively uncomplicated situation of homogenous transpression during constant incremental strain. More common geological situations are expected to be even more complex, because strain within shear zones is often recognised to be heterogenous on a variety of scales. Volume change is also very likely to occur in shear zones.

The simplified model of transpression (Fig. 1 of Sanderson & Marchini, 1984), seems to have great relevance to actual transpression zones on a regional scale. The upward "extrusion" of deforming material in the transpression zone will occur in preference to lateral extrusion and downward thickening if the gravitational force acting upon the upper ("free") surface is less than the confining pressure acting on the other bounded surfaces. This is consistent with the "flower structures" recorded in areas that have experienced transpression (*e.g.* Sylvester & Smith 1976). An important feature of this model is that the vertical component of deformation decreases in magnitude with depth; *i.e.* gently plunging stretching lineations will predominate at depth, with more steeply plunging stretching lineations more common at higher structural levels (Fig. 6.3).

During progressive deformation, fragments of mid- and lower-crustal shear zone rocks can migrate to higher crustal levels, to give a heterogeneity of shear sense and structural style. Reactivation of the shear zone, together with deep erosion, can lead to further heterogeneity.

---

<sup>1</sup> The term "flattening" [*sensu stricto*], applies to axially symmetric shortening (Lister & Snoke, 1984, p.618). Sanderson & Marchini (1984) use the term in a more general sense, for oblate strains ( $k < 1$ ).

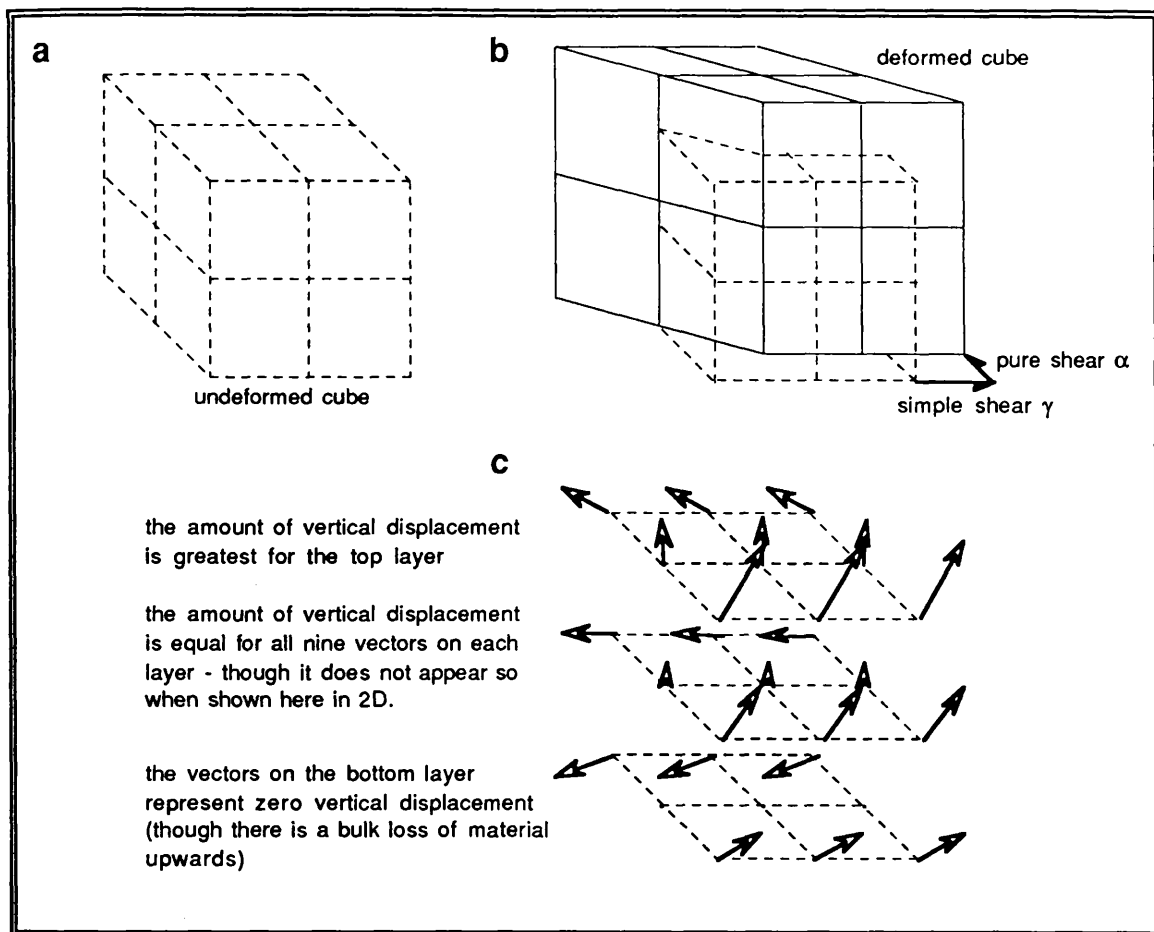


Fig. 6.3. Transpressional deformation of a unit cube, from the model shown in Fig.1 of Sanderson & Marchini (1984), showing that vertical displacements are greater at higher structural levels. (a) undeformed cube (divided into three horizontal layers) (b) deformed cube, due to transpressional stress (c) displacement vectors for the three horizontal grid layers of the original cube.

### 6.3.3. Deformation in four dimensions

An important conclusion of the previous section (6.3.2.) is that the relationship between regional-scale plate motion and outcrop-scale stretching lineations can be complex (*c.f.* Shackleton & Ries 1984). This applies to both brittle deformation (Chapter 4) and ductile deformation (Chapter 5). In order to even begin to adequately understand the complexity of this relationship, it is imperative to analyse geological structures in three-dimensions. Plane strain has received undue attention from structural geologists, even though the mathematical theory, the methodology of data collection, and the presentation of interpretations of three-dimensional structure are all well established and widely used in other branches of science (the mathematics of three-dimensional geometry was founded two thousand years ago by Euclid, the methodology of field collection of 3D data

is well developed [e.g. Ramsay & Huber 1983], and the presentation of 3D interpretation is widely used in computer aided design).

A second important conclusion is that our knowledge of progressive deformation is rather limited. Future research should aim to further investigate how deformations develop in the fourth dimension, time. This may not always be easy, because the resolution of geochronological measurement is sometimes poor. In this respect, the analysis of active modern day environments may often prove more fruitful than the study of ancient tectonism.

I think that it is particularly unfortunate that current trends in research strategy in the geological sciences seem to be moving inexorably towards specialisation, particularly specialisation in fields that can offer immediate economic return. There is room for great specialisation in structural geology, but this should be balanced with a degree of diversification in which integration with other scientific disciplines can lead to a broader understanding of geological structures.

Diversification is essential: not only should geologists study structures in three dimensions, they should also study the fractional dimension of geological structures. Do fracture patterns display scale-independent self-similarity? Do mylonites show chaotic turbulent flow? Can Andersonian behaviour ever be realised in rock, or is it the heterogeneities that exist in rock (at several scales) that actually determine how brittle deformation is manifested? The validity of using Euclidean geometry to describe nature is being questioned in many branches of science, and must now also be done in structural geology.

Diversification is also needed to study temporal relationships. Uniformitarianism - "the present is the key to the past" - is an axiom of geology still widely taught. As a guideline it is perhaps important, because modern-day environments often have fewer of the limitations that exist in the fragmented geological record. Yet as a scientific law uniformitarianism is invalid, because it is a metaphysical statement, a statement of *belief*, rather than scientific 'fact'. An alternative belief is that the earth has no steady-state behaviour, that there is no 'average' in plate tectonics of the earth's crust. Is the structural evolution of the earth *chaotic*?

## 6.4 Interpretation of the significance of HBC mylonites

The implications of the synthesis and discussion presented in sections 6.2 to 6.4 are important to the interpretation of the "mode of microplate accretion in the Highland Borders", because they provide one possible explanation for the heterogeneity of local shear sense that characterises the HBC mylonites (see section 6.2). Thus, the steeply-plunging stretching lineations (typifying many of the central and north-eastern HBC exposures) need not be structurally incompatible with the gently-plunging stretching lineations (that typify many of the south-western HBC exposures), but instead might be interpreted as representing different levels of a major terrane-scale transpressional deformation event (see Fig. 6.3). Progressive deformation, repeated fault reactivation, and differential erosion (*i.e.* generally deeper erosion in the south-east), have given the HBC mylonites their enigmatic heterogeneity and complexity.

This hypothesis, that (some of) the ductile deformation within the HBFZ represents transpressional deformation, *still* cannot yet be *adequately* tested with the evidence that I have both collected in the field, and collated from many previous studies. The possibility certainly still remains that some mylonitic components of the HBC are not temporally connected, but instead formed during entirely different deformational episodes (or perhaps even belong to entirely different tectonostratigraphic terranes). This is explored further in the next section.

## 6.5 Theoretical concepts of terrane tectonics

This section introduces some concepts in terrane geology that are of importance in interpreting the ductile deformation in the HBFZ. The section forms a basis for further interpretation of the data of section 5.2, to be presented in section 6.7.

### 6.5.1. Plate tectonics and terrane tectonics

In the 1960's the geological sciences were completely revolutionised by the theory of plate tectonics, which provided an all-embracing theory that helped geologists relate the geological record to lithospheric processes operating at the present time. The overall effect of plate tectonic theory has been to radically enlarge the scale of understanding of earth scientists, who

in general had previously been limited to tackling problems on an outcrop or a regional scale.

There have been two fundamental areas of modification<sup>1</sup> in plate tectonic theory since its inception (Wilson 1965). One was the realisation that lithospheric plates are not rigid, but deform by *flexure* in response to interplate stress and intraplate loading. The other modification resulted from the study of destructive plate boundaries.

Plate tectonic theory originally predicted the repeated opening and closing of oceans, and the consequential splitting and subsequent collision of continental plates (Wilson 1966), and this repetition of tectonic events became known as the "Wilson cycle" (Windley 1984). The study of *destructive* plate boundaries (so called because the Benioff zone returns oceanic crust back to the mantle), has since revealed them to be sites of significant growth of continental crust<sup>2</sup>. This is believed to occur by two processes: firstly, by the intrusion and underplating of the continental crust by rising diapirs, derived from the differentiation of sinking oceanic crust (*e.g.* the Andes), and secondly, by the accretion of microplates (of oceanic, continental, or hybrid character).

Microplate accretion along a continental margin can lead to incredible structural and stratigraphical complexity. As an example; the geology of Indonesia is complicated, and presently not well understood. Imagine, however, the even greater chaos that will result when the Australian plate shunts the myriad of Indonesian islands into collision with Vietnam and China.

Such complexity was recognised in the Cordilleran orogenic belt, when it was realised that the entire western margin of the American continent was composed of a tectonic collage of unrelated microplates.

Palaeomagnetic studies (Beck 1976) suggested that many of the microplates had been carried hundreds, or even thousands of kilometres on oceanic crust now subducted beneath North and South America. These discoveries encouraged some geologists to adopt a new methodology in their research, involving the identification and analysis of "tectono-stratigraphic terranes" (Coney *et al.* 1980, Ben-Avraham *et al.* 1981)

---

<sup>1</sup> There have been countless hypotheses that have helped to refine rather than modify plate tectonic theory. A third major change in the theory may result from chaos theory (*e.g.* Gleick 1987), including the recognition of fractal geometries in geological processes (see Mandelbrot 1982).

<sup>2</sup> Hence, the production and differentiation of oceanic crust, and the return of the residual magma to the mantle, may represent the most efficient method of mantle segregation, allowing heat loss from the earth's interior, and producing a geoid that has more gravitational stability.

Tectonostratigraphic terranes are defined by Jones *et al.* (1983) as "fault-bounded geologic entities of regional extent, each characterized by a geologic history that is different from the histories of contiguous terranes".

Jones *et al.* (1983) further qualify their definition of terranes with some fundamental comments about terrane analysis:

"The basic question that must be asked while analyzing stratigraphic sequences of possibly distinct terranes is whether or not the inferred geologic histories are compatible with the present spatial relations. This decision is not always easy to make, and is heavily dependant on the quality and quantity of geologic controls that are available to the analyzer. The degree of differences noted between terranes is thus variable, and classifications will differ according to the judgement, experience, and competency of the analyzer. New data always require reexamination of existing terrane classifications, and it is expected that new combinations or subdivisions will result from additional palaeontological, geologic, and geophysical research. In this regard, terrane nomenclature is similar to stratigraphic nomenclature, and is subject to continuous revision as data accumulate and concepts evolve".

These comments form an important statement about the philosophy of terrane analysis. The possibility (or probability) that orogenic belts *might* be composed of unrelated lithospheric fragments should preclude geologists working in such belts from assuming geological continuity, yet many *geometric* reconstructions (*i.e.* balanced cross-sections) of orogenic belts (such as the Alps and Himalayas) still make such assumptions.

Terrane analysis demands a change of emphasis in geological reasoning, and requires the rejection of the geological principle of adopting the *simplest* solution as the most likely hypothesis. This is a progressive step in scientific methodology.

Terrane analysis has helped to further our understanding of other orogenic belts, including the Caledonide-Appalachian Chain (*e.g.* Barker & Gayer 1985; Hutton & Dewey 1986; Hutton 1987). However, some of the recently presented research on British Caledonide terranes suggests that the rigorous rationale of terrane analysis has not been universally adopted. Jones *et al.* (1983) point out that; "a critical feature of terrane analysis is that geologic and geophysical data must be clearly separated from plate tectonic interpretations concerning the genetic relations among terranes". There may currently be a danger in British Caledonide research that some fault-bounded blocks are *assumed* to be terranes, and that the term 'terrane' is in some way synonymous with 'large scale strike-slip'. This is fundamentally not so! Importantly, in the Western Cordillera the identification of a terrane is based primarily on its internal stratigraphy (*not* on the presence of a fault boundary), and need not carry any genetic or even plate tectonic implication (Coney *et al.* 1980).

There are additional complexities and uncertainties associated with the analysis of ancient terranes and terrane boundaries, in comparison with modern accretion zones, because of the following considerations;

- 1) repeated reactivation of terrane boundaries is likely (*e.g.* Goldstein 1989)
- 2) fault zones can act as pathways for repeated fluid flow and metasomatism
- 3) repeated magnetic overprinting is likely
- 4) whole terranes and their boundaries are more likely to be completely buried by overlying strata

Consequently, terranes and their boundaries tend to become overprinted ("homogenised") by later tectonic events, or become buried by the products of subsequent depositional episodes. Even those that do not experience post-accretion complications can be difficult to interpret;

- 5) the biostratigraphical record is not as detailed or refined for earlier periods
- 6) the global pattern of sea floor spreading is unknown for the Proterozoic and Palaeozoic (unlike the Mesozoic and Caenozoic).

These complications have the important implication for the analysis of ancient terranes that most ancient terranes will be difficult to identify as truly allochthonous with any degree of certainty. Most terranes may therefore be regarded as "suspect" (following the terminology of Coney [1978], and Coney *et al.* [1980]), but their affinity might never be proven, even after very thorough and painstaking research.

In summary, terrane analysis involves a more realistic and objective methodology than previous geological practise, but care should be taken to separate objective observation from imaginative and creative interpretation<sup>1</sup>.

#### 6.5.2. Problems associated with structural and stratigraphical correlations

In using terrane analysis to interpret orogenic belts, great importance is placed upon structural and stratigraphical correlations. Because some degree of subjectivity is involved in all correlation, the conclusions of terrane analysis must constantly be reviewed as data are updated.

---

<sup>1</sup> The final comment is not meant as a rejection of the need for interpretation, which, when done skilfully, will involve both imagination and creativity. It is generally the *interpretation* of data that leads to a greater understanding of the significance of ones data, and allows other scientists to view their own work in a wider context. However, raw data must always be presented, to allow them to be progressively reinterpreted in conjunction with new data, as they becomes available.

The *largest* block of structurally homogenous rock presently exposed in the HBC is probably less than one metre in diameter! This is because late brittle deformation was pervasive. At an outcrop scale, few geologists would debate the correlation of adjacent blocks that have identical field appearance, separated only by mesofractures that show little evidence of displacement. However, other correlations might be more controversial. For example, the positive identification of a fragment of Dalradian within the HBC (or the identification of Dalradian clasts in HBC or ORS basins) is extremely difficult to prove beyond reasonable doubt. What are the diagnostic characteristics of the Dalradian terrane that enable it to be distinguished from all other terranes, including possible terranes now not seen in the British/Irish sector of the Caledonides?

Some of the causes of difficulties in correlation are as follows:

- 1) exposure is limited in much of the Highland Borders. Is it justifiable to correlate adjacent exposures of similar lithologies that are separated by a gap in exposure? How similar must the lithologies be? How great can an exposure gap be before correlation is doubted?
- 2) lateral variations in stratigraphy are commonplace in many geological environments. Consequently, some valid correlations between equivalent lateral variants may be missed.
- 3) too little is understood about the interplay between sedimentation and tectonics. Can a basin avoid receiving sediment from an adjacent orogenic belt? How reliable and/or significant are palaeocurrent data in interpreting the direction of regional sediment transport?
- 4) structural correlations are fraught with difficulty, because deformation in fault zones often gives rise to fault-parallel fabrics, and adjacent blocks can have similar fabric geometries produced at widely differing times.
- 5) biostratigraphic correlation relies upon precise knowledge of the stratigraphic range of faunal specimens.
- 6) fault zones act as sites of repeated reactivation, metamorphism, and metasomatism, all of which tend to "homogenise" the field appearance of rocks of widely different origin.

It is complications such as these that prompted Jones *et al.* (1983) to comment that "the degree of differences noted between terranes is thus variable, and classifications will differ according to the judgement, experience, and competency of the analyzer."

In reality, no structural or stratigraphic correlation can be *proven*. Careful research might provide *support* for a hypothesis that two blocks are

tectonostratigraphically equivalent, but correlation will always involve some degree of subjectivity.

### 6.5.3. The mode and timing of microplate docking in the Highland Borders of Scotland: philosophical discussion

In this section I shall attempt broaden the discussion of the research, to give a wider perspective to the research presented in thesis, particularly that given in Chapter 5, and to thereby show how the status of the science that I have documented in Chapters 5 and 6 differs in some respects from that given in the earlier chapters.

In common with the preceding chapters of this thesis, the science presented in Chapter 5 is based on individual "scientific" observations and measurements. However, the science here differs in the methodology that I have adopted in interpreting those individual observations to form hypotheses.

Such a statement of scientific philosophy demands much further explanation and discussion!

For example, in Chapter 2, the observation that Permo-Carboniferous dykes show little displacement across the HBFZ, leads to the hypothesis that the HBFZ has not moved significantly since Permo-Carboniferous times. Similarly, in Chapter 4, the observations that (1) triaxial compression in controlled experiments can give rise to four sets of fractures that have orthorhombic symmetry, and (2) that some rocks in central Scotland have four sets of fractures that have orthorhombic symmetry, leads to the hypothesis that central Scotland has experienced triaxial compression. What hypotheses can be derived from the observations presented in Chapter 5? Before I attempt to answer this question, I must make an important digression, in order to refute and reject inductivism as a scientific method.

The two hypotheses from chapters 2 and 4 given above, can in no way be considered to be scientific "facts". Both hypotheses might be modified or rejected after further scientific observations have been made. For example, if the dykes that cut the HBFZ were re-dated as Tertiary, the first hypothesis would be modified. Should further experiment into rock deformation show that triaxial deformation only gives rise to four fractures sets under unrealistic P/T/t conditions, then the second hypothesis would be rejected. In this respect, both hypotheses conform to the falsificationist view of

scientific theory (e.g. Popper 1968), and show that inductivism is inadequate.

The fallibility of observation also provides problems for the inductivist; different geologists working on the same problem will gather different data from the same outcrop. Thus, inductivism is logically invalid, because there must always be a *potential* gap between perception and reality.

There are many hypotheses contained in chapters 2 to 4, and in general all share the features of the two examples discussed above. All are capable of being falsified to a greater or lesser extent (e.g. the hypothesis that "central Scotland experienced a heterogeneous triaxial deformation that was sinistrally transpressive with respect to the HBFZ in mid-Devonian times", is more falsifiable than the hypothesis that "mesofracture station 21 experienced triaxial compression at some unspecified time").

The important feature of the hypotheses presented in the preceding chapters is that they all conform to and support a set of coherent and logical scientific theories. For example, I have not documented any clear observations that suggest that Reches theory of triaxial stress must be rejected. And the mesofracture analysis has led to modification and expansion, but *not* rejection, of the Harland model of simple transpression.

The science in *this* chapter serves to demonstrate the inadequacy of the falsificationist view of scientific theory. Although highly falsifiable hypotheses can be formulated from the observation statements presented in section 5.2, many such hypotheses can be shown to be speculative and rather irrelevant. For example, the following assertions are highly falsifiable:

- 1) all shear zone movement within the HBFZ was sinistral,
- 2) there was 1,326 km of sinistral movement on the HBFZ between 465 Ma and 430 Ma.

There are serious problems with forming hypotheses in this way. Consider the second assertion, concerning the amount of HBFZ displacement at a specific time. Ostensibly, this bold conjecture is highly falsifiable, because it makes *very specific* claims about the mode and timing of fault movement. Yet, in order for scientific progress to be made, such assertions must be testable in a practical way. What research strategies can be adopted now to try to falsify the hypothesis? What observations that I have recorded in section 5.2 help to falsify or confirm the conjecture? *In fact, most hypotheses that could be proposed for ductile HBFZ movements cannot yet be readily tested, and this is the most important difference between the science here compared with that of preceding chapters.* This is discussed in more detail later.

The first assertion, that all movement in the HBFZ is sinistral, is much more acceptable to sophisticated falsificationists, because it is highly falsifiable *and* appears very testable. Should further field work in the Highland Borders reveal a mylonite with "reliable" dextral shear sense indicators, then the original assertion has been falsified. However, there are three serious difficulties in adopting this method of scientific reasoning:

- 1) the overall philosophy of the falsificationists has been adopted by some geologists working in the British Caledonides, yet, as I have already alluded to in section 6.5.1, this approach conflicts with the philosophy of terrane analysis as outlined by Coney (1980), Jones *et al.* (1983), and others. To the inductivists, terranes are "innocent until proven guilty", whereas to the falsificationists, terranes are "guilty until proven innocent" (this is much more exciting!). In terrane analysis, however, *all* terranes are "suspect", to a greater or lesser degree as more and more scientific observations are accumulated.
- 2) falsificationism has led to serious *practical* difficulties in British Caledonide research, because highly conjectural assertions (made by falsificationists) have been assumed by inductivists to be based on induction, and hence have been adopted by them as scientific facts. These "facts" can then be used as the basis for further hypotheses by falsificationists and inductivists alike, leading to further conjectures, inductions, and "facts", all of which having varying degrees of scientific validity. There have been two centuries of research in the British Caledonides to allow this process to develop, but the problem seems particularly acute at present because falsificationism now has unprecedented support amongst Caledonide geologists.

The fundamental importance of separating fact from speculation was emphasised by Hutton (1987, and pers. comm.), yet in practise this often proves impossible. As an example: Hutton (1987, p. 406-407) takes a conjecture about lower Silurian sinistral transpression in Clew Bay, as a "fact" that forms the basis for further conjecture on the nature of Caledonide terrane movements. Similarly, in several parts of this thesis I have structured the text to try to separate fact from interpretation, but there must be many examples of interpretations and conjectures that have crept into the "data" sections. Objectivity and impartiality must be strived for when making scientific observation statements, but in practise this is impossible to achieve completely. Much of research performed by the survey geologists in the late-nineteenth to early-twentieth centuries has retained long-lasting usefulness and relevance. This is principally because objectivity of observation was emphasised,

and clear distinction can normally be made between their observation and their interpretation (it may also be partially due to the low theory dependence of their observations).

- 3) falsificationism is logically invalid because it fails to account for the complex nature of some scientific theories. For example, if I find a HBC mylonite with dextral shear sense indicators, does this really falsify the hypothesis that "all shear zone movement within the HBFZ was sinistral"? Of course it doesn't *necessarily* falsify the assertion; perhaps the "dextral" mylonite was originally sinistral, but has been rotated by subsequent fault movement.

These logical difficulties led philosophers to explain scientific theories not in terms of individual observation statements, but rather in terms of "structures" of observations and theories, all of which can have some degree of interdependency. Viewing science in this way can help understand the difficulties inherent in Highland Border research, and might lead to the adoption of more fruitful research strategies in the future.

So, I believe that falsificationism fails to provide a strategy of research into HBFZ terrane analysis, on *philosophical, practical* and *logical* grounds. One attempt at developing the falsificationists view of scientific theory was made by Lakatos (1974), who views theories as forming "research programmes", comprised of a "hard core" of basic assumptions, together with a "protective belt" of additional hypotheses that protect the "hard core" from falsification (a trivial example has already been given; the "hard core" theory that "all movement in the HBFZ was sinistral", is protected from falsification by the "protective" hypothesis that "dextral mylonites are actually sinistral mylonites that have been rotated"). According to Lakatos, the hard core of research programmes must not be rejected or modified (this statement forms the "negative heuristic"), and research programmes should include some guidelines outlining how research should be developed (these form the "positive heuristic").

In the broad research programme of terrane analysis, the "hard core" theory is that orogenic belts can be comprised of distinct tectonostratigraphic terranes. There is a wealth of theories - the "protective belt" - that are concerned with the character of terranes, the nature of their boundaries, the ways in which they accrete with the orogenic margin, *etc. etc.* At present, terrane analysis in general is a *progressive* research programme, because it is continuously leading to novel predictions and hypotheses regarding the nature of orogenic belts.

Lakatos' view of science helps to explain the difficulty that I have in interpreting the science presented in section 5.2. Although terrane analysis is, in general, a highly progressive research programme, this chapter is mainly concerned with only one small part of terrane analysis; the analysis of a "disrupted terrane". At present, the positive heuristic of terrane analysis gives little guidance to the future research of disrupted terranes. So, how should disrupted terranes be analysed?

Although it might at present be difficult to see how the analysis of disrupted terranes will become as progressive as other parts of terrane analysis, this may be overly pessimistic, because the research programme is still immature (stone-age man just discovering fire might have had difficulty contemplating manned space-flight!).

However, there is perhaps a genuine difficulty in establishing a positive heuristic in the analysis of disrupted terranes because the geology of such terranes seems so complex, given our present understanding and vision. Often, such immaturity of scientific theory is due to lack of appropriate scientific instruments (for instance, would chaos theory ever have evolved without digital computers?), but this is probably not so in terrane geology. Our problem is not one of technical development, but rather one of scale and time. Previously, I stated that many theories that might be inferred from the data in section 5.2 are not independently testable. Strictly speaking this is not so; theoretically they can be tested, because our observational skills are probably adequate, and instrumentation is well developed. The problem is a practical one; to adequately test even a simple hypothesis might, for some disrupted terranes, require an inordinate number of observation measurements, in total taking an unreasonable amount of time. This is exacerbated by the *scale* of terranes; attempting to derive a coherent and testable regional-scale interpretation, given the common complexity at outcrop-scale, sometimes seems fraught with difficulties.

An alternative view of scientific theories as "structures", was developed by Kuhn (1970), based on the complete rejection of falsificationism. Again, this can help to explain the difficulty that I have in interpreting the science presented in section 5.2.

Kuhn's view is that a "mature" science can be explained by a single paradigm (the "disciplinary matrix"), that is difficult to define, but nevertheless gives guidance to the development of the science which it governs. Mature science is followed by periods of scientific revolution in which the original paradigm is rejected (the acceptance of plate tectonic

theory is a good example of scientific revolution). Importantly, mature science is *preceded* by a "pre-science" stage, in which fundamental theories are poorly defined and research lacks direction. The development from pre-science to mature science is impossible before the necessary scientific apparatus, analytical techniques, and supporting theories are developed (for example, Newton's theory of gravitation was not formulated before the mathematical development of calculus). This may be of relevance to this thesis; the analysis of disrupted terranes may be in a "pre-science" stage of scientific development. Progress isn't possible until the paradigm of "disrupted terrane analysis" can be given some coherency and substance.

**In summary:** rigorous terrane analysis demands that conjectures that would have previously appeared trivial or irrelevant must now be challenged. The complexity inherent in the HBC *disrupted* terrane makes some of these conjectures extremely difficult to be tested thoroughly.

The science in Chapter 5 differs from that in preceding chapters because many possible hypotheses concerning HBFZ ductile deformation are not independently testable, given the time constraints of this research project. This may be a significant contributory factor in the difficulty that geologists have had in establishing a coherent strategy of research, and in formulating a unifying hypothesis in which disrupted terranes can be interpreted.

The discussion presented in this section has important implications for this thesis, and for other research projects that study disrupted terranes.

- 1) It is fundamentally important to try to separate observation statements from interpretation and conjecture. Of course, total objectivity is ultimately impossible (because of the "theory dependence of observation", and "the infinite regress" of Plato), but practically speaking, much improvement *can* be made by geologists working in terrane analysis.
- 2) To force a detailed interpretation of observation statements is often inappropriate, at least at this stage in the development of the analysis of disrupted terranes, particularly when such interpretations might be subsequently treated as "facts" by other geologists. The observation statements presented in section 5.2 might, at some time in the future, help to develop a "protective belt" to a Lakatosian type "disrupted terrane" research programme, or might help to form a Kuhnian paradigm, but as yet, I can give little more significance than this to much of the data. In a way, I feel that this is in keeping with the whole philosophy of terrane analysis.

- 3) Speculation and imaginative interpretation of regional geology can play an important part in helping to formulate the "protective belt" or the "disciplinary matrix". This can be recognised historically in the development of many of the great scientific theories, and also helps to explain the acclaim received by modern-day tectonicists such as J.F. Dewey. Their ability is that they can provide a loose "framework" of understanding, in which other geologists can more easily explain their own observations and small-scale hypotheses. For this reason, I have included a regional-scale speculative interpretation of HBFZ movement history (section 6.7), but I cannot over-emphasise that this should not be taken as a coherent and independently testable hypothesis founded on an adequate and entirely supportive base of observation statements (for example, compare the "validity" of section 6.7 with section 4.8 - the strain partitioning model for simple transpression).

In the next section I shall attempt to overcome the difficulties that I have expressed here, in order to try to give some direction to the development of the analysis of disrupted terranes.

#### 6.5.4. A strategy for the future analysis of disrupted terranes

There is a marked difference between the analysis of coherent terranes compared with analysis of terrane boundaries and disrupted terranes. In disrupted terranes coherency is low and deformation is high. Disrupted terranes can generally be repeatably sub-divided into smaller and smaller contiguous units. The terrane nomenclature is rather arbitrary in this situation.

Consequently, whereas coherent terranes can be readily analysed to give information on their origin and affinity, disrupted terranes will only yield this information in certain circumstances (for example, a disrupted terrane may include blocks that have very diagnostic geochemistry or stratigraphy that is already recognised in other coherent terranes elsewhere in the orogen). Instead, disrupted terranes can contain information about the timing and sense (and amount?) of terrane displacement.

Paradoxically, in the HBC most of the limited amount of information about the age of tectonism is derived from stratigraphic rather than structural data (see section 6.6.1), but for disrupted terranes that have no biostratigraphical record, this would be completely invalid.

In addition, I think it is important to stress the subjectivity associated with the strategy that I chose to try to interpret the HBC. Section 6.6 is an

attempt at the *correlation* of HBC stratigraphy and history, and this forms the basis of HBC interpretation in section 6.7 (given due recognition of the difficulties that exist in such correlation, as outlined in section 6.5.2). In general, terrane analysis relies on geological correlation (Jones *et al.* 1983), but I believe that the reliability and validity of *any* correlation in the HBC must be considered questionable.

At the very least, geologists should openly recognise, rather than conceal, the subjectivity associated with HBC correlation.

The usefulness of a disrupted terrane in the study of orogenic belts lies not in being able to unravel or re-assemble that terrane, but rather in the evidence of terrane movements that it may contain. Consequently, research in disrupted terranes, unlike coherent terranes, should not concentrate on *correlation*, but should aim to describe and interpret individual blocks *in isolation* (*i.e.* individual fault-bounded pods and individual outcrops, within the disrupted terrane)<sup>1</sup>.

Palaeontological data cannot be used to establish a *highly objective* tectono-stratigraphy for the *whole* terrane. The data can be used in isolation to constrain the ages of individual fault rocks.

The initiation of future research projects to analyse disrupted terranes should start with the identification of a significant number of well-exposed shear zones that have not been severely overprinted by subsequent geological processes. The principal aim of the project should be to study these shear zones for evidence of shear sense and timing of deformation. Future research should therefore also aim to develop ways in which fault fabrics can be precisely dated.

#### 6.5.5. Concluding remarks concerning objectivity and subjectivity

At the risk of repetition, I shall now try to summarise the arguments presented in section 6.5. Given the observational data presented in section 5.2, it is possible to interpret the significance of the data in a way that is broadly "scientific". Yet, it is important to stress the inherent subjectivity of such interpretation.

As an example, consider the mathematical expression

$$a^2 = b^2 + c^2 - 2bc \cos A$$

<sup>1</sup> Thus outcrop mapping is essential, at a scale at which *significant* structural boundaries and exposure gaps can be accurately recorded. The location of field samples can then be recorded accurately, and where possible the location should also be marked indelibly on the outcrop.

This formula is the cosine rule. A mathematician can regress back through a series of logical steps, using other theorems (including Pythagoras' in this instance) to prove or disprove the validity of the equation. Regression is not indefinite: sooner or later the whole argument will depend on a number of fundamental axioms (in the above case, the axioms of Euclidean geometry). If one were to define a completely different reference frame with a new set of axioms, a whole new set of theorems could be developed. Thus, mathematical science can be seen to have very high objectivity.

In contrast, consider two conclusions from this thesis:

- (a) the present-day HBFZ is still a site of significant crustal weakness
- (b) there was major terrane accretion along the HBFZ during the Upper Ordovician.

Both these hypotheses can be regressed back to a (large and complicated) set of fundamental geological axioms. In formulating the first hypothesis, there is little uncertainty, assuming that one accepts the fundamental axioms of geology relating to earthquakes, faults, and plate tectonics. Objectivity appears to be high.

However, when formulating (or regressing) the second hypothesis one encounters many uncertainties, even though the fundamental axioms of geology remain. For instance, when regressing the second hypothesis, a question that immediately arises concerns the very low proportion of HBC rocks that show high shear strain (see section 6.2.1.). Some possible reasons (the "protective belt" of theories) are presented in section 6.2.1., *but the hypothesis remains inherently subjective until such a problem is resolved.*

So there is more uncertainty associated with some scientific hypotheses than with others, but there are no simple formulae for quantifying such uncertainty. Such subjectivity arises not out of "experimental error", but from unanswerable questions that arise when a hypothesis is formulated.

Sections 6.6 and 6.7 present subjective plate tectonic interpretations of the significance of the HBC. My aim was to make them *consistent* with the field data described in Chapter 5, but this in no way implies that the model presented in the *only* valid interpretation.

## 6.6 Interpretation of ductile deformation along the HBFZ

### 6.6.1. An Interpretation of regional HBC stratigraphy

As outlined in section 6.5 the identification and analysis of tectonostratigraphic terranes involves the assimilation and interpretation of stratigraphical data, involving recourse to biostratigraphal, lithostratigraphal, geochemical, and/or magnetostratigraphical information as appropriate. This section aims to summarise the stratigraphy of the HBC by jointly interpreting the data that I presented in section 5.2, together with the data from the many previous studies referenced therein. In the interpretation of HBC tectonostratigraphy, *biostratigraphical* data is generally more useful (but not necessarily more *reliable*) than other types of stratigraphic data, and consequently I have placed greater importance on biostratigraphical information in my tectonostratigraphic interpretations.

The stratigraphy of the HBC has been studied by geologists for over two hundred years; a full and detailed history of research on HBC stratigraphy is given in Curry *et al.* 1984. The rediscovery of a Lower Arenig fauna within the HBC (Curry *et al.* 1982), together with subsequent palaeontological investigation (Curry *et al.* 1984, Dorning 1985, Ingham *et al.* 1985, Curry 1986, Whelan 1988) has allowed the basis of a HBC biostatigraphy to be constructed and refined (Fig. 6.4).

Bluck *et al.* in Curry *et al.* 1984 divided the HBC into four lithostratigraphic units, supported by biostratigraphic correlation wherever possible (see section 6.6.2 for a discussion of the difficulties associated with such interpretations):

Rock assemblage 1: serpentinites, amphibolites, and tectonites (*i.e.* rocks of possible ophiolitic affinity). The age of this assemblage is poorly constrained, though an unpublished age of  $540 \pm ?$  exists for the amphibolite on Bute (Tim Dempster, pers. comm. 1990). Re-dating is still in progress. Some of the rocks of this assemblage, particularly the tectonised serpentinites, may have acted preferentially as zones of repeated high shear strain (with associated fluid flow), thus obliterating much of the evidence of their primary character and age.

Rocks of assemblage 1 may represent several separate tectonostratigraphic units, and it is possible that continuing work may further sub-divide this assemblage.

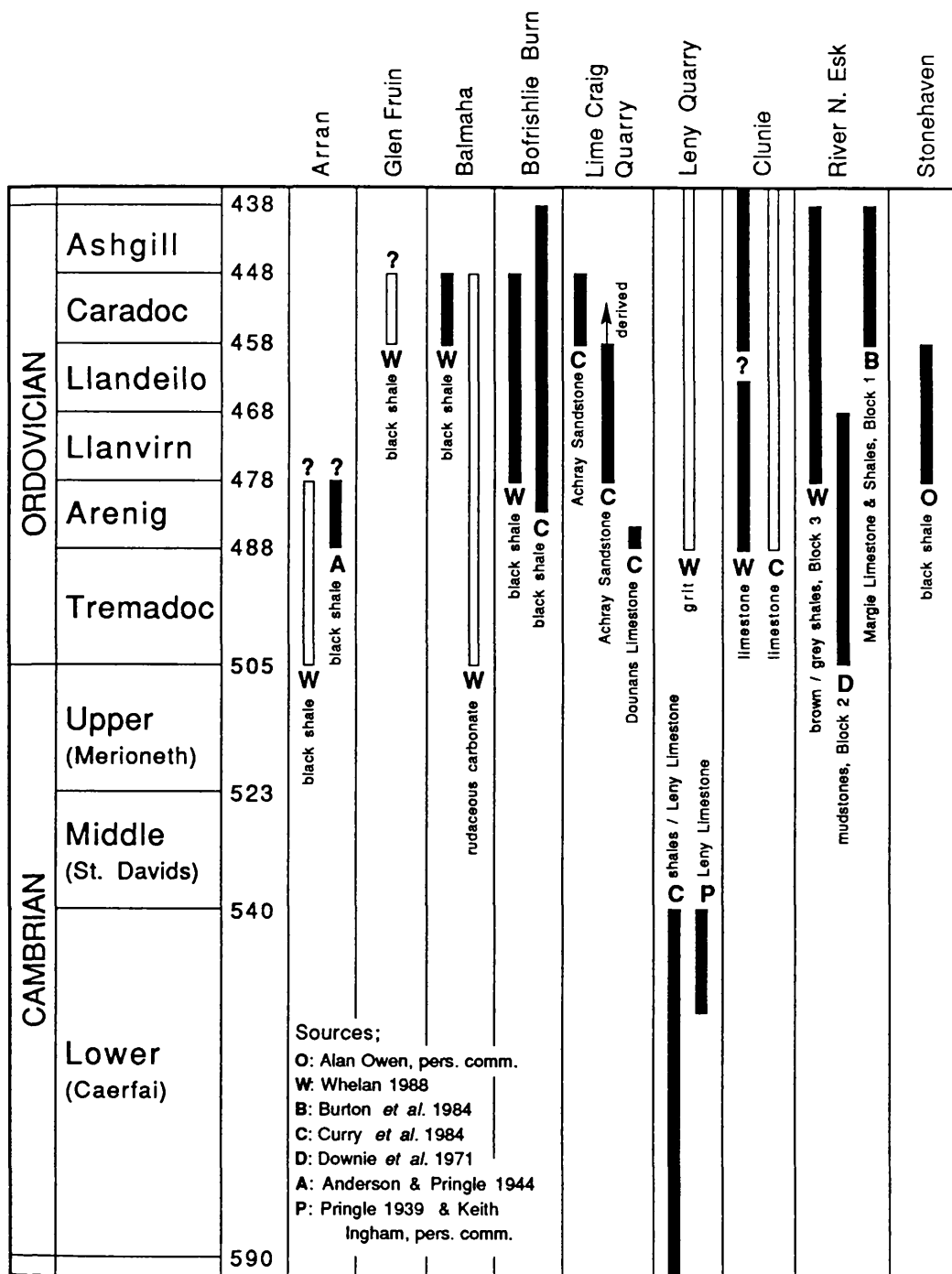


Fig. 6.4. A summary of biostratigraphic data from the Highland Border Complex. Solid bars apply to specimens identified with a high degree of confidence (generally to species level), while hollow bars relate to specimens of more unclear palaeontological affinity. Question marks (?) refer to other uncertainties (specimens now missing, uncertain stratigraphical range, etc.). The locations of the HBC sections are shown in Fig. 5.1. The timescale is from Harland *et al.* 1982.

Rock assemblage 2: carbonates, and sedimentary serpentinite conglomerates (note that some HBC serpentinite conglomerates are probably tectonic in origin). It has been assumed that assemblage 2 sits unconformably on assemblage 1 (Curry *et al.* 1984), but this is unproven.

The Lime Craig serpentinite conglomerate contains a component of detritus that has Archean  $T_{DM}$  ages, with a mid-Proterozoic thermal overprint (Dempster & Bluck 1990).

Rock assemblage 3: black shales, cherts, tuffs, spilites, and quartz-wacke turbidites, probably Llanvirn to Llandeilo in age (though the Arran black shales have been assigned an Arenig age).

Some of the turbidites of this assemblage contain basic or ultrabasic rock fragments (Curry *et al.* 1984, p.129).

Rock assemblage 4: sandstones, conglomerates, and limestones of Upper Ordovician age, sitting unconformably on assemblage 2 (at Balmaha) and assemblage 3 (at Bofrishlie Burn). Assemblage 4 includes (some of ?) the Loch Lomond Clastics (Henderson & Robertson 1982), the Achray Sandstone (Curry *et al.* 1984), and the Margie Limestone (Barrow 1901). Many of the samples contain abundant slate, shale, chert, and basic-ultrabasic fragments.

The biostratigraphic data, together with lithostratigraphical correlation, allows a tentative *interpretation* of the geological history of the HBC to be attempted. Inferred relationships between the four rock assemblages are shown in Fig. 6.5.

The above interpretation suggests that most (but *not* necessarily all) of the HBC might represent a single tectonostratigraphic terrane. The affinity of the Lower Cambrian Leny limestone remains unclear, though it almost certainly can no longer be considered to be Dalradian (Rogers *et al.* 1989). Further information about the ages of the various components of assemblage 1 is needed before the inter-relationships of this assemblage with the Leny sequence can be elucidated.

The interpretation given in Fig. 6.5 shows two phases of tectonism affecting the HBC. The younger of these occurred at some time between the Caradoc and Llandovery, and is deduced from the difference between cleaved HBC arenites of assemblage 4, and the overstepping undeformed Wenlock ORS. The earlier phase of tectonism occurred in late Llandeilo or early Caradoc times, and is deduced from the difference in structural complexity between HBC assemblage 4, and the unconformably underlying HBC rocks of assemblages 3 and 2.

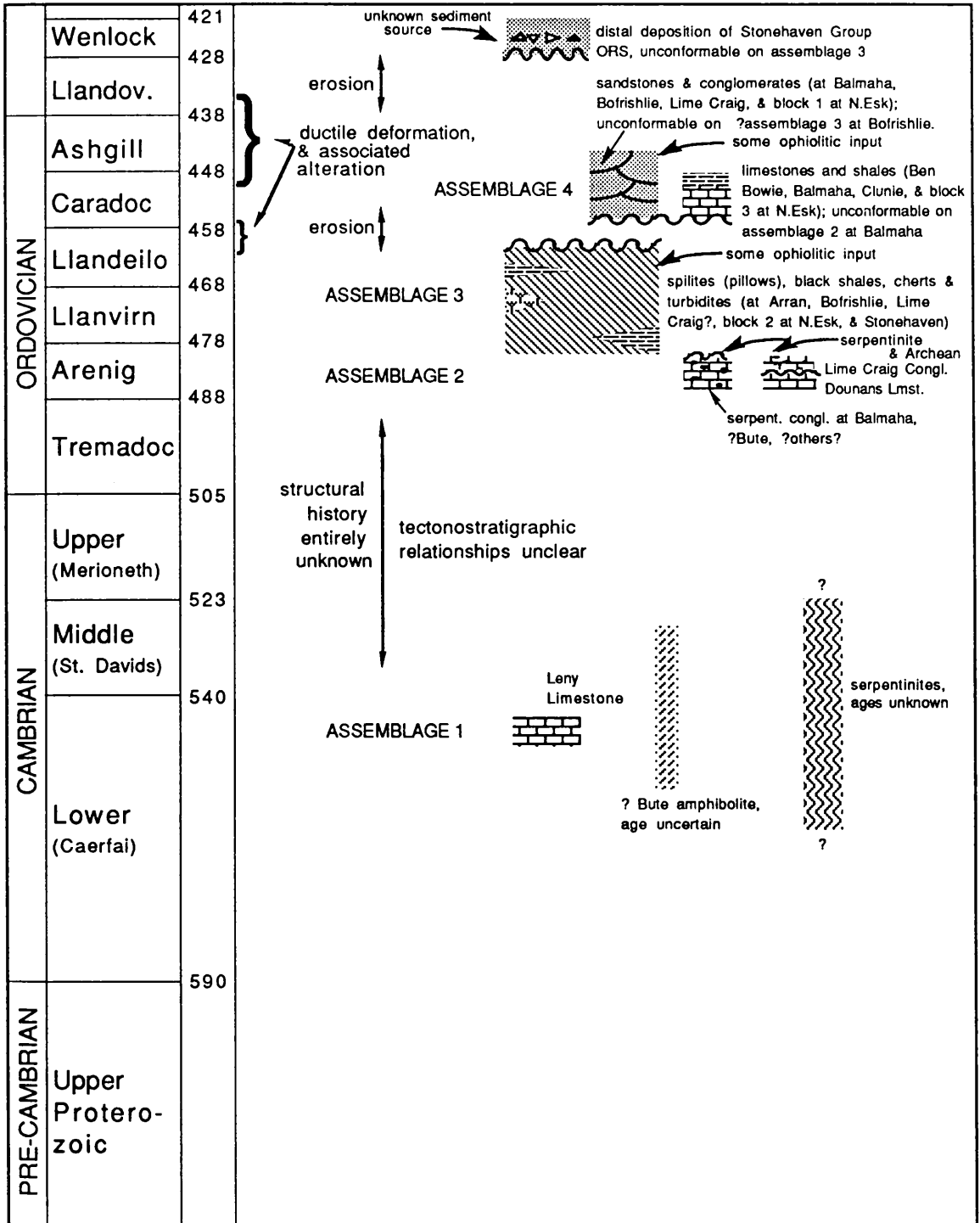


Fig. 6.5. An interpretation of the tectonostratigraphy of the HBC, showing the inferred structural and temporal relationships between the four rock assemblages proposed by Bluck *et al.* (in Curry *et al.* 1984). The timescale is from Harland *et al.* 1982.

Other phases of tectonism may also have affected the HBC, but evidence for these is ambiguous. For instance, because the tectonostratigraphical relationships between assemblage 1 and the other assemblages are unknown, it is unclear whether the high structural

complexity and metamorphic grade of the amphibolites and serpentinites of assemblage 1 is due to

- 1) tectonism<sup>1</sup> *prior* to deposition of assemblages 2 and 3, or
- 2) the same Llandeilo/Caradoc tectonic event described in the preceding paragraph, or
- 3) the same Caradoc/Llandovery tectonic event described in the preceding paragraph.

Options (2) and (3) are both possible because subsequent deformation events (*e.g.* in mid-Devonian times) may have structurally juxtaposed both high and low strain rocks that had been deformed in the same tectonic event, in regions of varying shear strain<sup>2</sup>. This ambiguity is removed when assemblages can be seen to be separated by unconformable rather than structural boundaries.

#### 6.6.2. The HBFZ as a terrane boundary

This section attempts to test the hypothesis that the Dalradian Highlands and the HBC are two distinctly separate tectonostratigraphic terranes, by comparing the geological history of the two tracts.

The rediscovery of a stratigraphically diagnostic fauna within the HBC (Curry *et al.* 1982) led to the hypothesis that the geological histories of the Dalradian Highlands and the HBC *were* incompatibly different from Arenig through to Caradoc times (Curry *et al.* 1982, 1984, Bluck 1985). It is possible to test for geological *incompatibility* along the HBFZ because radiometric age determinations of Dalradian thermal events give ages that are broadly synchronous with palaeontological age determinations of HBC sedimentation. The HBC stratigraphy was taken to represent distal basin deposition on oceanic crust (Curry *et al.* 1982). At this time (460-440 Ma) the Dalradian terrane was undergoing regional uplift and D4 ductile deformation (Dempster 1985), an event that would be expected to yield large volumes of proximal detritus into adjacent sedimentary basins (Bluck 1985). None of this detritus has yet been identified within the HBC.

This evidence is now generally taken to have greater scientific validity than previous theories, which had suggested a shared *structural* history between the two terranes, based on structural correlation between D1/D2 in the HBC and Dalradian (Harris 1962, Harris 1969, Harris & Fettes 1972). The

---

<sup>1</sup> *i.e.* a possible terrane accretion event (see section 6.7).

<sup>2</sup> This is particularly plausible with serpentinites and carbonated serpentinites, because these lithologies tend to focus stress and hence act as zones of high shear strain.

recent re-dating of the minimum age of Grampian D1/D2 deformation ( $590 \pm 2$  Ma; Rogers *et al.* 1989) has given great support to the refutation of *structural* correlation between the HBC and the Dalradian. Clearly, such broad correlation now seems impossible, as the components of the HBC that have yielded microfossils appear to have been deposited 50-150 Ma *after* Grampian D1/D2 deformation.

The apparent misunderstandings that resulted from spurious structural correlations along the HBFZ should serve to demonstrate that the geology in fault zones can be complicated and misleading, and that any lithological or structural correlations within fault zones can be so fraught with difficulties. Fault zones are often associated with fault-parallel fabrics, and adjacent blocks could have similar fabric geometries produced at widely differing times. With the benefit of hindsight, it is now clear that these considerations might have a wide relevance to fault zones in general.

Though the recent radiometric and palaeontological data have helped to refute structural correlation between the HBC and the Dalradian, they have also altered our understanding of Caledonide geology sufficiently to suggest that a reappraisal of the status of the HBFZ as a terrane boundary is now relevant. To re-emphasise a conclusion from the previous section; most ancient terranes will be difficult to identify as truly allochthonous with any degree of certainty - new data always require re-examination of existing terrane classifications. The existing theory that the HBFZ is a tectonostratigraphic terrane boundary must now be tested once again.

The tectonostratigraphic interpretation of the HBC was given in Fig. 6.5. Compare this with an interpretation for the Dalradian terrane (a "suspect" terrane at this stage of the analysis) for the equivalent time period, in Fig. 6.6.

Comparison of Figs. 6.5 and 6.6 allows incompatibility between the Dalradian and the HBC to be tested. I will now discuss this in more detail, starting with the earliest time period and working forward in time.

No comparison or test of compatibility is possible for the Precambrian histories of the two suspect terranes, because there is no evidence of a HBC basement, and no rocks of Precambrian age have yet been identified within the HBC. For example, it is theoretically possible for a basement to the HBC to have collided with the Dalradian block prior to 590 Ma, *causing* D1/D2

deformation. However, not only is there is no evidence to suggest this, but such "theories" are probably not falsifiable<sup>1</sup>. (*i.e.* not "testable").

The postulate of Rogers *et al.* 1989 (conclusion 4, p.796), that D3 crustal thickening of the Dalradian terrane could be related to emplacement of HBC ophiolites (and thus representing the interaction of the two terranes as early as 520 Ma) is interesting, but cannot yet be addressed given the present lack of data. Furthermore, what little evidence we have does not count in favour of their speculation. The tectonostratigraphic position of the Leny Limestone is of extreme importance in these deliberations. It is difficult to envisage how the Leny rocks might have acted as a basement to the serpentinites and amphibolites of assemblage 1, and this implies either that the serpentinites/amphibolites are older than the Leny Limestone, or that the serpentinites/amphibolites and the Leny Limestone actually represent two (or more) different tectonostratigraphic terranes. If the serpentinites/amphibolites *are* older than Late Lower Cambrian, they are unlikely to have caused a crustal thickening event any later than the Middle Cambrian, because it appears that only very young oceanic crust is buoyant enough to be obducted (J.F. Dewey, pers. comm.). This apparent logical difficulty in the postulate of Rogers *et al.* would not exist if the timing of D3 was shown to be Lower Cambrian in age!

Such convoluted speculation shows the fragility and complexity of possible theory. A more worthwhile conclusion is that future research should aim to constrain the timing of D3 Dalradian deformation, and the age of components of assemblage 1 of the HBC; such research would allow the hypothesis of Rogers *et al.* 1989 to be adequately tested.

Comparison of Dalradian and HBC geological history is also difficult for the Arenig to Llandeilo timespan. This period appears to be a time of inactivity for the Dalradian, contemporaneous with the deposition of assemblages 2 and 3 of the HBC. The geochemical evidence suggests that assemblages 2 and 3 *do* represent an ophiolite sequence of overall MORB character (Robertson & Henderson 1984), perhaps equivalent to the Tyrone ophiolite described by Hutton *et al.* (1985). However, such *difference* in geological history does not conclusively prove complete *incompatibility* at this time. The data are consistent with the HBC representing an ophiolite that was either:

a) generated far from the Dalradian continental margin [*i.e.* no compatibility], or

---

<sup>1</sup> Hence, this is speculation rather than theory, and is therefore invalid according to falsificationists such as Popper (*e.g.* Popper 1968)

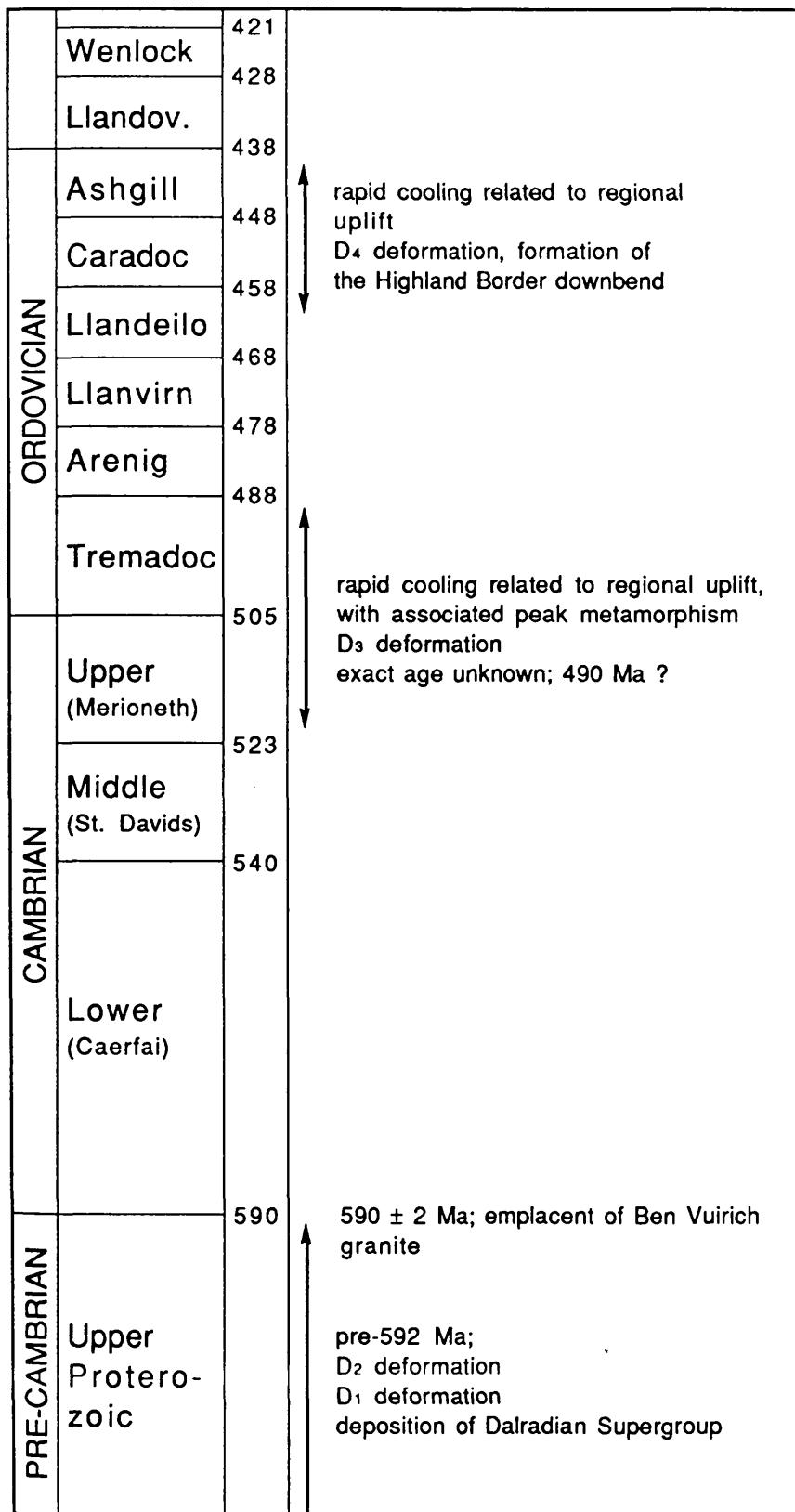


Fig. 6.6. An interpretation of the geological history of the Dalradian terrane. The timescale is from Harland *et al.* 1982. Data are principally from Rodgers *et al.* 1989, Dempster 1985, and references therein.

b) formed adjacent to or within the Dalradian continental crust, and was generated in response to rifting (or the initiation of rifting) of the crust [i.e. some degree of compatibility].

Whether the latter scenario suggests sufficient "incompatibility" to justify the identification of the HBC and the Dalradian as two separate terranes, perhaps depends upon one's own interpretation of the definition of terranes given by Jones *et al.* (1983) in section 6.5.1. This comment is a recognition of the greater subjectivity inherent in the identification of ancient terranes, compared with their Mesozoic and Cenozoic counterparts.

In Caradoc to Ashgill times the change in HBC sedimentation from a distal to a more proximal character is marked by the angular unconformity between assemblage 4 and assemblages 3 and 2 (see Fig. 6.5). Arenites of assemblage 4 are at least partially derived from an ophiolitic source. The Caradoc to Ashgill HBC stratigraphy may reflect the inversion, or the closure, or the initiation of closure of the Arenig to Llandeilo HBC basin. At this time Dalradian rocks were undergoing rapid regional uplift, probably associated (at least temporally) with the formation of the D4 Highland Border downbend (Dempster 1984, 1985). This D4 event deformed the major pre-existing D1/D2 Tay Nappe structure, down-folding the nappe to give the Highland Border steep belt (Shackleton 1953). Such uplift and tectonism would give rise to an orogen with significant topographic relief, and according to Bluck (1985) this event should yield a large amount of detritus southwards, into a basin that occupied the present position of the HBC, yet no Dalradian detritus has been identified with certainty within the HBC.

However, some complications exist. The original argument for geological incompatibility between the two terranes was based on ophiolite generation and pelagic sedimentation in the HBC being synchronous with progressive D1 to D4 deformation and uplift in the Dalradian (Curry *et al.* 1982). But our understanding of the geological histories of both terranes has advanced (Figs. 6.5, 6.6), and this argument is now untenable. Only the Caradoc/Ashgill HBC sediments were deposited synchronously with a Dalradian uplift event (*i.e.* D4), and at present not enough is known about the provenance of these HBC sediments to satisfactorily disprove an interaction between the Dalradian orogen and the HBC basin. Such a provenance study should be an important area of future HBC research.

During Llandovery times both the HBC and the Dalradian appear to be relatively inactive, rendering compatibility/incompatibility difficult to prove. The Wenlockian Stonehaven Group sits unconformably on the deformed HBC, thus marking the upper time limit of ductile deformation of the HBC. Because little is known about the provenance of the Stonehaven

Group it cannot yet be determined whether or not these beds represent a sedimentological terrane linkage. The earliest hypothesised terrane linkages are:

- 1) a sedimentary provenance link indicated by granite clasts from the Dalradian terrane deposited in Lower Devonian conglomerates of the Dunnottar Group at Stonehaven (Haughton 1988, Haughton *et al.* 1990),
- 2) a palaeomagnetic linkage of the Lintrathen type ignimbrites across the HBFZ (Trench & Haughton 1990).

So, does the HBFZ separate two (or more) distinct tectonostratigraphic terranes? On balance, I feel that the majority of evidence favours significant geological incompatibility between the HBC and Dalradian, and therefore the two have a *highly suspect* relationship. However, it is important that this is not overstated, and I firmly believe that the available evidence is incapable of conclusively proving incompatibility.

Interestingly, an important line of evidence in this discussion comes from the structural data presented in sections 5.2 and 5.3. The identification of mylonitic rocks within the HBC is evidence that "significant" movement has occurred on the HBFZ. In a general way this supports hypotheses of geological incompatibility between the HBC and Dalradian, and suggests terrane-scale movements. This line of reasoning represents a marked departure from the methodology described by Coney *et al.* (1980) and Jones *et al.* (1983), in which individual terranes are defined by their geological histories, *not* on the structural histories of their boundaries. Is this modification in methodology acceptable?

### **6.7. A speculative account of the mode and timing of microplate docking (and post-accretion movements) along the HBFZ.**

This section is an attempt to collate and synthesise the structural and stratigraphical data already discussed, to give a coherent interpretive model for terrane accretion on the HBFZ. A summary of post-accretion deformation is also given, in order to show how the Dalradian/HBC terrane boundary has been disrupted by later tectonic events.

In general, the model becomes less speculative for later time periods, because data for later periods are more numerous and more reliable; this is clear from Figs. 6.5 and 6.6. The suggestions for the Precambrian and

Cambrian are very poorly constrained, whereas the later time periods are based on much supporting evidence.

The inherent subjectivity of this interpretation cannot be over-emphasised. This is discussed in detail in section 6.5.

#### Precambrian:

The Dalradian Supergroup was deposited in extensional basins during the break-up of a Proterozoic Supercontinent (Anderton 1982, 1985; Glover & Winchester 1989), with the Southern Highland Group representing deposition on the thermally-subsiding Laurentian continental margin. In the SW Southern Highlands the Dalradian seems to have prograded onto oceanic crust (Graham 1986; this is suggested by the inferred heat flow during later Grampian metamorphism).

The phase of extension ended (or at least was interrupted) with the collision of an unknown terrane with the Dalradian block, giving the regional D1/D2 deformations. The collision occurred along a precursor to the present-day HBFZ<sup>1</sup>, but the unknown terrane was shunted along the continental margin by continued oblique subduction, and much evidence of Precambrian collision within the HBFZ has been lost during subsequent deformation. The basement rocks in the Ox mountains may be a remnant of the unknown terrane. Subduction beneath the Laurentian margin at some time between Late Proterozoic and Lower Cambrian is deduced from the presence of eclogites in a *mélange* at Ballantrae ( $576 \pm 32$  Ma; Sm-Nd, Hamilton *et al.* 1984).

#### Lower Cambrian:

HBC history was probably initiated in Lower Cambrian times, with the generation of oceanic crust, now seen as amphibolites and serpentinites of assemblage 1. This was then overlain by the Leny Limestone sequence. The HBC rocks may have formed in a back-arc basin to the Midland Valley batholithic and volcanic arc described by Blüch (1985). The palaeogeographic position of the Midland Valley and the HBC, with respect to the Dalradian terrane, is unknown, but proximity to the Laurentian margin is indicated by the provinciality of the Leny fauna.

#### Middle Cambrian - Tremadoc:

Further terrane collision may have occurred along the Laurentian margin on a precursor to the present-day HBFZ, to cause D3 Dalradian

---

<sup>1</sup> or along a boundary then lying to the SE, if part of the Dalradian was subsequently sliced out by later deformational events.

deformation and metamorphism. It is not clear whether this D3 event actually represents the accretion of assemblage 1 of the HBC onto the Dalradian terrane, or whether D3 was caused by the accretion of another unknown terrane, not seen along the HBFZ at the present day. [The available evidence favours the latter, because the Llanvirn - Llandeilo histories of the two terranes are *probably* incompatible. This model, therefore, incorporates a later docking event between the HBC and the Dalradian.]

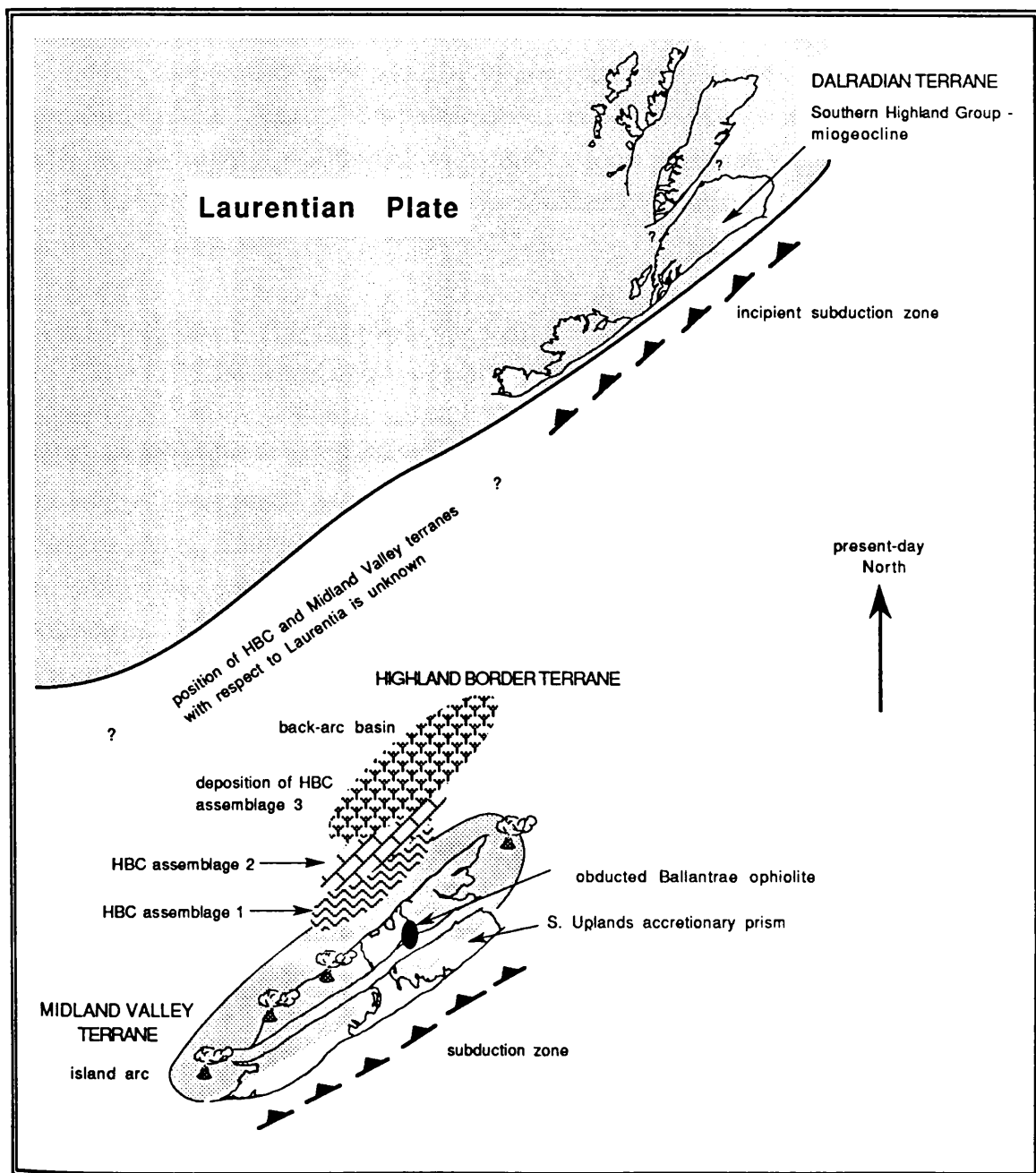


Fig. 6.7. Palaeogeographic reconstruction of the Scottish/Irish Laurentian margin in Llanvirn-Llandeilo times.

### Arenig:

Assemblage 2 of the HBC was deposited, derived from both Archean rocks and nearby serpentinites. The palaeogeographic position of this part of the HBC is unknown, but deposition probably took place on top of older HBC rocks (*i.e.* assemblage 1) and the Midland Valley arc.

At this time the Ballantrae ophiolite was obducted onto the Midland Valley basement (Bluck *et al.* 1980).

### Llanvirn - Llandeilo (Fig. 6.7):

HBC deposition continued with assemblage 3, in part derived from ophiolitic rocks. Again, the palaeogeographic position of this part of the HBC is unknown, but deposition probably took place on top of older HBC rocks (*i.e.* assemblages 1 & 2) and the Midland Valley arc.

### Late Llandeilo - early Caradoc (Fig. 6.8):

The HBC back-arc basin started to close obliquely, and the HBC experienced intense deformation. The original stratigraphical and palaeogeographical relationships were mostly destroyed, and the HBC became a "disrupted" terrane. HBC rocks were plastered onto the Dalradian margin along sinistrally transpressive shear zones. Transpressional mylonites were formed at different structural levels along the terrane boundary. Mid-crustal mylonites, with shallow-dipping stretching lineations, formed in shear zones at Clew Bay and Slieve Gamph in Ireland, and at Glen Sannox, Toward, and Innellan in Scotland. The *upper* crustal expression of this deformation is represented by a mylonitic thrust at the River N.Esk, and by oblate strains with or without steep stretching lineations in many of the HBC rocks in Scotland.

At this time D4 Dalradian deformation initiated, with the formation of the Highland Border downbend, in response to compression caused by terrane accretion.

### Caradoc - Ashgill (Fig. 6.9):

HBC deposition (assemblage 4) occurred unconformably upon older HBC rocks. The older HBC units acted as the sediment source for the arenites and conglomerates of assemblage 4. Deformation of the HBC continued, further destroying evidence of the earlier HBC history.

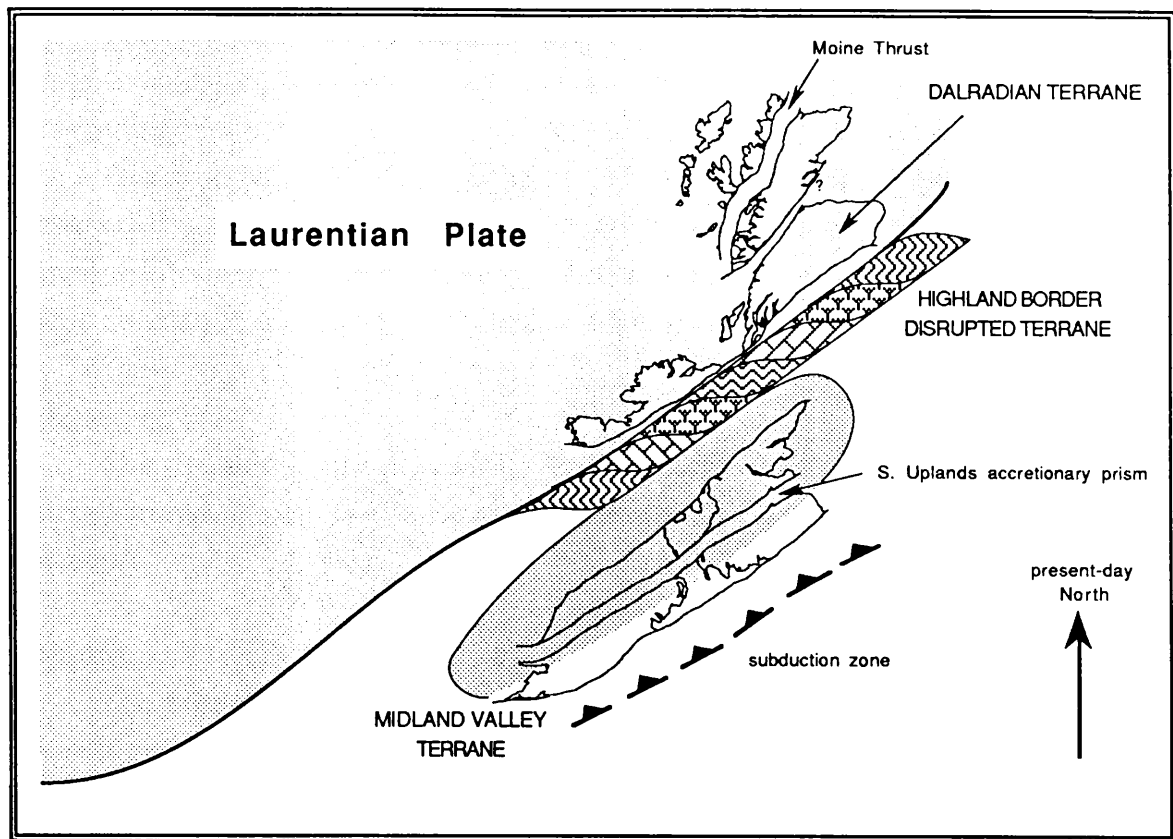


Fig. 6.8. Palaeogeographic reconstruction of the Scottish/Irish Laurentian margin in Late Llandeilo - early Caradoc times.

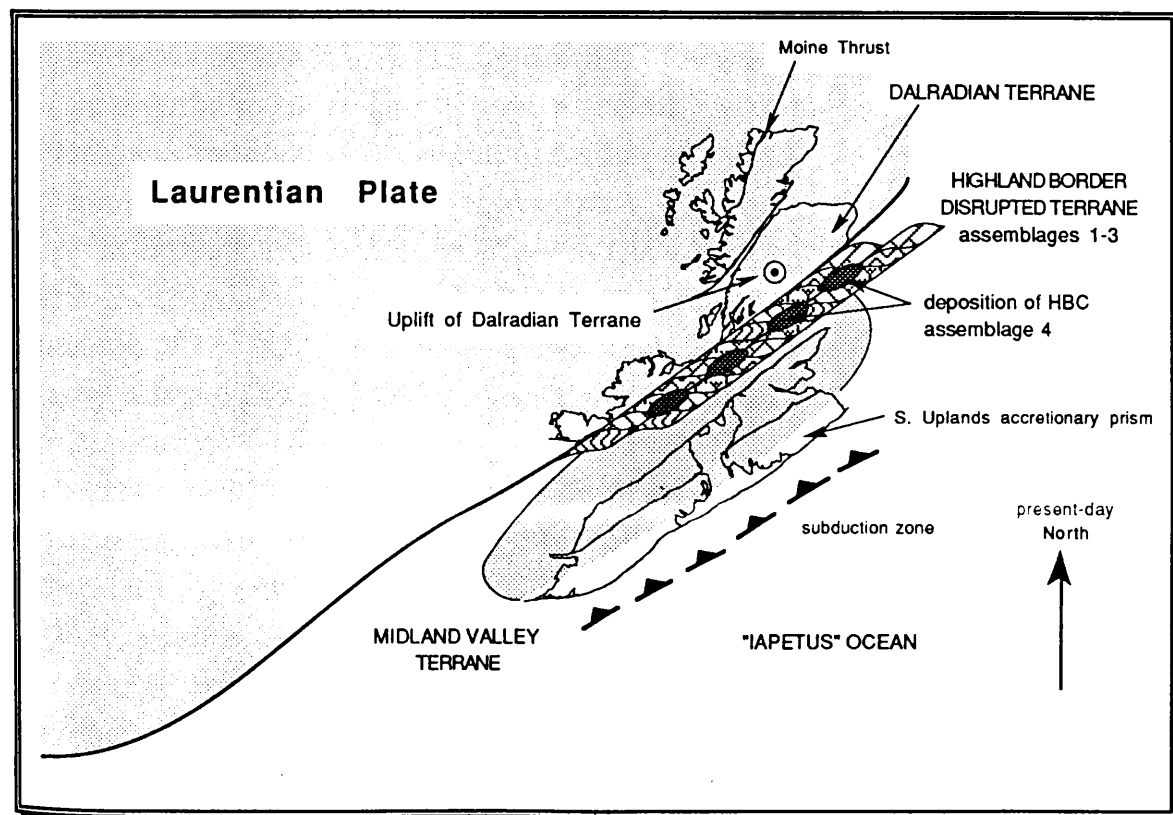


Fig. 6.9. Palaeogeographic reconstruction of the Scottish/Irish Laurentian margin in Caradoc - Ashgill times.

The Dalradian terrane started to undergo rapid uplift in response to terrane collision, but did not act as a major sediment source for those fragments of assemblage 4 of the HBC that are exposed today.

The final collision of the Midland Valley arc and the Dalradian terrane marked the end of D4 downbend formation, and preserved a width of several kilometres of HBC mélange across the terrane suture [this width was later shortened by subsequent deformation events].

#### Llandovery:

The uplifted Dalradian, HBC, and Midland Valley blocks (now all incorporated as part of the Laurentian continent) were denudated by rapid erosion.

#### Wenlock:

The Stonehaven group was deposited unconformably upon the weathered HBC at Slug Head (Stonehaven). The sediments are of unknown provenance, but seem to represent distal sedimentation, implying that the Dalradian and Midland Valley blocks were peneplaned by this time.

#### Ludlow-Gedinnian:

The HBC was further disrupted at this time, though evidence of HBFZ movements in Scotland is circumstantial. This deformation event was probably due to continuing terrane accretion along the Laurentian margin, which was progressively migrating further outboard (*i.e.* seaward) as terranes accreted to the existing continent.

In Ireland, a deformation phase in Clew Bay was broadly synchronous with the intrusion of the Corvock Granite (Hutton & Dewey 1986), which is dated at  $387 \pm 12$  Ma (Rb/Sr; O'Connor *et al.* 1983). The Lough Talt and Easky adamellites may also represent continued sinistral shear in Ireland in Pridoli times.

The Loch Tay/Killin/Tyndrum fault array are thought to have initiated in Late Silurian times (Watson 1984; Hutton 1987), though this remains uncertain. Deposition of coarse ORS conglomerates started in the Midland Valley, possibly in a series of pull-apart basins (Peter Haughton, pers. comm.; Brian Bluck, pers. comm.). This depositional event records a provenance linkage between the Dalradian and the Midland Valley (Haughton 1988, Haughton *et al.* 1990).

Coarse, angular breccias and conglomerates of local origin are deposited on the Dalradian, interbedded with the Lintrathen-type ignimbrites. Vulcanism is pervasive in the Midland Valley.

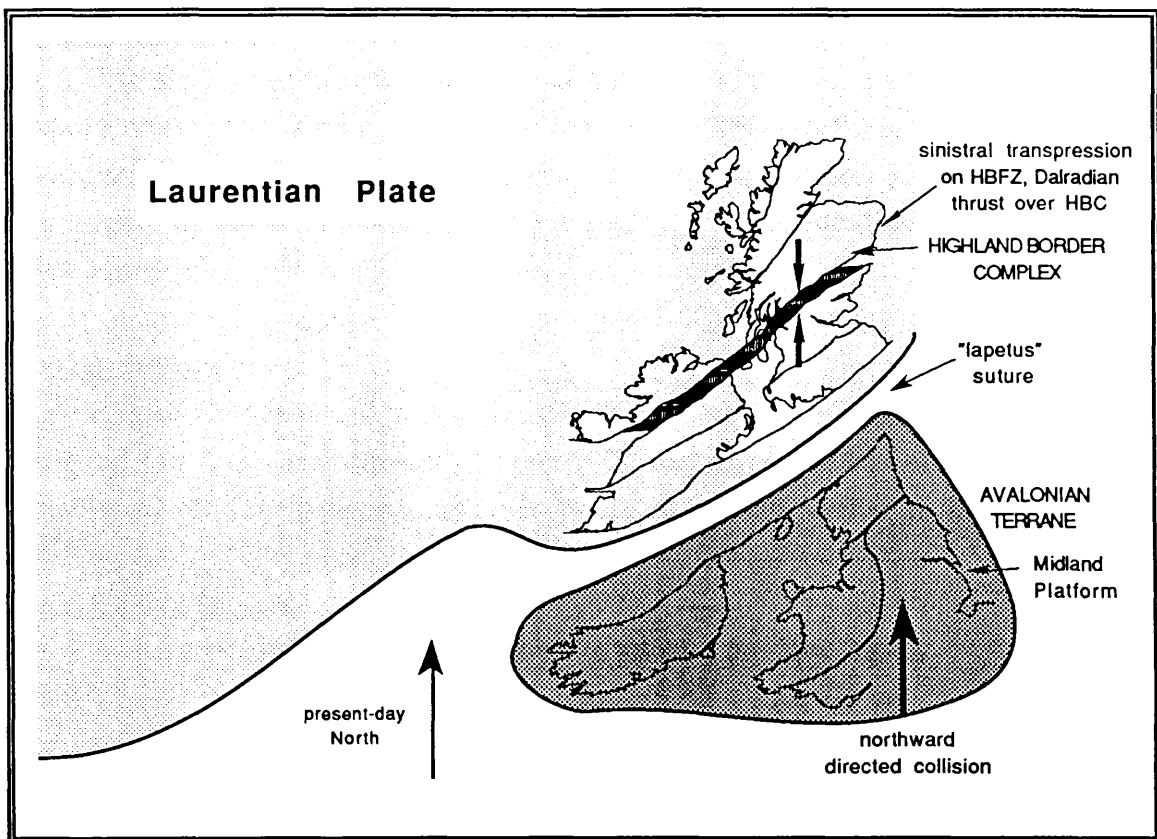


Fig. 6.10. Palaeogeographic reconstruction of the Scottish/Irish Laurentian margin in Emsian times.

#### Emsian - Givetian (Fig. 6.10):

Central Britain suffered north - south compression; this was probably due to the collision of Avalonia (also termed "Cadomia" or "Acadia"), which incorporates the Midland Platform, with the Laurentian continent. Brittle deformation was widespread over much of Northern England (Soper *et al.* 1987).

The deformational event caused the obliquely orientated HBFZ to experience sinistral transpression. The HBC suffered pervasive brittle deformation, causing further reduction in the size of the blocks that comprise the disrupted terrane.

The Lower ORS beds deposited on the Midland Valley and Dalradian terranes were shortened to form large asymmetrical folds, though any continuity of ORS above the HBFZ was lost when the Dalradian was thrust over the HBFZ onto the Midland Valley. The small, localised uplift resulting from this thrusting provided a proximal source of Dalradian material that was deposited in the Upper ORS of the Midland Valley.

### Upper Devonian:

The structural blocks flanking the HBFZ were once again eroded, then locally covered by Upper ORS conglomerates. Though there is little evidence of significant fault displacement, deposition may have occurred in small pull-apart basins (Bluck 1980) that form during localised block movements.

### Carboniferous:

Regional extension caused localised reactivation along the HBFZ. Normal faulting downfaulted Upper ORS and Lower Carboniferous southwest of Aberfoyle, but the effects are unknown farther to the NE.

### Late Carboniferous:

A quartz-dolerite and dolerite dyke swarm cut the HBFZ.

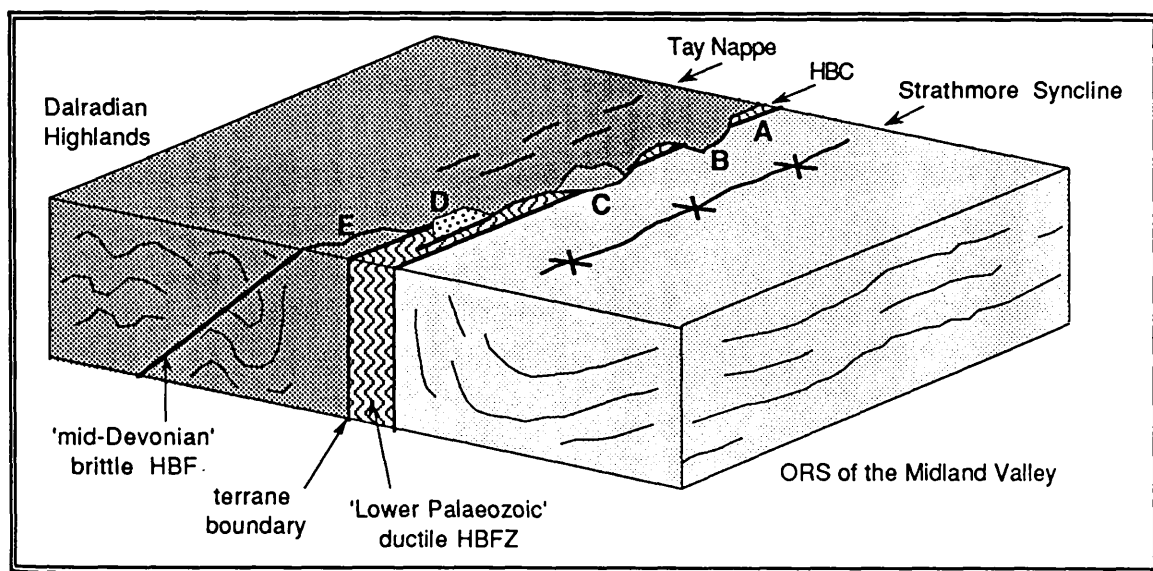


Fig. 6.11. Schematic block diagram showing the overall present-day structure of the HBFZ in Scotland. Five typical structural scenarios are shown (A-E). A the most common structure of the HBFZ; the HBC melange separates the Dalradian and Midland Valley terranes. B the HBC has either been faulted out, or is buried by overthrust Dalradian (*i.e.* the present-day erosion level is not deep enough) - *e.g.* Glen Shee. C L.ORS sediments that were deposited on top of the Dalradian terrane are juxtposed against L.ORS of the Midland Valley - *e.g.* Tayside. D U.ORS basins in the HBFZ produced by localised extensional faulting during the Upper Devonian and/or Carboniferous - *e.g.* Balmaha. E erosion is sufficiently deep enough to expose the actual Lower Palaeozoic (ductile) terrane boundary between the HBC and Dalradian terranes - *e.g.* Bute, Toward (and Ireland?).

Post-Carboniferous (Fig. 6.11):

The HBFZ, marking the site of the Ordovician Laurentian margin, was denudated, exposing the repeatedly disrupted HBC mélange. Overall, the deepest crustal sections are exposed in the S.W., rather than the N.E., though repeated fault movements from the Ordovician to Carboniferous have ensured that rocks from different structural levels are juxtaposed all along the fault zone.

# CHAPTER 7: CONCLUSIONS

This thesis documents and interprets evidence for displacements along the Highland Boundary Fault Zone ("HBFZ"). The important conclusions of this thesis are as follows:

## 7.1 Conclusions relating to terrane accretion along the HBFZ

1. The HBFZ is a major crustal fracture with a long and complex structural history. Brittle deformation along the HBFZ was superimposed upon pre-existing fabrics produced by ductile deformation.
2. The Highland Border Complex in Scotland contains very few, well exposed mylonites. The mylonites described in this thesis contain kinematic indicators that show varying senses of shear.
3. The *interpretation* of structural data from the HBFZ in Scotland, together with data from the HBFZ in Ireland, gives an apparent balance of evidence in favour of major terrane accretion along the HBFZ during the Lower Palaeozoic. In this respect, the unseen Midland Valley basement is 'highly suspect' with respect to the Dalradian; the boundary between these two tectonostratigraphic terranes is marked by the HBC 'disrupted terrane' or *mélange*.
4. The balance of evidence supports a palaeo-tectonic model in which the HBFZ has a long history of terrane accretion and terrane dispersal, with sinistral transpression occurring in the Llandeilo and/or Caradoc and again in the Ashgill and/or Llandovery. It must be stressed that the overall objectivity of this hypothesis is low, and consequently, the model, though consistent with the available data, must *not* be considered as the only possible palaeogeographical solution.
5. A period of End-Silurian regional tectonism has been documented by Caledonide geologists, but I did not recognise evidence of this in central Scotland; however, my lack of recognition must *not* be taken to imply that this event did not exist, rather that mesofracture analysis did not distinguish it.

6. The influence of active tectonics during the deposition of L.ORS sediments along the HBFZ is poorly understood.
7. Central Scotland was pervasively deformed in mid-Devonian times. This phase of deformation may have been due to continuing terrane accretion of Avalonia onto the developing Laurentian margin to the south.
8. Mid-Devonian brittle strain was low in magnitude, but widespread in aerial extent. Upper crustal deformation was manifested as large-wavelength folds, as well as prolific arrays of brittle meso- and macro-faults and fractures.
9. Regional evidence suggests that the HBFZ experienced thrust and/or strike-slip components of deformation. This is validated and further constrained using a brittle microtectonic study.
10. A mesofracture analysis of central Scotland, comprising geometric and kinematic analyses of 2,600 mesofractures from 40 sampling stations, generally shows that deformation produced *either* one conjugate pair of vertical strike-slip faults and/or shear joints, *or* four sets of steep, syn-genetic, oblique-slip faults and/or shear joints.
11. The results of the mesofracture analysis are important on both a small and large scale. Results from individual stations can be dynamically interpreted by a general model of three-dimensional or 'triaxial' brittle deformation, in which conjugate fracture pairs represent biaxial strain, and four fracture sets represent triaxial strain. The maximum principal strain is horizontal and compressive for all the stations in Scotland that show this type of deformation. The intermediate principal strain is vertical, and is neutral (biaxial strains) or extensional (triaxial strains), whilst the minimum principal strain is horizontal and extensional (hence triaxial strains are oblate, *i.e.* flattening). These conclusions corroborate an earlier study of fractured pebbles (Ramsay 1962,1964).
12. Collectively, the dynamic mesofracture interpretations allow regional mid-Devonian stress (and strain) to be inferred. The overall results imply that regional compression was orientated approximately north-south, suggesting that the pre-existing HBFZ should have experienced transpressive strain. However, the mesofracture interpretations from stations adjacent to the HBFZ are inconsistent with existing models of

transpression. Consideration of the geometry of the large-scale folds in the northern Midland Valley helps to constrain this problem, and confirms the inapplicability of existing transpression models in explaining mid-Devonian tectonism in central Scotland. Instead, I propose an alternative model in which transpressive strain across the pre-existing HBFZ is partitioned into two components: a pure shear component that is taken up in the regions flanking the fault, and a simple shear component that is restricted to the fault itself.

13. The "end-member" strain-partitioning model is more relevant to the HBFZ than previous transpression models, but is nevertheless too simplistic to thoroughly explain the deformation seen in central Scotland, where several components of deformation can be recognised: pure shear folds in the northern Midland Valley; simple shear within the HBFZ; some simple shear in small domains of L. ORS adjacent to the HBFZ; southerly overthrusting of the Dalradian on top of the HBFZ; combined pure and simple shear (*i.e.* 'more normal' transpression) in the Dalradian north of the HBFZ; and irrotational triaxial (oblate) strain outwith the transpression zone.

14. The influence of active tectonics during the deposition of U.ORS and L. Carboniferous sediments along the HBFZ is poorly understood.

15. During regional Carboniferous extension the HBFZ was locally re-activated, down-faulting Upper ORS sediments on the Gualann Fault Zone. Elsewhere in the northern Midland Valley, Lower ORS rocks are only locally affected by this deformational event.

16. The HBFZ is cut by a small number of Late Carboniferous dykes. This suggests that at least some parts of the HBFZ have not experienced significant displacement since Late Carboniferous times.

## 7.2 Conclusions relating to geological processes

A. In general, terrane analysis offers a more realistic and objective methodology of studying orogenic belts than previous research strategies, but only when all terranes are viewed as 'suspect' until shown to be otherwise. In practice, however, the analysis of *disrupted* terranes remains inherently problematical, and it may be difficult to ever *prove* that such

terrane are exotic, allochthonous, or actually contiguous; some disrupted terranes might always best be classified as 'suspect'.

B. The analysis of 'disrupted' terranes is particularly problematical at present, because a coherent methodology of research has not yet been adequately formulated. Future analyses of disrupted terranes should concentrate on the structural interpretation and dating of mylonite zones produced during terrane accretion, in order to constrain the timing, sense, and possibly the amount of terrane displacement. In general, the interpretation of disrupted terranes should avoid over-dependence upon structural, palaeontological, geochemical, and lithological *correlation*, because of the inherent unreliability of many such correlations.

C. Structural geology has given undue attention to the analysis of deformation in two-dimensions, particularly when analysing brittle deformation. Plane strain is just one limiting case, in a whole spectrum of *three-dimensional* crustal deformation, and the analysis of geological structures must reflect this. Furthermore, deformation cannot happen instantaneously, and structural geologists should aim to further understand the effect of time (the fourth dimension) during *progressive* deformation.

D. Existing models of transpression may be invalid for transpressive reactivation of pre-existing faults. The "strain-partitioning model" is an alternative model in which transpressive strain across a pre-existing fault is partitioned into two components: a pure shear component that is taken up in the regions flanking the fault, and a simple shear component that is restricted to the fault itself.

E. The strain-partitioning model may have wide implications for deformation along other fault zones; in particular, it predicts that widespread stretching directions need not necessarily be parallel to the overall direction of regional shortening.

F. The strain-partitioning model is an "end-member" model that should be considered in conjunction with the "homogeneous transpression" model of Sanderson & Marchini (1984). In reality, reactivation of pre-existing faults is likely to involve components of both transpression models.



Plate 1. Photomicrograph of sample J148(1), from the N.Esk Fault. Crossed Polars. Magnification X20. See page 104. Quartz grains are fractured and internally strained. Grain size reduction has occurred primarily by cataclasis. Top right of the field of view shows the internal composition and structure of a slickenside 'surface', composed of phyllosilicates. The slickenside is approximately 0.5mm thick, and in hand specimen appears as a black, highly polished, striated surface.

Between view shows the typical plastic deformation of quartz grains, including grain size diminution, internal grain rotation, non-fusible, irregular polyhedral, and new grain and new grain growth.

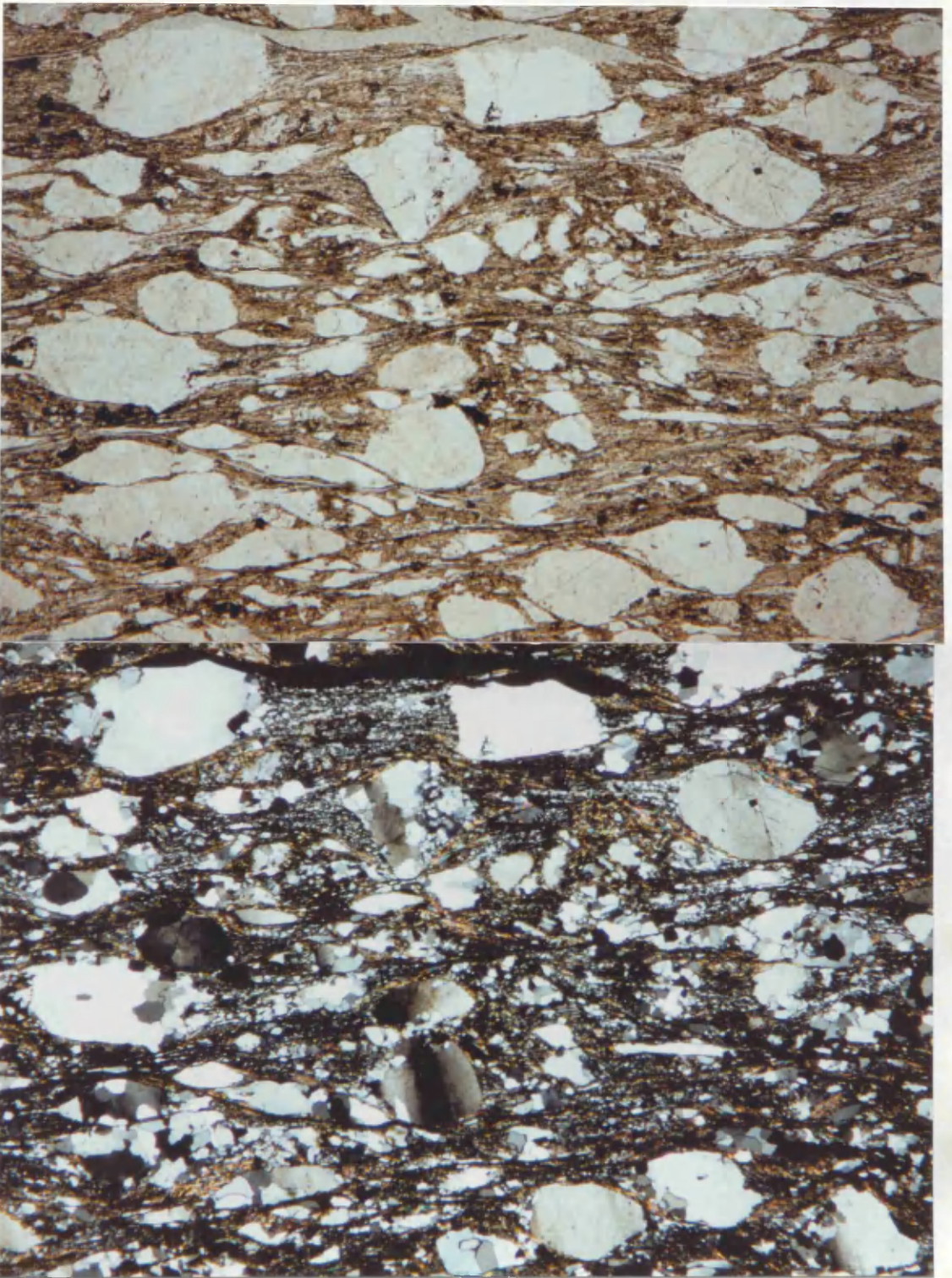


Plate 2. Photomicrograph of sample J165(2), of a quartz-mica mylonite, from Toward. Top: Plane Polarized Light; below: Crossed Polars. Magnification X20. See page 123.

Top view shows the anticlockwise (sinistral) asymmetry of  $\sigma$ -type rotated porphyroclasts, and the sinistral S-C fabric development, defined by micas and elongated quartz grains.

Bottom view shows the crystal-plastic deformation of quartz grains, including grain-size diminution, serrated grain contacts, kink-banding, incipient polygonisation, and sub-grain and new-grain growth.

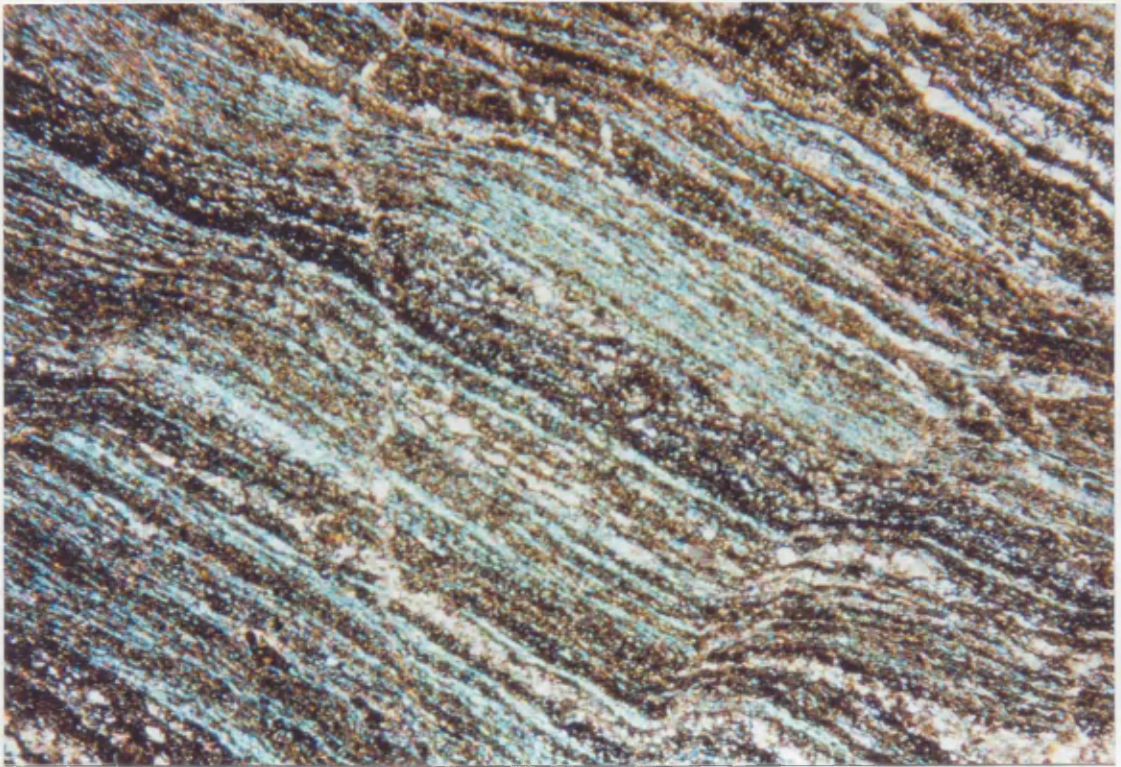


Plate 3. Photomicrograph of sample B0012(3), of ultramylonite from Corloch, Arran. Crossed Polars. Magnification X20. See page 127.

A feint dextral S-C fabric relationship is scarcely visible at this low magnification, but its petrographic appearance is easy to distinguish from the post-mylonitisation crenulation folds shown in this photograph. Note that the significance of the shear sense has been disguised by the subsequent phases of folding.

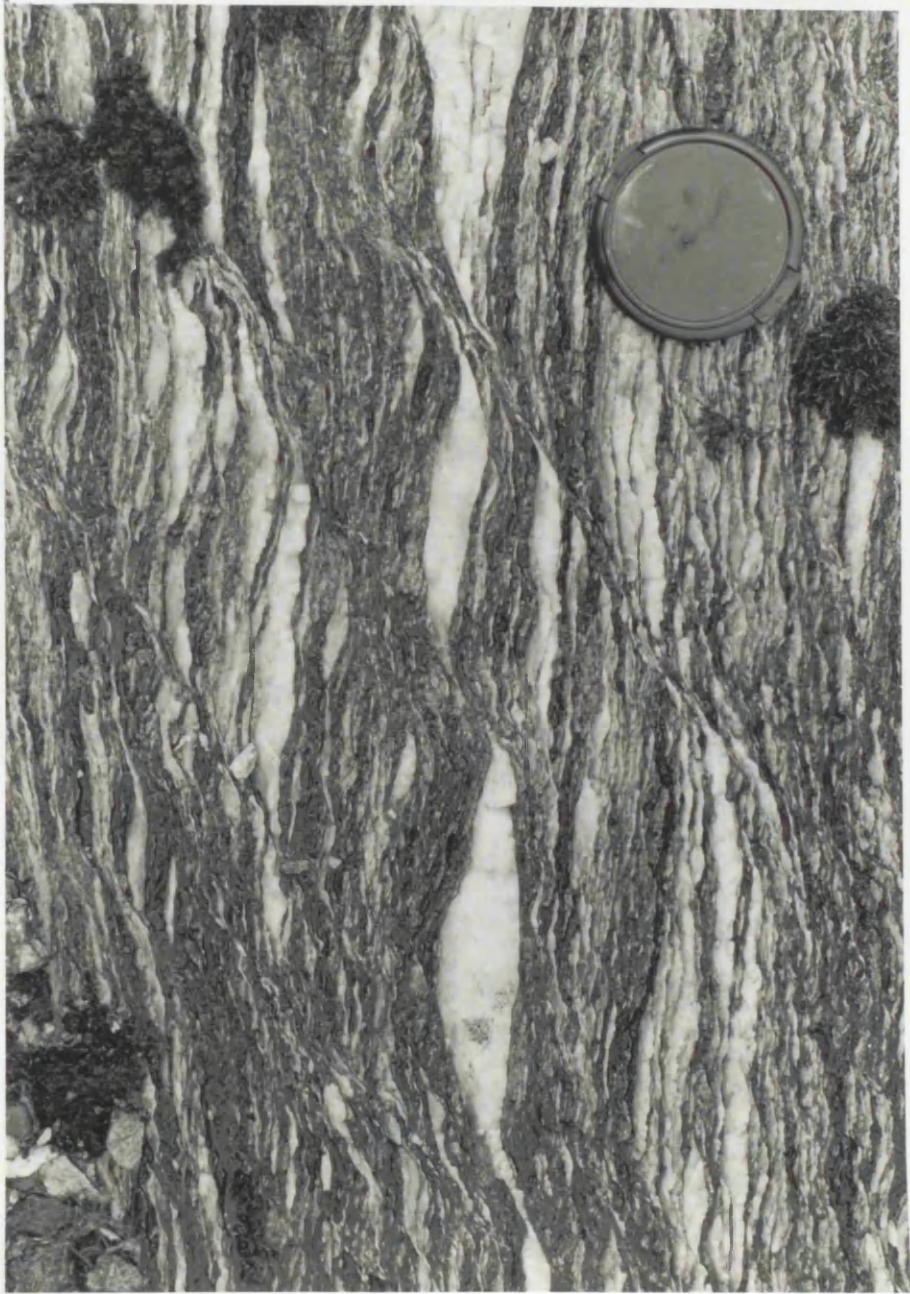


Plate 4. Photograph of sinistral shear bands from Callow Loughs, Ox Mountains. Lens cap is 55mm in diameter. See page 130.

## References

- Aleksandrowski, P. 1985. Graphic determination of principal stress directions for slickenside populations: an attempt to modify Arthaud's method. *Journal of Structural Geology* **7**, 73-82.
- Allan, D.A. 1928. The geology of the Highland Border from Tayside to Noranside. *Transactions of the Royal Society of Edinburgh: Earth Sciences* **56**, 57-88.
- Allan, D.A. 1940. The geology of the Highland Border from Glen Almond to Glen Artney. *Transactions of the Royal Society of Edinburgh: Earth Sciences* **60**, 171-193.
- Anderson, E.M. 1942. *The dynamics of faulting and dyke formation with applications to Britain*. Oliver & Boyd, Edinburgh.
- Anderson, E.M. 1951. *The dynamics of faulting*. Oliver & Boyd, Edinburgh (2nd edition).
- Anderson, J.G.C. 1943. The Highland Border Series in Bute. *Nature* **152**, 277.
- Anderson, J.G.C. 1946. The geology of the Highland Border: Stonehaven to Arran. *Transactions of the Royal Society of Edinburgh: Earth Sciences* **61**, 479-515.
- Anderson, J.G.C. & Pringle, J. 1944. The Arenig rocks of Arran, and their relationship to the Dalradian Series. *Geological Magazine* **81**, 81-87.
- Anderton, R., Bridges, P.H., Leeder, M.R. & Sellwood, B.W. 1979. *A dynamic stratigraphy of the British Isles*. Allan & Unwin, London.
- Anderton, R. 1980. Distinctive pebbles as indicators of Dalradian provenance. *Scottish Journal of Geology* **16**, 143-152.
- Anderton, R. 1982. Dalradian deposition and the late Precambrian-Cambrian history of the N.Atlantic region: a review of the early evolution of the Iapetus Ocean. *Journal of the Geological Society of London* **139**, 421-431.
- Anderton, R. 1985. Sedimentation and tectonics in the Scottish Dalradian. *Scottish Journal of Geology* **21**, 407-436.
- Andrews, J. 1986. Accomodation of obliquely convergent displacement in a transpressional segment of the San Andreas Fault Zone, Mecca Hills, California. Abstracts of the Geological Society of London conference on the "interactions between thrust and strike-slip tectonics".
- Angelier, J. 1989. From orientation to magnitudes in palaeostress seterminations using fault slip data. *Journal of Structural Geology* **11**, 37-50.

- Armstrong, M. & Paterson, I.B. 1970. *The Lower Old Red Sandstone of the Strathmore Region*. Institute of Geological Sciences Report no. 70/12.
- Armstrong, M., Paterson, I.B., & Browne, M.A.E. 1985. *Geology of the Perth and Dundee district*. Memoirs of the British Geological Survey, Sheets 48W, 48E, 49.
- Astin, T.R. 1983. Discussion on implications for Caledonian plate tectonic models of chemical data from volcanic rocks of the British Old Red Sandstone. *Journal of the Geological Society of London* **140**, 315.
- Aydin, A. & Reches, Z. 1982. Number and orientations of fault sets in the field and in experiments. *Geology* **10**, 110-112.
- Bailey, E.B. & Holtedahl, O. 1938. *Northwestern Europe Caledonides. Regionale Geologie der Erde, 2*. Leipzig.
- Ballance, P.F. & Reading, H.G. (editors). 1980. *Sedimentation in oblique-slip mobile zones*. Special Publications of the International Association of Sedimentologists **4**.
- Bamford, D., Nunn, K., Prodehl, C. & Jacob, B. 1977. LISP-B-III. Upper crustal structure of northern Britain. *Journal of the Geological Society of London* **133**, 481-488.
- Bamford, D., Nunn, K., Prodehl, C. & Jacob, B. 1978. LISP-B-IV. Crustal structure of northern Britain. *Geophysical Journal of the Royal Astronomical Society* **54**, 43-60.
- Bamford, M.L.F., & Ford, M. 1988. Comment on "Orogen-parallel extension and oblique tectonics: the relation between stretching lineations and relative plate motions". *Geology* **16**, 859.
- Barker, A.J. 1990. *Metamorphic textures and microstructures*. Blackie, New York.
- Barker, A.J. & Gayer, R.A. 1985. Caledonide-Appalachian tectonic analysis and evolution of related oceans. In *The tectonic evolution of the Caledonide-Appalachian orogen* (ed. Gayer, R.A.). Vieweg & Sohn, Braunschweig, 126-165.
- Barrow, G. 1901. On the occurrence of Silurian (?) rocks in Forfarshire and Kincardineshire along the eastern border of the Highlands. *Quarterly Journal of the Geological Society of London* **57**, 328-345.
- Barrow, G. 1912. On the geology of Lower Deeside and the Southern Highland Border. *Proceedings of the Geological Association* **23**, 274-290.
- Beck, M.E. Jnr. 1976. Discordant palaeomagnetic pole positions as evidence of regional shear in the western Cordillera of North America. *American Journal of Science* **276**, 694-712.
- Beck, M.E. Jnr. 1984. Introduction to the special issue on correlations between plate motions and Cordilleran tectonics. *Tectonics* **3**, 103-105.

- Bell, T.H. & Etheridge, M.A. 1973. Microstructures of mylonites and their descriptive terminology. *Lithos* 6, 337-348.
- Ben-Avraham, Z., Nur, A., Jones, D. & Cox, A. 1981. Continental accretion: from oceanic plateaus to allochthonous terranes. *Science* 213, 47-54.
- Bergerat, F. 1987. Stress fields in the European Platform at the time of Africa-Eurasia collision. *Tectonics* 6, 99-132.
- Berthé, D., Choukroune, P., & Jegouzo, P. 1979. Orthogneiss, mylonite and non coaxial deformation of granites: the example of the South Armorican shear zone. *Journal of Structural Geology* 1, 31-42.
- Bevan, T.G. & Hancock, P.L. 1986. A late Cenozoic regional mesofracture system in southern England and northern France. *Journal of the Geological Society of London* 143, 355-362.
- Biddle, K.T. & Christie-Blick, N. (editors). 1985. *Strike-slip deformation, basin formation, and sedimentation*. Society of Economic Palaeontologists and Mineralogists Special Publications 37.
- Biddle, K.T. & Christie-Blick, N. 1985. Glossary - strike-slip deformation, basin formation, and sedimentation. In *Strike-slip deformation, basin formation, and sedimentation* (ed. Biddle, K.T. & Christie-Blick, N.). Society of Economic Palaeontologists and Mineralogists Special Publications 37, 375-386.
- Bluck, B.J. 1978. Sedimentation in a late orogenic basin: the Old Red Sandstone of the Midland Valley of Scotland. In *Crustal evolution in Northwestern Britain and adjacent regions*. (ed. Bowes, D.R. & Leake, B.E.). Geological Journal Special Issue 10, 249-278.
- Bluck, B.J. 1980. Evolution of a strike-slip fault-controlled basin, Upper Old Red Sandstone, Scotland. In *Sedimentation in oblique-slip mobile zones* (ed. Ballance, P.F. & Reading, H.G.). Special Publications of the International Association of Sedimentologists 4, 63-78.
- Bluck, B.J. 1983. Role of the Midland Valley of Scotland in the Caledonian Orogeny. *Transactions of the Royal Society of Edinburgh: Earth Sciences* 74, 119-136.
- Bluck, B.J. 1984. Pre-Carboniferous history of the Midland Valley of Scotland. *Transactions of the Royal Society of Edinburgh: Earth Sciences* 75, 275-295.
- Bluck, B.J. 1985. The Scottish paratectonic Caledonides. *Scottish Journal of Geology* 21, 437-464.
- Bluck, B.J. 1990. Terrane provenance and amalgamation: examples from the Caledonides. *Philosophical Transactions of the Royal Society of London* (in press).

- Bluck, B.J., Halliday, A.N., Aftalion, M. & McIntyre, R.M. 1980. Age and origin of the Ballantrae ophiolite and its significance to the Caledonian orogeny and the Ordovician timescale. *Geology* 8, 492-5.
- Booth 1985. *Structural, stratigraphic and metamorphic studies in the South-East Scottish Dalradian Highlands*. University of Edinburgh (unpublished PhD thesis).
- Borradaile, G.J. & Poulsen, K.H. 1981. Tectonic deformation of pillow lava. *Tectonophysics* 79, T17-T26.
- Borradaile, G.J. 1981. Minimum strain from conglomerates with ductility contrast. *Journal of Structural Geology* 3, 295-297.
- Bott, M.H.P. 1959. The mechanics of oblique slip faulting. *Geological Magazine* 96, 109-117.
- Boue, A. circa 1820. *Essai geologique sur l'Ecosse*. Paris.
- Boyer, S.E. & Elliot, D. 1982. Thrust systems. *American Association of Petroleum Geologists Bulletin* 66, 1196-1230.
- Bowes, D.R. & Leake, B.E. (editors). 1978. *Crustal evolution in Northwestern Britain and adjacent regions*. Geological Journal Special Issue 10.
- Brown, P.E., Miller, J.A., Soper, N.J. & York, D. 1965. Potassium-argon age pattern of the British Caledonides. *Proceedings of the Yorkshire Geological Society* 35, 103-138.
- Buisson, G. & Leblanc, M. 1985. Gold-bearing listwaenites (carbonatized ultramafic rocks) from ophiolite complexes. In *Metallogeny of basic and ultrabasic rocks* (ed. Gallagher, M.J., Ixer, R.A., Neary, C.R. & Prichard, H.M.). Institute of Mining and Metallurgy.
- Buist, D.S. 1953. Part I. *The igneous rocks of Bute*. University of Durham (unpublished PhD thesis).
- Burton, C.J. 1984. Chitinozoa and the age of the Margie Limestone of the North Esk. *Proceedings of the Geological Society of Glasgow* 124/125, 27-32.
- Busk, H.G. 1929. *Earth flexures*. Cambridge University Press.
- Butler, R.W.H. 1982. The terminology of structures in thrust belts. *Journal of Structural Geology* 4, 239-245.
- Butler, R.W.H. & Coward, M.P. 1984. Geological constraints, structural evolution, and deep geology of the Northwest Scottish Caledonides. *Tectonics* 3, 347-366.
- Butts, C. 1939. Tyrone Quadrangle. *Topographic and Geologic Atlas of Pennsylvania no.96*. United States Geological Survey.

- Campbell, R. 1911. Preliminary note on the geology of south-eastern Kincardineshire. *Transactions of the Royal Society of Edinburgh: Earth Sciences* **48**, 63-69.
- Campbell, R. 1913. The geology of south-eastern Kincardineshire. *Transactions of the Royal Society of Edinburgh: Earth Sciences* **48**, 923-960.
- Chalmers, A.F. 1982. *What is this thing called Science?* - second edition. Open University Press.
- Christie-Blick, N. & Biddle, K.T. 1985. Deformation and basin formation along strike-slip faults. In *Strike-slip deformation, basin formation, and sedimentation* (ed. Biddle, K.T. & Christie-Blick, N.). Society of Economic Palaeontologists and Mineralogists Special Publications **37**, 1-34.
- Cloos, H. 1928. Experimente zur inneren Tektonik. *Centralbl. f. Mineral. u. Pal.* **1928B**, 609-621.
- Cocks, L.R.M. & Fortey, R.A. 1982. Faunal evidence for oceanic separations in the Palaeozoic of Britain. *Journal of the Geological Society of London* **139**, 465-478.
- Cobbing, E.J. 1964. The Highland Boundary Fault in East Tyrone. *Geological Magazine* **101**, 496-501.
- Coney, P.J. 1978. Mesozoic-Cenozoic Cordilleran plate tectonics. *Geological Society America Memoirs* **152**, 33-50.
- Coney, P.J. 1989. Structural aspects of suspect terranes and accretionary tectonics in western North America. *Journal of Structural Geology* **11**, 107-125.
- Coney, P.J., Jones, D.L. & Monger, J.W.H. 1980. Cordilleran suspect terranes. *Nature* **288**, 329-333.
- Cooper, M.A. 1983. The calculation of bulk strain in oblique and inclined balanced sections. *Journal of Structural Geology* **5**, 161-165.
- Coward, M.P. 1976. Strain within ductile shear zones. *Tectonophysics* **34**, 181-197.
- Coward, M.P. & Ries, A.C. (editors). 1986. *Collision Tectonics*. Geological Society of London Special Publication no. 8.
- Coward, M.P., Dewey, J.F. & Hancock, P.L. (editors). 1987. *Continental extensional tectonics*. Geological Society of London Special Publications **28**.
- Curry, G.B. 1986. Fossils and tectonics along the Highland Boundary Fault in Scotland. *Journal of the Geological Society of London* **143**, 193-198.

- Curry, G.B., Bluck, B.J., Burton, C.J., Ingham, J.K., Siveter, D.J., & Williams, A. 1984. Age, evolution and tectonic history of the Highland Border Complex, Scotland. *Transactions of the Royal Society of Edinburgh: Earth Sciences* 75, 113-133.
- Curry, G.B., Ingham, J.K., Bluck, B.J., & Williams, A. 1982. The significance of a reliable Ordovician age for some Highland Boundary rocks in Central Scotland. *Journal of the Geological Society of London* 139, 451-454.
- Dahlstrom, C.D.A. 1969. Balanced cross sections. *Canadian Journal Earth Sciences* 6, 743-757.
- Daubree, A. 1879. *Etudes synthetiques de geologie experimentale*. Dunod, Paris.
- Davison, C. 1924. *A history of British earthquakes*. Cambridge University Press.
- Davidson, K.A.S., Sola, M., Powell, D.W. & Hall, J. 1984. Geophysical model for the Midland Valley of Scotland. *Transactions of the Royal Society of Edinburgh: Earth Sciences* 75, 175-181.
- Dempster, T.J. 1984. Localised uplift in the Dalradian. *Nature* 307, 156-159.
- Dempster, T.J. 1985. Uplift patterns and orogenic evolution in the Scottish Dalradian. *Journal of the Geological Society of London* 142, 111-128.
- Dempster, T.J. & Harte, B. 1986. Polymetamorphism in the Dalradian of the central Scottish Highlands. *Geological Magazine* 123, 95-104.
- Dempster, T.J. & Bluck, B.J. 1989. The age and origin of boulders in the Highland Border Complex: constraints on terrane movement. *Journal of the Geological Society of London* 146, 377-379.
- Dentith, M.C., Tench, A. & Bluck, B.J. (*in prep.*). Geophysical constraints on the nature of the Highland Boundary Fault in Scotland.
- De Souza, H.A.F. 1979. *The geochronology of Scottish Carboniferous volcanism*. University of Edinburgh (unpublished PhD thesis).
- Dewey, J.F. 1963. The Lower Palaeozoic stratigraphy of central Murrisk, County Mayo, Ireland, and the evolution of the South Mayo Trough. *Quarterly Journal of the Geological Society of London* 119, 313-344.
- Dewey, J.F. 1965. Nature and origin of kink-bands. *Tectonophysics* 1, 459-494.
- Dewey, J.F. 1971. A model for the Lower Palaeozoic evolution of the early Caledonides of Scotland and Ireland. *Scottish Journal of Geology* 7, 219-240.
- Dollar, A.T.J. 1950. Catalogue of Scottish Earthquakes 1916-1949. *Transactions of the Geological Society of Glasgow* 21, 283-361.

- Dorning, K.J. 1986. Acritarch microflora from the Ordovician of North Glen Sannox, Isle of Arran, Scotland. British Lower Palaeozoic Palynomorph Working Group Report 1985, 9-13.
- Downie, C., Lister, T.R., Harris, A.L. & Fettes, D.J. 1971. *A palynological investigation of the Dalradian rocks of Scotland*. Institute of Geological Sciences Report no. 71/9.
- Du Toit, A. 1905. The Lower Old Red Sandstone rocks of the Balmaha-Aberfoyle region. *Transactions of the Geological Society of Edinburgh* 8, 315.
- Elliot, D. 1982. The construction of balanced cross-sections. *Journal of Structural Geology* 5, 101.
- Ellis, M.A. & Watkinson, A.J. 1987. Orogen-parallel extension and oblique tectonics: the relation between stretching lineations and relative plate motions. *Geology* 15, 1022-1026.
- Ellis, M.A. & Watkinson, A.J. 1988. Reply to comment on "Orogen-parallel extension and oblique tectonics: the relation between stretching lineations and relative plate motions". *Geology* 16, 859-861.
- Etchecopar, A., Vasseur, G. & Daignieres, M. 1981. An inverse problem in microtectonics for the determination of stress tensors from fault striation analysis. *Journal of Structural Geology* 3, 51-65.
- Faill, R.T. 1969. Kink Band Structures in the Valley and Ridge Province, Central Pennsylvania. *Geological Society America Bulletin* 80, 2539-2250.
- Faill, R.T. 1973. Kink-band folding, Valley and Ridge Province, Pennsylvania. *Geological Society America Bulletin* 84, 1289-1314.
- Francis, E.H., Forsyth, I.H., Read, W.A. & Armstrong, M. 1970. Geology of the Stirling District. B.G.S. memoirs 39.
- Friend, P.F., Harland, W.B. & Hudson, J.D. 1963. The Old Red Sandstone and the Highland Boundary in Arran. *Transactions of the Geological Society of Edinburgh* 19, 363-425.
- Friend, P.F., Harland, W.B. & Smith, A.G. 1969. Reddening and fissuring associated with the Caledonian unconformity in north-west Arran. (abstract) Geological Association (London) 717, 2.
- Galdeano, C.S. de. 1987. Strike-slip faults in the southern border of the Vera basin (Almeria, Betic Cordilleras). *Estudios geol.* 43, 435-443.
- Garfunkel, Z. & Ron, H. 1985. Block rotation and deformation by strike-slip faults: 2. The properties of a type of macroscopic discontinuous deformation. *Journal of Geophysical Research* 90, 8589-8602.
- Geike, Sir A. 1897. In *Annual Report for 1896*. Memoirs of the Geological Survey.

- George, T.N. 1960. The stratigraphical evolution of the Midland Valley. *Transactions of the Geological Society of Glasgow* 24, 32-107.
- Gibbs, A.D. 1983. Balanced cross-section construction from seismic sections in areas of extensional tectonics. *Journal of Structural Geology* 5, 153-160.
- Gibbs, A.D. 1984. Structural evolution of extensional basin margins. *Journal of the Geological Society of London* 141, 609-620.
- Girard, P., Schwerdtner, W.M. & Mareschal, J.-C. 1988. Comment on "Orogen-parallel extension and oblique tectonics: the relation between stretching lineations and relative plate motions". *Geology* 16, 857-859.
- Gleick, J. 1987. *Chaos*. Penguin.
- Glover, B.W. & Winchester, J.A. 1989. The Grampian Group: a major Late Proterozoic clastic sequence in the Central Highlands of Scotland. *Journal of the Geological Society of London* 146, 85-96.
- Goldstein, A.G. 1989. Tectonic significance of multiple motions on terrane-bounding faults in the northern Appalachians. *Geological Society America Bulletin* 101, 927-938.
- Graham, J.R., Richardson, J.B. & Clayton, G. 1983. Age and significance of the Old Red Sandstone around Clew Bay, NW Ireland. *Transactions of the Royal Society of Edinburgh: Earth Sciences* 73, 245-249.
- Graham, J.R., Leake, B.E. & Ryan, P.D. 1985. *The Geology of South Mayo*. 1:63360 map. University of Glasgow.
- Graham, C.M. 1986. The role of the Cruachan Lineament during Dalradian evolution. *Scottish Journal of Geology* 22, 257-270.
- Gregory, J.W. 1910. Problems of the South-Western Highlands. *Transactions of the Geological Society of Glasgow* 14, 1-29.
- Gunn, W. 1899. On the Old Volcanic rocks of the Island of Arran. *Transactions of the Geological Society of Glasgow* 2, 174-191.
- Gunn, W. 1903. *The geology of north Arran, south Bute and the Cumbraes*. Memoirs of the Geological Survey of the United Kingdom.
- Gunn, W. 1905. On a volcanic series associated with the schists of North Glen Sannox, Arran. *Transactions of the Geological Society of Glasgow* 12, 192-195.
- Gunn, W., Clough, C.T., & Hill, J.B. 1897. *The geology of Cowal*. Memoirs of the Geological Survey of the United Kingdom.
- Hall, J., Powell, D.W., Warner, M.R., El-Isa, Z.H.M., Adesanya, O. & Bluck, B.J. 1983. Seismological evidence of shallow crystalline basement in the Southern Uplands of Scotland. *Nature* 305, 418-420.

- Hall, J., Powell, D.W., Warner, M.R., El-Isa, Z.H.M., Adesanya, O. & Bluck, B.J. 1984. Seismological evidence of shallow crystalline basement in the Southern Uplands of Scotland - reply to comment by Oliver & McKerrow. *Nature* 309, 89-90.
- Hamilton, P.J., Bluck, B.J. & Halliday, A.N. 1984. Sm-Nd ages from the Ballantrae complex, S.W. Scotland. *Transactions of the Royal Society of Edinburgh: Earth Sciences* 75, 183-187.
- Hancock, P.L. 1985. Brittle microtectonics: principles and practise. *Journal of Structural Geology* 7, 437-457.
- Hancock, P.L. 1986. Faulting. *Geology Today*, September-October, 150-151.
- Hancock, P.L. & Atiya, M.S. 1979. Tectonic significance of mesofracture systems associated with the Lebanese segment of the Dead Sea transform fault. *Journal of Structural Geology* 1, 142-153.
- Hancock, P.L. & Bevan, T.G. 1987. Brittle modes of foreland extension. In *Continental extensional tectonics*.(ed. Coward, M.P., Dewey, J.F. & Hancock, P.L.). Geological Society of London Special Publications 28, 127-137.
- Hancock, P.L., Al-Kadhi, A., Barka, A.A. & Bevan, T.G. 1987. Aspects of analysing brittle structures. *Annales Tectonicae* 1, 5-19.
- Hanmer, S.K. 1982. Vein arrays as kinematic indicators in kinked anisotropic materials. *Journal of Structural Geology* 4, 151-160.
- Hanmer, S.K. 1986. Asymmetrical pull-aparts and foliation fish as kinematic indicators *Journal of Structural Geology* 8, 111-122.
- Harding, T.P. 1985. Seismic characteristics and identification of negative flower structures, positive flower structures and positive structural inversion. *American Association of Petroleum Geologists Bulletin* 69, 582-600.
- Harding, T.P. 1988. Comment on "State of stress near the San Andreas fault: implications for wrench tectonics". *Geology* 16, 1151-1152.
- Harland, W.B. 1971. Tectonic transpression in Caledonian Spitzbergen. *Geological Magazine* 108, 27-42.
- Harland, W.B., Cox, A.V., Llewellyn, P.G., Pickton, C.A.G., Smith, A.G. & Walters, R. 1982. *A geological timescale*. Cambridge University Press.
- Harper, C.T. 1967. The geological interpretation of potassium - argon ages of metamorphic rocks from the Scottish Caledonides. *Scottish Journal of Geology* 3, 46-66.
- Harper, D.A.T., Williams, D.M. & Armstrong, H.A. 1989. Stratigraphical correlations adjacent to the Highland Boundary fault in the west of Ireland. *Journal of the Geological Society of London* 146, 381-384.

- Harris, A.L. 1962. *Dalradian geology of the Highland Border near Callander*. Geological Survey of Great Britain Bulletin no. 19, 1-15.
- Harris, A.L. 1969. The relationships of the Leny Limestone to the Dalradian. *Scottish Journal of Geology* 5, 187-190.
- Harris, A.L. 1973. Excursion 8: Aberfoyle. In *Excursion Guide to the Geology of the Glasgow District* (ed. Bluck, B.J.). Geological Society of Glasgow, 69-75.
- Harris, A.L. & Fettes, D.J. 1972. Stratigraphy and structure of Upper Dalradian rocks of the Highland Border. *Scottish Journal of Geology* 8, 253-264.
- Harris, L.B. & Cobbold, P.R. 1985. Development of conjugate shear bands during bulk simple shearing. *Journal of Structural Geology* 7, 37-44.
- Harte, B. & Dempster, T.J. Regional metamorphic zones: tectonic controls. *Philosophical Transactions of the Royal Society of London* A321, 105-127.
- Hashimoto, M. & Uyeda, S. (editors). 1983. *Accretion tectonics in the Circum-Pacific regions*. Terra Sci. Pub. Co., Tokyo.
- Haughton, P.D.W. 1988. A cryptic Caledonian flysch terrane in Scotland. *Journal of the Geological Society of London* 145, 685-703.
- Haughton, P.D.W., Rogers, G. & Halliday, A.N. 1990. Provenance of Lower Old Red Sandstone conglomerates, SE Kincardineshire: evidence for the timing of Caledonian terrane accretion in central Scotland. *Journal of the Geological Society of London* 147, 105-120.
- Hempton, M.R. & Nether, K. 1986. Experimental fracture, strain and subsidence patterns over an échelon strike-slip faults: implications for the structural evolution of pull apart basins. *Journal of Structural Geology* 8, 597-605.
- Henderson, W.G. 1981. Jasper pebbles in the Dalradian at the Highland Boundary. *Scottish Journal of Geology* 17, 179-183.
- Henderson, W.G. & Robertson, A.H.F. 1982. The Highland Border rocks and their relation to marginal basin development in the Scottish Caledonides. *Journal of the Geological Society of London* 139, 433-450.
- Henderson, W.G. & Fortey, N.J. 1982. Highland Border rocks at Loch Lomond and Aberfoyle. *Scottish Journal of Geology* 18, 227-245.
- Horsfield, W.T. 1980. Contemporaneous movement along crossing conjugate normal faults. *Journal of Structural Geology* 2, 305-310.
- Hossack, J.R. 1983. A cross-section through the Scandinavian Caledonides constructed with the aid of branch-line maps. *Journal of Structural Geology* 5, 103-112.

- House, M.R., Richardson, J.B., Chaloner, W.G., Allen, J.R.L., Holland, C.H. & Westoll, T.S. 1977. *A correlation of the Devonian rocks of the British Isles*. Geological Society of London Special Report 7.
- Huang, Q. 1988. Computer-based method to separate heterogenous sets of fault-slip data into sub-sets. *Journal of Structural Geology* **10**, 297-299.
- Hutchison, A.G. 1925. A lava-flow at the base of the Kincardineshire Downtonian. *Transactions of the Geological Society of Edinburgh* **12**, 69-73.
- Hutton, D.H.W. 1982. A tectonic model for the emplacement of the Main Donegal Granite, N.W. Ireland. *Journal of the Geological Society of London* **139**, 615-632.
- Hutton, D.H.W. 1987. Strike-slip terranes and a model for the evolution of the British and Irish Caledonides. *Geological Magazine* **124**, 405-425.
- Hutton, D.H.W. 1988. Granite emplacement and tectonic controls: inferences from deformation studies. *Transactions of the Royal Society of Edinburgh Earth Sciences* **79**, 245-255.
- Hutton, D.H.W. 1990. The geology of the Tyrone Inlier, Northern Ireland. Abstracts from "Tectonics of the British Isles" conference, Durham University, March 1990.
- Hutton, D.H.W., Aftalion, M. & Halliday, A.N. 1985. An Ordovician ophiolite in County Tyrone, Ireland. *Nature* **315**, 210-212.
- Hutton, D.H.W. & Dewey, J.F. 1986. Palaeozoic terrane accretion in the Western Irish Caledonides. *Tectonics* **5**, 1115-1124.
- Ikin, N.P. 1979. The mafic and ultramafic rocks of the Highland Border. University of Wales (unpublished PhD thesis).
- Ikin, N.P. 1983. Petrochemistry and tectonic significance of the Highland Border Suite mafic rocks. *Journal of the Geological Society of London* **140**, 267-278.
- Ikin, N.P. & Harmon, R.S. 1981. D/H and  $^{18}\text{O}/^{16}\text{O}$  ratios and mineralogy of serpentinites from the Highland Border Fracture-Zone, Scotland. *Bulletin Mineralogie* **104**, 795-800.
- Ikin, N.P. & Harmon, R.S. 1983. A stable isotope study of serpentinitisation and metamorphism in the Highland Border Suite, Scotland, U.K. *Geochimica et Cosmochimica Acta* **47**, 153-167.
- Imrie, Lt.-Col. 1812. A description of the strata which occur in ascending from the Plains of Kincardineshire to the Summit of Mount Battoc, one of the most elevated points in the Eastern District of the Grampian Mountains. *Transactions of the Royal Society of Edinburgh* **6**, 3-19.

- Ingham, J.K., Curry, G.B. & Williams, A. 1985. Early Ordovician Dounans limestone fauna, Highland Border Complex, Scotland. *Transactions of the Royal Society of Edinburgh: Earth Sciences* 76, 481-513.
- Jackson, J. & McKenzie, D. 1983. The geometrical evolution of normal fault systems. *Journal of Structural Geology* 5, 471-482.
- Jaeger, J.C. & Cook, N.G.W. 1969. *Fundamentals of rock mechanics*. Methuen, London.
- Jehu, T.J. 1912. Discovery of fossils in the Boundary Fault Series, near Aberfoyle. *Geological Magazine* 49, 469-470.
- Jehu, T.J. 1914. Note on the Highland Border Series near Aberfoyle. *Geological Magazine* 51, 402-404.
- Jehu, T.J. & Campbell, R. 1917. The Highland Border rocks of the Aberfoyle District. *Transactions of the Royal Society of Edinburgh: Earth Sciences* 52, 175-212.
- Johnson, M.R.W. 1967. Mylonite zones and mylonite banding. *Nature* 213, 246-247.
- Johnson, M.R.W. & Frost, R.T.C. 1977. Fault and lineament patterns in the southern Highlands of Scotland. *Geologie en Mijnbouw* 5, 287-294.
- Johnson, M.R.W. & Harris A.L. 1965. Is the Tay Nappe post Arenig? *Scottish Journal of Geology* 1, 217-219.
- Johnson, M.R.W. & Harris A.L. 1967. Dalradian-?Arenig relations in part of the Highland Border, Scotland, and their significance in the chronology of the Caledonian Orogeny. *Scottish Journal of Geology* 3, 1-16.
- Johnstone, G.S. 1973. *The Grampian Highlands (amended 3rd edition)*. Institute of Geological Sciences.
- Johnstone, G.S. & Smith, D.I. 1965. Geological observations concerning the Breadalbane hydro-electric project, Perthshire. *Geological Survey of Great Britain Bulletin* 22.
- Jones, C. & McCaffery, K. 1989. Field guide to the Ox Mountains (5-10 January 1989). Department of Geology, Durham University.
- Jones, D.L., Siberling, N.J., Gilbert, W. & Coney, P. 1982. Character, distribution and tectonic significance of accretionary terranes in the central Alaska range. *Journal of Geophysical Research* 87, 3709-3717.
- Jones, D.L., Howell, D.G., Coney, P. & Monger, J.W.H. 1983. Recognition, character, and analysis of tectonostratigraphic terranes in western North America. In *Accretion tectonics in the Cirum-Pacific regions* (ed. Hashimoto, M. & Uyeda, S.). Terra Sci. Pub. Co., Tokyo, 21-35.
- Kennedy, W.Q. 1955. The tectonics of the Morar anticline and the problem of the North-west Caledonian front. *Quarterly Journal of the Geological Society of London* 110, 357- 390.

- Kennedy, W.Q. 1958. The tectonic evolution of the Midland Valley of Scotland. *Transactions of the Geological Society of Glasgow* **23**, 106-133.
- Kent, D.V. 1988. Further palaeomagnetic evidence for oroclinal rotation in the central folded Appalachians from the Bloomsburg and the Mauch Chunk Formations. *Tectonics* **7**, 749-759.
- King, B.C. & Rast, N. 1956. The small-scale structures of South-Eastern Cowal, Argyllshire. *Geological Magazine* **93**, 185-195.
- King, G. 1983. The accomodation of large strains in the upper lithosphere of the earth and other solids by self-similar fault systems: the geometrical origin of b-value. *Pageoph.* **121**, 761-815.
- Kissel, C., Laj, C., Poisson, A., Savasçin, Y., Simeakis, K. & Mercier, J.L. 1986. Palaeomagnetic evidence for Neogene rotational deformations in the Aegean domain. *Tectonics* **5**, 783-796.
- Kligfield, R., Hunziker, J., Dallmeyer, R.D. & Schamel, S. 1986. Dating of deformation using K-Ar and  $^{40}\text{Ar}/^{39}\text{Ar}$  techniques: results from the Northern Apennines. *Journal of Structural Geology* **8**, 781-798.
- Knipe, R.P. 1985. Footwall geometry and the rheology of thrust sheets. *Journal of Structural Geology* **7**, 1-10.
- Knipe, R.P. 1989. Deformation mechanisms - recognition from natural tectonites. *Journal of Structural Geology* **11**, 127-146.
- Koenemann, F. 1986. A universal stage method for very fine-grained crystal aggregates. *Journal of Structural Geology* **8**, 941-942.
- Kohlbeck, F. & Scheidegger, A.E. 1977. On the theory of the evaluation of joint orientation measurements. *Rock Mechanics* **9**, 9-25.
- Kralik, M., Klimat, K. & Riedmüller, G. 1987. Dating fault gouges. *Nature* **321**, 315-317.
- Krantz, R.W. 1988. Multiple fault sets and three-dimensional strain: theory and application. *Journal of Structural Geology* **10**, 225-237.
- Kuhn, T.S. 1970. *The Structure of Scientific Revolutions*. University of Chicago Press.
- Lagarde, J.L. & Michard, A. 1986. Stretching normal to the regional thrust displacement in a thrust-wrench shear zone, Rehamna Massif, Morocco. *Journal of Structural Geology* **8**, 483-492.
- Lakatos, I. 1974. Falsification and the Methodology of Scientific Research Programmes. In *Criticism and the Growth of Knowledge* (eds. Lakatos, I. & Musgrave, A.). Cambridge University Press, 91-196.
- Lambert, R.St.J. & McKerrow, W.S. 1976. The Grampian Orogeny. *Scottish Journal of Geology* **12**, 271-292.

- Lambert, R.St.J. & McKerrow, W.S. 1984. Comparison of the San Andreas Fault system with the Highland Boundary fault system in Scotland. *Transactions of the American Geophysical Union* 56, 1193.
- Lamont, A. 1930. A guide to the rocks of Bute. *Transactions of the Buteshire Natural History Society* 10, 63-67.
- Lapworth, C. 1885. The highland controversy in British geology; its causes, course and consequences. *Nature* 32, 558-559.
- Larter, R.C.L. & Allison, I. 1983. An inexpensive device for modelling strike-slip fault zones. *Journal of Geological Education* 31, 200-205.
- Leake, B.E., Tanner, P.W.G., Singh, D. & Halliday, A.N. 1983. Major southward thrusting of Dalradian rocks of Connemara, western Ireland. *Nature* 305, 210-213.
- Leblanc, M. 1986. Co-Ni arsenide deposits, with accessory gold, in ultramafic rocks from Morocco. *Canadian Journal Earth Sciences* 23, 1592-1602.
- Leeder, M.R. 1982. Upper Palaeozoic basins of the British Isles - Caledonide inheritance versus Hercynian plate margin processes. *Journal of the Geological Society of London* 139, 481-494.
- Leggett, J.K., McKerrow, W.S. & Eales, M.H. 1979. The Southern Uplands of Scotland: a Lower Palaeozoic accretionary prism. *Journal of the Geological Society of London* 136, 755-770.
- Leggett, J.K., McKerrow, W.S. & Soper, N.J. 1983. A model for the crustal evolution of southern Scotland. *Tectonics* 2, 187-210.
- Lister, G.S. & Price, G.P. 1978. Fabric development in a quartz-feldspar mylonite. *Tectonophysics* 49, 37-78.
- Lister, G.S. & Williams, P.F. 1979. Fabric development in shear zones: theoretical controls and observed phenomena. *Journal of Structural Geology* 1, 283-397.
- Lister, G.S. & Snoke, A.W. 1984. S-C mylonites. *Journal of Structural Geology* 6, 617-638.
- Longman, C.D., Bluck, B.J. & van Breemen, O. 1979. Ordovician conglomerates and the evolution of the Midland Valley. *Nature* 280, 578-581
- Lyell, C. 1825. On a dyke of serpentine, cutting through sandstone, in the county of Forfar. *Edinburgh Journal of Science* 1, 112-118.
- Maltman, A. 1984. On the term 'soft-sediment deformation'. *Journal of Structural Geology* 6, 589-592.
- Mandelbrot, B.B. 1982. *The fractal geometry of nature*. Freeman, San Francisco.
- Mandl, G. 1987. Discontinuous fault zones. *Journal of Structural Geology* 9, 105-110.

- Marshall, J.E.A. 1989. The palynology of the Stonehaven Group, north east Scotland and its stratigraphical implications. *Palaeontological Association Abstracts*.
- Max, M.D. 1989. The Clew Bay Group: a displaced terrane of Highland Border Group rocks (Cambro-Ordovician) in Northwest Ireland. *Geological Journal* **24**, 1-17.
- Max, M.D. & Riddihough, R.P. 1975. Continuation of the Highland Boundary Fault in Ireland. *Geology* **3**, 206-210.
- Means, W.D. 1987. A newly recognized type of slickenside striation. *Journal of Structural Geology* **9**, 585-590.
- Mellie, R. 1990. The man on the telly. *Viz* **42**.
- Mitra, G. 1984. Brittle to ductile transition due to large strains along the White Rock thrust, Wind River mountains, Wyoming. *Journal of Structural Geology* **6**, 51-61.
- Moody, J.D. & Hill, M.J. 1956. Wrench-fault tectonics. *Geological Society America Bulletin* **67**, 1207-1246.
- Mount, V.S. & Suppe, J. 1987. State of stress near the San Andreas fault: implications for wrench tectonics. *Geology* **15**, 1143-1146.
- Murrell, S.A.F. 1977. Natural faulting and the mechanics of brittle shear failure. *Journal of the Geological Society of London* **133**, 175-189.
- MacCulloch 1824. On the limestone of Clunie, in Perthshire, with remarks on trap and serpentine. *Edinburgh Journal of Science* **1**, 1-15.
- MacDonald, R. 1980. Trace element evidence for mantle heterogeneity beneath the Scottish Midland Valley in the Carboniferous and Permian. *Philosophical Transactions of the Royal Society of London A* **297**, 245-247.
- McCallien, W.J. 1938. The rocks of Bute. *Transactions of the Buteshire Natural History Society* **12**, 84-112.
- McCoss, A.M. 1986. Simple constructions for deformation in transpression/transension zones. *Journal of Structural Geology* **8**, 715-718.
- McCoss, A.M. 1988. Restoration of transpression/transension by generating the three-dimensional segmented helical loci of deformed lines across structure contour maps. *Journal of Structural Geology* **10**, 109-120.
- McEwan, T.J. 1981. Brittle deformation in pitted pebble conglomerates. *Journal of Structural Geology* **3**, 25-37.
- McKerrow, W.S., Leggett, J.K., & Eales, M.H. 1977. Imbricate thrust model of the Southern Uplands of Scotland. *Nature* **267**, 237-239.

- McLean, A.C. 1978. Evolution of fault-controlled ensialic basins in north-western Britain. In *Crustal evolution in Northwestern Britain and adjacent regions*. (ed. Bowes, D.R. & Leake, B.E.). Geological Journal Special Issue 10, 325-246
- Naylor, M.A., Mandl, G. & Sijpesteijn, C.H.K. 1986. Fault geometries in basement-induced wrench faulting under different initial stress states. *Journal of Structural Geology* 8, 737-752.
- Norris, D.K. 1958. Structural conditions in Canadian coal mines. *Bulletin of the Geological Survey of Canada* 44, 1-53.
- Norrell, G.T., Teixell, A. & Harper, G.D. 1989. Microstructure of serpentinite from the Josephine ophiolite and serpentinisation in retrogressive shear zones, California. *Geological Society America Bulletin* 101, 673-682.
- Nur, A. & Ben-Avraham, Z. 1983. Break-up and accretion tectonics. In *Accretion tectonics in the Cirum-Pacific regions* (ed. Hashimoto, M. & Uyeda, S.). Terra Sci. Pub. Co., Tokyo, 3-18.
- O'Connor, P.J., Long, C.B. & Hennessy, J. 1983. Radioelement geochemistry of Irish Newer Caledonian granites. *Geological Survey of Ireland Bulletin* 3, 125-140.
- Oertel, G. 1965. The mechanism of faulting in clay experiments. *Tectonophysics* 2, 343-393.
- Pankhurst, R.J., Andrews, J.R., Phillips, W.E.A. & Sanders, I.S. 1976. Age and structural setting of the Slieve Gamph igneous complex, Co. Mayo, Eire. *Journal of the Geological Society of London* 132, 327-336.
- Passchier, C.W. & Simpson, C. 1986. Porphyroclast systems as kinematic indicators. *Journal of Structural Geology* 8, 831-843.
- Paterson, I.B. & Harris, A.L. 1969. *Lower Old Red Sanstone ignimbrites from Dunkeld, Perthshire*. Institute of Geological Sciences Report no. 69/7.
- Petit, J.P. 1987. Criteria for the sense of movement on fault surfaces in brittle rocks. *Journal of Structural Geology* 9, 597-608.
- Phillips, W.E.A. 1973. The pre-Silurian rocks of Clare Island, Co. Mayo, Ireland, and the age of the metamorphism of the Dalradian in Ireland. *Quarterly Journal of the Geological Society of London* 129, 585-606.
- Platt, J.P. 1984. Secondary cleavages in ductile shear zones. *Journal of Structural Geology* 6, 439-442. [See erratum; J.S.G. 6, 749.]
- Platt, J.P. & Vissers, R.L.M. 1980. Extensional structures in anisotropic rocks. *Journal of Structural Geology* 2, 397-410.
- Pollard, D.D. & Aydin, A. 1988. Progress in understanding jointing over the past century. *Geological Society America Bulletin* 100, 1181-1204.
- Popper, K.R. 1968. *The Logic of Scientific Discovery*. Hutchinson, London.

- Pringle, J. 1939. *The discovery of Cambrian trilobites in the Highland Border rocks near Callander, Perthshire*. Report of the British Association for the Advancement of Science, p252.
- Pringle, K. 1941. On the relationship of the green conglomerate to the Margie Series in the North Esk, near Edzell; and on the probable age of the Margie Limestone. *Transactions of the Geological Society of Glasgow* 20, 136-140.
- Ramsay, D.M. 1962. The Highland Boundary Fault: reverse or wrench fault. *Nature* 195, 1190-1191.
- Ramsay, D.M. 1964. Deformation of pebbles in Lower Old Red Sandstone conglomerates adjacent to the Highland Boundary Fault. *Geological Magazine* 101, 228-248.
- Ramsay, J.G. 1967. *Folding and fracturing of rocks*. McGraw-Hill, New York.
- Ramsay, J.G. 1980. Shear zone geometry: a review. *Journal of Structural Geology* 2, 83-99.
- Ramsay, J.G. & Graham, R.H. 1970. Strain variation in shear belts. *Canadian Journal Earth Sciences* 7, 786-813.
- Ramsay, J.G. & Huber, M.I. 1983. *The techniques of modern structural geology. Volume 1: strain analysis*. Academic Press, London.
- Ramsay, J.G. & Huber, M.I. 1987. *The techniques of modern structural geology. Volume 2: folds and fractures*. Academic Press, London.
- Reches, Z. 1978. Analysis of faulting in three-dimensional strain field. *Tectonophysics* 47, 109-129.
- Reches, Z. 1983. Faulting of rocks in three-dimensional strain fields II. Theoretical analysis. *Tectonophysics* 95, 133-156.
- Reches, Z. & Dietrich, J.H. 1983. Faulting of rocks in three-dimensional strain fields I. Failure of rocks in polyaxial, servo-controlled experiments. *Tectonophysics* 95, 111-132.
- Richardson, J.B., Ford, J.H. & Parker, F. 1984. Miospores, correlation and age of some Scottish Lower Old Red Sandstone sediments from the Strathmore region (Fife and Angus). *Journal of Palaeontology* 3, 109-124.
- Ridley, J. 1986. Parallel stretching lineations and fold axes oblique to a shear zone displacement direction - a model and observations. *Journal of Structural Geology* 8, 647-653.
- Robertson, A.H.F. & Henderson, W.G. 1984. Geochemical evidence for the origins of igneous and sedimentary rocks of the Highland Border, Scotland. *Transactions of the Royal Society of Edinburgh: Earth Sciences* 75, 135-150.

- Robertson, S. 1987. Early sinistral transpression in the Lower Old Red Sandstone of Kincardineshire, Scotland. *Scottish Journal of Geology* **23**, 261-268.
- Rogers, G., Dempster, T.J., Bluck, B.J. & Tanner, P.W.G. 1989. A high precision U-Pb age for the Ben Vuirich granite: implications for the evolution of the Scottish Dalradian Supergroup. *Journal of the Geological Society of London* **146**, 789-798.
- Ron, H. 1987. Deformation along the Yammuneh, the restraining bend of the Dead Sea transform: palaeomagnetic data and kinematic implications. *Tectonics* **6**, 653-666.
- Ron, H., Freund, R., Garfunkel, Z. & Nur, A. 1984. Block rotation by strike-slip faulting: structural and palaeomagnetic evidence. *Journal of Geophysical Research* **89**, 6256-6270.
- Ron, H., Aydin, A. & Nur, A. 1986. Strike-slip faulting and block rotation in the Lake Mead fault system. *Geology* **14**, 1020-1023.
- Rushton, A.W.A. & Phillips, W.E.A. 1973. A specimen of *Protospongia hicksi* from the Dalradian of Clare Island, Co. Mayo, Ireland. *Palaeontology* **16**, 223-230.
- Rushton, A.W.A. & Tripp, R.P. 1979. A fossiliferous lower Canadian (Tremadoc) boulder from the Benan conglomerate of the Girvan District. *Scottish Journal of Geology* **15**, 321-327.
- Russell, M.J. & Smythe, D.K. 1983. Origin of the Oslo Graben in relation to the Hercynian-Alleghenian Orogeny and lithospheric rifting in the North Atlantic. *Tectonophysics* **94**, 457-472.
- Ryan, P.D., Max, M.D. & Kelly, T. 1983. Ophiolitic melange separates ortho- and para-tectonic Caledonides in Western Ireland. *Nature* **301**, 50-52.
- Sanderson, D.J. 1982. Models of strain variation in nappes and thrust sheets: a review. *Tectonophysics* **88**, 201-233.
- Sanderson, D.J. & Marchini, W.R.D. 1984. Transpression. *Journal of Structural Geology* **6**, 449-458.
- Shackleton, R.M. 1957. Downward facing structures of the Highland Border. *Quarterly Journal of the Geological Society of London* **113**, 361-392.
- Shackleton, R.M. & Ries, A.C. 1984. The relation between regionally consistent stretching lineations and plate motions. *Journal of Structural Geology* **6**, 111-117.
- Sibson, R.H. 1977. Fault rocks and fault mechanisms. *Journal of the Geological Society of London* **133**, 191-213.
- Sibson, R.H. 1980. Transient discontinuities in ductile shear zones. *Journal of Structural Geology* **2**, 165-171.

- Sibson, R.H. 1985. A note on fault reactivation. *Journal of Structural Geology* 7, 751-754.
- Sibson, R.H. 1989. Earthquake faulting as a structural process. *Journal of Structural Geology* 11, 1-14.
- Simpson, C. & Schmid, S.M. 1983. An evaluation of criteria to deduce the sense of movement in sheared rocks. *Geological Society America Bulletin* 94, 1281-1288.
- Smellie, W.R. 1916. The igneous rocks of Bute. *Transactions of the Geological Society of Glasgow* 15, 334-372.
- Smith, D.I. 1961. Patterns of minor faults in the south Central Highlands of Scotland. *Geological Survey of Great Britain Bulletin* 17.
- Smith, P.J. & Bott, M.H.P. 1975. Structure of the crust beneath the Caledonian Foreland and Caledonian Belt of the North Scottish shelf region. *Geophysical Journal of the Royal Astronomical Society* 40, 187-205.
- Soper, N.J. 1986. Geometry of transecting, anastomosing solution cleavage in transpression zones. *Journal of Structural Geology* 8, 937-940.
- Soper, N.J. & Hutton, D.H.W. 1984. Late Caledonian sinistral displacements in Britain: implications for a three-plate collision model. *Tectonics* 3, 781-794.
- Soper, N.J., Webb, B.C. & Woodcock, N.H. 1987. Late Caledonian (Acadian) transpression in north-west England: timing, geometry and geotectonic significance. *Proceedings of the Yorkshire Geological Society* 46, 175-192.
- Stark, J. 1905. The Highland Boundary Fault in Arran. *Transactions of the Geological Society of Glasgow* 12, 292-293.
- Stephens, W.E. & Halliday, A.N. 1984. Geochemical contrasts between the late Caledonian granitoid plutons of northern, central and southern Scotland. *Transactions of the Royal Society of Edinburgh: Earth Sciences* 75, 259-273.
- Sugden, T. 1987. Kinematic indicators: structures that record the sense of movement in mountain chains. *Geology Today*, May-June, 93-99.
- Suppe, J. 1983. Geometry and kinematics of fault-bend folding. *American Journal of Science* 283, 684-721.
- Suppe, J. 1985. *Principles of structural geology*. Prentice-Hall, New Jersey.
- Sylvester, A.G. 1988. Strike-slip faults. *Geological Society America Bulletin* 100, 1666-1703.
- Sylvester, A.G. & Smith, R.R. 1976. Tectonic transpression and basement-controlled deformation in san Andreas fault zone, Salton trough, California. *American Association of Petroleum Geologists Bulletin* 66, 2081-2102.

- Tanner, P.W.G. 1989. The flexural slip mechanism. *Journal of Structural Geology* **11**, 635-655.
- Tchalenko, J.S. 1970. Similarities between shear zones of different magnitudes. *Geological Society America Bulletin* **81**, 1625-1640.
- Tchalenko, J.S. & Ambrayeses, N.N. 1970. Structural analysis of the Dasht-e-Bayaz (Iran) earthquake fractures. *Geological Society America Bulletin* **81**, 41-60.
- Thirlwall, M.F. 1981. Implications for Caledonian plate tectonic models of chemical data from volcanic rocks of the British Old Red Sandstone. *Journal of the Geological Society of London* **138**, 123-138.
- Thirlwall, M.F. 1983. Discussion on implications for Caledonian plate tectonic models of chemical data from volcanic rocks of the British Old Red Sandstone: reply to Dr. T.R. Astin. *Journal of the Geological Society of London* **140**, 315-318.
- Thirlwall, M.F. 1988. Geochronology of Late Caledonian magmatism in northern Britain. *Journal of the Geological Society of London* **145**, 951-967.
- Thirlwall, M.F. & Bluck, B.J. 1984. Sr-Nd isotope and chemical evidence that the Ballantrae 'ophiolite', S.W. Scotland, is polygenetic. In *Ophiolites and oceanic lithosphere* (ed. Gass, I.G., Lippard, S.J. & Shelton, A.W.). Geological Society of London Special Publications **13**, 215-230.
- Thorning, L. 1974. Palaeomagnetic results from Lower Devonian rocks of the Cheviot Hills, northern England. *Geophysical Journal of the Royal Astronomical Society* **36**, 487-496.
- Torsvik, T.H. 1985. Magnetic properties of the Lower Old Red Sandstone lavas in the Midland Valley, Scotland; palaeomagnetic and tectonic considerations. *Physics of the Earth and Planetary Interiors* **39**, 194-207.
- Traquair, R.H. 1912. Note on the fish-remains collected by Messrs R. Campbell, W.T. Gordon, and B.N. Peach in Palaeozoic Strata at Cowie, Stonehaven. *Geological Magazine* **9**, 511.
- Tremlett, W.E. 1973. Excursion 9: Balmaha. In *Excursion Guide to the Geology of the Glasgow District* (ed. Bluck, B.J.). Geological Society of Glasgow, 75-81.
- Trench, A. 1988. *Palaeomagnetic studies in the Scottish Paratectonic Caledonides*. University of Glasgow (unpublished PhD thesis).
- Trench, A. & Haughton, P.D.W. 1990. Palaeomagnetic and geochemical evaluation of a terrane-linking ignimbrite: evidence for the relative position of the Grampian and Midland Valley terranes in late Silurian time. *Geological Magazine* **127**, 241-257.

- Turcotte, D.L. 1983. Mechanisms of crustal deformation. *Journal of the Geological Society of London* **140**, 701-724.
- Turcotte, D.L. 1986. A fractal model for crustal deformation. *Tectonophysics* **132**, 261-269.
- Upton, B.G.J., Aspen, P. & Graham, A. 1976. Pre-Palaeozoic basement of the Scottish Midland Valley. *Nature* **260**, 517-518.
- Upton, B.G.J., Aspen, P. & Chapman, N.A. 1983. The upper mantle and deep crust beneath the British Isles: evidence from inclusions in volcanic rocks. *Journal of the Geological Society of London* **140**, 105-121.
- van Breemen, O. & Bluck, B.J. 1981. Episodic granite plutonism in the Scottish Caledonides. *Nature* **291**, 113-117.
- Walsh, J.J. & Watterson, J. 1988. Analysis of the relationship between displacements and dimensions of faults. *Journal of Structural Geology* **10**, 239-247.
- Watson, J.V. 1984. The ending of the Caledonian Orogeny in Scotland. *Journal of the Geological Society of London* **141**, 193-214.
- Whelan, G.M. 1988. *The palynology of selected Ordovician localities in Scotland*. University of Glasgow (unpublished PhD thesis).
- White, S.H., Burrows, S.E., Carreras, J., Shaw, N.D. & Humphreys, F.J. 1980. On mylonites in ductile shear zones. *Journal of Structural Geology* **2**, 175-187.
- Wickham, J.S. 1988. Comment on "State of stress near the San Andreas fault: implications for wrench tectonics". *Geology* **16**, 1152-1153.
- Wilcox, R.E., Harding, T.P. & Seely, D.R. 1973. Basic wrench tectonics. *American Association of Petroleum Geologists Bulletin* **57**, 74-96.
- Williams, G.D. & Chapman, T.J. 1986. The Bristol-Mendip foreland thrust belt. *Journal of the Geological Society of London* **143**, 63-73.
- Williams, P.F. 1985. Multiply deformed terrains - problems of correlation. *Journal of Structural Geology* **7**, 269-280.
- Wilson, J.T. 1965. A new class of faults, and their bearing on continental drift. *Nature* **207**, 343-347.
- Wilson, J.T. 1966. Did the Atlantic close and then re-open? *Nature* **211**, 676-681.
- Windley, B.F. 1984. *The evolving continents*. Second edition. John Wiley & sons, Chichester.
- Wise, D.U., Dunn, D.E., Engelder, J.T., Geiser, P.A., Hatcher, R.D., Kish, S.A., Odom, A.L. & Schamel, S. 1984. Fault-related rocks: suggestions for terminology. *Geology* **12**, 391-394.

- Wojtal, S. & Mitra, G. 1988. Nature of deformation in some fault rocks from Appalachian thrusts. *Geological Society America Special Paper* **222**, 17-33.
- Woodcock, N.H. 1986. The role of strike-slip fault systems at plate boundaries. *Philosophical Transactions of the Royal Society of London* **A317**, 13-27.
- Woodcock, N.H. & Naylor, M.A. 1983. Randomness testing in three-dimensional orientation data. *Journal of Structural Geology* **5**, 539-548.
- Woodcock, N.H. & Fischer, M. 1986. Strike-slip duplexes. *Journal of Structural Geology* **8**, 725-736.

# Appendix 1: MESOFRACTURE ANALYSIS USING A COMPUTER

## A1.1 Introduction

There are several advantages of using computers to plot orientation data:

- 1) plotting by computer is orders of magnitude faster than plotting by hand.
- 2) rapid plotting facilitates a trial and error approach. This allows the user to find the most effective way of presenting the data.
- 3) computer-generated plots are as accurate as the input data will allow: bug-free programs do not make mistakes.

The Structural Orientation Database System ("SODS") was written in 1988 by Colin Farrow (Dept. of Geology & Applied Geology, Glasgow Univ.). SODS allows geological orientation data to be stored, analysed, sorted and displayed graphically. The plotting routines in SODS use "S", a high level language and software system for data analysis and graphics, which runs under the UNIX operating system. The simplicity of the SODS system allows unlimited expansion and customization of the graphics macros for individual applications; the only requirement is a basic knowledge of programming in "S".

The Mesofracture Analysis Stereonet System ("MASS") is an example of such expansion. A package of macros described in the following pages sorts, plots, contours, and statistically analyses fault, joint, and lineation data. Display is in colour using the Tektronix 4107 terminal (or equivalent).

## A1.2 Summary of MASS macros

- ?paps(userref1,userref2) plots each fracture type separately.
- ?paps2(userref1,userref2) as ?paps, but plots over existing plots.
- ?pufs(userref1,userref2,startcol/2/) colour contour plot of undifferentiated fractures.
- ?BWpufs(userref1,userref2,startlty/2/,charsze/0/) as ?pufs, but produces a monochrome plot.
- ?faces(userref1,userref2,startcol/2/) Each fracture type in the data set is contoured separately and superimposed on the plot.

- ?BWfaces(userref1,userref2,startlty/2/,charsze/0/) as ?faces, but produces a monochrome plot.
- ?linp1(userref1,userref2,segsize/10/,surftype/0/) plots all the lineation data without distinguishing between different fault types.
- ?linp2(userref1,userref2,segsize/10/,surftype/0/) separates fractures into sets of different movement sense, and plots each set in a different colour.
- ?rose2(az,new/T/,start/0/,step/30/) plots "equal distance" rose diagrams
- ?ear(az,new/T/,circs/T/,meen/400/,step/30/,start/0/) plots "equal area" rose diagrams.
- ?segstat(ordata,polar/T/) statistical analysis of data limited to a specific segment of the stereonet.
- ?quad(userref1,userref2,pole/F/) quadrant statistics for the analysis of triaxial deformation.

### A1.3 Details of the MASS structure

MASS is a modular system comprising several controlling macros with mnemonic names. These controlling macros are partially interactive: some information is entered when the macro is called, whilst the user is prompted for other information as the programme runs. The controlling macros each call several sorting and plotting macros (these are prefixed by "?rj..").

The modularity of the system allows the system to be expanded easily. Those parts of a plotting routine common to most routines (e.g. extracting the orientation data from the SODS database ) need not be re-written for each one. In addition, this system allows other SODS users to incorporate the appropriate macros with minimal modification, for their own individual use.

#### A1.3.1. Details of the MASS controlling macros

All of the controlling macros have the following features in common:

- 1) the macros extract data from a user reference number ("userref1") as entered in the SODS database for each sample site.
- 2) two separate groups of data can be combined by giving two user reference numbers ("userref1" & "userref2") when the controlling macro is called.
- 3) the plots are automatically labelled for the total number of data plotted, the number of data of each fracture type, the symbols and/or colours used for each fracture type plotted, and the values of the contours where appropriate.

- 4) colours and line types are incremented automatically in "numerical order" (colours and lines have numerical labels in S. Note that the line type assigned to a given number may vary according to the type of terminal or plotter used).

### A1.3.2 Details of MASS commands

#### A. Plotting the fracture plane data

Colour plotting of fracture orientation data is done using the "paps" (plot all planes stereonet) macros:

`?paps(userref1,userref2)` extracts and sorts the data into different types of fractures, then plots poles to fracture planes in different colours

`?paps2(userref1,userref2)` as `?paps`, but is used to plot the data on top of existing plots. For example, the raw data can be superimposed on top of a contoured plot.

#### B. Contoured plots of the fracture plane data

Plots can be contoured in monochrome or colour.

`?pufs(userref1,userref2,startcol/2/)` contours a plot of undifferentiated fault senses, (in colour), *i.e.* the data are not separated into different types of fracture. The user is prompted to input whether joints should be included in the plot.

'startcol' is an optional value of the colour of the first contour (default is '2' which is normally 'red' on the tek4107).

`?BWpufs(userref1,userref2,startlty/2/,charsze/0/)` as `?pufs`, but produces a black and white plot.

'startlty' is an optional value of the line type of the first contour line (default is '2', a dotted line on the tek4107).

'charsze' is an optional value for the character size used to label the contours. Default is '0'; the contours are not labelled.

`?faces(userref1,userref2,startcol/2/)` separates the orientation data into different types of fracture. Each fracture type is contoured separately and superimposed on the plot. Each contour is shown in a different colour. Remember that the plots can be unintelligible if too many fracture types are shown, especially when individual clusters overlap.

'startcol' is an optional value of the colour of the first contour (default is '2' which is normally 'red' on the tek4107).

?BWfaces(userref1,userref2,startlty/2/,charsze/0/) as ?faces, but produces a black and white plot. Each contour is shown in a different line type.

'startlty' is an optional value of the line type of the first contour line.(default is '2', a dotted line on the tek4107).

'charsze' is an optional value for the character size used to label the contours. Default is '0'; the contours are not labelled.

### C. Plotting lineation data

Slickenside data can be plotted using the "?linp" (lineation plotting) macros:

?linp1(userref1,userref2,segsze/10/,surftype/0/) plots all the lineation data without distinguishing between different fault types. The corresponding fault plane data can either be plotted as full great circle traces, or as partial great circles to keep the plot as legible as possible.

'segsze' is the angular size of the segment used for partial great circles. Default is 10°.

'surftype' is an optional value that determines the type of surface shown. '1' calls the "great" function to show full great circle traces; '2' calls "pgc" function to print partial great circles; '3' prints both. (Default is '0'; fault traces are not shown).

?linp2(userref1,userref2,segsze/10/) separates different senses of fault surface and plots each sense in a different colour. The fault plane data can either be plotted as full great circle traces, or as partial great circles to keep the plot as legible as possible.

'segsze' is the angular size of the segment used for partial great circles. Default is 10°.

'surftype' is an optional value that determines the type of surface shown. '1' calls the "great" function to show full great circle traces; '2' calls "pgc" function to print partial great circles; '3' prints both. (Default is '0'; fault traces are not shown).

### D. Rose diagrams

These macros plot 2D orientation data (*i.e.* azimuth values measured in the horizontal plane). Note that the plots take directional data in which a

direction, rather than just a trend, is specified (therefore the macros must be modified for fault-trend analysis *etc.*).

`?rose2(az,new/T/,start/0/,step/30/)` plots rose diagrams using the normal "equal distance" algorithm.

'az' is a vector of azimuthal data.

'new' is a logical flag to allow different datasets to be superimposed (using the same radius scale as the first plot).

'start' allows the first segment to be drawn at azimuths other than the north (0/360°) mark.

'step' is the circular class interval used for counting. Default is 30° segments.

`?ear(az,new/T/,circs/T/,meen/400/,step/30/,start/0/)` plots "equal area" rose diagrams.

'az' is a vector of azimuthal data.

'new' is a logical flag to allow different datasets to be superimposed (using the same radius scale as the first plot).

'circs' is a logical flag that plots circles of radius 10,20,30,40%.

'meen' plots an arrow at the azimuth given, to show the mean value of the circular data. If the argument given is greater than 360 (as is the default value), no arrow is shown. At the moment the macro doesn't calculate the mean, but this would be an obvious improvement for the future.

'step' is the circular class interval used for counting. Default is 30° segments.

'start' allows the first segment to be drawn at azimuths other than the north (0/360°) mark.

## E. Circular statistics for 3D deformation

These macros are designed to test clusters of data within datasets statistically, and also to test for geometric symmetry (for instance, pure shear plane strain deformation results in tetragonal symmetry. Pure shear non-plane strain deformation gives orthogonal geometrical symmetry [Reches 1978]).

`?segstat(ordata,polar/T/)` uses the "STATIS" function (an S function, written into SODS, that calls the "STATIS" program, which was designed by Nigel Woodcock [Dept. of Earth Sciences, Cambridge University] to statistically analyse orientation data). Only a specified

segment of the stereonet is analysed; the start and end values of the segment are entered by the user as the programme runs.

'ordata' is a two column matrix of orientation data.

'polar' is a logical flag to indicate whether data are planes or poles.

Default is T: data are polar.

?quad(userref1,userref2,pole/F/) quadrant statistics for 3D deformation.

This macro prompts for a  $\sigma_1$  direction, then rotates the data about  $\sigma_1$ , using a mirror plane parallel to  $\sigma_1$ , and another perpendicular to  $\sigma_1$ .

'pole' is a logical flag to indicate whether data are planes or poles.

Default is F: data are planar.

# Appendix 2: CONSTRUCTING GEOLOGICAL CROSS-SECTIONS USING A COMPUTER

## A2.1 Introduction

"KINKS" is a computer program that constructs geological cross-sections from surface dip data. Section balancing techniques that are currently used generally involve making assumptions about the pre-deformation state of the now-deformed rock: the amount of deformed material must be capable of being "restored" to its original shape. In contrast, the basic approach used here is to construct folds by making assumptions about the fold geometry, and hence no knowledge of the undeformed state of the rock is needed. This is particularly advantageous where an undeformed foreland sequence is no longer present, or where knowledge is limited in poorly studied areas. This approach can therefore be used as an alternative or in conjunction with established section drawing methods.

An important limitation of the program is that a *parallel fold geometry* is assumed.

There are several advantages of using computers to draw cross-sections:

- 1) plotting by computer is orders of magnitude faster than plotting by hand.
- 2) rapid plotting facilitates a trial-and-error approach. This allows the user to consider many different plots and reject those that are geologically unrealistic.
- 3) computer generated plots are as accurate as the input data will allow.

KINKS uses a construction that conserves bed thickness and bed length, and hence produces cross-sections that are inherently restorable. The program is therefore most useful where deformation has been accommodated by bedding-parallel flexural slip mechanisms. The construction used was developed by Geoff Tanner (Dept. of Geology & Applied Geology, Glasgow University), based on the work of John Suppe (Suppe 1985), as an alternative to the Busk construction (Busk 1929), and approximates rounded folds as a series of straight line segments. As in the Busk construction, fold "hinges" are assumed to be midway between two dip-readings, and the hinge bisects the interlimb angle ("hinge" here is used as the point at which the degree of curvature [Busk], or the angle of dip

[Kink] changes). This approach allows straight-limbed folds (kink and chevron folds) to be constructed using the same algorithm.

## A2.2 Limitations of the program

1) The program forces fold geometries to be parallel (preserving bed-thickness). Large inaccuracies will result if KINKS is used in areas where other classes of fold shape predominate.

2) The sections are two- rather than three-dimensional. The program is simply an attempt to predict sub-surface geometry, rather than kinematics (and therefore more interpretation must be done by the program user; less is done by the program itself). Consequently, interpolation between several parallel 2D traverses, or between a grid of 2D traverses would not be complicated (though the results would be less well constrained than 3D balancing methods).

Facilities for graphical display of 3D sections are well developed in comparison with our ability to collect and process 3D data.

3) the program forces bed-length to be preserved, allowing no thickening or attenuation of beds. This causes bed-lines to double back on themselves where fold axes intersect (Fig. A2.1). The apparent space problem created by KINKS is an artifact of the construction used, and is avoided in folds observed in the field in several ways. For example, folds can rupture to form fold and thrust belts; or underlying rocks might have more ductile rheology, and hence deform to give other fold geometries.

## A2.3 Program structure

The main body of KINKS is 365 lines (11508 characters) of Fortran77 code. Input data are processed to give a matrix of  $x$  and  $z$  values (*i.e.* horizontal and vertical coordinates) ready for plotting. Data input can be from keyboard (slow but interactive), or from datafile (much quicker if you are familiar with the program format). Data processing is extremely rapid (typically less than a second).

The plotting routines are not included in the main program, as they are dependent upon the type of device and the type of operating system used. The output from KINKS, however, is simply a matrix of coordinates, and so is simple enough for use with any plotting device.

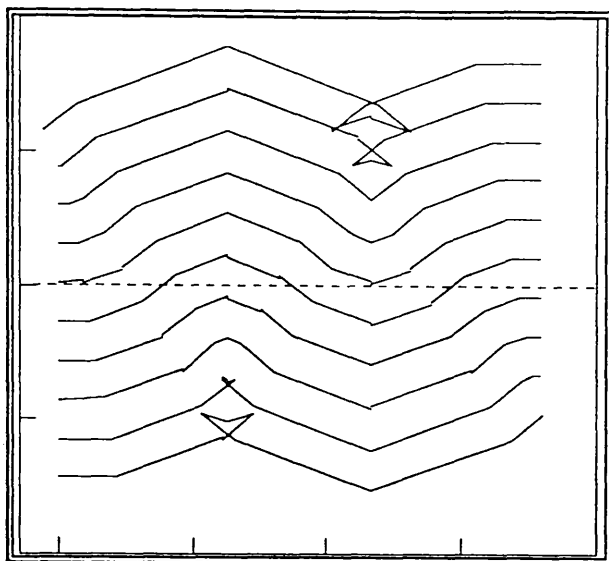


Fig. A2.1. Geometrical space problems are indicated by "looping" bed-lines. These space problems are shown in this way because the program forces the preservation of bed-length and bed-thickness.

The cross-sections presented here were drawn using "KINKPLOT", a program written in "S". S is a high level language and software system for data analysis and graphics routines, and runs under the UNIX operating system. KINKPLOT calls KINKS to perform the computations, then plots the matrix that KINKS produces (Fig. A2.2).

## A2.4 Examples of geological cross-sections

### A2.4.1. Foreland fold and thrust belts

KINKS is most useful in areas of large-wavelength, open folding, typical of the external parts of foreland fold belts close to the deformation front. Here fold geometries are often parallel or sub-parallel, and shortening by flexural slip is common.

Complications arise where thrusts have propagated beyond the level of the present day topographic surface, because the program assumes that all deformation is accomplished by parallel folding. Blind thrusts, however, *can* be recognised, because realistic fold geometries at the surface are matched at depth by intersecting fold traces showing potential space problems (*i.e.* geologically representing a departure from bedding-parallel simple shear).

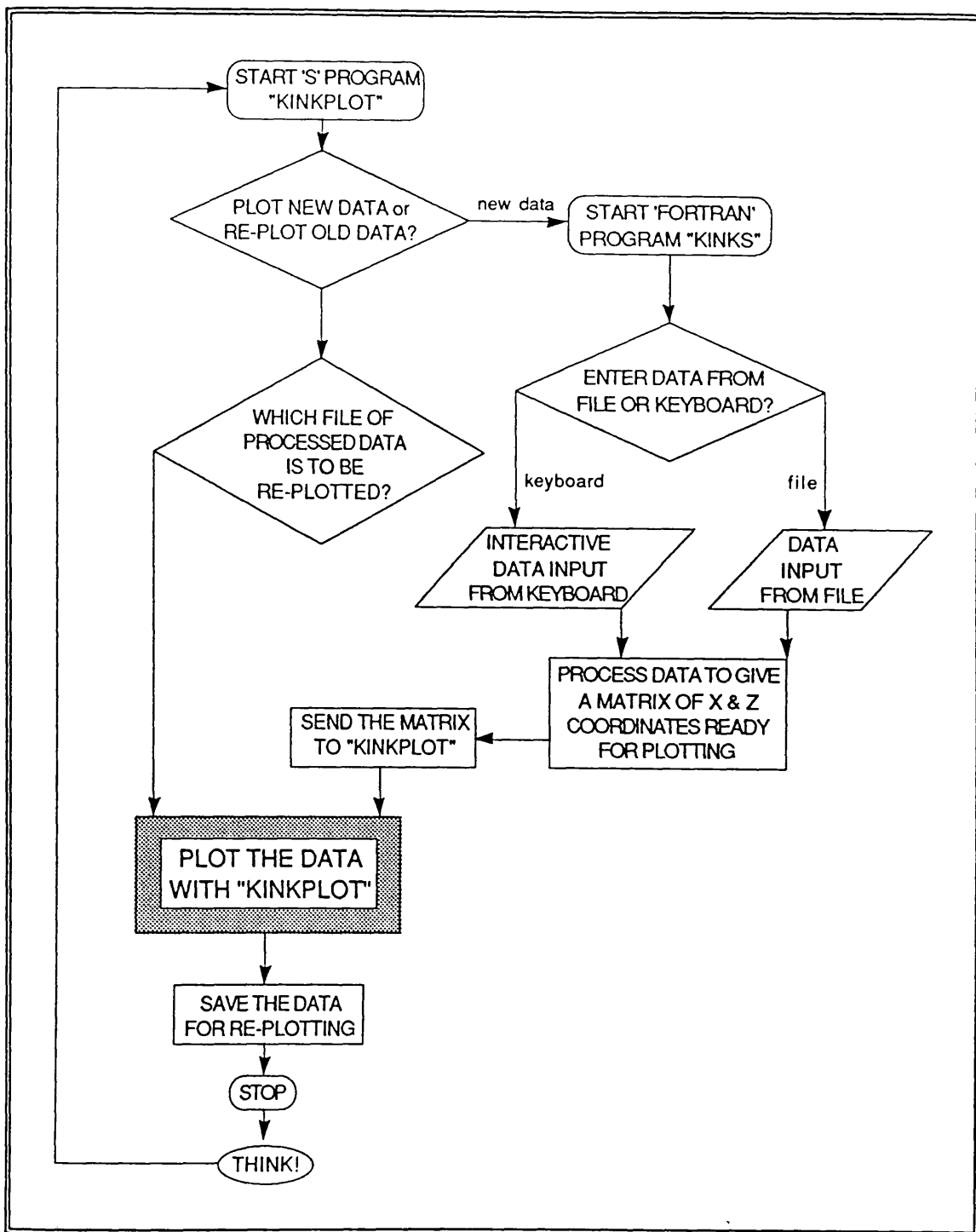


Fig. A2.2. Flowchart, showing the structure of the S program "KINKPLOT" and the FORTRAN program "KINKS".

### Variscan foreland fold belt, S.W.England

The Bristol-Mendip fold belt has been interpreted as a thin-skinned piggy-back foreland thrust belt of Variscan age (Williams & Chapman 1986). The Bristol to Cheddar section shown (Fig. A2.3) represents part of the belt in which most thrusts did not propagate as far as the present day land

surface The data are from B.G.S. 1:63,360 sheets 280 (Wells) and 264 (Bristol). The section is from G.R. ST 500500 to ST 500800.

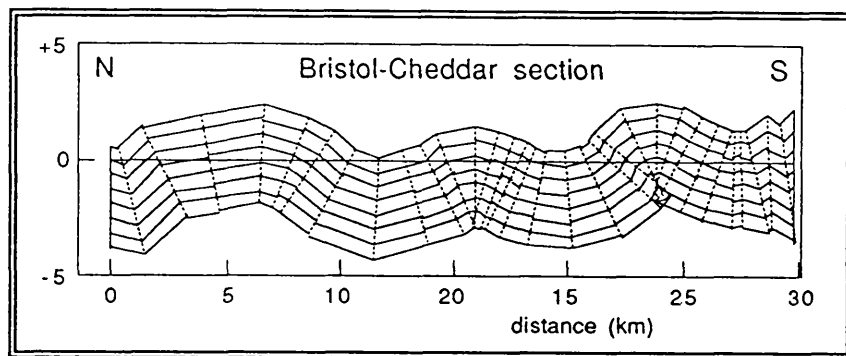


Fig. A2.3. True-scale cross-section constructed for the Bristol-Cheddar transect

### Caledonide foreland fold belt, Asker, S.E. Norway

Para-autochthonous Caledonide deformation is well preserved in the Lower Palaeozoic sediments of the Oslo Graben. In the field the style of folding is strongly dependent on lithology. Arenites and calc-arenites of Lower Llandovery age form flexural-slip folds with angular hinges and planar limbs. These rocks are underlain by Ordovician shales in which pervasive flexural-slip has given rise to attenuation of beds on fold limbs and thickening in fold hinges. Similarly, Upper Llandovery limestones have partially deformed by ductile flow to give non-parallel fold geometries. Furthermore, the folds have been tightened during the later stages of progressive foreland deformation. Consequently, the section shown in Fig. A2.4 requires careful interpretation: not all of the space problems evident at depth need indicate the presence of blind thrusts.

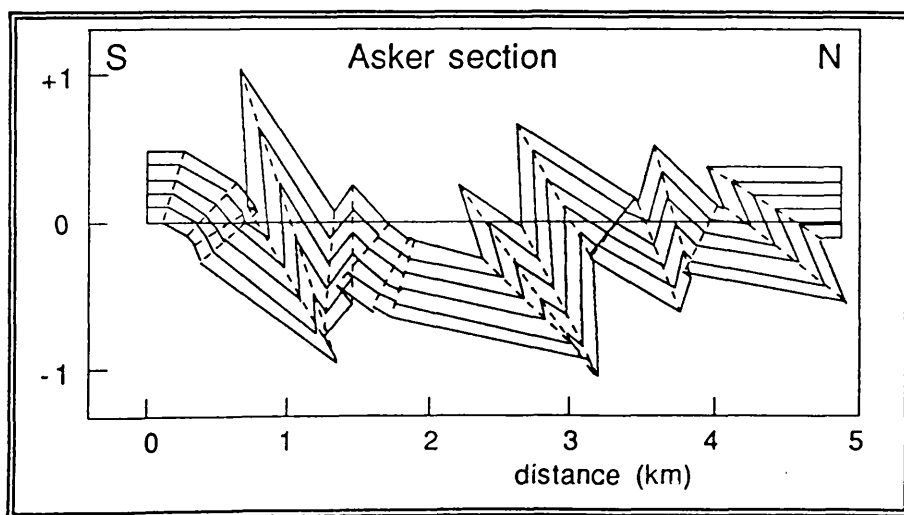


Fig. A2.4. True-scale cross-section constructed for Asker section, Norway.

### A2.4.2. Kink-band folds

#### **Valley and Ridge Province, Pennsylvania, U.S.A.**

Folds in the Valley and Ridge Province, ranging in wavelength from metres to kilometres, have geometries that are similar to kink-band geometries widely recognised on a smaller scale (Faill 1969,1973). The section shown in Fig. A2.5 is based on data from the U.S. Geological Survey (Butts 1939). In the field, fold limbs are seen to be planar, hinges are angular, and evidence of flexural slip is widespread. Consequently, the angularity depicted is real, unlike sections in which rounded folds are approximated as a series of straight-line segments.

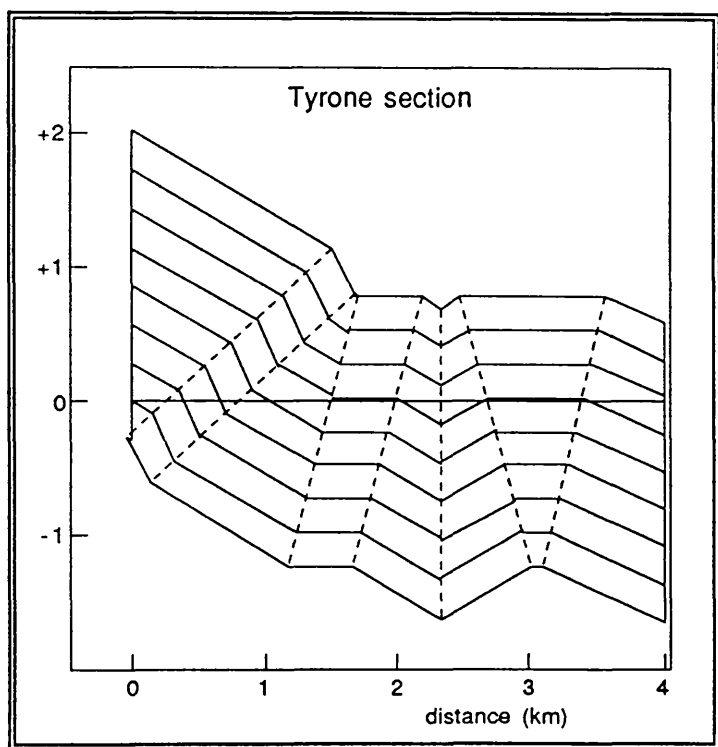


Fig. A2.5. True-scale cross-section, Tyrone, Pennsylvania.

### A2.4.3. Transpressional folds

#### **Mid-Devonian folds of the Midland Valley of Scotland**

"Kinks" was originally written to enable predictions to be made about the sub-surface geometry of the Strathmore syncline - Sidlaw anticline (Fig. A2.6). This is discussed in more detail in chapter 4 and Appendix 3.

### A2.4.4. Chevron folds

The main use of "Kinks" for chevron folds is to provide a rapid plotting facility, as little interpretation is generally required with folds of this

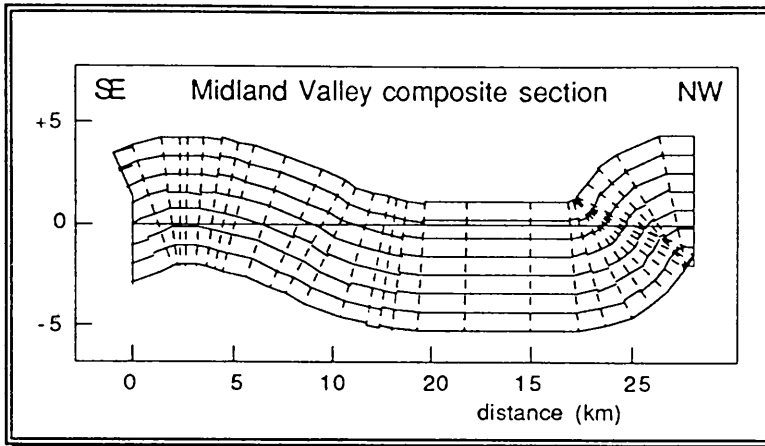


Fig. A2.6. True-scale composite cross-section constructed for the Midland Valley of Scotland.

type because their geometry is so well constrained. In fact, at present "Kinks" is less accurate for chevrons than plotting by hand. This is because the position of the fold traces on the line of section is not input into the computer by the program user, but is guessed to be midway between the two limb dip-data points.

### Grytviken, S.Georgia

The section shown in Fig. A2.7 is from South Georgia, south Atlantic (Tanner, 1990). Widespread chevron folding was caused by the Mid-Cretaceous closure of a turbidite back-arc basin sequence. Deformation increases in intensity to the N.E., with tightening of interlimb angles and progressive overturning of the folds.

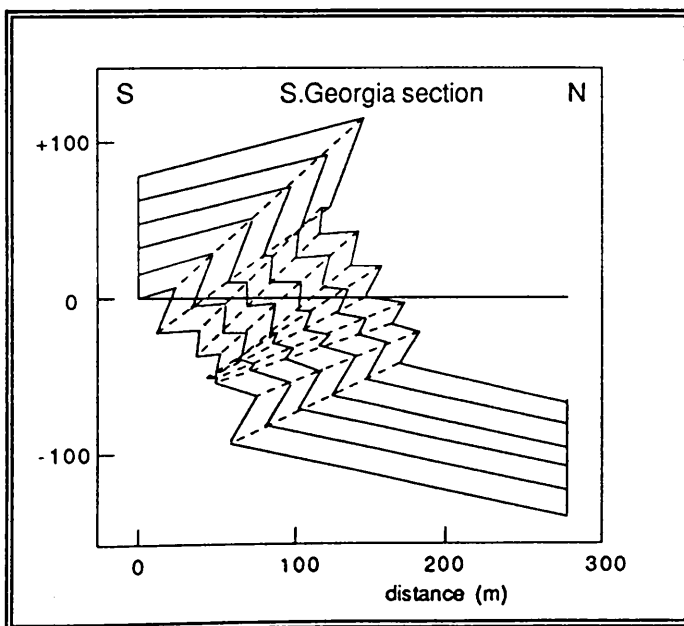


Fig. A2.7. True-scale cross-section for Grytviken, S.Georgia, south Atlantic.

## A2.5 Program Listings

```

PROGRAM kinklinesegments

C  declarations -----
   REAL seprate(40), midpt(40), kinkline(40), gradkinkl(40), dippt(40),
radkinkl(39), pi, kinklintcept(39), graddip(40), sectionlength,
linesepr, vertlinsepr, dipintcept(40), raddip(40), startzord,
intersect
   INTEGER count1, count2, count3, maxdips, dip(40), numidpts, numdippts,
numcflines, abovexaxis
   DIMENSION intersect(2,41,30)
   CHARACTER*1 info, toendit, dipsense(40), sepunits, wichlimb(39)

C  open channel 14 to store the final matrix
C  and to store the parameters needed for plotting -----
10  open (14, file="xzpoints")

C  initialisations -----
   count1 = 1
   count2 = 0
   maxdips = 40
   pi = 3.1415926

C  introduction -----
15  print*, " "
   print*, "This program will construct a cross-section of kink-line"
   print*, "segments given some surface dip data. For a discussion"
   print*, "of the assumptions and limitations of this method of X-S"
   print*, "construction, enter 'H' ,otherwise press any key."
   print*, " "
   read*, info
   IF (info .EQ. 'H'.OR. info .EQ. 'h') THEN
     print*, " "
     print*, "OK, info not yet written!"
   ENDIF

C  enter the data -----

C  first enter the units of measurement; metres or kilometres.
   print*, " "
   print*, "Next, you will be prompted to enter your data. You need to"
   print*, "type in some distances, either in METRES or in KILOMETRES."
   print*, "You must consistently use one OR the other. Enter 'm' for"
   print*, "metres, or 'k' for kilometres."
20  read*, sepunits
   print*, " "

C  next enter the perpendicular separation between bed lines
   print*, "Now enter the required perpendicular spacing between the"
   print*, "bed-lines (ie the true 'bed' thickness)."
   read*, linesepr
   print*, " "

C  how many bedlines are required
   print*, "How many bed-lines do you want on the section?"
   read*, numoflines
   print*, " "
   print*, "Of these",numoflines,"bed-lines, how many should start above"
   print*, "the ground surface?"
   read*, abovexaxis

C  Next enter the surface dip data
   print*, "Next enter the surface dip data. Keep the data in the"
   print*, "correct spatial order, starting with the reading at the left-"
   print*, "hand end of your section, finishing at the right-hand end of"
   print*, "the section."
   print*, "the section."

```

```

print*, "Note, there is a maximum no. of",maxdips,"dip readings per "
print*, "cross-section. To increase this you must change the"
print*, "'declarations' in the program."
print*, " "
print*, "Enter the first dip value. It must, of course, be between "
print*, "0 and 90 degrees. After that you must specify whether the dip"
print*, "DIRECTION is to the left ('L') or to the right ('R'), as you"
print*, "look at the section."
30 print*, "Some examples: 34 R .. 65 L .. 12 L etc."
print*, " "

C IF loop to input any number of dip readings -----
32 IF (toendit .NE. 'Y' .AND. toendit .NE. 'y') THEN
    print*, " "
    print*, "Enter value number",count1," and its direction."
    read*, dip(count1), dipsense(count1)

C check the data -----
    IF (dip(count1) .LT. 0 .OR. dip(count1) .GT. 90 .OR. (dipsense(count1) .NE.
'R' .AND. dipsense(count1) .NE. 'L')) THEN
        count2 = count2 + 1

        IF (count2 .EQ. 1) THEN
            print*, "There's an error in your data input. Try again, dummy !"
            GOTO 32
        ENDIF

        IF (count2 .EQ. 2) THEN
            print*, "Are you crazy ? Enter it again, pea-brain !"
            GOTO 32
        ENDIF

        IF (count2 .GE. 3) THEN
            print*, "This is beyond a joke. Your I.Q. is rated at "
            print*, "          ",count2 * -100
            GOTO 32
        ENDIF
    ENDIF
ENDIF

C Is there any more data to be entered -----
print*, " "
print*, "Is that all the dip data to be entered? Enter 'Y' or 'N'."
read*, toendit

C If its not the last entry then
C enter the spacing between the dip readings
    IF (toendit .NE. 'Y' .AND. toendit .NE. 'y') THEN
        print*, " "
        print*, "What is the distance between dip reading",count1," and"
        print*, "dip reading",count1 + 1
        read*, seprate(count1)

C This bit is very important- there are two possibilities in drawing the
C section between any two points: one puts a fold hinge between the two
C points; the other keeps the two points on the same fold limb. IMPORTANT
-----
print*, " "
print*, "The next bit is very important. If you don't understand the"
print*, "significance of the question, you should quit and look at"
print*, "the methodology of this method of section drawing."
print*, " "
print*, "Will the next dip data point lie on the same fold limb, "
print*, "or is there a fold hinge between the points ? "
print*, "Enter 'q' to quit"
print*, "      'b' to return to the beginning of the program for help"
print*, "      's' if the points are on the same limb of a fold"
print*, "      'o' if the points are on opposite limbs of a fold"
read*, wichlimb(count1)
-----

```

```

C 'if' loop to allow quitting -----
  IF (wichlimb(count1) .EQ. 'q' .OR. wichlimb(count1) .EQ. 'Q') THEN
    GOTO 1000
  ENDIF

C 'if' loop to allow user to go back to beginning and get help -----
  IF (wichlimb(count1) .EQ. 'b' .OR. wichlimb(count1) .EQ. 'B') THEN
    GOTO 10
  ENDIF

  ENDIF

C increment the counter(s) -----
C (line below: no. of mid pts. must = one less than the no. of dip datas.)
  numidpts = count1 - 1
  numdippts = count1
  count1 = count1 + 1

C check that not too many values are to be entered -----
  IF (count1 .EQ. maxdips) THEN
    print*, " "
    print*, "This must be your last data entry. To enter more you must "
    print*, "change the array length, now set at", maxdips, "in the "
    print*, "'DECLARATIONS' part of the program, and also change the "
    print*, "constant 'maxdips' in the 'INITIALISATION' section."
    print*, " "
  ENDIF

C go back to start of IF loop to input the next dip data. -----
  GOTO 32

  ELSE
    print*, "OK, that's the end of the data entry."
    print*, " "
  ENDIF

-----
-----

C Now do the meaty bit! Manipulate the data ready to draw the Suppe section
-----
C First manipulate the DIP data to get it into coordinates and gradients
  DO 200 k = 1, numdippts

C change the format of the dip direction to be between 0 and 180' ....
C ... measured anticlockwise from left of section. eg 20 R = 160' ....
C ... 20 L = 20' 50 R = 130' etc.

  IF (dipsense(k) .EQ. 'R' .OR. dipsense(k) .EQ. 'r' ) THEN
    dip(k) = 180 - dip(k)
  ENDIF

C change the angle to radians, and then from an angle to a gradient
  raddip(k) = dip(k) * 2 * pi / 360
  graddip(k) = tan(raddip(k))

200 CONTINUE

C initialise -----
  dippt(1) = 0

C set up mid-points between the dip-data points using the separations inputted.

  DO 250 i = 1, numidpts
    midpt(i) = dippt(i) + ( seprate(i) / 2 )

C This is important- this bit uses the variable 'wichlimb' to make
C the kink-line either the ACUTE angular bisector (wichlimb = 'o')
C [ie the kink-line is a fold axis ], or the perpendicular to the
C angular bisector, that is the OBTUSE bisector (wichlimb = 's')
C [the kink-line is not a real fold axis]

```

```

IF (wichlimb(i) .EQ. 'o' .OR. wichlimb(i) .EQ. 'O') THEN
C   kink-line is the angular bisector
   kinkline(i) = (dip(i) + dip(i + 1)) / 2

ELSE
C   kink-line is the perpendicular to the angular bisector
   kinkline(i) = 90 + ((dip(i) + dip(i + 1)) / 2 )

ENDIF

C   keep the kink-lines less than 180 degrees
IF (kinkline(i) .GE. 180 ) THEN
   kinkline(i) = kinkline(i) - 180
ENDIF

C   convert the degrees to radians
radkinkl(i) = kinkline(i) * 2 * pi / 360

C   and convert the angle to a gradient
gradkinkl(i) = tan(radkinkl(i))

C   find the intercept of the kinkline with the z-axis
kinklintcept(i) = 0 - (gradkinkl(i) * midpt(i) )

C   set up the x-coordinate of each dip point
dippt(i+1) = dippt(i) + seprate(i)

250  CONTINUE

C   set up a final, extra kink-line :- a vertical line at the right-
C   hand end of the section, with a x-coord at the far right dip-point
gradkinkl(numidpts + 1) = 1001
midpt(numidpts + 1) = dippt(numidpts)

-----
C   Use nested DO loops to set up a 3D array, 'intersect(k,m,i)'
C   'k' always equals 2; k=1 is the x ordinate, k=2 is the z ordinate.
C   'm' is equal to number of intersections on each bedline: 'numintsperline'.
C   'i' is the number of bedlines: 'numoflines'.
-----

C   set up the z coordinate for the starting (i.e. top) bedline
IF (dipsense(1) .EQ. 'L') THEN
vertlinsep = linesep/(cos(raddip(1)))
ELSE
vertlinsep = linesep/(cos(raddip(1))) * -1
ENDIF
startzord = vertlinsep * abovexaxis
print*, "vertlinsep is",vertlinsep

C   section extends from zero point to the last dip-point:
sectionlength = dippt(numdippts)

DO 380 i = 1,numoflines

C   set up the first coordinate of each dip line on the z-axis
intersect(1,1,i) = 0
intersect(2,1,i) = startzord

DO 350 m = 2,numidpts + 2
C   'number of midpts + 2' :- to include the vertical kink-line at right-
C   hand end of section and the start point of each line

C   the starting point for the bed-line segment takes the finishing
C   point of the last segment
C   I pity anyone trying to understand this !

```

```

C      find the intercept of the dip-line segment with the z-axis
C      using the equation for a straight line  $c = z - g.x$ 
C      dipintcept(m-1)= intersect(2,m-1,i)-(graddip(m-1)* intersect(1,m-1,i))

-----

C      find the intercepts between diplines and midpoint lines

C      if the dip of either the kink-line or the bed-line is near to infinity
C      the algorithms break down. So, use two IF loops to overcome this.
C      'Infinity' is set arbitrarily at > 1000

      IF (graddip(m-1) .GT. 1000) THEN
C      x-coord is the same as the previous intersection point
      intersect(1,m,i) = intersect(1,m-1,i)

      intersect(2,m,i) = (gradkinkl(m-1) * intersect(1,m,i))

      ENDIF

      IF (gradkinkl(m-1) .GT. 1000) THEN
C      kinkline is vertical and x-coord is intecept of kinline with x-axis
      intersect(1,m,i) = midpt(m-1)
      intersect(2,m,i) = (graddip(m-1) * intersect(1,m,i))+ dipintcept(m-1)
      ENDIF

      IF (graddip(m-1) .LE. 1000 .AND. gradkinkl(m-1) .LE. 1000) THEN
C      standard algorithm for intersecting lines.
      intersect(1,m,i)=(kinklntcept(m-1)- dipintcept(m-1))/(graddip(m-1)-
gradkinkl(m-1) )
      intersect(2,m,i) = (graddip(m-1) * intersect(1,m,i)) + dipintcept(m-1)
      ENDIF

350      CONTINUE

-----

C      increment the starting point for each bed-line by the line separation
      startzord = startzord - vertlinsep

380      CONTINUE

C      initialise
      count3 = 0

C      send the values for number of lines and the number of intersects per line
      write(14,430) numoflines
      write(14,430) numdippts + 1

C      send the 'intersect' matrix to channel 14
C      the number of intersections per bedline = number of dip points + 1
      DO 405 i = 1,numoflines
      DO 400 m = 1,numdippts + 1
      write(14,420) (intersect(k,m,i), k = 1,2 )
400      CONTINUE
405      CONTINUE

-----

420      format(3 f 10.1)
430      format(I2)

      close(14)

100C      END

```

```

# ----- KINKPLOT -----
#
# Richard Jones
#
# Version 1.0 16/7/90
#
# This source file of S commands is written for use with the
# fortran program "KINKS", to construct geological cross-sections.
# KINKS generates a series of XZ coordinates for the cross-section.
# This program will plot those coordinates using the S "plot" function.
#
# set up the plotting parameters -----
tek4107
par(mai=c(0,0,5,0))
title(main="WELCOME TO KINKS",col=2, cex=3)
#
# Plotting or Re-plotting? -----
# The program can plot existing data-sets of coordinates already generated by
# this program from KINKS data, or can plot the data for the first time:
# this is a time saving option to allow multiple copies of plots.
#
print()
print("Enter 'P' to process and plot new data.")
print("Enter 'R' to re-plot data that has already been processed.")
wotinput <- read(,length=1)
if (wotinput=="P" | wotinput=="p") {
  print("List of files suitable for processing:")
  sys('ls CKP*')
  sys('CK.compiled')
  toplot <- read('xzpoints', mode=REAL)
  sys('rm xzpoints') } else {
  print()
  print("Here is a list of shell files that have already")
  print("been processed ready for plotting:")
  sys('ls plot*')
  print()
  print("Type in the name of the file to be plotted")
  wotfile <- read(,length=1)
  toplot <- read(wotfile, mode=REAL)
  rm (wotfile) }
#
# Now split up the data from "toplot" dataset -----
nl <- toplot[1] # = number of lines
ni <- toplot[2] # = number of intersections per line
tni <- (2*ni*nl) + 2 # = total number of intersections
gotlot <- toplot[3:tni] # = all the coordinate data
xzints <- array(c(gotlot), c(2,ni,nl)) # create the xz matrix
rm (tni,gotlot,toplot)
print()
#
# allow section to fill screen or to be true-scale -----
print("Should the section be true scale or should it be automatically ")
print("stretched to fill the screen. Enter 'T' or 'S':")
shape <- read(,length=1)
par(mai=c(1.2,1,1,0.3))
#
# Plot the data, true-scale or stretched -----
if (shape=="T" | shape=="t") {
  par(pty = "s")
  plot(xzints[1, ,1], xzints[2, ,1], type='l', col=4, xlim=range(xzints),
  ylim=range(xzints)) } else {
  plot(xzints[1, ,1], xzints[2, ,1], type='l', col=4, ylim=range(xzints[2, ,])) }
for(cnt1 in 2:nl) {
  lines(xzints[1, ,cnt1],xzints[2, ,cnt1], col=cnt1) }
print("What should the sub-title of the section be? Enter a character string:")
print("If the string is more than one word, use quotes:")
sts <- read(,length=1)
title("Kink-fold Cross-Section",sts,"distance (m)", "elevation (m)")
origin <- c(xzints[1,ni,1],0)
secend <- c(0,0)
lines(origin,secend, lty=3)

```

```

for (cnt2 in 1:ni ) {
  xhinge <- c(xzints[1,cnt2,1],xzints[1,cnt2,nl])
  zhinge <- c(xzints[2,cnt2,1],xzints[2,cnt2,nl])
  lines(xhinge,zhinge, lty=2)
}
#
# Allow data to be saved -----
print("Do you want to save this data, to allow replotting/editing ?")
print("Enter 'Y' or 'N' :")
tosave <- read( ,length=1)
if (tosave== "N" | tosave=="n") {
  print("OK, all the data is deleted.") } else {
  print("Type in the filename where this data is to be stored:")
  print("Use the prefix 'plot'. eg plotALPS, plotHIMALAYAS.")
  fn <- read( ,length=1)
  cbf <- c(nl,ni,xzints)
  write(cbf,fn)
  rm (fn,cbf)
}
rm (ni,nl,origin,xzints,secend,xhinge,zhinge,tosave,shape,wotinput,sts)
# -----

```

# Appendix 3: THE ROTATION OF LINEATIONS DURING FLEXURAL-SLIP FOLDING

## A3.1 Introduction

This appendix investigates the change in orientation of lineations during folding. Palaeomagnetic vectors are a type of geological lineation, and the aim of this work is to examine whether palaeomagnetic data can be used as a constraint in the analysis of individual folds. This has particular relevance to the mid-ORS Midland Valley transpressional deformation discussed in Chapter 4. The generalised geometrical conclusions have a wider significance, and can be applied to other types of geological lineation, such as palaeocurrent data and structural lineations.

Firstly, an important limitation of this discussion must be emphasised: the results presented below apply only to folds with parallel profile geometry (Ramsay 1967), that have developed *entirely* by flexural-slip (*i.e.* no flexural flow has occurred).

Parallel folds are the easiest class of folds to describe geometrically, and other classes of folds will cause lineations to rotate along different (and more complicated) paths.

## A3.2 The orientation of a palaeomagnetic vector with respect to tilted bedding

The geometry of a palaeomagnetic lineation, "P", after tilting is shown in Fig.A3.1. Tilting has occurred about a fixed horizontal axis. The changes in orientation of the lineation are considered in relation to a plane that (1) is perpendicular to bedding, and (2) contains the palaeomagnetic vector, "P". This plane is of great importance, because during parallel folding by flexural-slip it always remains perpendicular to bedding (this is generally not the case with non-parallel fold geometries). The line "L" is the intersection of this perpendicular plane with bedding.

I = the initial plunge (*i.e.* "inclination") of P. This angle remains constant during parallel folding by flexural-slip

A = the pitch of line L within the plane of bedding

d = the angle of dip of bedding

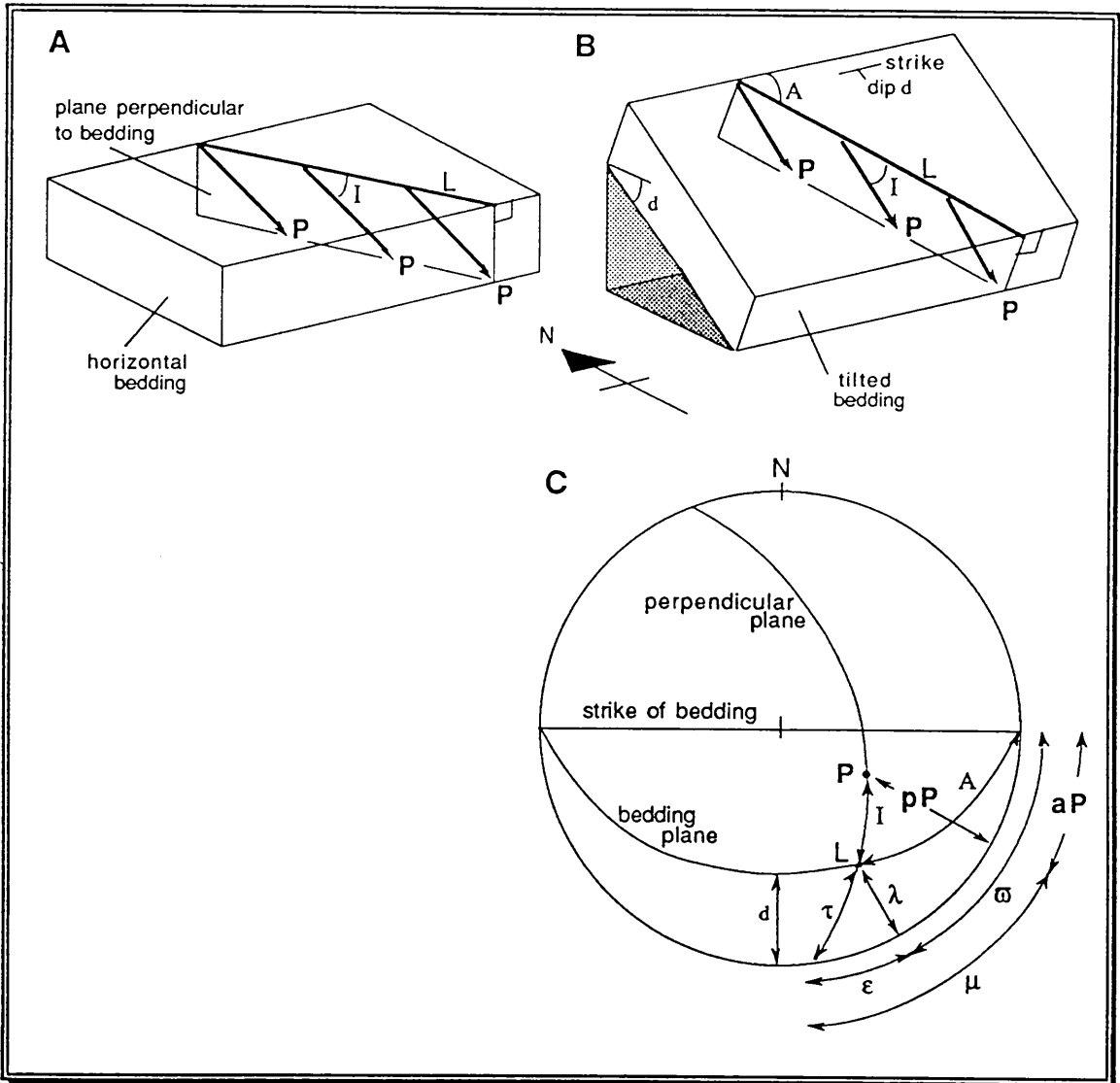


Fig. A3.1. The orientation of a palaeomagnetic vector  $P$  during folding. (A) initial orientation, horizontal bedding. (B) orientation after tilting. (C) lower hemisphere stereonet showing the relationships between the azimuth and plunge of  $P$  and  $L$  and the other angles described by the equations in the text, after tilting.

From Fig A3.1 we see that:

$$\text{plunge of } L, \lambda = \sin^{-1}(\sin A * \sin d)$$

Eq. A3.1

Let  $\varpi$  be the angle between the strike of bedding and the azimuth of  $L$

$$\varpi = \cos^{-1}(\cos A / \cos \lambda)$$

Eq. A3.2

Thus equations A3.1 and A3.2 can be used to give the plunge and azimuth of  $L$ . These angles are used below to derive the strike and dip of the perpendicular plane after tilting, and subsequently the plunge and azimuth of  $P$ :

Let  $\epsilon$  be the angle between the azimuth of L and the strike of the plane that is perpendicular to bedding and that contains L and P, such that:

$$\tan(\varpi + \epsilon) = \tan A / \cos d \quad \text{Eq. A3.3}$$

Let  $\Delta$  be the angle of dip of the plane that is perpendicular to bedding and that contains L and P

$$\Delta = \cos^{-1} (\cos A * \sin d) \quad \text{Eq. A3.4}$$

Let  $\tau$  be the pitch of L in the plane that is perpendicular to bedding and that contains L and P

$$\tau = \tan^{-1} (\tan d * \sin A) \quad \text{Eq. A3.5}$$

plunge of P, $pP = \sin^{-1} [\sin \Delta * \sin(I + \tau)]$	Eq. A3.6
--	----------

Let  $\mu$  be the angle between the azimuth of P and the strike of the plane that is perpendicular to bedding and that contains L and P

$$\mu = \tan^{-1} [\cos \Delta * \tan(I + \tau)] \quad \text{Eq. A3.7}$$

The azimuth of P (with respect to the strike of bedding) is related to  $\mu$  as follows:

azimuth of P, $aP = \mu - (\varpi + \epsilon)$	Eq. A3.8
--	----------

Equations A3.6 and A3.8 can be re-written to show that the plunge and azimuth of a lineation after folding can be expressed solely in terms of the three variables A, I and d, as defined in Fig A3.1.

Equations A3.4 and A3.5 are substituted into Eq. A3.6 to give the plunge of P:

plunge of P, $pP = \sin^{-1} [(\cos d * \sin I) + (\sin A * \sin d * \cos I)]$	Eq. A3.9
--	----------

Equations A3.3, A3.4, A3.5, and A3.7 are combined with Eq. A3.8 to give the azimuth of P (measured in the horizontal plane, *with respect to the fold axis*):

azimuth of P, $aP = \tan^{-1} \{ [(\cos A * \sin d * \tan I) + (\cos A * \sin A * \sin d * \tan d) - (\tan A / \cos d) + (\tan A * \sin A * \tan I * \tan d / \cos d)] / [1 + (\tan^2 d * \sin^2 A)] \}$	Eq. A3.10
--	-----------

### A3.3 The orientation of palaeomagnetic vectors around parallel folds

The above equations (Eq. A3.1 - Eq. A3.10) can be directly applied to show how the orientations of surface lineations and palaeomagnetic vectors vary around a parallel fold. It is assumed here that the fold axis is orientated perpendicular to maximum compression, so that the hinge undergoes no rotation or migration as the fold tightens. In general this should be valid for folds that develop due to pure shear deformation.

If the above assumption holds, then the variable  $A$  (see Fig A3.1) remains constant during fold development, and the lineation "L" traces out a small circle path on the stereonet (Fig A3.2), as was shown by Ramsay (1967, chapter 8). The palaeomagnetic vector,  $P$  follows a similar trace, with a pitch dependant upon  $A$  and  $I$ .

Let  $\rho$  be the pitch of the plane traced by  $P$  around a parallel fold

$$\rho = \cos^{-1}(\cos A * \cos I) \quad \text{Eq. A3.11}$$

(i.e. the pitch is a function of the magnetic declination and inclination).

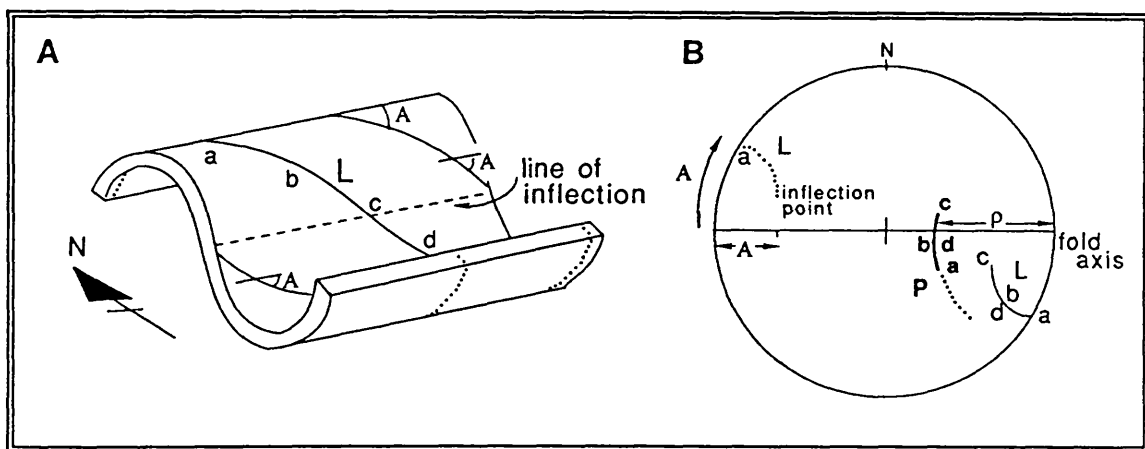


Fig. A3.2. The orientation of a lineation around a parallel fold (see Fig. A3.1 for notation). (A) sketch of parallel fold showing lineation L. Four points, 'a-d' are shown: 'a' lies on the fold hinge, 'c' marks an inflection point where the curvature of the fold limb changes sense. (B) schematic lower hemisphere Wulff net showing the trace of lineation L with points 'a-d', and palaeomagnetic vector  $P$  with equivalent positions 'a-d'. The solid line segments show L and  $P$  orientations for the south facing limb; the dotted traces relate to the hidden north facing limbs.

### A3.4 Parallel folds that form during simple shear

The change in orientation of geological lineations and palaeomagnetic vectors, after folding has occurred, will depend upon:

- 1) the initial orientation of the lineations/vectors with respect to bedding
- 2) the style and geometry of the folding
- 3) the amount of simple shear acting during fold development.

In general, the effect of simple shear strain on fold geometry has not been considered by palaeomagnetists. For example, the palaeomagnetists' "fold-test" uses the geometry of folds (and more lately the style of folding as well) to constrain the orientation of vectors prior to folding (more specifically, to test the age of a component of magnetism with respect to the age of the folds). Conversely, structural geologists have recently used palaeomagnetic vectors to understand the geometry of folds (*e.g.* Kent 1988). This section considers the theoretical effects of a simple shear component acting during fold development.

Many wrench faults are characterised by zones of en-échelon folding (Moody & Hill 1956), and such folds have been modelled in clay-box experiments (Wilcox *et al.* 1973). The folds initiate with axes perpendicular to the maximum incremental stress, *i.e.* at 45° to the shear zone boundaries for simple shear. During progressive simple shear, as modelled in clay-box experiments, the folds are seen to rotate towards the zone boundaries.

The rotation of fold axes can occur passively for ductile rheologies (such as clay, or rock at elevated temperature and pressure), and the fold axes, once formed, may follow the rotation of any other type of geological lineation, such that:

$$\phi' = \phi + \gamma \quad (\text{from Ramsay 1967, equation 3-71}) \quad \text{Eq. A3.12}$$

where;       $\phi$  = initial orientation of line  
                   $\phi'$  = final orientation of line after simple shear  
                   $\gamma$  = shear strain

In this analysis I have assumed that parallel folds occur by elastic rather than plastic deformation (*i.e.* there is no *internal* deformation of the folded layers by flexural flow), and this implies that passive rotation of fold axes is not possible. Instead, the fold axes might follow the rotation of the finite strain ellipse:

$$\tan (2\theta') = 2\gamma / \gamma^2 \quad \text{Eq. A3.13a}$$

$$\therefore \theta' = [\tan^{-1} (2 / \gamma)] / 2 \quad \text{Eq. A3.13b}$$

This requires that the fold axes move through the rock, causing a significant volume of rock to passively change position from one fold limb, through the hinge, onto the opposing fold limb (Fig. A3.3).

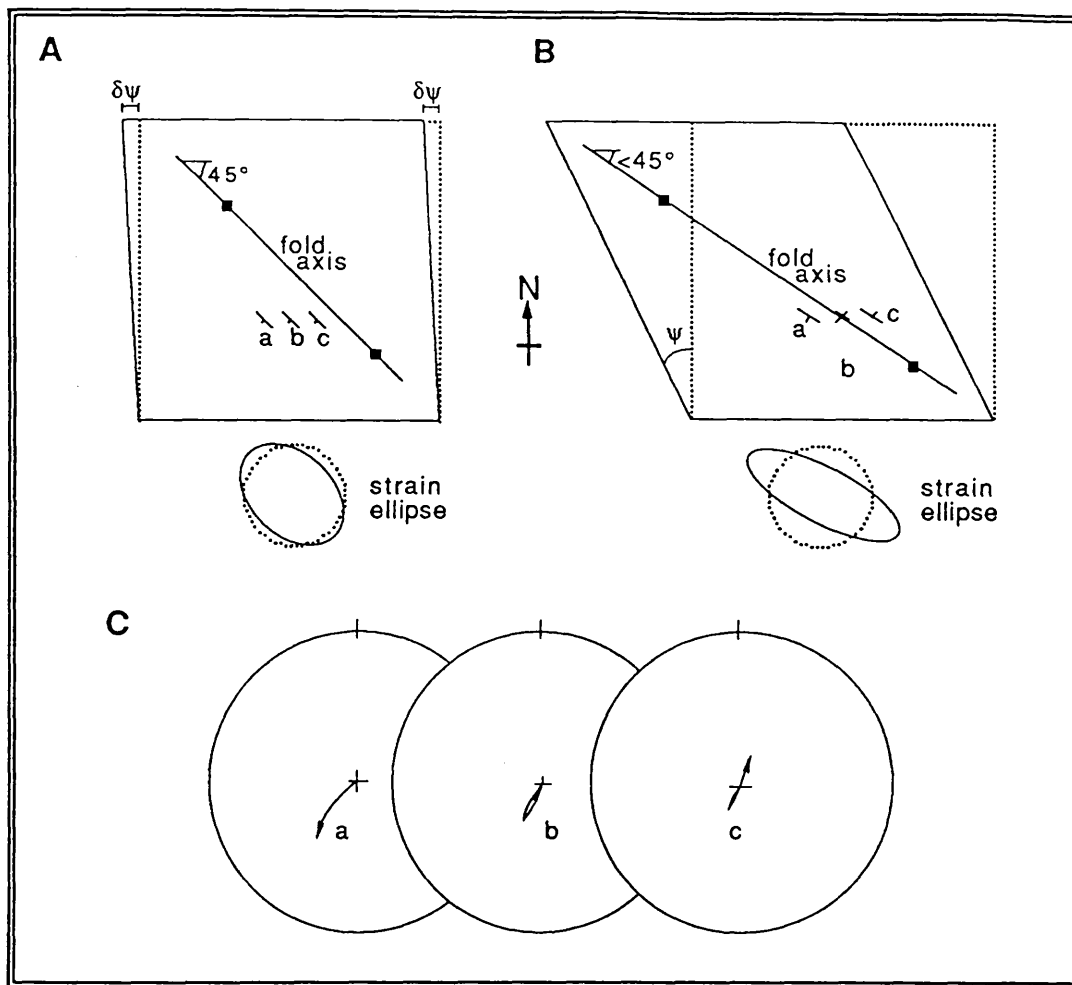


Fig. A3.3. Rotation of an antiformal fold hinge during *progressive* simple shear (plan view). (A) initiation of fold at  $45^\circ$  to shear zone boundary. (B) fold axis rotates (anticlockwise) relative to "fixed" points a, b, and c: point 'a' remains on the same fold limb, point 'b' now lies on the antiformal axis, whereas the axis has passed through position 'c'. Note that the fold axis also increases in length. (C) lower hemisphere schematic Wulff nets showing the rotation paths of the poles to bedding at points a-c.

Fig. A3.3 serves to show the heterogeneity of all deformation manifested by folding. The points a-c are just three examples of all the possible points in the deforming zone, and the actual orientation path experienced by every point is unique during progressive rotation of the fold hinge. The orientation path for each point will therefore depend not only on the shear strain, but also on the position of the point with respect to folds, and on the geometry of the folds (*i.e.* wavelength, amplitude, and the shape of the fold profile).

It must be emphasised that the heterogeneity of deformation inherent in folded rocks precludes a full detailed description of the generalities of simple shear folds. Further assumptions must be made in order to remove two of the three unknown parameters stated at the start of this section.

As an example, I shall now consider the change in orientation of a palaeomagnetic vector during folding in a simple shear zone. The following assumptions apply;

- 1) the folds have a parallel style produced entirely by elastic deformation
- 2) there is no shortening or extension across the simple shear zone (*i.e.* deformation is *not* transpressional)
- 3) fold axes migrate, *in order to maintain parallelism with the long axis of the finite strain ellipse.*

As shown in section A3.2 the angle  $A$  remains constant during non-rotational folding (see Fig. A3.1). The third assumption is important, because it determines how the angle  $A$  will change during during fold axis migration:

$$A - A' = \theta - \theta' \quad \text{Eq. A3.14}$$

The orientation *path* of each point in the deformation zone will be complex and unique (because  $A$  and  $d$  in Eqs. A3.9 and A3.10 are constantly changing). However, at any stage of progressive simple shear a transect of points across the zone will follow equation A3.11, such that

$$\rho' = \cos^{-1}(\cos A' * \cos I) \quad \text{Eq. A3.15}$$

As an example, consider a north/south left-lateral simple shear zone (similar to the east-west zone shown in Fig. A3.3). Let the palaeomagnetic vector plunge at  $50^\circ$  towards  $205^\circ$  prior to deformation. Deformation is considered for four stages of increasing shear strain (Fig. A3.4).

- (1) The onset of deformation (Fig. A3.4a). The fold axes initiate at  $45^\circ$  to the shear zone boundary, *i.e.*  $\theta_1$  is at  $045^\circ$ - $225^\circ$ .  $A$  is equal to  $20^\circ$  ( $225^\circ - 205^\circ = 20^\circ$ ), and the palaeomagnetic vectors at each point in the deformation zone start to change orientation.

- (2) Shear strain,  $\gamma = 0.5$  (Fig. A3.4b)

$$2\theta' = \tan^{-1}(2 / 0.5) \quad \therefore \theta' = 38.0^\circ \quad (\text{from Eq. A3.13b})$$

*i.e.* fold axis orientated at  $038^\circ$ - $218^\circ$

$$A' = \theta' - \theta + A \quad \therefore A' = 13.0^\circ \quad (\text{from Eq. A3.14})$$

$$\rho' = \cos^{-1}(\cos A' * \cos I) \quad \therefore \rho' = 52.8^\circ \quad (\text{from Eq. A3.15})$$

(3) Shear strain,  $\gamma'' = 1.0$  (Fig. A3.4c)

$$2\theta'' = \tan^{-1}(2 / 1.0) \quad \therefore \theta'' = 31.7^\circ \quad (\text{from Eq. A3.13b})$$

*i.e.* fold axis orientated at  $032^\circ$ - $212^\circ$

$$A'' = \theta'' - \theta + A \quad \therefore A'' = 6.7^\circ \quad (\text{from Eq. A3.14})$$

$$\rho'' = \cos^{-1}(\cos A'' * \cos I) \quad \therefore \rho'' = 50.3^\circ \quad (\text{from Eq. A3.15})$$

(4) Shear strain,  $\gamma''' = 2.0$  (Fig. A3.4d)

$$2\theta''' = \tan^{-1}(2 / 2.0) \quad \therefore \theta''' = 22.5^\circ \quad (\text{from Eq. A3.13b})$$

*i.e.* fold axis orientated at  $023^\circ$ - $203^\circ$

$$A''' = \theta''' - \theta + A \quad \therefore A''' = -2.7^\circ \quad (\text{from Eq. A3.14})$$

the negative sign shows that the fold hinge is now orientated anticlockwise of L.

$$\rho''' = \cos^{-1}(\cos A''' * \cos I) \quad \therefore \rho''' = 50.1^\circ \quad (\text{from Eq. A3.15})$$

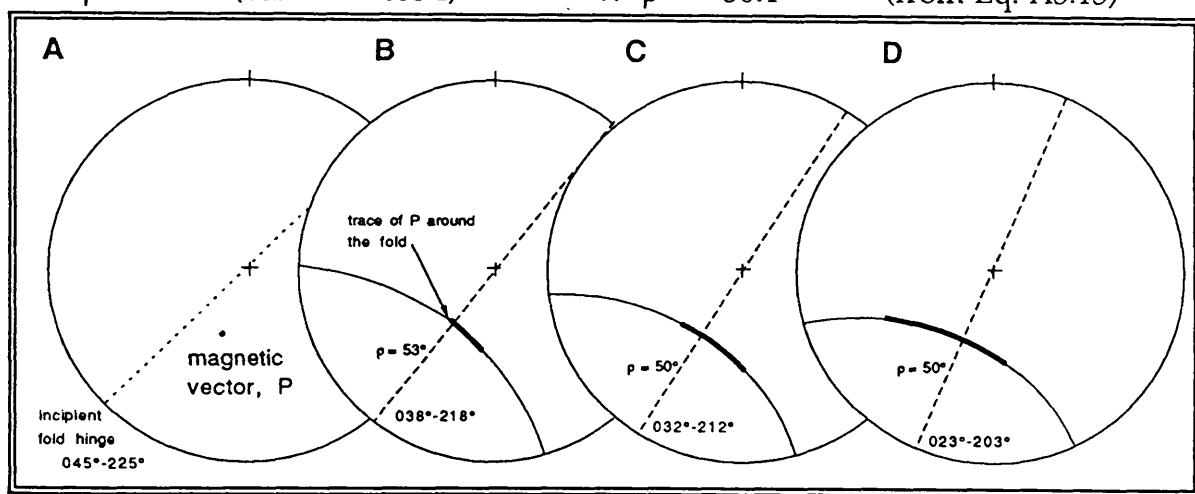


Fig. A3.4. Schematic lower hemisphere Wulff nets showing the change in orientation of a palaeomagnetic vector around folds produced in a N/S simple shear zone. Four stages are shown (A-D), corresponding to  $\gamma$  values of  $\delta\gamma$ , 0.5, 1.0, and 2.0. Note how the length of traces of the vectors on the stereonet increase as the folds tighten (this is because the dip of bedding at the inflection points increases as the folds tighten). The exact position of P on the vector trace can be ascertained by solving equations A3.9 and A3.10 for various values of 'd' around the fold surface.

The above analysis can be expanded to allow for departure from one of its assumptions, namely, that deformation is not transpressional. This is considered in the following section.

## A3.5 Transpressional parallel folds

### A3.5.1 Introduction

During transpression, folds develop in response to components of both pure and simple shear. Consequently the equations describing simple shear

deformation must be modified, using the transpressional strain matrix of Sanderson & Marchini (1984).

The orientation of the finite strain ellipse,  $\theta'$ , is given by

$$\tan (2\theta') = 2\gamma / (\alpha^2 + \gamma^2 - 1) \quad \text{Eq. A3.16}$$

where  $\alpha$  is the ratio of deformed to undeformed width of the transpression zone. (More specifically, Eq. A3.16 gives the orientation of the longer principal axis, of the finite strain ellipsoid, *in the XY plane*).

In order to demonstrate the theoretical change in orientation of magnetic vectors some assumption must be made about the deformation path. A well-defined deformation path was outlined by Harland (1970) in his model for "simple transpression" (see section 4.7, and Fig.4.27).

### A3.5.2 Fold development in the Harland model of simple transpression

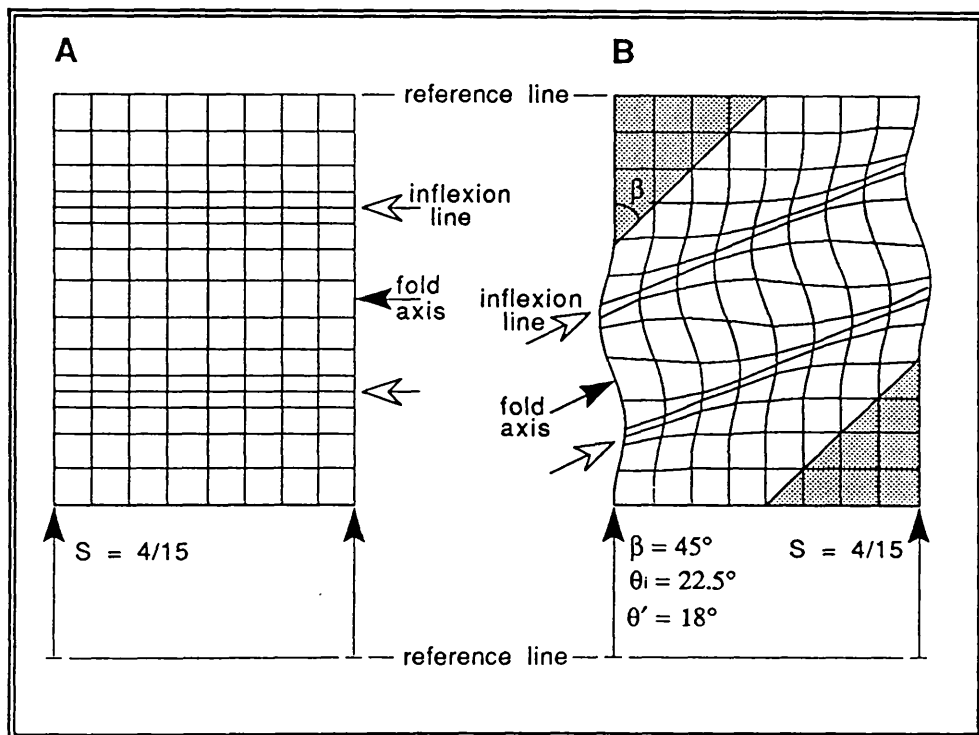


Fig. A3.5. Schematic diagram comparing the deformation of a regular 5mm grid, manifested as buckle folding, (A) by pure shear, and (B) by simple transpression. Plan view.

For simple transpression (from Sanderson & Marchini 1984, p.453),

$$\alpha = (1-S)^{-1} \quad \text{Eq. A3.17}$$

$$\gamma = S(1-S)^{-1} \cot\beta \quad \text{Eq. A3.18}$$

where  $S$  is the shortening and  $\beta$  is the angle between regional shortening and the transpression zone boundaries. For a given value of  $\beta$ , Eq. A3.18 can be substituted into Eq. A3.16 to show how the strain ellipse

changes orientation during transpressional shortening (see Figs. 4.29, 4.30). For a given amount of shortening, the corresponding value of  $\theta'$ , and therefore values for  $A'$  and  $\rho'$ , can be ascertained, using equations A3.13, A3.14, and A3.15.

By way of example, consider a deformational zone experiencing north-south simple transpressional shortening. The zone boundaries are orientated at  $030^\circ$ - $210^\circ$  (*i.e.*  $\beta = 30^\circ$ ), magnetic inclination is  $+10$  (*i.e.* pointing downwards), and magnetic declination is towards  $160^\circ$ . The variation of the parameters used to describe transpression is shown graphically for shortening from 0 to 100% ( $S: 0 \rightarrow 1$ ):

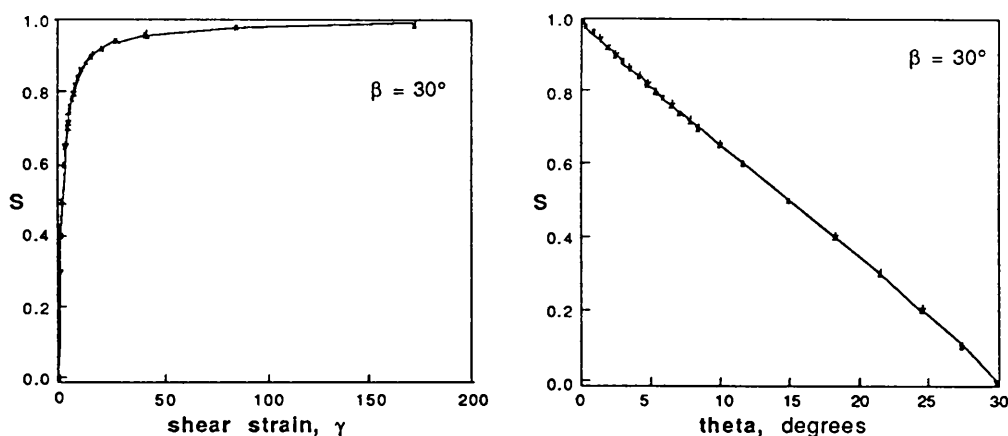


Fig. A3.6. Left graph: variation in shear strain during simple transpressional shortening, from Eq. A3.18. Right graph: orientation of the largest horizontal axis of the finite strain ellipse during simple transpressional shortening, from Eq. A3.16.

It is important to realise that it is difficult to reconcile the transpression equation A3.16 with the model of simple transpression as originally envisaged by Harland (1971, figure 3; see Fig. 4.27). Harland believed that folds would initiate perpendicular to the regional shortening direction, then start to rotate. However, equation A3.16 shows that at the onset of shortening the long axis of the strain ellipse is *not* perpendicular to the direction of regional shortening, because of the effect of the simple shear component.

Consequently, if fold hinges develop parallel to the long axis of the strain ellipse (at least at the time of fold *initiation*) then folds will form oblique to regional  $\sigma_1$ , and the conceptual model of Harland must be slightly revised.

In the above example, Fig. A3.6 shows that at the onset of shortening, buckle folds will initiate at  $30^\circ$  to the zone boundary (*i.e.* at  $060^\circ$ - $240^\circ$ ). Therefore  $A_{\text{initial}}$  will be  $80^\circ$  ( $= 240^\circ - 160^\circ$ ).

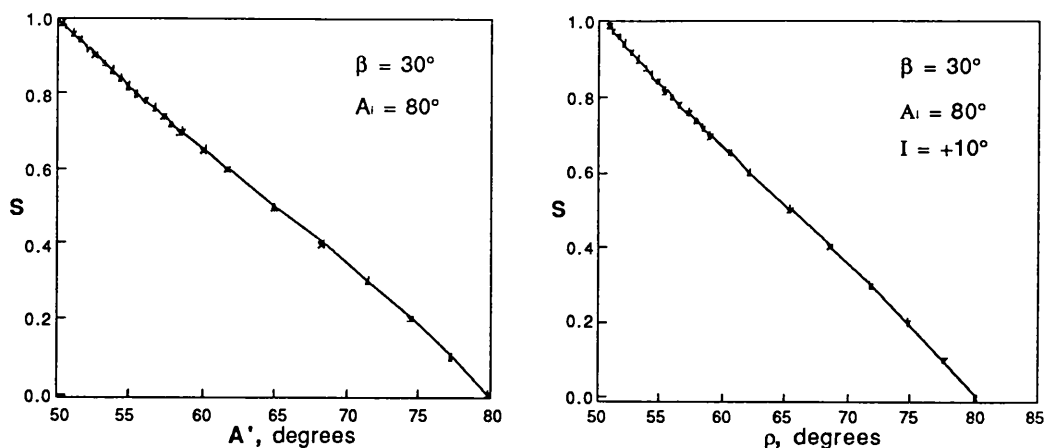


Fig. A3.7. Left graph: orientation of fold hinges during simple transpressional shortening, from Eq. A3.14. Right graph: variation in the pitch of a plane traced out by a magnetic vector around parallel folds during simple transpressional shortening, from Eq. A3.15.

These results can be used to predict the orientation of folds, and hence the trace of the possible orientations of the folded magnetic vector, for any given stage of the transpressional shortening. For instance, at 40% shortening ( $S = 0.4$ ),  $\theta' = 18^\circ$ , and  $p' = 69^\circ$ . This is shown in Fig. A3.8A.

It is interesting to compare these conclusions with the orientations of folds and folded magnetic vectors that would result from pure shear deformation of the same deforming zone used in the above example (Fig. A3.8B). In this case  $\beta = 90^\circ$ , and the regional shortening direction is perpendicular to the zone boundaries at  $120^\circ$ - $300^\circ$ . Such folds are non-rotational, and their axes would be orientated parallel to the zone boundaries, as described in section A3.3. The transpressional folds of Fig. A3.8A always maintain a parallel fold geometry, and "untilting" the vector data about the fold axis ( $048^\circ$ - $228^\circ$ ) will give perfect clustering.

Furthermore, not only will the data be perfectly clustered, but the resultant palaeo-declination and palaeo-inclination thus derived (from which a palaeo-pole can be inferred), will be accurate. This, of course, is logical, though not necessarily immediately obvious, because one of the assumptions of this analysis is that fold hinges rotate through the deforming zone, *without body rotation of the zone*. (deformation is entirely elastic). The mathematical proof of this is obtained by solving equations A3.9 and A3.10 for  $d=0$ , for any stage of transpressional shortening, including both the situations shown in Fig. A3.8.

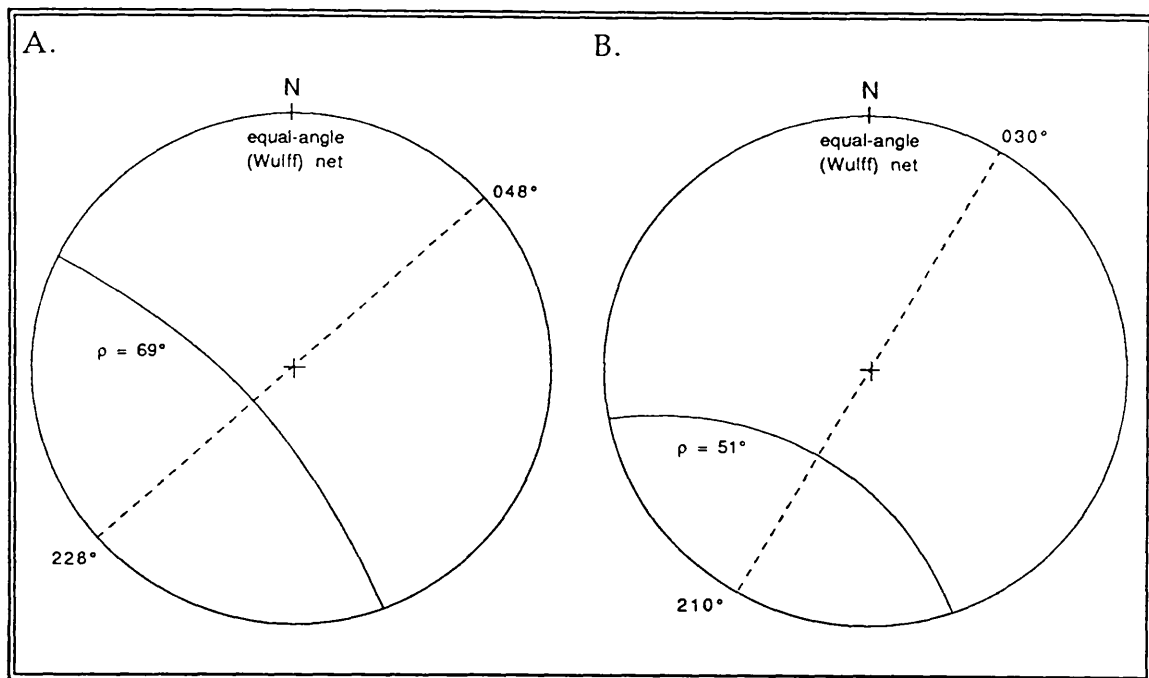


Fig. A3.8. Stereonets comparing the orientation of a magnetic vector around parallel folds. (A) after 40% simple transpressional shortening (see text for details of other parameters). (B) after pure shear deformation of the same deforming zone (*i.e.*  $\beta = 90^\circ$ ; compression orientated  $120^\circ$ - $300^\circ$ ; fold hinges do not rotate).

This conclusion is of importance to the palaeomagnetist, because it shows that standard method of untilting data from parallel folds used by palaeomagnetists is probably still valid, even when rotating hinge migration has occurred. It does, however, also demonstrate that there are many assumptions underlying this conclusion, and should encourage palaeomagnetists to plot the uncorrected data, before 'blindly' tilt-correcting them.

There is a practical limit to the application of the theoretical analysis outlined in this appendix. An inherent assumption of the analysis is that deformation is elastic. When the elastic limit of a material is reached, the material either yields (resulting in brittle failure), or deforms plastically. At this point, deformation can no longer occur in the way described in this appendix.

The significance of the analysis is now clear. Unlike the measured palaeo-declination and palaeo-inclination, the value of  $\rho$  *does* vary during transpressional folding.

Consequently, the  $\rho$ -value could be used to help describe the deformation state, by removing one unknown variable in the transpression equations.

For example, the value of  $\rho$ , derived from palaeomagnetic measurement, could be used to measure  $\beta$  in a deforming zone in which the zone boundaries are not well defined in the field (that is providing that the direction of regional shortening is known, and the deformation path is identified or assumed).

### A3.5.3 Further discussion of the application of the Harland model of simple transpression to the mid-Devonian folding in the Midland Valley

In section 4.7.4 I showed that the current models for transpression cannot be applied to the mid-Devonian folds of the Midland Valley, because folds can only achieve parallelism with the deformation zone boundaries at infinite transpressional shortening. Section 4.8 describes an alternative model of transpression, in which folds develop parallel to the transpression zone boundary.

This section attempts to use the theory developed in this appendix to analyse existing palaeomagnetic data, in order to further constrain the geometry of the Midland Valley folds, and to try to use the data to test the transpression models.

The geometrical parameters:

- (1) Regional  $\sigma_1$  is taken to be due north-south (with respect to magnetic north), from the results of the mesofracture analysis presented in section 4.6.
- (2) The HBFZ is taken to be a zone boundary, and hence  $\beta$  is approximately  $60^\circ$ .
- (3) Palaeomagnetic declination,  $D$ , =  $218^\circ$  ( $225^\circ$  with respect to grid north), and inclination,  $I$  =  $+46^\circ$ . This is derived from the data of Torsvik (1985), who derived a Lower Devonian palaeo-pole from L.ORS rocks of the Sidlaw Anticline. The validity of the values of  $D$  and  $I$  should *not* depend upon whether rotating hinge migration has occurred (see section A3.5.2); this is an important inference, because it suggests that it is reasonable to use the conclusions of Torsvik's data to further analyse the data itself (*i.e.* circular logic is avoided).

Are the assumptions of the analysis valid?

- (1) The geometry of the mid-Devonian folds is probably (though not certainly) parallel, as discussed in section 4.7.1.
- (2) The L.ORS rocks seem to have displayed elastic rheology during fold formation. The field evidence suggests that brittle failure (giving rise to

the mesofracture arrays), occurred *after* fold formation, because the orientation of mesofracture geometries is maintained across the fold axes (*c.f.* figure 17 of Hancock 1985). However, the mesofracture and fold geometries *are* coaxial and are broadly synchronous, implying a close genetic link between the two types of deformation.

The rotational component of mesofracture deformation observed in some stations close to the HBF has serious consequences for the theoretical analysis of Appendix 3, because block-faulting back-rotations will lead to an inaccurate measurement of palaeomagnetic declination. However, Torsvik's data were taken from the Sidlaw anticline, well away from the HBFZ (see Fig. 1.1).

The palaeomagnetic data:

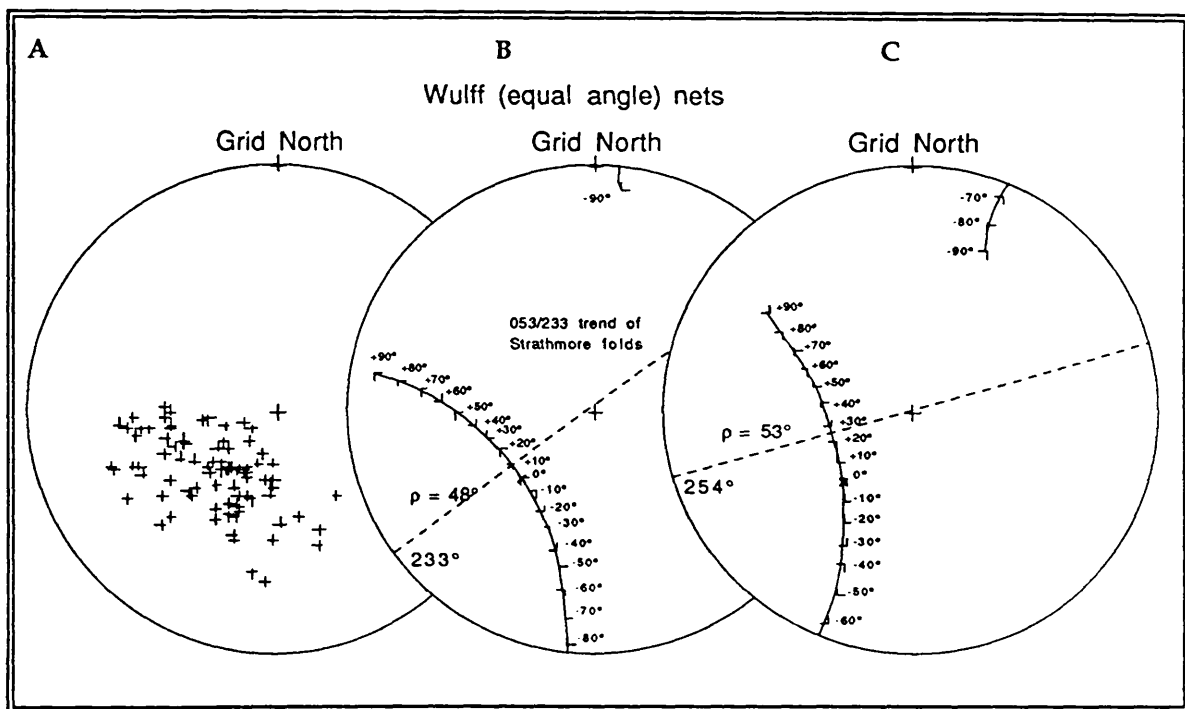


Fig. A3.9. (A) lower hemisphere Wulff net selectively showing some of the data from Torsvik (1985). Only Group 1 data are shown (interpreted as pre-folding magnetic component), and negative polarities are converted to lie in the lower hemisphere. (B) & (C) theoretical vector traces, with several positions of P (these are calculated by substituting various values of bedding dip,  $d$ , into equations A3.9 and A3.10): (B) predicted vector trace assuming the folds formed by pure shear, orthogonal to the HBFZ. (C) theoretical vector trace predicted for rotating folds forming after 10% north-south simple transpressional shortening, using the analysis of section 3.5.2.

## Discussion:

The data shown in Fig. A3.9 is broadly consistent with the mid-Devonian folding having been formed by pure shear, orthogonal to the HBFZ, as proposed in my strain partitioned transpression model. *However, the error on the data is too large to preclude other interpretations from being discounted.* Some of the error in Torsvik's calculation of D and I may result from difficulties in measuring the true palaeo-horizontal in the ORS lavas and red-beds, whilst some of the spread seen in the untilted data (Fig. A3.9) may be due to undulations of strike on the fold limbs, or small rotations on later faults. However, the main problem in this study is that the palaeo-declination is orientated close to the axis of folding, and that data are taken from shallowly dipping fold limbs. Consequently, all the vector data are predicted to cluster close to the trace of the axial plane on the net.

Some recent data from Glenberrie, on the steep limb of the Strathmore syncline was given by Trench & Haughton (1990). Unfortunately, the magnetic vectors appear to have been back-rotated (strike 085), probably by mid-Devonian brittle faulting, and so the data are difficult to incorporate into an analysis of Torsvik's study.

### A3.5.4 Computer programs used to model transpression

```
MACRO PMT(Incl,pitchL,hingeor,add/F/)
#
# ----- Richard Jones -----
#
# this macro calculates the plunge and azimuth of a palaeomagnetic vector for
# different positions around a folded surface.
# The variables and equations are explained in Appendix 3 of my thesis
#
# Version 2.2  11/7/90
#
# -----
#
print("NOTE: great care is needed with the sign conventions",quote=F)
print(" used in the equations of Appendix 3. Always check the",quote=F)
print(" results of this macro to see if they are reasonable!",quote=F)
#
#
?T(I) <- $1 * torads      # the inclination of palmag vector
?T(A) <- $2 * torads      # the pitch of "L"
?T(ho) <- $3              # the orientation of the fold hinge
#
print("Enter a vector of dip values. Enter '100' for a range",quote=F)
print("of dips from +90 to -90, in 10 degree increments.",quote =F)
?T(d) <- read()
if (?T(d)==100) ?T(d) <- c(-9,-8,-7,-6,-5,-4,-3,-2,-1,0,1,2,3,4,5,6,7,8,9)*10
?T(d) <- ?T(d) * torads
#
#
# ---- calculate the vector of plunge values for P, using Eq.A3.9 ----
#
QpP <- asin( (cos(?T(d))*sin(?T(I))) + (sin(?T(A))*sin(?T(d))*cos(?T(I))) )
QpP <- QpP * todeg      # convert back from radians to degrees
```

```

#
#
# ---- calculate the vector of 'azimuth' values for P, using Eq.A3.10 -----
#
?T(z1) <- cos(?T(A)) * sin(?T(d)) * (?tan(?T(I)))           # Equation 10a
?T(z2) <- cos(?T(A)) * sin(?T(A)) * sin(?T(d)) * (?tan(?T(d))) # Equation 10b
?T(z3) <- (?tan(?T(A))) / cos(?T(d))                         # Equation 10c
?T(z4) <- (?tan(?T(A))) * sin(?T(A)) * (?tan(?T(I))) * (?tan(?T(d))) / cos(?T(d)) #10d
?T(z5) <- 1 + ( (?tan(?T(d))) * (?tan(?T(d))) * sin(?T(A)) * sin(?T(A)) ) #10e
?T(z6) <- ( ?T(z1) + ?T(z2) - ?T(z3) + ?T(z4) ) / ?T(z5)   # Equation 10
?T(z6) <- atan(?T(z6)) * todegS                             # convert back from radians to degrees
QaP <- ?T(ho) + ?T(z6)                                       # change the angle to an azimuth
#
#
# ---- now validate the data to plot on lower hemisphere stereonet -----
#
# first change all 'upward' plunges to point downward:
for (i in 1:len(QpP)) {
  if (QpP[i] < 0) {
    QpP[i] <- abs(QpP[i])
    QaP[i] <- QaP[i] - 180
  }
}
# now change all azimuths to lie between 0 and 360
for (i in 1:len(QaP)) {
  if (QaP[i] < 0) QaP[i] <- QaP[i] + 360
  if (QaP[i] > 360) QaP[i] <- QaP[i] - 360
}
# and round the data to nearest integer
QpP <- round(QpP)
QaP <- round(QaP)
#
#
# ---- print out the results -----
#
print("Plunge of P =", QpP, quote=F)
print("Azimuth of P =", QaP, quote=F)
#
# combine the QpP and QaP into one matrix of orientation data
Qor <- matrix(c(QaP, QpP), ncol=2, byrow=F)
# plot on a Wulff net
?stereo(Qor, "+", T, $4)
#
#
#zap(T*)           # remove the local macro variables, but not the results
END

```

```

MACRO TPsimple(beeter/60/, hay/40/, eye/50/)
#
# ----- CHANGE IN ORIENTATION OF STRAIN ELLIPSE & FOLD AXES IN -----
# -----SIMPLE TRANSPRESSIVE REGIMES -----
#
# ----- Richard Jones -----
#
# version 1.0 5.7.90
#
# This macro describes the changes in orientation of a lineation (eg a
# palaeomagnetic vector) during transpressional shortening that is manifested
# as buckle folds that have PARALLEL fold geometry.
# The figure numbers and equations quoted refer to my thesis, where the theory
# of transpression is developed and discussed.
#
#
# ----- First calculate how shear strain varies during simple -----
# ----- transpression -----
#
beta <- $1 * torads           # see Fig. 4.27 for definition of beta
#
# get a vector of shortening values ("S") to use as increments of shortening:

```

```

print("Enter a vector of S values",quote=F)
print("Transtension: S < 0   Transpression: 0 < S < 1",quote=F)
print("Just enter the value '100' to use a typical range of S values",quote=F)
print("",quote=F)
print("Corresponding pure and simple shear values are calculated",quote=F)
print("",quote=F)
ess <- read()
if (ess == 100) ess <-
c(0.1,10,20,30,40,50,60,65,70,72,74,76,78,80,82,84,86,88,90,92,94,96,98,99) *
.01
#
# now calculate variation in shear strain ("gama"):
gama <- (ess / (1 - ess)) * (cos(beta) / sin(beta))           # Eq. A3.18
#
#
# ----- Next calculate the change in orientation of the finite -----
# ----- strain ellipse during simple transpression -----
#
alpha <- 1/(1 - ess)                                         # Eq. A3.17
theeta <- (atan((2*gama)/((alpha*alpha)+(gama*gama)-1))) / 2  # Eq. A3.16
#
# ----- Now calculate the corresponding change in orientation of fold -----
# ----- axes, and the consequent value for 'ro' (see Fig. A3.1) -----
#
A <- $2 * torads                                             # see Fig. A3.1 for definition of beta
I <- $3 * torads                                             # see Fig. A3.1 for definition of beta
Aprime <- theeta - theeta[1] + A                             # Eq. A3.14
ro <- acos(cos(Aprime) * cos(I))                             # Eq. A3.15
#
#
# ----- now give the results, numerically & graphically -----
#
print("",quote=F)
print("Shortening used:",ess,quote=F)
print("Corresponding variation in gama:",gama,quote=F)
theeta <- theeta * todeg
print("Corresponding variation in theta:",theeta,quote=F)
Aprime <- Aprime * todeg
print("Corresponding variation in A:",Aprime,quote=F)
ro <- ro * todeg
print("Corresponding variation in ro:",ro,quote=F)
print("",quote=F)
#
par(pty="s")
#
plot(gama,ess,type="n",xlab="gamma",ylab="S",col=7)
lines(gama,ess,col=4)
text(gama,ess,"*",col=6)
title("VARIATION OF SHEAR STRAIN, SIMPLE TRANSPRESSION",col=2)
#
plot(theeta,ess,type="n",xlab="theta, degrees",ylab="S",col=7)
lines(theeta,ess,col=4)
text(theeta,ess,"*",col=6)
title("ROTATION OF STRAIN ELLIPSE, SIMPLE TRANSPRESSION",col=2)
#
plot(Aprime,ess,type="n",xlab="A, degrees",ylab="S",col=7)
lines(Aprime,ess,col=4)
text(Aprime,ess,"*",col=6)
title("VARIATION OF 'A' DURING SIMPLE TRANSPRESSION",col=2)
#
plot(ro,ess,type="n",xlab="ro, degrees",ylab="S",col=7)
lines(ro,ess,col=4)
text(ro,ess,"*",col=6)
title("VARIATION OF 'ro' DURING SIMPLE TRANSPRESSION",col=2)
#
rm(beta,ess,gama,alpha,theeta,A,I,Aprime,ro)
#
# NB the dataset name "gama" is used rather than "gamma". This is to avoid
# potential problems because 'gamma' is an S function.
# Similarly, 'ess' and 'theeta' are used.
#
END

```

### A3.6 Sign Conventions

Great care must be taken to use the correct signs for parameters when using the equations in this appendix. It is generally beneficial to quickly plot the data by hand, in order to understand the significance and to check the validity of the derived results.

Positive angles are measured in an anticlockwise sense. Consequently, sinistral shear strain is positive; dextral is negative. In the vertical plane, positive angles are measured downwards (to plot on the lower hemisphere of the stereonet).

I have adopted these conventions in the equations in this appendix, so, for example,  $\beta$  in the simple transpression model is measured from the zone boundary anticlockwise to the direction of regional  $\sigma_1$ . Thus positive values of  $\beta$  will give a component of left-lateral (*i.e.* positive) simple shear. The angle  $A$  is measured with respect to the fold hinge: if  $L$  has a greater azimuth than the fold hinge,  $A$  will be negative.

### A3.7 Summary

The theoretical arguments developed in this appendix aim to further our understanding of heterogeneous three-dimensional deformation, and show how palaeomagnetic data might be used to constrain such deformation. When applied to the mid-Devonian folds of the Midland Valley, the spread of available palaeomagnetic data is far too large to allow statistically significant interpretations to be made. Indeed, this may prove to be the limiting factor in many palaeomagnetic studies. However, the analysis presented in this appendix does provide a background in which the statistical validity of palaeomagnetic studies of folded rocks can be further understood.

The convoluted discussion developed here demonstrates a more important philosophical point; namely, that deformation is complex and is dependant upon many parameters. Though some parameters are inter-related, all must be specified before deformation can be fully described. This is generally not possible, and some assumptions must therefore be made. It is particularly important that palaeomagnetists understand the assumptions that are inherent in many of the methods they use to interpret their data, and that efforts are made to test and refine these assumptions.

